NASA CR-216

STUDY OF THE THERMAL PROCESSES FOR MAN-IN-SPACE

Prepared under Contract No. NASw-1015 by
AIRESEARCH MANUFACTURING COMPANY
Los Angeles, Calif.

for

NATIONAL AERONAUTICS AND SPACE ADMINISTRATION

For sale by the Clearinghouse for Federal Scientific and Technical Information
Springfield, Virginia 22151 – Price $6.00

FOREWORD

This report was prepared by personnel of the AiResearch Manufacturing Company, Los Angeles, California, under Contract NASw-1015. W. L. Burriss was principal investigator on the program. S. H. Lin, Ph.D., was responsible for the extravehicular suit heat balance studies. P. J. Berenson, Ph.D., conducted the shirtsleeves environment thermal and comfort studies. The contract was monitored by John Fuscoe of the Office of Advanced Research and Technology, Headquarters, the National Aeronautics and Space Administration, Washington, D.C.

ABSTRACT

2317/

Thermal control of the human body is analyzed for the environments obtained in spacecraft shirtsleeve cabins and extravehicular pressure suits to provide environmental design criteria applicable to extraterrestial missions. Basic heat and mass transfer correlations are used to establish dependence of the thermal processes and comfort criteria on atmospheric pressure and composition, gravity, ventilating velocity, gas temperature, humidity, and mean radiant temperature. The thermal and comfort criteria are analyzed for the lunar and zero-gravity shirtsleeve cabins. Extravehicular suit thermal control methods employing ventilation cooling, liquid-loop cooling, and radiation cooling are analyzed to determine the relative performance, limitations, and problems associated with various methods of extravehicular suit thermal control. Extravehicular suit heat balances are performed for earth orbital, lunar orbital, Mars orbital, lunar plane, and lunar crater environments.

CONTENTS

CONTENTS (Continued)

CONTENTS (Continued)

ILLUSTRATIONS

ILLUSTRATIONS (Continued)

ILLUSTRATIONS (Continued)

ILLUSTRATIONS (Continued)

ILLUSTRATIONS (Continued)

TABLES

NOMENCLATURE

A	Area, sq ft
A_v	Ventilating flow area, sq ft
C	Fraction of maximum evaporative capacity
CLO	Clothing heat transfer resistance; 1 CLO = 0.88 sq ft-^{0}F-hr/Btu
C_p	Specific heat, Btu/lb-^{0}F
D_h	Hydraulic diameter, ft
D	Diffusion coefficient, ft^2/hr
E	Heat or mass transfer effectiveness
F	Gray body view factor
Gr	Grashof number, dimensionless
H	Mass ratio, lb/lb of pure ventilating gas
L	Characteristic length, ft
L	Clothing thickness, ft
M	Metabolic rate, Btu/hr
Nu	Nasselt number, dimensionless
P	Total pressure, psia, and partial pressure, psia
Pr	Prandtl number, $(C_p\mu/k)$ dimensionless
Q	Heat transfer rate, Btu/hr
R	Gas constant, ft lb/lb-^{0}F
Re	Reynolds number, dimensionless
Sc	Schmidt number, $\mu/\rho D$, dimensionless
T	Temperature, ^{0}F or ^{0}R
V	Velocity, ft/min
W	Power, watts

d	Diameter, ft
g	Fraction of earth gravity
h	Heat transfer coefficient, Btu/hr-ft^2-^{0}F
h_D	Mass transfer coefficient, ft/hr
h_{fg}	Heat of vaporization, Btu/lb
k	Thermal conductivity, Btu/hr-ft-^{0}F
m_w	Mole fraction water vapor
$\dot{m}$	Mass flow, lb/hr
$\dot{q}$	Volume flow, cfm
t	Time, hr
x	Distance, ft
α	Solar absorptivity
γ	Angular position in orbit, degrees
ε	Thermal emissivity
η_f	Fan efficiency
σ	Stefan-Boltzmann constant
σ_d	Density ratio = $\rho/0.0765$
μ	Viscosity, lb/hr-ft
ρ	Density, lb/ft^3
ϕ	Orbital inclination relative to solar radiation, degrees
ω	Angular position around body, degrees

Subscripts

a	Atmosphere
b	Body, suit

Subscripts (Continued)

c	Clothing, convection
i	In
l	Latent
o	Out
r	Radiation
s	Skin
w	Wall

SECTION I

INTRODUCTION AND SUMMARY

This document reports and summarizes a study program concerned with the heat transfer mechanism involved in cooling the human body in space and lunar environments. The work described was performed under NASA Contract NASW-1015.

In lunar and space missions, if man is to function optimally, he must be maintained in a comfortable environment that provides a suitable thermal balance. This does not mean that it is essential to provide in space an exact duplication of man's terrestrial environment, for it is evident that man can adapt satisfactorily to a fairly wide range of environmental conditions without detectable degradation of his performance. Providing a comfortable environment does require, however, that the heat removal from the body be accomplished at temperature levels that are acceptable from the standpoint of comfort and physiological needs.

In summary, space environments impose the following unique problems in cooling of the human body:

Heat transfer constraints - The heat transfer modes that operate in a normal terrestrial environment may be eliminated or impaired in space or lunar environments. For example, the natural convective heat transfer mode important in a normal earth environment is essentially eliminated at reduced gravity. Also, the radiative heat transfer mode may not be available when the body is encased in a thermally insulated space suit or in a cabin with wall temperature approaching skin temperature. In addition, the effectiveness of ventilating gas flow may be reduced with lowered ambient pressure. (Most spacecraft missions anticipate use of cabin pressures less than 14.7 psia.)

High metabolic rates - The high metabolic rates that may obtain while work is being performed in pressurized suits and/or in low-traction environments will complicate the cooling problem. Estimates of the effect of low-traction environments on the metabolic rate are somewhat speculative at present, although there is evidence that the metabolic rate will be significantly increased for performance of a given task at reduced gravity.

Thermal adequacy- The combination of high metabolic rates and the reduced heat rejection rates results in the problem of providing adequate cooling, particularly where ventilation serves as the primary means of cooling with the crew in pressure suits.

Physiological stress - Because of the reduction of certain modes of heat rejection from the body in spacecraft environments, there will be a tendency for the attainment of high sweat rates and high body temperatures in both the shirtsleeve and pressure-suit environments. High sweat rates are undesirable from both a comfort and a physiological standpoint, but may be unavoidable under certain conditions. There is some indication

of a serious problem in providing an adequate water intake under the conditions of high average latent heat loads to avoid dehydration of the body. Reduction in sweat rates to the minimum level (insensible perspiration) appears to be highly desirable, but may not be possible in practice. It is important that, whatever the design sweat rate, the environment provide adequate evaporative cooling capacity for removal of the moisture from the surface of the body at acceptable body temperature levels. If the environment requires attainment of high body temperatures during normal operation, the safety margin represented by heat storage capability available for emergency conditions will be correspondingly reduced. That is, from the standpoint of both comfort and safety, it is highly undesirable to operate near the limits of human tolerances.

Definition of comfort zone - The conventional ASHRAE comfort zone criteria are not necessarily applicable to space systems, because different heat transfer processes may predominate in cooling of the human body. Therefore, it will be necessary to establish system design criteria applicable to reduced ambient pressures, reduced gravity, and pressure suits.

The approach to solution of these problems used in this study involved analysis of the human body heat transfer and thermal control processes for the environmental conditions encountered in space missions. This has involved study of the relevant data applicable to a terrestrial environment in order to determine the interrelationships between the controlling temperature parameters and the heat transfer mechanisms. Fundamental heat transfer correlations were then examined to estimate the effects of such environmental factors as atmospheric composition, temperature and pressure, environmental wall temperature, ventilating gas velocity, and gravity. The study considered the function of the heat transfer mechanisms (1) in both shirtsleeve and pressure-suit environments, (2) under reduced (zero to 1/6 g) gravitational fields, (3) under reduced (3.5 to 14.7 psia) ambient pressures, and (4) for metabolic rates corresponding to activities ranging from rest to high work rates. The environmental criteria were then formulated from heat balances for the body, considering the available latent and sensible cooling capacity of the environment within the limitations imposed by comfort considerations. The comfort criteria developed in the study were based upon maintenance of skin temperatures and sweat rates within specified ranges determined from physiological investigations.

The design criteria for the shirtsleeeve environment in lunar and spacecraft cabins have been determined in terms of the ventilating gas flow and environmental temperatures tradeoffs for various atmospheric pressures and compositions.

Environmental control of the body in a pressure suit environment has been studied for ventilation, liquid-loop, conduction, and radiation cooling methods. Availble test data have been analyzed and correlated to provide the basis for performance estimates.

Extravehicular suit heat balances were analyzed for orbits about the earth, the moon, and Mars, for the surfaces of the moon and Mars, and for the lunar crater environment by means of computer programs which are given in the Appendixes to this report.

SECTION 2

LITERATURE SURVEY

INTRODUCTION

This section of the report is devoted to a survey of the available literature applicable to the problem of providing man with a suitable thermal environment in extraterrestrial ambients. This has involved compiling information concerning: (1) man's physiological requirements with respect to thermal regulation and acceptable temperature levels and transfer rates; (2) the metabolic rates that can be expected in confined quarters, reduced gravity, and pressurized suits; (3) human comfort criteria applicable to spacecraft environments; and (4) internal and external heat balances for pressure and extravehicular suits in various space environments.

PHYSIOLOGICAL CHARACTERISTICS OF MAN

General

Analysis of the energy transfer processes between man and his environment, (and critical evaluation of the generality of the various comfort criteria summarized in the following section) requires awareness of the physiological mechanisms by which man responds to his thermal environment. The physiological parameters related to human thermal comfort are sweat rate, skin surface temperature, and body internal temperature; only small changes in the latter two can be tolerated without discomfort. Some latent heat rejection by evaporation occurs due to respiratory water loss, but most occurs at the skin surface, where water is deposited by the sweat glands and by diffusion of water through the skin. The remaining energy, termed sensible heat, is transported from the deep body tissues to the skin by the flow of blood and then transferred to the atmosphere by a combination of convection and radiation heat transfer.

Energy Balance for Body

Man normally dissipates waste heat by a combination of heat transfer processes including natural convection, forced convection, radiation, conduction, and evaporation of moisture. The heat balance for the body is given by

$$Q_{metabolic} = Q_{work} + Q_{latent} + Q_{sensible} + Q_{stored} \qquad (2\text{-}1)$$

Any deficit in cooling is accompanied by heat storage, an undesirable condition that can be tolerated for only a limited time. Although heat storage in limited amounts can be tolerated before physical collapse occurs, it will be assumed to be intolerable for a normal steady-state operating condition. That is, the condition for thermal adequacy requires zero heat storage for normal operation.

The thermal adequacy criterion requires the attainment of a heat balance for the body (without heat storage) at temperature levels consistent with the interrelated factors of comfort, physiology, and minimum sweat rate. These factors will be considered subsequently.

Heat Storage Limit

The body heat storage rate is usually estimated as a function of the change in the weighted average of skin and rectal temperatures, as follows:

$$Q_{stored} = 0.83\ W \frac{d}{dt} (T_{body}) \qquad (2\text{-}2)$$

where W = body mass, lb

$$T_{body} = \frac{1}{3} T_{skin} + \frac{2}{3} T_{rectal}$$

The average heat capacity of the body tissues is given as 0.83 Btu/lb ^{0}F in Equation (2-2). A heat storage tolerance limit of approximately 600 Btu is generally accepted for men with a body mass of 150 lb (Ref. 15). This represents a 4.6^{0}F rise in average body temperature. Because of the greater temperature increases experienced in the muscle masses during periods of high physical activity, this limit is somewhat conservative. For example, it is known that rise in temperature of the muscles, representing about 43 percent of the mass of the body, will be approximately 400 percent of the rise in rectal temperature. This factor would indicate a heat storage tolerance of approximately 1000 Btu for the same increase in rectal and skin temperatures as would correspond to the previously cited 600 Btu limit. Recent pressure suit heat balance studies by Wortz et al. (Ref. 30) appear to justify a 1000-Btu heat storage limit for exercising subjects. In addition, it should be noted that the different heat storage characteristics of various areas of the body may be important in analyzing and interpreting apparently anomalous data sometimes obtained in suit tests.

Work Output

The portion of the metabolic rate appearing as external work output will vary with the nature of the task and the work level. It has been found that the mechanical efficiency for performance of a given task remains relatively constant, although the work capacity will vary greatly with different individuals.

The concepts of positive and negative work are important in evaluating man's energy requirements. Negative work, which is represented, for example, by lowering a weight in a gravitational field, is accomplished at a lower energy expenditure than the positive work required for the equivalent reverse action. Thus, walking downhill or downstairs requires significantly less energy than walking uphill or upstairs. The metabolic energy cost, above resting values, for performance of negative work has been found to be from 19 to 42 percent of that for performance of the equivalent positive work.

Figure 2-1 shows the external work output as a function of metabolic rate for: (1) exercising on a bicycle ergometer in light clothing (Ref. 5);

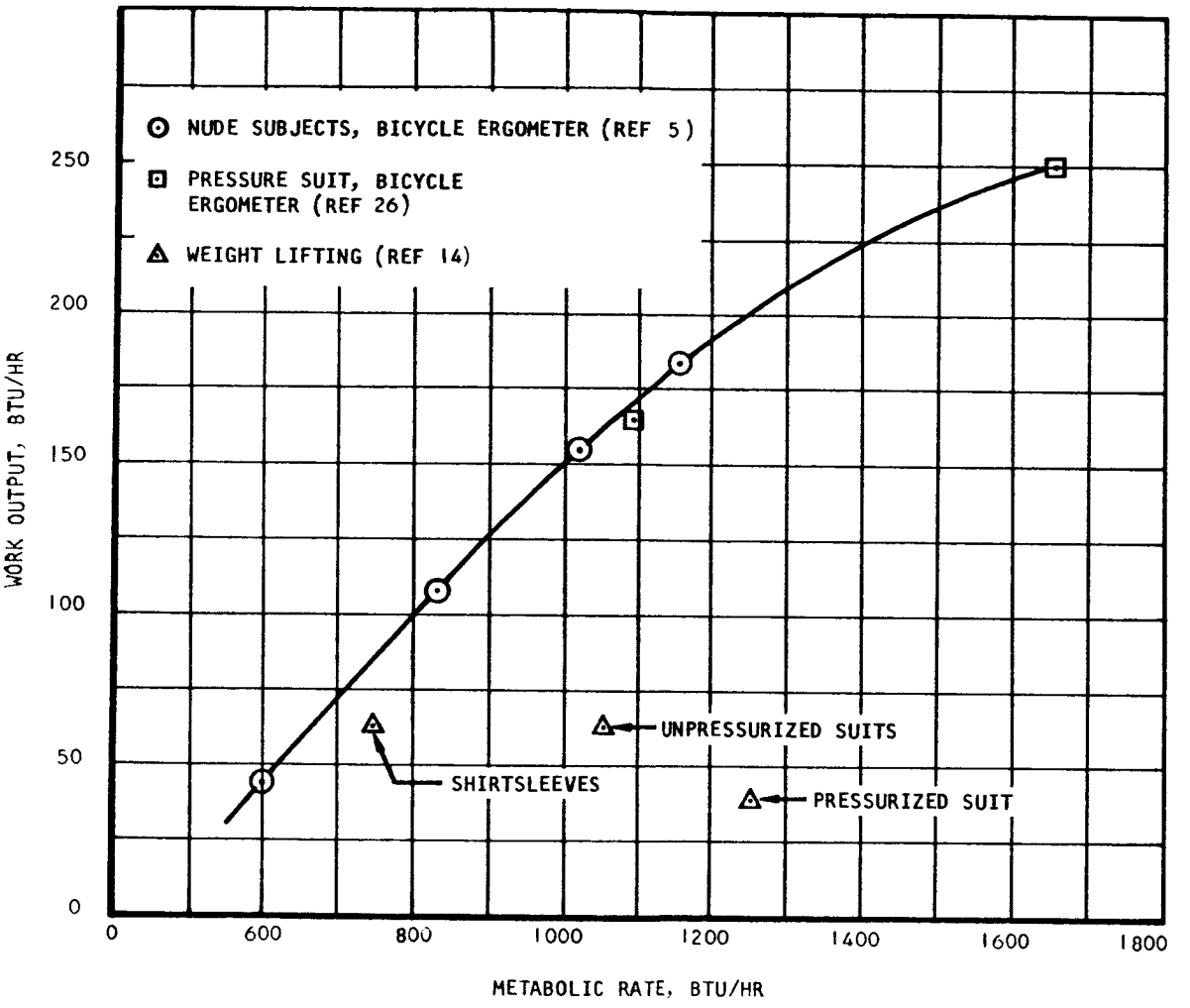

Figure 2-1. Work Output vs Metabolic Rate

(2) exercising on a bicycle ergometer in an unpressurized prototype Apollo suit (Ref. 26); and (3) exercising with lifting-weights on a wall exerciser (Ref. 14). In all of these cases, the external work output can be measured directly. However, in the case of tasks such as walking on a horizontal plane, estimating the work output for purposes of design energy balances will be more difficult, since it cannot be measured directly. As a consequence, it appears that for the task of walking in a pressurized suit on the lunar surface, it will be necessary to neglect work output in formulation of the heat balances for body cooling. Because of the increase in metabolic rates due to working in pressurized suits, it appears that it will not be conservative to make any allowance for work output in formulation of the energy balances for the performance of other extravehicular tasks, since a significant part of the increased energy input will be expended in moving the suit.

Evaporative Cooling

The evaporative cooling capacity of the environment will be an important factor in establishing human comfort conditions. Correlations of experimental data for evaporative cooling capacity have been prepared by different investigators.

Assuming the body to be totally wet, the following expression has been given for the maximum evaporative cooling rate of a nude body (Ref. 15).

$$Q_{\ell max} = 0.0408 \sqrt{\frac{T_a V\rho}{536}} \; A \; (P_s - P_a)_{H_2O} \text{ Btu/hr} \qquad (2\text{-}3)$$

The expression $(P_s - P_a)_{H_2O}$ represents the difference in water vapor partial pressure between the evaporative surface (skin) and the ambient. The case of a completely wet body will be obtained only under thermal stress conditions and in humid environments. Also, clothing could significantly reduce the maximum evaporative cooling of the body to be obtained in a given situation. From the comfort standpoint as well as from the physiological standpoint, it is not desirable to approach the evaporative cooling limit. One of the criteria to be considered in the discussion of human comfort involves as an index the ratio of the evaporative cooling required to maintain a heat balance to the maximum possible evaporative cooling.

Nelson et al. (Ref. 12) give an appropriate expression for the evaporative loss from the body, as follows:

$$Q_\ell = 0.0261 \; (V\rho)^{0.4} (P_s - P_a)_{H_2O} \; AC \text{ Btu/hr} \qquad (2\text{-}4)$$

where C represents the fraction of the body covered with sweat. The case of C = 1.0 corresponds to a maximum evaporative capacity with a fully wet body surface. The case of C = 0.1 approximates the insensible moisture loss from the body provided by diffusion of through the skin. The maximum evaporative heat loss given by Equation (2-3) is substantially greater than that expressed by Equation (2-4). The variation shown may be an indication of experimental accuracy or biological variance. As mentioned previously, the evaporative cooling capacity will provide the basis for one of the comfort design criteria

to be evolved. In subsequent sections of this report, the dependence of the evaporative cooling capacity parameter on pressure and gravity will be determined by use of established mass-transfer correlations. Both of these correlations described here are based upon experimental data for heat transfer from the human body. In the section following, the dependence of the sweat rate on the relevant temperature control parameters will be discussed.

Thermoregulatory Mechanisms

In a normal environment, man may be exposed during the course of a day's activities to a wide range of external ambients and, at the same time, may sustain considerable variation in metabolic rate. Consequently, the body has a number of provisions for thermal control that permit adaptation to a rather wide range of conditions. The purpose of the thermoregulatory system is to maintain the internal temperature of the body at a certain level, called the "set-point," which is specific for an individual. Set-point variances due to individual differences are small, falling in the range represented by 98.0 $\pm 0.5^{\circ}F$, for a number of subjects (Ref. 3). The principal thermoregulatory mechanisms available for temperature control are the following:

1. Control of blood flow to the skin

2. Control of sweat production

3. Control of metabolic heat production by shivering

One of the major heat regulating provisions of the body involves control of the blood flow to the skin, since this blood flow serves to convey heat from the internal tissues, where it is generated, to the skin, where it is dissipated. Thus, under cold conditions, the body attempts to conserve heat by reducing the flow of blood to the skin areas by constriction of the peripheral blood vessels. Under hot conditions, vasodilation and increased peripheral blood flow occur with the onset of active sweating.

The heat dissipation pathways subject to thermoregulatory control involve sensible heat transfer by radiation and convection and latent heat transfer by evaporation of moisture from the skin. The range of heat rejection rate over which thermoregulatory control is effective will be small for sensible heat transfer compared with that for latent heat transfer. For example, it can be shown that the heat rejection rate from the body by radiation and convection will normally vary with skin temperature by approximately 20 Btu/hr-$^{\circ}F$. Therefore, in going from a comfortable skin temperature of $88^{\circ}F$ to the upper limit of $98^{\circ}F$, the heat rejection rate by radiation and convection is increased by only 200 Btu/hr. As will be seen, a considerably greater range of control is available in the sweat mechanism.

At internal temperatures above the set-point, vasodilation and active sweating occur; at internal temperatures below the set-point, vasoconstriction and increased metabolism due to shivering occur. Skin temperature will modify these effects, making possible such physiological anomalies as simultaneous sweating and shivering (with a high internal temperature and a low skin temperature).

Sweat Rate

Kerslake (Ref. 7) found the sweat rate to be a linear function of the skin temperature and heat flux, as follows:

$$\frac{Q_\ell}{A} = C_1 \left(T_s - T_{so} + \frac{C_2 Q_t}{A}\right) \qquad (2\text{-}5)$$

The constants C_1 and C_2 vary somewhat with the individual; T_{so} was found to remain relatively constant at 93.9°F for several test subjects. On the basis of this functional dependence, Kerslake concluded that control of the sweat mechanism was centered in the deep skin area. The deep skin temperatures that correlated the observed sweat rates were obtained from the expression

$$T_{ds} = T_s + \frac{C_2 Q_t}{A} \qquad (2\text{-}6)$$

Thus, the constant C_2 was considered to represent the thermal resistance of the skin. The coefficient, C_1, was found to range from 10 to 17 Btu/hr-ft^2-°F while the coefficient C_2 varied from 0.065 to 0.085 °F-ft^2-hr/Btu. At a heat flux of 50 Btu/hr-ft^2, the deep skin temperature will be from 3.2 to 4.2°F higher than the skin temperature. The skin temperature will depend upon how the heat flux is to be dissipated (by sensible heat rejection or by evaporation of sweat).

In more recent work using improved experimental techniques, Benzinger (Ref. 1,2,3) found that the eccrine sweat rate is controlled by the hypothalamus and is dependent upon the cranial internal temperature only for skin temperatures above approximately 91.4°F; it is suppressed by reduced skin temperature at skin temperatures less than 91.4°F. As shown in Figure 2-2, the sweat rate is highly sensitive to internal temperature for skin temperatures above 91.4°F and internal temperatures above 98.4°F. For any given internal temperature above approximately 98.4°F, sweat rates are seen to be diminished by approximately 320 Btu/hr for every °F decrease in level of skin temperature. It will be noted that this is in agreement with the range for a similar parameter (C_2 in Equations (2-5) and (2-6) obtained in the previously cited work of Kerslake). The combination of reduced skin temperature and elevated internal temperature (produced by working in low-temperature environments) shown in Figure 2-2 would be representative of an unusual (although not impossible) environment. The more common environmental situation for active sweating would be represented by skin temperatures in excess of 91.4°F. However, the condition shown by Figure 2-2 may be representative of the situation obtained where the body is cooled directly by conduction using one of the techniques analyzed in this report.

Insensible Water Loss

The insensible water loss (which is not subject to thermoregulatory control) from the body is represented by diffusion through the skin and by water vapor content of the respiratory products. Wortz *et al.* (Ref. 18) found that the respiratory water loss varies with metabolic rate, pressure,

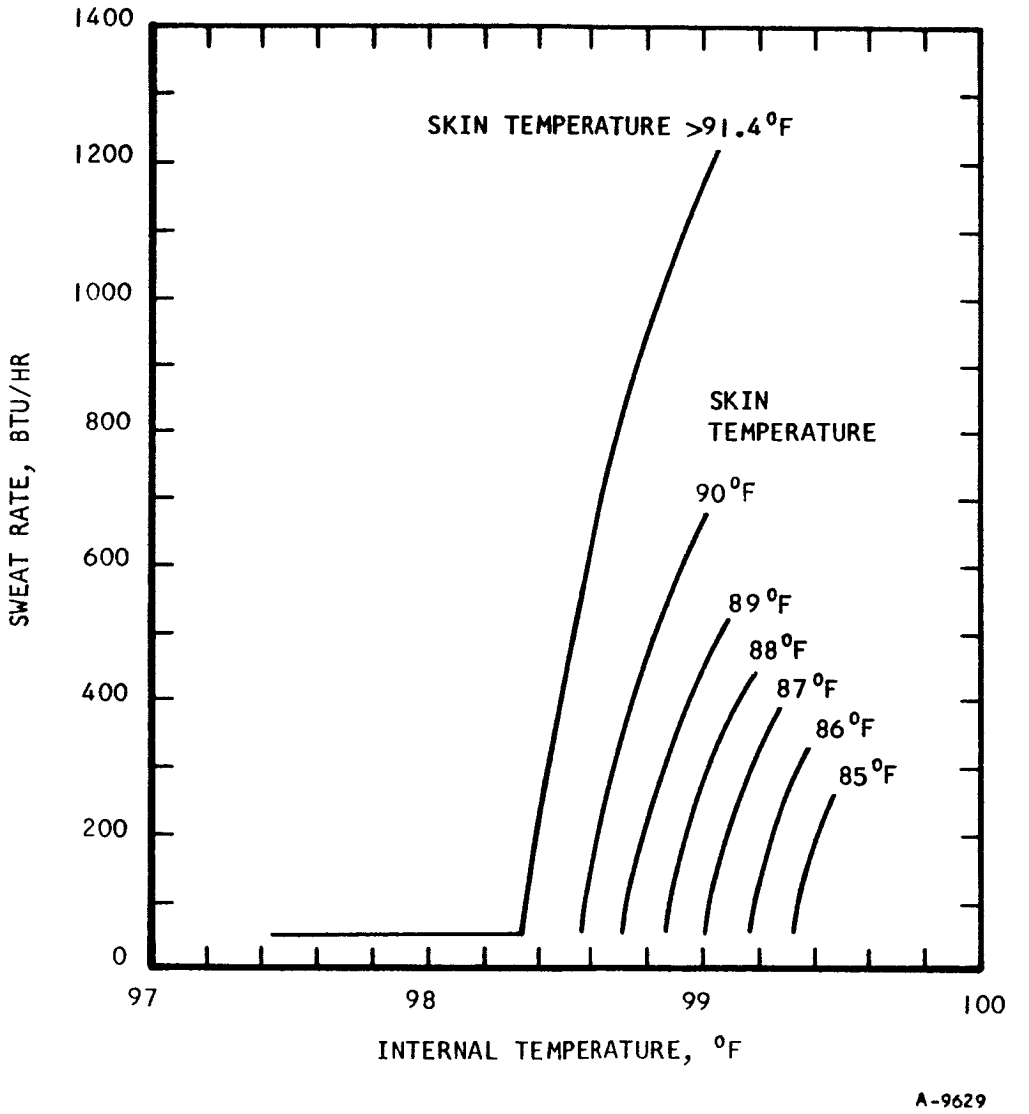

Figure 2-2. Intensity of Thermoregulatory Sweating During Cold Reception at the Skin

dry-bulb temperature, and dew-point temperature of the breathing gas. Figure 2-3 shows the respiratory water loss as a function of metabolic rate for representative environmental conditions. The insensible water vapor loss by diffusion through the skin is influenced by the vapor pressure gradient, the skin temperature, and the barometric pressure (Ref. 15). Under normal conditions with respect to skin temperature (91°F) and humidity (50°F dew-point), the insensible moisture loss by diffusion through the skin will range from approximately 0.04 lb/hr (at 14.7 psia) to 0.06 lb/hr (at 5.0 psia). Therefore, it can be shown that the minimum moisture loss from the body will vary from approximately 0.075 lb/hr to 0.10 lb/hr for a metabolic rate of 500 Btu/hr.

Skin Properties

The properties of the skin listed in Table 2-I (Ref. 15) are important in the analysis of human comfort.

The "conductance" of the body represents the heat flux dissipated by the body divided by the difference between the skin temperature and the internal temperature. The effective conductance of the body can vary over a range from 3.5 to 48 Btu/hr-ft^2-°F, depending whether vasodilation or vasoconstriction prevails.

The skin temperature and thermal sensation data listed in Table 2-I are applicable to test subjects at rest. It will be shown subsequently in the report that decreased skin temperature levels will be preferable at increased metabolic rates.

Skin Temperature

Skin temperature is primarily a function of the thermal environment of the body and the resulting heat exchanger with the ambient. Decreasing environmental temperatures result in reduced skin temperatures. Decreasing ambient pressures lead to increased skin temperatures, presumably because of the lower rates of heat transfer. On the other hand, skin temperature decreases with increasing work load because of sweating.

By analysis of human calorimetric data, Herrington (Ref. 50) was able to derive a linear first-order equation relating skin temperature to ambient air temperature, radiant temperature, metabolic heat input, and evaporative heat loss:

$$T_s = 0.286\ T_a + 0.142\ T_w + 0.0265M + 0.0232Q_\ell + 53.39 \qquad (2\text{-}7)$$

where T_s, T_a, T_w refer, respectively, to mean skin surface, air, and wall temperatures, and M and Q_ℓ to metabolism and evaporation. This expression is applicable to activities while: seated with normal clothing in a terrestrial environment; air velocities are about 10 to 20 ft/min; and the average of air and wall temperatures is between 50°F and 80°F. Because of the thermoregulatory effects represented by vasodilation and active sweating, this expression is limited to conditions where skin temperatures less than 94°F are obtained.

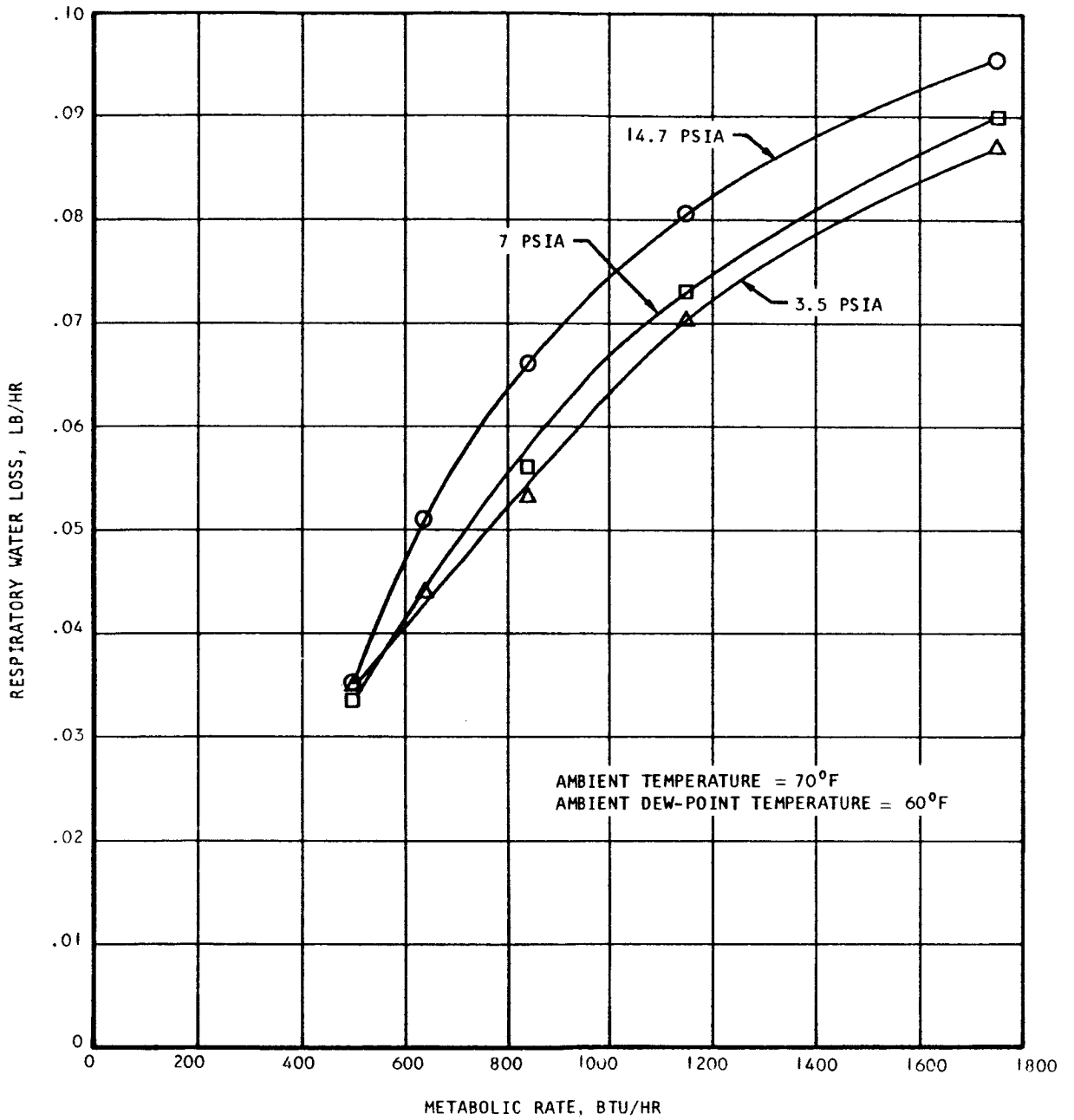

Figure 2-3. Respiratory Water Loss

TABLE 2-I

PROPERTIES OF THE SKIN (REF. 15)

Approximate values of the physical dimensions of whole skin for the "average man": 154 lb, 5'7"

Weight	8.8 lb	4 kg
Surface area	20 sq ft	1.8 m^2
Volume	3.7 qt	3.6 liters
Water content	70 - 75%	
Specific gravity	1.1	
Thickness	0.02 - 0.2 in.	0.5 - 5.0 mm

Approximate values for thermal properties of skin:

Heat production	40 Btu/hr
Conductance	3.3 to 48 Btu/ft^2-hr-^0F
Thermal conductivity (k)	(.363 ±.0726) Btu/ft-hr-^0F, at 73.4 to 77^0F ambient
Diffusivity (k/pc)	27.1 x 10^{-4} ft^2/hr (surface layer .0102 in. thick)
Thermal inertia (kpc)	13.6 to 60.5 Btu^2/ft^4-hr-^0F
Heat capacity	~0.8 Btu/lb-^0F

Skin temperature and thermal sensation:

Pain threshold for any area of skin 113^0F (45^0C)

When mean weighted skin temperature is:	The typical sensation is:
above 95^0F (35^0C)	unpleasantly warm
93^0F (34^0C)	comfortably warm
below 88^0F (31^0C)	uncomfortably cold
86^0F (30^0C)	shivering cold
84^0F (29^0C)	extremely cold

When the hands reach:	When the feet reach:	They feel:
68^0F (20^0C)	73.5^0F (23^0C)	uncomfortably cold
59^0F (15^0C)	64.5^0F (18^0C)	extremely cold
50^0F (10^0C)	55.5^0F (13^0C)	painful and numb

Approximate optical properties of skin:

Emissivity (infrared)	~0.99
Reflectance (wave-length dependent)	Maximum 0.6 to 1.1μ Minima < 0.3 and > 1.2μ
Transmittance (wave-length dependent)	Maxima 1.2, 1.7, 2.2, 6, 11μ Minima 0.5, 1.4, 1.9, 3, 7, 12μ
Solar reflectivity of surface	
Very white skin	42%
5 "white" subjects	28 - 40%, average 34%
6 "colored" subjects	19 - 24%, average 21%
Very black skin	10%
Solar penetration--very white skin	45.5% passes 0.1 mm depth 39.6% passes 0.2 mm depth 32.0% passes 0.4 mm depth 19.0% passes 1.0 mm depth 10.2% passes 2.0 mm depth
Solar penetration--very dark skin	75% passes 0.1 mm depth 40% absorbed in the melanin layer 35% passes 0.2 mm depth

By use of a combined black-globe temperature parameter replacing both the gas and wall temperatures, the equation can be used for gas velocities up to 100 ft/min. The evaporation rate, Q_ℓ, is determined by the following equation:

$$Q_\ell = 0.228\ M \tag{2-8}$$

Combination of the two equations for elimination of the evaporation rate leads to the following expression for the skin temperature:

$$T_s = 0.286\ T_a + 0.142\ T_w + 0.0318\ M + 53.39 \tag{2-9}$$

Unfortunately, Equation (2-9) is restricted to low metabolic rates, a terrestrial environment, and a fixed split between sensible and latent cooling. As a consequence, this will be of limited utility in the present study, which is concerned with high metabolic rates and an extraterrestrial environment.

It will be important to design the environmental control system to provide suitable skin temperatures because of its importance in establishing comfort. According to Kerslake (Ref. 9), a mean skin temperature of approximately 91.4°F is near optimum for resting subjects; with mean skin temperatures in excess of 94.0°F, active sweating is obtained; with mean skin temperatures less than 86.0°F, metabolic heat generation by shivering is obtained. Thus, the two limits in skin temperature can be identified, one represented by excessive sweating, the other by shivering. Within these two limits there exists the range for optimum human comfort. In the analysis of the shirtsleeve cabin, the optimum skin temperature will be assumed at 91.4°F, since the metabolic rates obtained should be those for sedentary activities. For the pressure suit environment, on the other hand, it will be necessary to consider the dependence of the skin temperature comfort zone on metabolic rate. Figure 2-4, for example, shows the variation in mean skin temperature with metabolic rate for both ventilated suits and liquid-cooled garments. Essentially no sweating is obtained in the liquid-cooled garment, whereas with the ventilated suit most of the cooling is obtained by evaporation of sweat.

Internal Temperature

As indicated previously, internal temperature is an important factor in the thermoregulation of the body. The internal temperature is to some extent a function of the external environment, but is less so than the skin temperature. Even under conditions where thermal adequacy is provided, there will be a tendency for increased internal temperature at higher metabolic rates. This is illustrated by Figure 2-5, which shows the "neutral-zone" internal temperature range as a function of metabolic rate. The neutral zone represents the conditions obtainable without thermal stress (as in a hot environment, for example). The neutral range depicted in the curve can be accounted for by individual differences and by thermal acclimatization of subjects with repeated exposures. Shown for comparison in Figure 2-5 are the internal temperatures obtained in ventilated suits and in liquid-cooled garments.

In addition to the previously described effects of internal temperature on the thermoregulatory mechanisms, there are biochemical effects, called the q_{10} effects, resulting from the temperature dependence of the chemical reaction

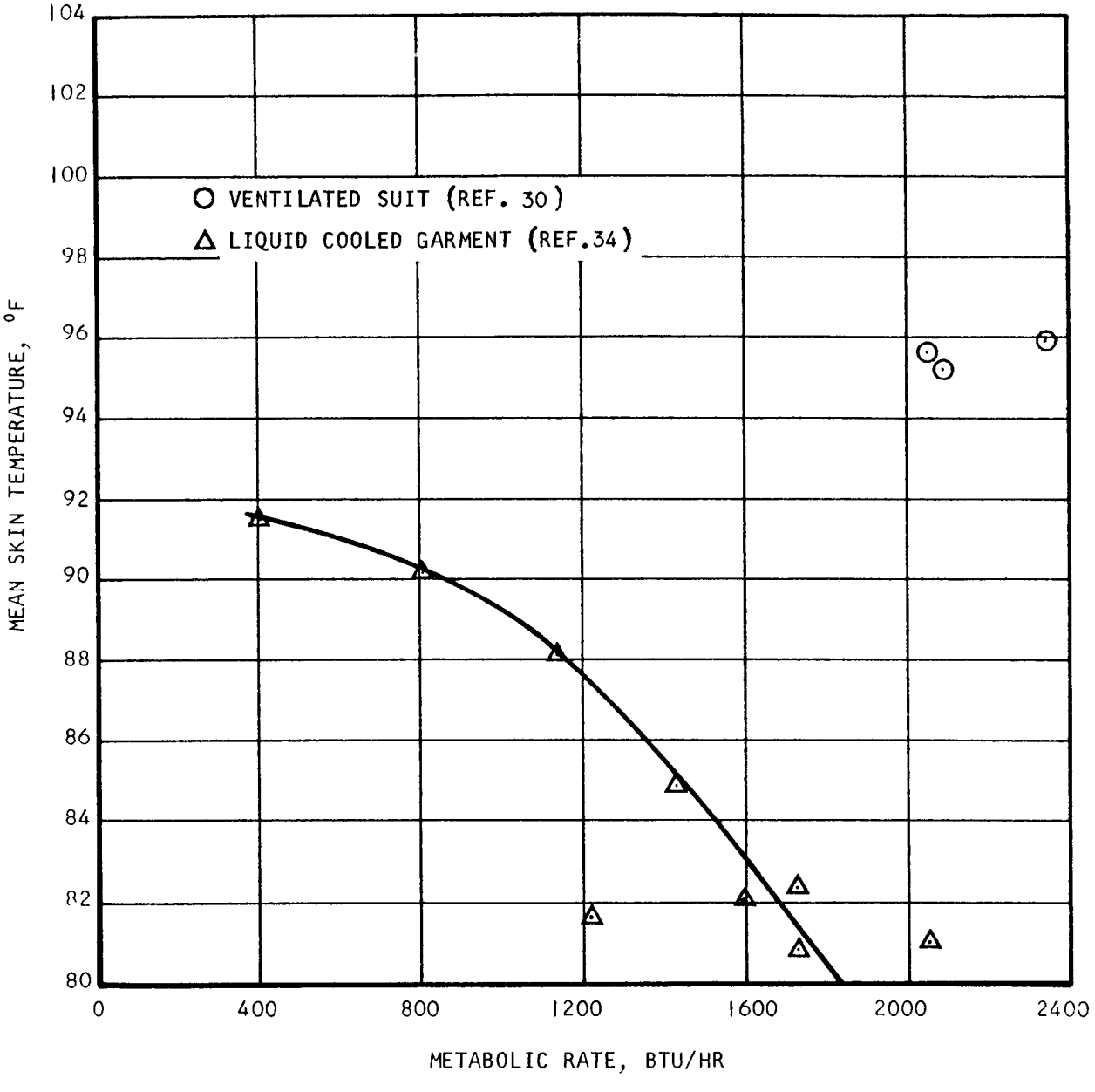

Figure 2-4. Mean Skin Temperature as a Function of Metabolic Rate

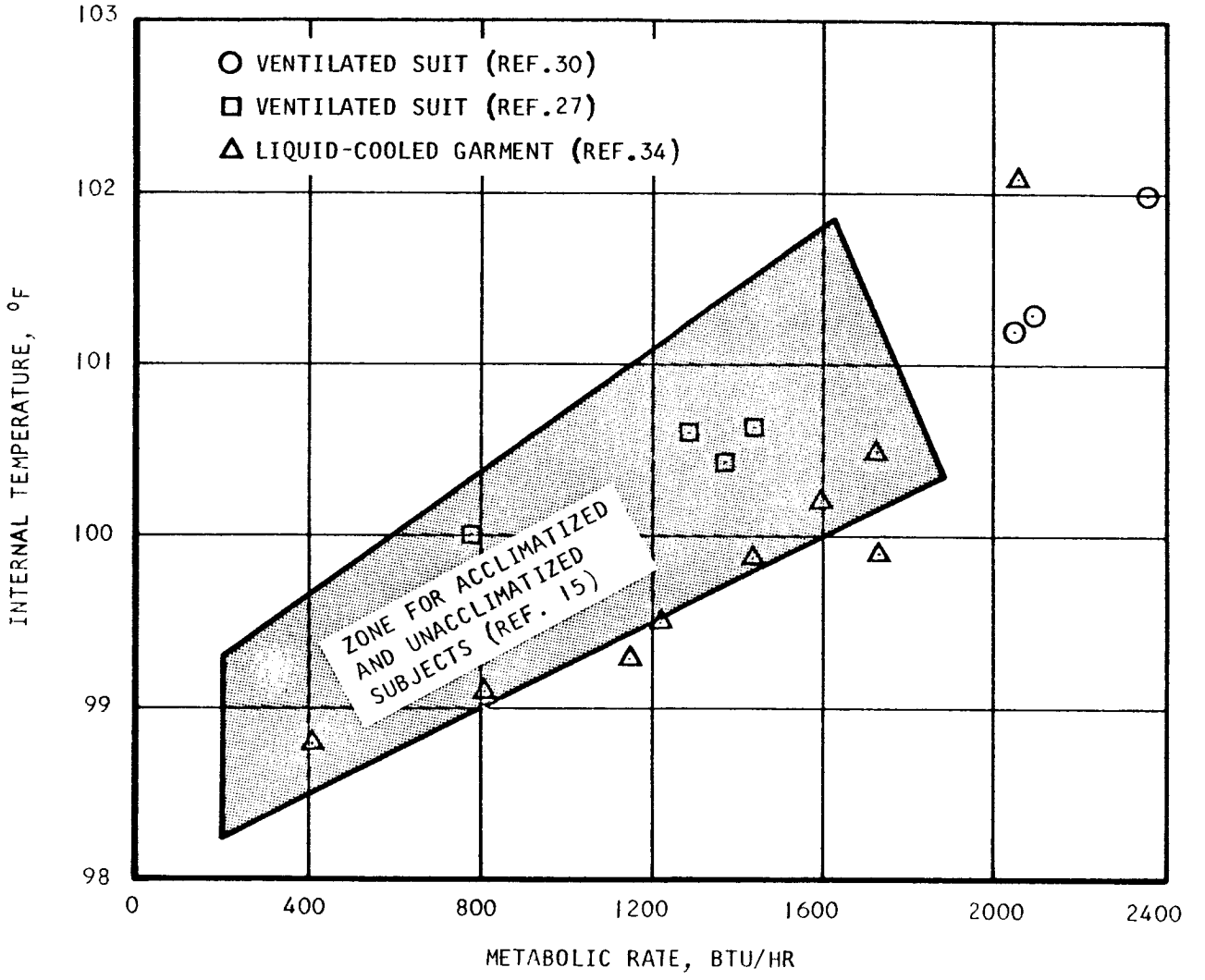

Figure 2-5. Neutral Zone Internal Temperature

rates which provide metabolic energy. That is, at temperatures above approximately 98 °F, there will be approximately a 7-percent increase in metabolic rate per °F increase in internal body temperature. Similarly, at temperatures less than about 98°F there will be a corresponding decrease in metabolic rate due to a spontaneous decrease in chemical reaction rate. The q_{10} effect is important in considering the thermal tolerance limits for human endurance. It will be noted that if the body is unable to adjust suitably to the environment, and the internal temperature falls outside the control range, the q_{10} effect operates to provide a more severe condition, by decreased metabolic heat output under cold conditions, and by increased metabolic heat output during hot conditions.

Regional Requirements

As shown in Figure 2-6, various areas of the body have differing thermal characteristics and requirements that may be important in human thermal comfort analysis. For example, Kerslake (Ref. 8) found that resting test subjects preferred temperatures varying from 83.5°F at the hands and feet to 94.2°F for the head and torso.

Provision will be required for removal of the insensible perspiration, even when the body is maintained at conditions where active sweating is not obtained. This is ordinarily accomplished by atmospheric gas flow over the surface of the body to remove the water vapor. Therefore, the areas of the body characterized by high moisture production rates will require a relatively large part of the total ventilating flow. This will be particularly important in ventilation-cooled pressure suits. The face and head areas will usually be adequately cooled by the breathing gas flow to the helmet. The groin and armpit areas present special problems in suit ventilation systems because of the high variability of the cooling requirement and the inaccessibility of these areas to the total suit flow. The palms of the hands and the soles of the feet are high sweat rate areas. The hands are difficult to cool (or heat) because of the requirement for minimum bulk in the gloves.

Means of mass removal other than ventilation could be applied to the problem of moisture removal from a pressure suit. For example, it may be possible to provide moisture removal by use of adsorbents or by diffusion through permeable membranes.

METABOLIC RATES

The metabolic rate represents the energy production rate of the body obtained by the oxidation of food. Thus, the process of metabolism is associated with production of energy, consumption of food and oxygen, and production of metabolic waste products (water, carbon dioxide, urine, and feces). Obviously, the material balance aspects of metabolism will be important to the design of spacecraft life-support systems, since these systems must have adequate capability to process the required materials. Since most of the metabolic energy will ultimately appear as waste heat, it is important that the environmental control system provide for removal of this waste heat from the body under conditions that are acceptable from the comfort and physiological standpoints.

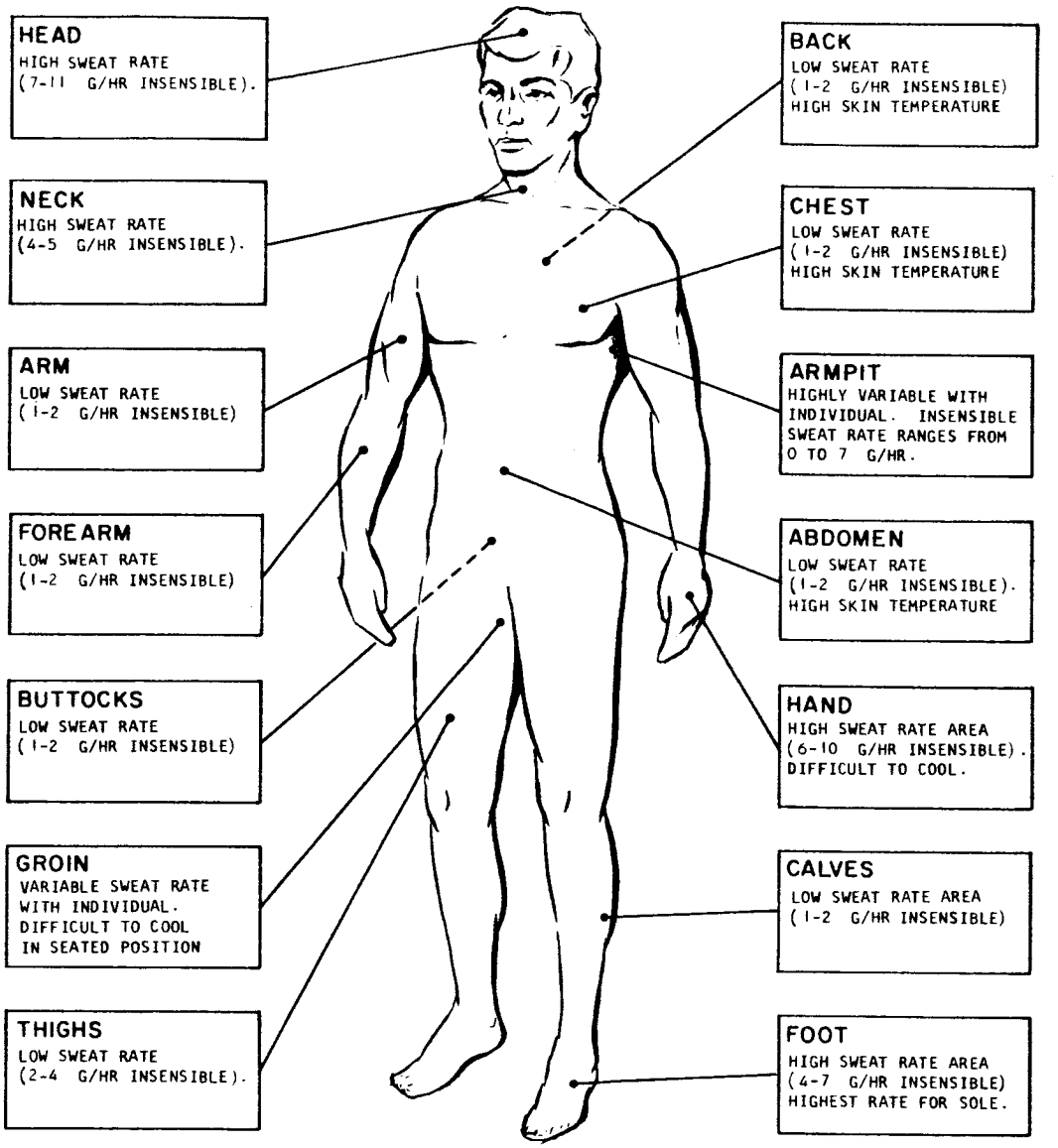

Region	Preferred temperature (^{o}F)	Heat loss Btu/hr	Area Ft^2	Skin conductance $Btu/ft^2/hr/^{o}F$
Head	94.4	15.9	2.15	1.61
Chest	94.4	32.6	1.83	3.87
Abdomen	94.4	17.9	1.29	3.02
Back	94.4	49.3	2.48	4.31
Buttocks	94.4	33.0	1.94	3.70
Thighs	91.4	47.7	3.55	1.76
Calves	87.5	58.0	2.15	2.35
Feet	83.5	39.7	1.29	1.98
Arms	91.4	33.4	1.07	4.10
Forearms	87.5	34.2	0.86	3.45
Hands	83.5	63.5	0.75	5.45

Figure 2-6. Regional Cooling Requirements of the Human Body

Metabolic rate will depend upon many factors, including, in particular, body size, activity, and body internal temperature. Table 2-2 shows metabolic rates representative of various typical activities in a normal terrestrial environment (Ref. 15). Average design metabolic rates on the order of 500 Btu/hr have been selected for the Mercury, Gemini, and Apollo spacecraft. Since the crew is restricted to rather sedentary activities in these spacecraft, use of this design metabolic rate is probably conservative. Sealed cabin experiments in space cabin simulators by Welsh et al. (Ref. 16,17) involving two men for up to 30-day durations suggest that average metabolic rates on the order of 330 to 380 Btu/hr will be obtained in space cabins.

The metabolic rates obtained on earth may be subject to considerable variation when applied to the conditions that will be obtained in spacecraft environments. The effects due to pressurized suits and reduced gravity will be discussed in the sections following:

TABLE 2-2

METABOLIC EXPENDITURE FOR TYPICAL ACTIVITIES

Activity	Metabolic Rate (Btu/hr)
Sleeping	300
Sitting at rest	400
Piloting a DC-3 in level flight	400
Writing (seated)	430
Writing (standing)	480
Instrument landing DC-4	590
Medium assembly work	680
Taxi-ing DC-3	680
Sheet metal work	760
Driving truck	790
Machining	800
Repair vehicle	820
Slow walking	900
Walking 2.5 mph on firm flat road	660-1140
Walking under water	700-1700
Walking 3.3 mph on plowed field	850
Walking in 12 to 18-in. snow	3010

Pressurized Suits

Significant increases in metabolic energy expenditure will be obtained for working in pressurized suits because of the restrictions to movement

afforded by the pressurized suit. Present extravehicular space suits represent an extension of aircraft full-pressure suits, in which the pilot is restricted in motion and limited to more-or-less sedentary activity levels, with the suit serving as a backup to the vehicle pressure shell. However, in future extravehicular space missions, greater mobility will be required, since man will perform fairly extensive physical tasks, such as walking on the lunar surface. Figure 2-7 illustrates the increase in metabolic rate obtained in state-of-the-art space suits for the task of walking on a treadmill with the suit pressurized to 3.5 psi (Ref.27,29,30).

Streimer et al. (Ref.14) report metabolic rates for walking 1.0 mph (in three different suits pressurized to 3.5 psig) of 1875, 2530, and 3150 Btu/hr as compared with the metabolic rates for walking in the same suits unpressurized of 792, 946, and 1100 Btu/hr. Walking 1.0 mph in normal clothing was found to require an average metabolic energy expenditure of 675 Btu/hr. From these data, it was observed that encasing a man in an unpressurized suit led to a 17- to 63-percent increase in metabolic rate, while pressurizing the suit results in a 178- to 367 percent increase in metabolic rate relative to walking in normal clothing. The suits used here are aircraft (Mark II and Mark IV) full-pressure suits and the data are not necessarily applicable to spacecraft extravehicular suits, although the magnitude of the increase in metabolic rate obtained in these tests is comparable to that observed for the Apollo and Gemini suits.

Relatively little information is available concerning the metabolic rates associated with performance in pressurized suits of tasks other than walking on a treadmill. Part of the problem here is in defining the nature of the activities in sufficient detail to permit development of test procedures that provide adequate simulation of the tasks to be performed. During free-space extravehicular excursions, there will be no requirement for walking; movement under zero-gravity conditions will probably be accomplished by use of the arms. Thus, it appears reasonable to assume that arm and shoulder movements will predominate for tasks such as egress through hatches, replacement of components, and repair operations. Most of the metabolic data obtained for arm and shoulder movements in pressurized suits are highly variable. For example, in one series of tests involving arm movements in a Gemini suit pressurized to 3.5 psig, the observed metabolic rates varied over a range from 600 to more than 1500 Btu/hr for performance of presumably the same operation. In this case, part of the performance spread was attributed to factors such as suit fit and personnel acclimatization, since the lowest metabolic rates were obtained by a test subject who had extensive suit testing experience and the best fit with the suit.

Streimer et al. (Ref.14) reported metabolic rates for extension/flexion cycling, using a modified wall exerciser, in pressurized suits. A 46-percent increase was obtained in metabolic rate for performance of the task in an unpressurized suit, as compared with shirtsleeves. An additional 47-percent increase was observed when the suits were pressurized to 3.5 psig. Thus, a total increase in metabolic rate of 112 percent was observed for performance of the arm exercise (with an average power output of 500 to 660 ft-lb/min) in a pressurized suit as compared with shirtsleeves.

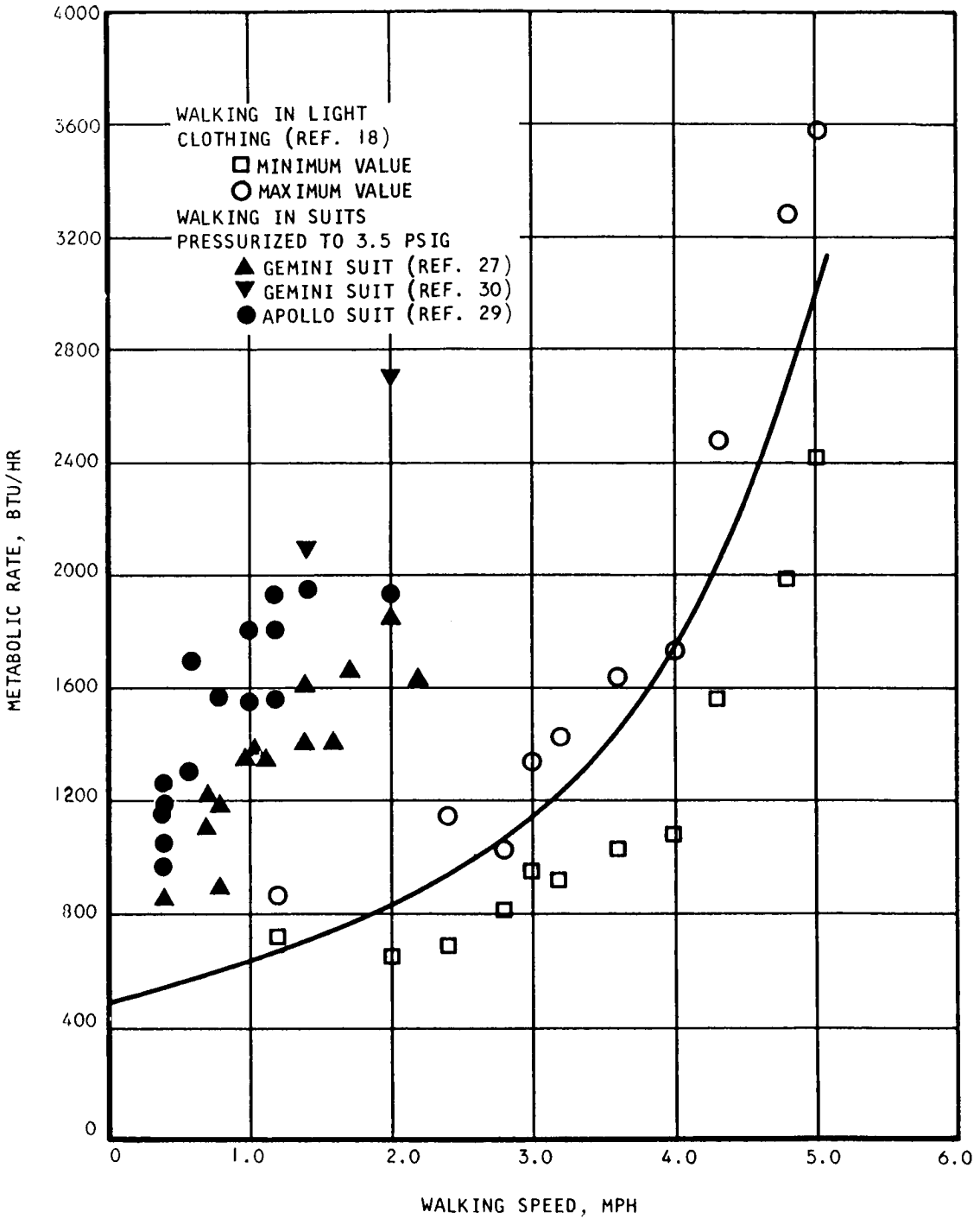

Figure 2-7. Energy Cost of Walking

Reduced Gravity

The effect of reduced gravity on metabolic rate is somewhat uncertain at the present time. It can be hypothesized that increased muscular activity will be required to provide restoring forces for body movement in reduced-traction environments. That is, it will be necessary to use muscular forces to provide restoring effects normally provided by gravity or friction. On the other hand, however, it can also be postulated that less work will be required in a weightless environment, since the body will not be working against a gravitational field, in order to maintain a standing position, for example.

Whether one effect or the other predominates would appear to depend upon the relative importance of gravitational and inertial forces. Margaria and Cavagna (Ref.11) studied the mechanism of human locomotion under subgravity conditions. Walking at 1 g is obtained by alternating conversion of potential energy into kinetic energy, with the kinetic and potential energy levels essentially out of phase. The shift from walking to running occurs at a critical speed (approximately 5.3 mph at 1 g) where the changes in kinetic energy are too high to be sustained only by changes of potential energy. In running, kinetic and potential energy are substantially in phase. Since the potential energy changes will substantially be reduced for locomotion in subgravity, the critical speed represented by transition from walking to running will be considerably lower for the lunar environment. Margaria and Cavagna conclude that locomotion on the lunar surface may not be possible by the walking mode and will probably be similar from a mechanical standpoint to the running mode. A jumping mode of locomotion is also postulated for the higher speeds. No conclusion is drawn concerning the energy requirements for the lunar environment, except for the statement that the metabolic energy expenditure will be less than that obtained at 1 g.

Lomonaco (Ref.10) reports an average 34-percent increase in metabolic rate for walking on a treadmill in light clothing with simulated reduced gravity conditions ranging from 1/2 to 1/20 g. Streimer et al. (Ref.4) observed a 12- to 15-percent increase in metabolic rate for extension/flexion cycling with the arms under simulated reduced-gravity (low-traction) conditions for the shirtsleeve and pressurized and unpressurized suit environments. In this case, one arm was used to do the work while the other arm was used to provide a counteracting force to maintain position in the low-traction environment.

On the other hand, other tests (Ref.6) indicate a reduced metabolic rate under subgravity conditions, amounting to 28-percent reduction for 2/5 g and 48-percent reduction for 1/6 g for walking on a treadmill. A recent Russian paper postulates a 30-percent decrease in metabolic rate for walking on the lunar surface. In fact, the prediction is made that walking on the lunar surface in a pressurized suit will require less metabolic energy expenditure than walking in normal clothing at 1 g. No substantiating data or analyses are presented for these conclusions.

Roth (Ref.44) presents a detailed review of the literature concerned with the mechanics of walking and concludes that an increase in metabolic rate can be expected for reduced-gravity environments.

COMFORT CRITERIA

General

A number of different indexes for human comfort have been advanced (Ref.19). The most common of these, used for the design of terrestrial air-conditioning systems, involve a comfort zone defined in terms of dry-bulb and wet-bulb temperatures. A large amount of literature is available concerning human comfort and physiology under a wide range of conditions in the earth environment. Unfortunately, because of important differences in gravity and pressure obtained in space environments, most of these data are not directly applicable to the design of spacecraft environmental control systems. The discussion here will be concerned with a critical review of different comfort criteria that have been proposed, to determine their general validity for all environments.

ASHRAE Comfort Chart

The conventional ASHRAE human comfort criterion such as that shown in Figure 2-8 is used for the design of air-conditioning systems, and is based upon data from subjects sitting at the rest in light clothing with no forced convection, and a terrestrial environment with respect to gravity, atmospheric composition, and pressure (Ref.19). The most recent ASHRAE data, noted on the chart as the lines labeled "slightly cool, comfortable," etc., show a much smaller effect of relative humidity than was indicated by the previously assumed dashed lines-of-equivalent-comfort. Figure 2-8 shows that, for the above stated conditions, a maximum number of subjects were comfortable at a dry-bulb temperature of 77°F, which is essentially independent of relative humidity. The boundaries of the comfort zone are 71.5°F, where a slightly cool sensation is reported, and 82°F, where a slightly warm sensation exists. The influence of relative humidity is shown to increase with increasing temperature. The ASHRAE Comfort Chart is applicable only for the conditions under which it was developed, but will prove useful in verifying general thermal comfort analyses.

Aircraft Environmental Limit Chart

Figure 2-9 is a chart showing the relative comfort requirements of a man and his ability to withstand various combinations of wet-bulb and dry-bulb temperatures in high-speed aircraft. In developing this figure, it was assumed that: (1) personnel are sitting and performing no more than light manual work; (2) standard temperature clothing (1 CLO) is worn; and (3) air motion is the equivalent of 200 ft/min linear velocity. The tolerance lines give the recommended maximum duration to the stated conditions. Figure 2-9 was prepared some time ago by the Air Force and does not take into account variations in the pressure or the composition of the atmosphere (Ref.24).

Dew-Point, Dry-Bulb Temperature Correlation

Since wet-bulb temperature is a function of gas density, and water vapor partial pressure is the controlling parameter in latent heat transfer, it is evident that comfort zone correlations based upon use of the wet-bulb temperature are not generally applicable to the reduced ambient pressures frequently

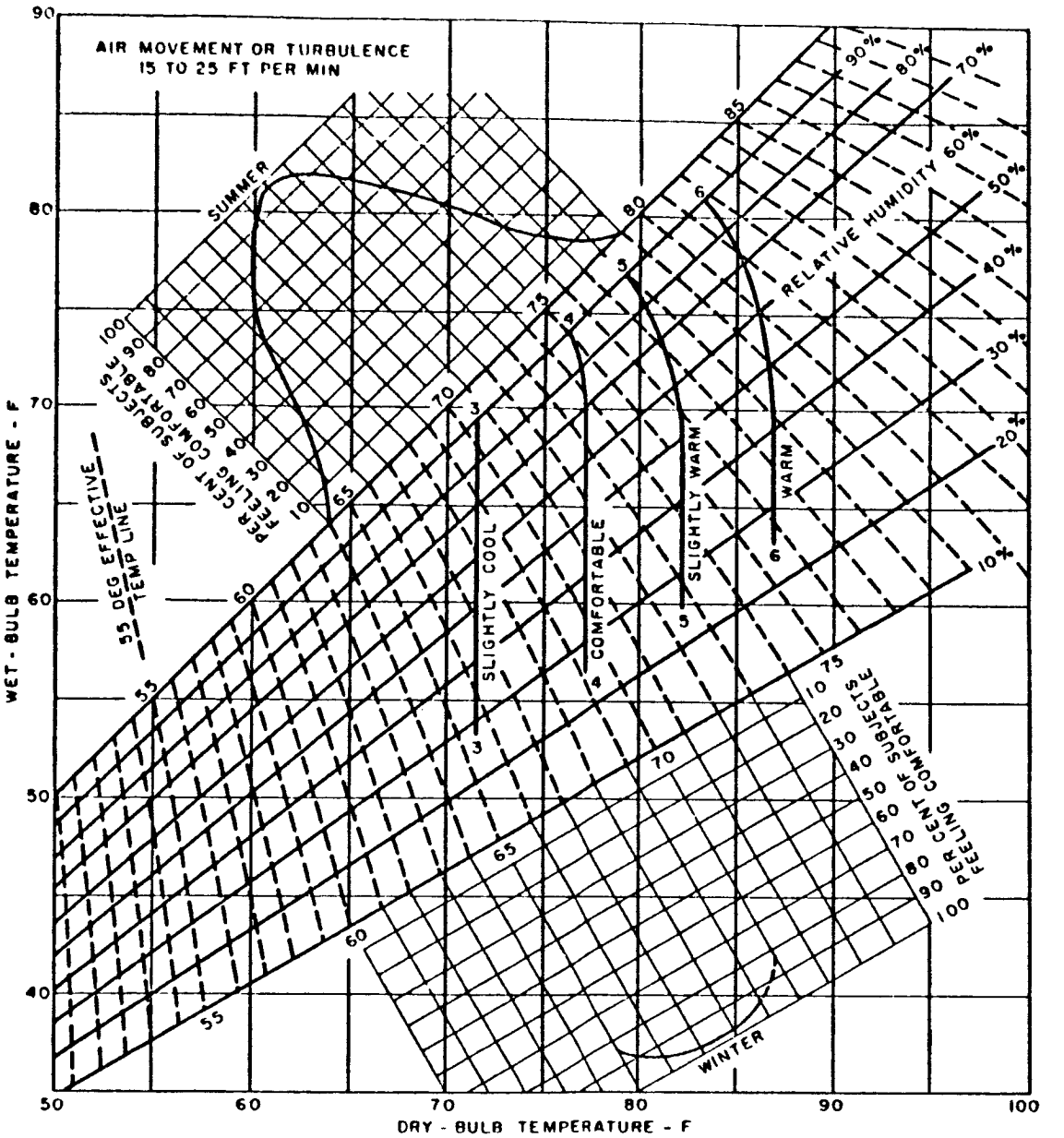

Figure 2-8. ASHRAE Comfort Chart (Ref. 19)

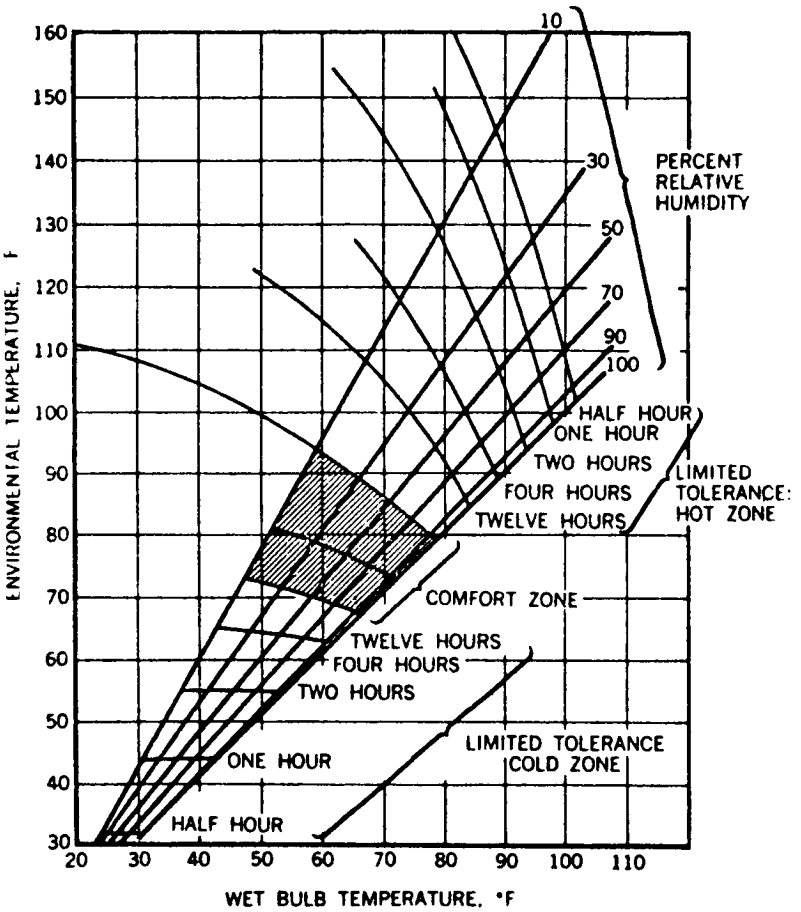

Figure 2-9. Thermal Requirements for Tolerance and Comfort in Aircraft (Ref. 24)

used in spacecraft environmental control systems. Figure 2-10 shows a somewhat more basic correlation of the unimpared performance zone as a function of dry-bulb and dew-point temperatures (Ref.21). Since dew-point temperature is a direct indication of water vapor partial pressure, this would appear to be suitable for reduced pressures. However, since the convection heat rejection rates from the body are a function of pressure and atmospheric fluid transport properties, it will not be possible to define comfort zone conditions independent of atmospheric pressure or composition. Also, the effect of reduced gravity on body cooling by the reduction or elimination of the natural convective heat transfer mode must be considered. Therefore, it appears that for a comfort zone criterion to be applicable to spacecraft environments, the correlation must consider the effect of reduced gravity, reduced pressure, and atmospheric composition on the heat rejection rates from the body.

Operative Temperature Comfort Correlation

Gagge, Rapp, and Hardy (Ref.20) describe a comfort criterion based upon a combination of the heat transfer coefficients and respective temperature potentials controlling each mode of sensible heat transfer. This relationship is derived from a simplified heat balance for the body, as follows:

$$Q = h_r(T_s - T_w) + h_c(T_s - T_a) \qquad (2\text{-}10)$$

Rearranging Equation (2-10) leads to

$$Q = \left[T_s - \frac{h_r T_w + h_c T_a}{h_r + h_c}\right](h_c + h_r) \qquad (2\text{-}11)$$

The "operative temperature," T_{op}, is defined as follows:

$$Q = (h_c + h_r)(T_s - T_{op}) \qquad (2\text{-}12)$$

Combining Equations (2-11) and (2-12), the operative temperature is then given by

$$T_{op} = \frac{h_r T_w + h_c T_a}{h_c + h_r} \qquad (2\text{-}13)$$

Therefore, T_{op} correlates the combined effects of radiation and convection cooling of the body and represents the hypothetical uniform temperature environment providing equivalent heat dissipation from the body for the same values of h_c and h_r; the difficult problem of predicting h_c and h_r remains. Comfort conditions were observed with nude subjects for operative temperatures between 85°F and 90°F using heat lamps to vary the radiation coefficient.

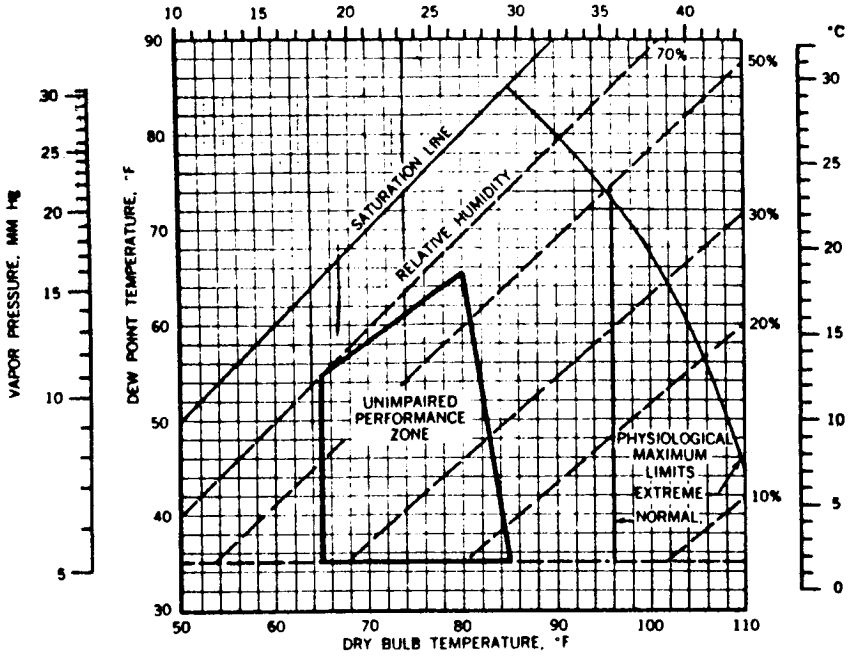

Figure 2-10. Temperature-Humidity Effects (Ref. 21)

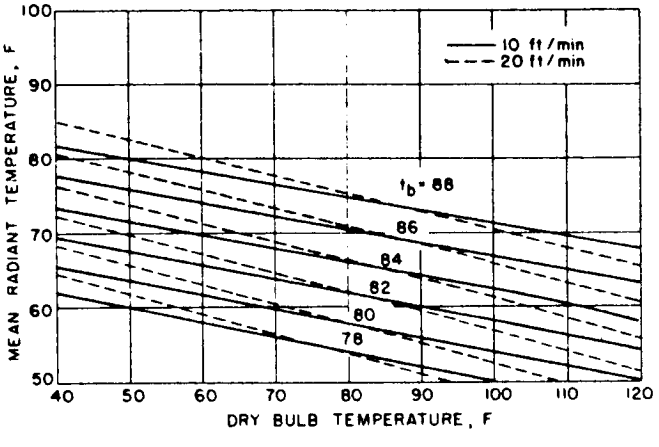

Figure 2-11. Comfort Criterion for 5.0 psia Space Cabin (Ref. 22)

Constant Skin Temperature Comfort Correlation

Jannsen (Ref.22) analyzed the sensible heat loss mechanisms from the human body obtained in a normal terrestrial environment and applied heat transfer correlations to estimate the heat rejection rates for zero-gravity shirtsleeve-environment space cabins. For radiation, the heat transfer model involved a man with an effective radiation area of 15.5 sq ft and an average thermal emissivity of 0.94. Forced-convection heat transfer was assumed to be represented by ventilating gas flow normal to a cylinder 1.0 ft in diameter with a total surface area of 19.5 sq ft. The following example expression was obtained by Jannsen for the sensible heat loss from the body in a pure oxygen atmosphere at 5.0 psia:

$$Q = 2.52\left[\left(\frac{T_c}{100}\right)^4 - \left(\frac{T_w}{100}\right)^4\right] + 0.932\, V^{0.466}\,(T_c - T_a)\ \text{Btu/hr} \qquad (2\text{-}14)$$

By determining the comfort zone conditions in terms of body surface temperature, Jannsen established a comfort design criterion for space cabins based upon maintenance of a mean body surface temperature assuming no latent heat loss. Figure 2-11 shows a thermal comfort correlation. If, for example, in a normal environment, comfort is obtained at a skin temperature of $86^{\circ}F$, a comfortable environmental temperature in a 5.0-psia cabin will be $72^{\circ}F$. This analysis does not consider the effect of the ambient environment on the latent cooling capacity. Since the evaporative cooling mechanism is not directly related to the sensible heat loss mechanism, the comfort criterion described by Jannsen is probably not sufficient without an additional factor that accounts for evaporative cooling.

Evaporative Capacity Comfort Correlation

Krantz (Ref.23) describes a comfort design criterion developed by Winslow *et al.* (Ref. 25) based upon the percentage of utilization of the maximum evaporative cooling capacity of the body. It was found that, on the hot side of comfortable conditions, sweat production was definitely related to the sensation of discomfort; on the cold side, skin temperatures below $90^{\circ}F$ produced a cool feeling. The maximum evaporative cooling capacity occurs when the body is completely covered with moisture. The sensation of comfort was related by Winslow *et al.* to the percentage of the body covered by moisture, as summarized in Table 2-3.

Approximately 10 percent of the maximum evaporative capacity was provided by insensible moisture loss from the body by respiration and by diffusion through the skin. Hence, this moisture loss is not subject to thermoregulatory control, and an indicated evaporative cooling requirement less than this amount represents overcooling of the body. The comfort design method described by Krantz involves analysis of the environmental conditions to estimate the sensible heat loss from the body. The metabolic rate is estimated for the activity level to be sustained. The difference between the metabolic rate and the sensible heat loss, therefore, is the required evaporative cooling. The environmental design conditions are then evaluated with respect to the maximum evaporative cooling capacity; if the required evaporative cooling represents from 10 to 25 percent of the maximum, the environment is in the

TABLE 2-3

EVAPORATIVE CAPACITY COMFORT CRITERION (REF. 25)

Percent of Maximum Evaporative Capacity	Comfort Level
0 to 10	Cold
10 to 25	Comfortable
25 to 70	Tolerable
70 to 100	Hot
Over 100	Dangerous

comfortable range. If it is outside this range, some of the environmental design factors (gas temperature, ventilating gas velocity, or wall temperature) should be changed to provide a comfortable environment. This comfort criterion accounts for all the important parameters and is applicable to all environments once general equations for estimating the various heat loss terms are developed.

Figures 2-12 and 2-13 show the maximum evaporative capacity given by Krantz (Ref. 23) for a normal terrestrial environment. The source or basis for these data is not discussed, although the values listed appear to be consistent with those of Nelson et al. (Ref. 12) with an allowance for natural convection.

This approach will be adapted in a modified form to the problem of defining comfort conditions for space environments. The sensible heat removal processes will be corrected for reduced pressure and reduced gravity through use of heat transfer correlations applicable to the specific process (forced convection, natural convection, radiation) The maximum evaporative capacity criteria can be corrected for reduced pressure and zero gravity by use of mass transfer correlations. For the case of lunar gravity and the shirtsleeve cabin, an additional correction representing natural convection at 1/6 g will be added to the evaporative capacity.

Suit Ventilation Cooling

Perhaps more critical than the high work rates are the problems associated with cooling the man in a space suit at the high metabolic rates Present space suits represent an extension of aircraft full-pressure suits using ventilation cooling. Because of the availability of high-pressure cooled bleed air from the aircraft air-conditioning system, pressure drop of the suit ventilating gas circuit is relatively noncritical in aircraft pressure suits. In the case of space systems, the ventilating gas is recirculated after purification in an atmospheric control system Because of the high power penalties, suit pressure drop is important. As a consequence, must of the development effort associated with the Project Mercury suit involved improvement of the suit internal ventilating system to reduce ventilating gas pressure drop. Figure 2-14 illustrates the improvement that has been made in the Mercury, Gemini, and Apollo suits, compared with the Mark IV suit

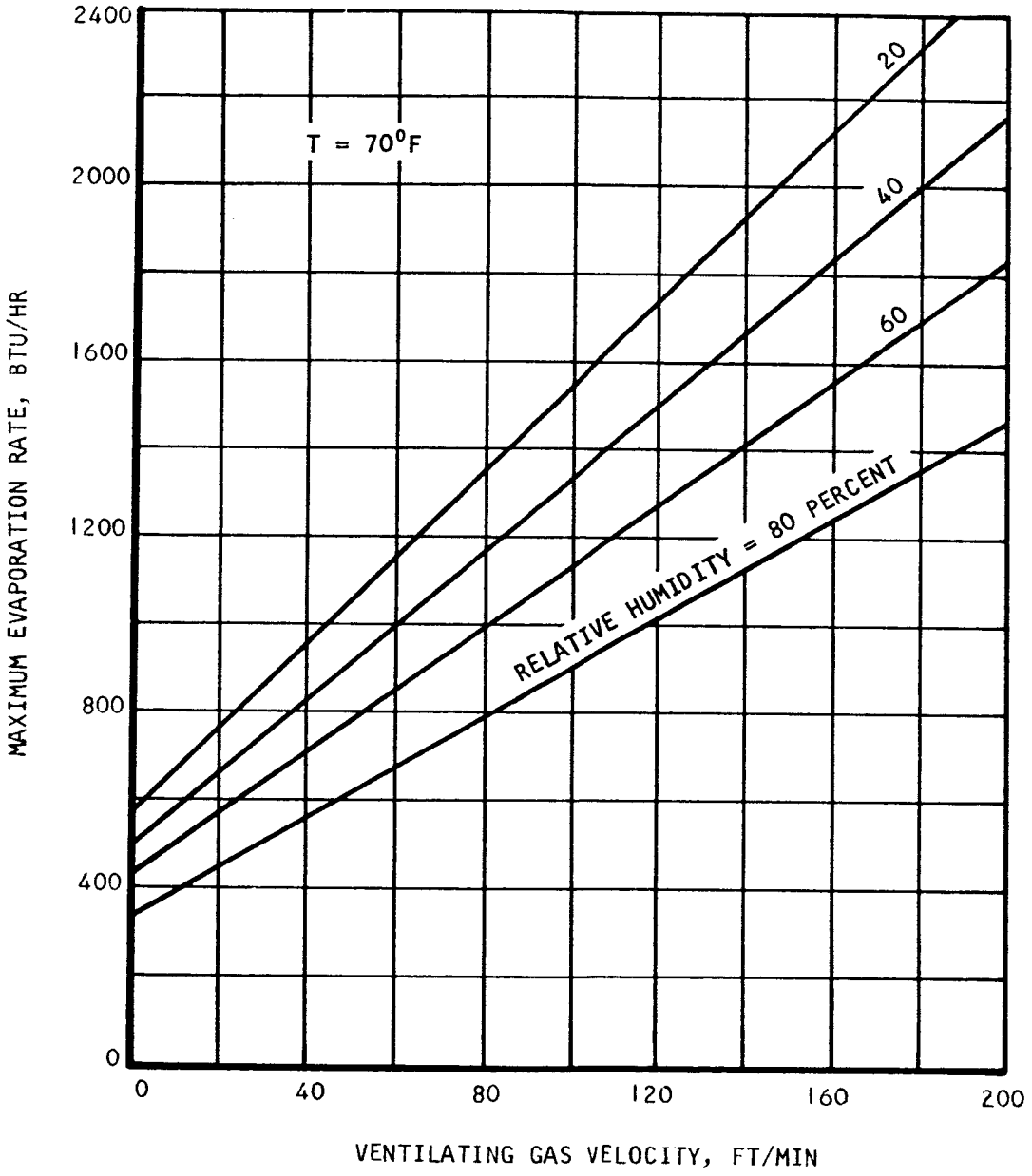

Figure 2-12. Maximum Evaporative Cooling Capacity vs Ventilating Gas Velocity

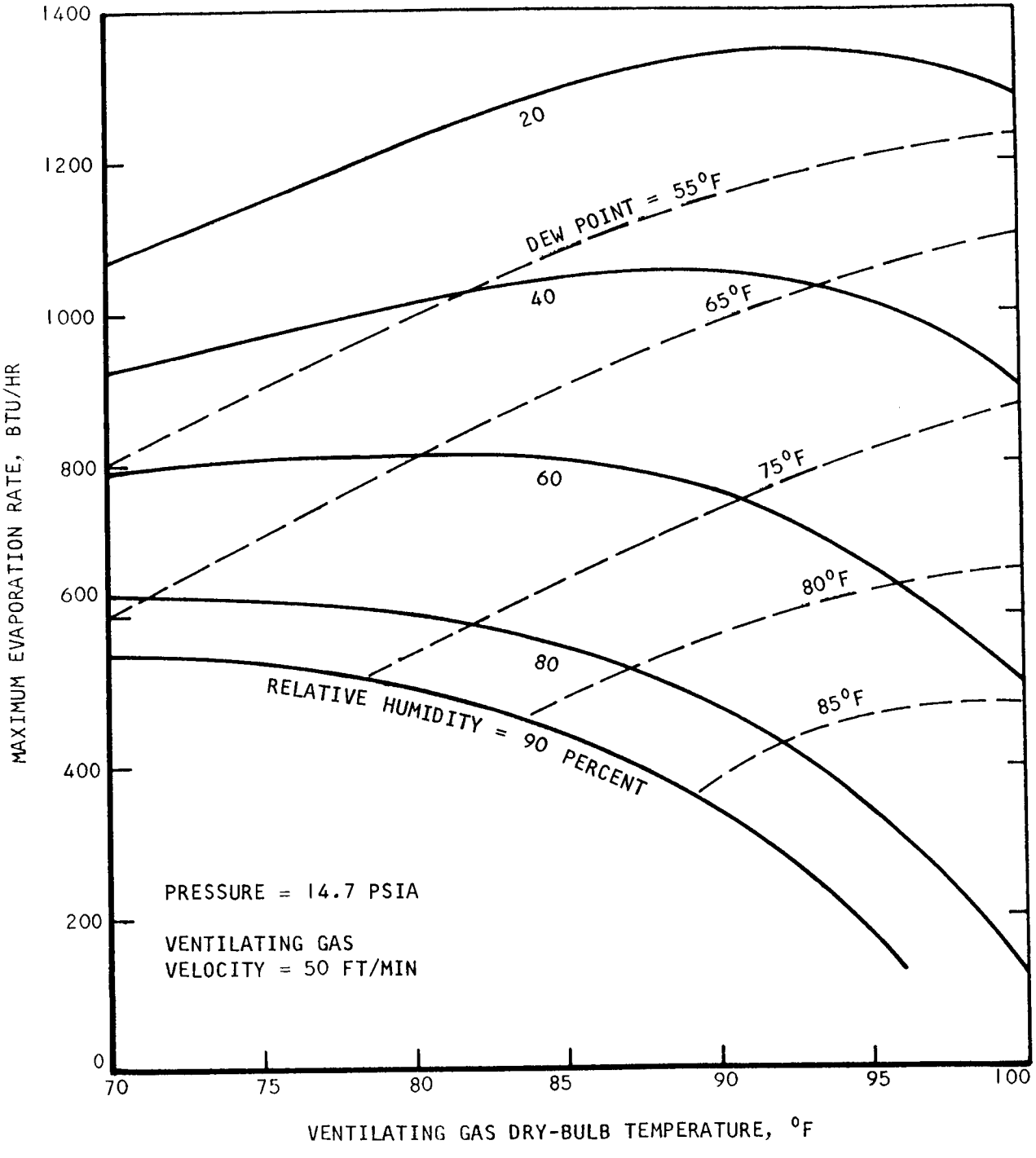

Figure 2-13. Maximum Evaporative Cooling Capacity vs Dry-Bulb Temperature (Ventilating Gas Velocity = 50 Ft/Min)

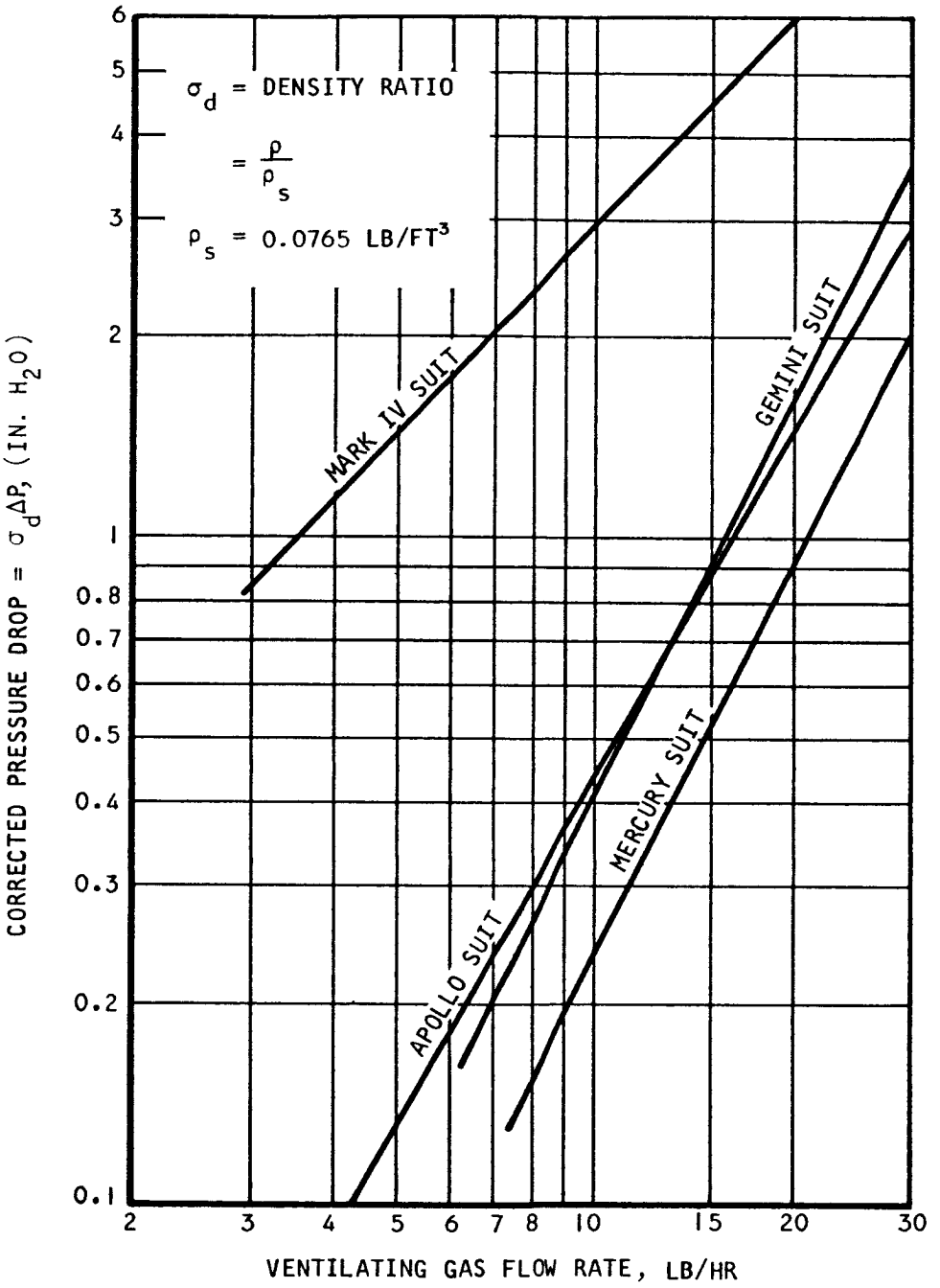

Figure 2-14. Suit Ventilating Flow Pressure Drop Correlation

There has been some question concerning the adequacy of ventilation cooling at high metabolic rates, based upon the first suit heat balance studies, in which the heat loss by radiation has been reduced to a low value by use of an efficient thermal insulating garment (Ref.29). The results of these studies are summarized in Figure 2-15 for the case of 15-cfm ventilating flow with the suit pressurized to 3.5 psi at altitude. At a metabolic rate of 1600 Btu/hr, the cooling deficit and indicated heat storage is probably in excess of 400 Btu/hr (with suit pressurized to 3.5 psig at a chamber pressure of 3.5 psia). Since the actual cooling provided by the ventilating gas loop averages about 900 Btu/hr for a metabolic rate of 1600 Btu/hr (which is measured independently from the heat balance by spirometer techniques), the cooling deficit could run as high as 700 Btu/hr, depending upon work output and efficiency. Figure 2-16 shows the results of pressurized suit tests conducted at sea-level ambient pressure with a suit ventilating flow of 15 cfm. In this case, an average heat removal rate of 1000 Btu/hr was obtained for a metabolic rate of 1600 Btu/hr. Comparison of Figures 2-15 and 2-16 suggests that tests at sea level could be misleading in determining the thermal adequacy of a system designed to operate at reduced pressures.

Albright (Ref.26) presents ventilating test data for an unpressurized Apollo prototype suit in which metabolic rates of 1080 and 1655 Btu/hr were produced by a bicycle ergometer. Table 2-4 summarizes the energy balance for the two test conditions (one test subject):

TABLE 2-4

APOLLO PROTOTYPE SUIT VENTILATING TEST RESULTS (REF.26)

	Condition 1	Condition 2
Metabolic output	1655 Btu/hr	1088 Btu/hr
Body heat loss	0	167
	1655 Btu/hr	1255 Btu/hr
Sensible heat removal	149 Btu/hr	121 Btu/hr
Latent heat removal	1292	956
Loss to ambient	-50	-50
Mechanical work	250	167
Heat removed	1641 Btu/hr	1194 Btu/hr

The heat removal rates reported by Albright were obtained at a ventilating gas flow rate of 15 cfm and a total pressure of 3.75 psia. In other tests, the heat removal rates were somewhat (10 to 15 percent) less, with little or no increase in cooling capacity obtained for ventilating flows in excess of approximately 15 cfm (shown in Figure 2-17). It should be noted that the ventilating performance given by Albright is somewhat better (with no indication of heat storage) than that reported by other investigators. The difference may be explained by variations in test conditions or test subjects, or, possibly, by modifications in the Apollo suit design for improved ventilating performance.

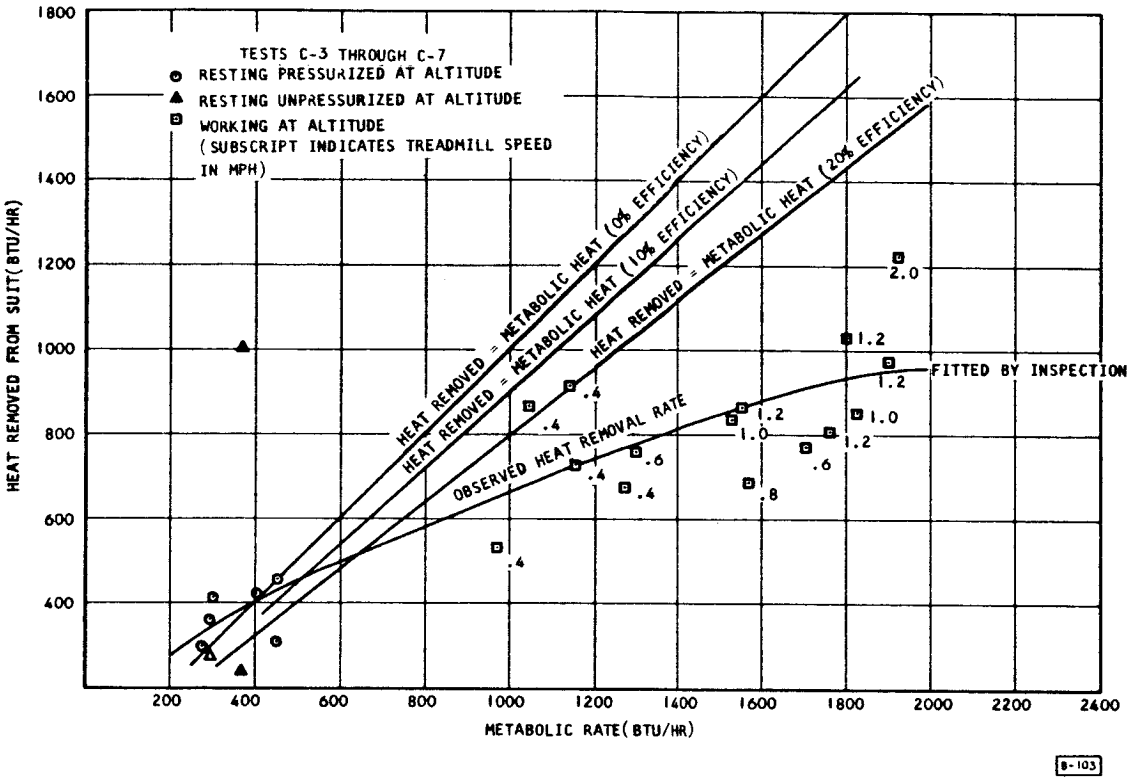

Figure 2-15. Suit Ventilation Cooling at Altitude (Ref. 29)

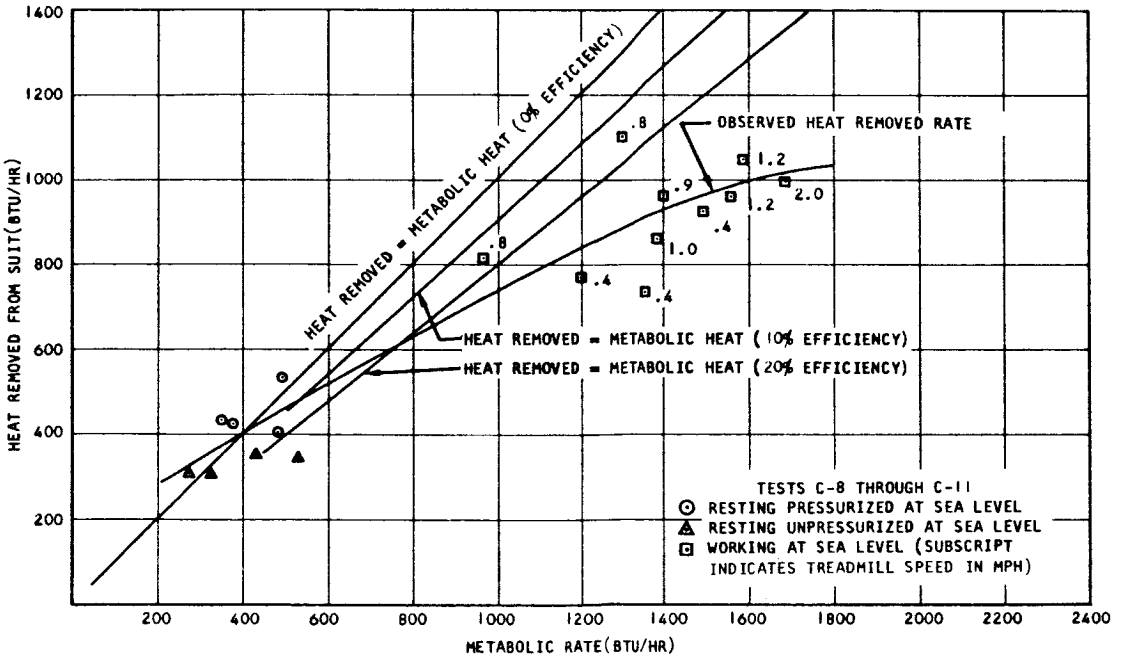

Figure 2-16. Suit Ventilation Cooling at Sea Level (Ref. 29)

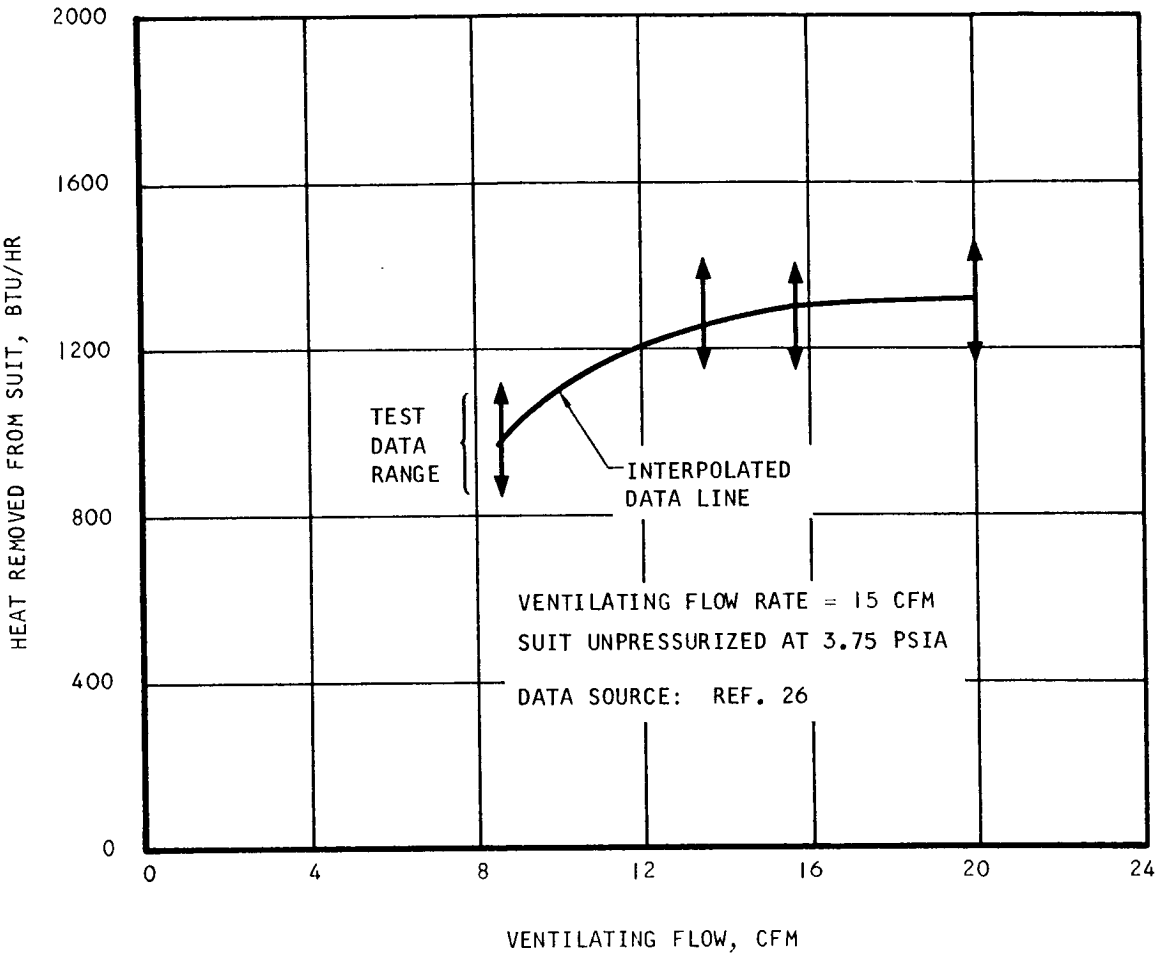

Figure 2-17. Suit Ventilation Cooling Heat Removal Rates

In a series of tests on the Gemini Model G2C pressure suit, Wortz et al. (Ref.30) investigated body heat balances for a ventilating flow of 17.1 cfm with the suits pressurized to 3.7 psig at sea level and 22,500-ft altitude chamber pressures. Results of these tests are summarized in Table 2-5 in the form of averages for the eight subjects which were obtained after a one-hour testing period. In some of these tests, the subjects approached the limit of their endurance (with rectal temperatures over 103°F and pulse rates in excess of 200 bpm). At the high metabolic rates obtained in these tests, cooling deficits ranging from 616 to 1296 Btu were obtained. Part of the observed cooling deficit may be represented by work output dissipated to the surroundings. Since the task involved walking a level treadmill in a pressurized suit, it is not possible to make a direct estimate of the work parameter. On the basis of the observed increase in body temperature with an allowance for increased temperature rise in the muscle masses, it is estimated that a maximum heat storage on the order of 1000 Btu was obtained. Thus, it appears that the work output under the most severe conditions is approximately 300 Btu/hr.

Suit Liquid-Loop Cooling

A liquid heat transport fluid loop can be used to convey waste heat from the suit to the system heat sink. Because of the relatively high bulk specific heats of liquid (water $\cong$62 Btu/ft^3-°F, oxygen $\cong$0.0045 Btu/ft^3-°F), the power requirement for heat transport by a liquid loop will be significantly lower than that for a gaseous transport loop. Water is the most likely heat transport fluid, because of its good heat transport properties, availability, and lack of toxicity.

Figure 2-18 shows the suit heat exchanger arrangement investigated by Felder and Sholsinger (Ref.35) which involves use of thermal transport panels containing liquid transport loop cooling coils. Ventilating gas is fed to the cooling panels, where it is directed to the skin for removal of insensible perspiration. Felder and Sholsinger report test results based on use of a man simulator; liquid-loop heat transfer effectiveness was in the range from 27 to 64 percent for 60 to 70 percent sensible heat removal, heat removal rates on the order of 50 Btu/hr-ft^2, and liquid transport fluid flows in the range from 1.5 to 2.5 lb/hr-ft^2. Subsequently, Bowen and Witte (Ref.31) report the results of manned tests on a suit cooling system using a thermal transport system of similar design.

Figure 2-19 illustrates the liquid-loop cooling method investigated by Burton and Collier (Ref.33). This approach involves heat removal from the body by conduction from the skin to tubes carrying a liquid heat transport fluid. The heat transport tubes are attached to a garment which maintains them in contact with the skin, as shown in Figure 2-20. Cooling was provided by 40 vinyl tubes (0.125-in. outside diameter, 0.060-in. bore diameter), each 4 ft long in the original design and 6 ft long in subsequent versions.

The cooling tubes provided a contact area of 0.3 ft^2 for the initial design and 0.45 ft^2 for the two later designs. Heat removal rates obtained with all designs were substantially in excess of those predicted by consideration of the thermal conductance of the skin and the heat transfer area of the

TABLE 2-5

AVERAGE CONDITIONS OBTAINED AFTER ONE HOUR IN VENTILATED PRESSURE SUIT (REF. 30)

	Metabolic Rate, (Btu/hr)	Average Skin Temp (^{o}F)	Rectal Temp (^{o}F)	17.1 cfm Ventilating Heat Removal			Suit Outlet Temp	
				Total (Btu/hr)	Sensible (Btu/hr)	Latent (Btu/hr)	Dry-Bulb	Dew-Point
Sea Level								
1.4 mph	2047	95.61	101.2	1331	308	1141	86.54	74.14
2.0 mph	2347	95.91	102.0	1342	271	1196	85.98	75.08
22,500 ft Altitude								
1.4 mph	2092	95.16	101.3	1186	304	920	82.53	67.25
2.0 mph	2703	95.99	102.1	1407	327	1182	83.25	70.80

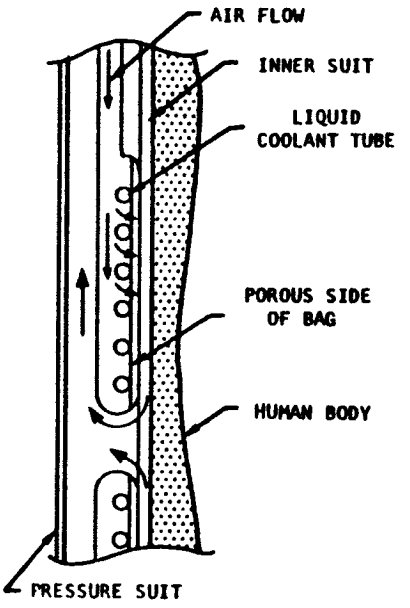

Figure 2-18. Body Cooling by Conduction and Forced Convection

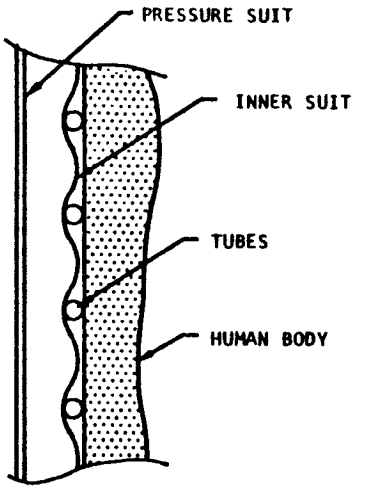

Figure 2-19. Body Cooling by Direct Conduction

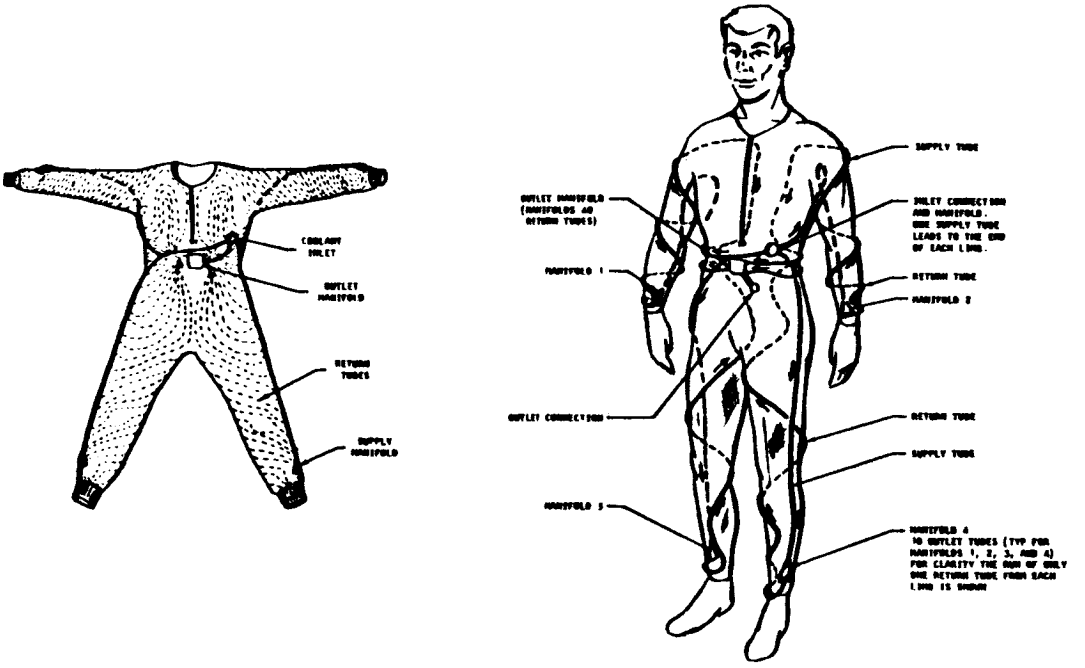

Figure 2-20. RAE Thermal Transport Assembly Design

cooling tubes. For example, at a heat removal rate of 404 Btu/hr, the coolant inlet temperature was 70.5°F and the coolant outlet temperature was 81.3°F. Assuming an average coolant temperature of 75.9°F, a mean skin temperature of 91.0°F, and an effective contact area of 0.45 ft^2, the overall heat transfer coefficient is 59 Btu/hr-ft^2-°F. The skin conductance under the condition of vasoconstriction represented by the test situation is approximately 3.3 Btu/hr-ft^2-°F. The heat flux from the body to the transport loop is 890 Btu/hr-ft^2. Assuming an internal temperature of 98.5°F with the skin temperature of 91.0°F, the corresponding heat flux from the body is estimated to be 24.7 Btu/hr-ft^2.

Figure 2-21 shows the heat transfer effectiveness as a function of coolant flow for two of the liquid-loop arrangements investigated by Burton and Collier. These data were obtained with sedentary test subjects who were insulated with mattresses. As a consequence of the low metabolic rates represented by the experimental condition, relatively low heat removal rates (from 300 to 400 Btu/hr) were obtained in these tests. However, in other tests at the NASA Manned Spacecraft Center, heat removal rates as high as 3400 Btu/hr were obtained with the test subject in an insulated garment on a treadmill using a coolant flow of 150 lb/hr with an inlet temperature near 32°F. It should be noted that the heat removal rates obtained by Burton and Collier involved use of a garment providing essentially complete coverage of the body (excepting the head, hands, and feet), although the actual prime heat transfer surface represented less than 3 percent of the total area of the body.

The principle of local cooling of the body has been investigated in detail by Wortz et al. (Ref.36,37) for the conditions obtained in a pressure suit at reduced pressure. Using three internal heat exchangers (one on the chest and one on each thigh), covering less than 15 percent of the surface area of the body, heat removal rates up to 750 Btu/hr were obtained for the thermal transport loop at metabolic rates averaging 1000 Btu/hr. Ventilating gas flow rates ranged from 2 to 6 cfm at 7.0 psia. No discomfort was reported by the test subjects as a result of local cooling. Adequate cooling was reported during several zero-ventilating-flow runs with the faceplate open. The 200- to 350-Btu/hr heat removal rates obtained under these conditions may be attributable to a combination of radiation and conduction. Figure 2-22 shows the heat removal rates reported by Wortz et al. for local area cooling of the body in a pressure suit environment.

Crocker, Webb, and Jennings (Ref.34) give test results for a liquid-cooled garment somewhat similar in design to those tested by Burton and Collier. In the tests reported, metabolic rate was varied parametrically by walking in a treadmill with the test subject in an insulated, impermeable overgarment. Heat transport fluid mass flow was varied from 1.9 to 6.1 lb/min, with the inlet temperature controlled in the range from 40 to 80°F depending upon metabolic rate. The garment heat removal rate appears to be primarily dependent upon inlet temperature and relatively independent of coolant flow rate, as shown in Figure 2-23. It can be deduced from this curve that it will be necessary to rather closely match coolant temperature with metabolic rate to provide the proper cooling effect. Figures 2-4 and 2-5 show the average skin and rectal temperatures as a function of metabolic rate using the liquid-cooled garment. An increasing metabolic rate occurs with a decreasing coolant temperature for

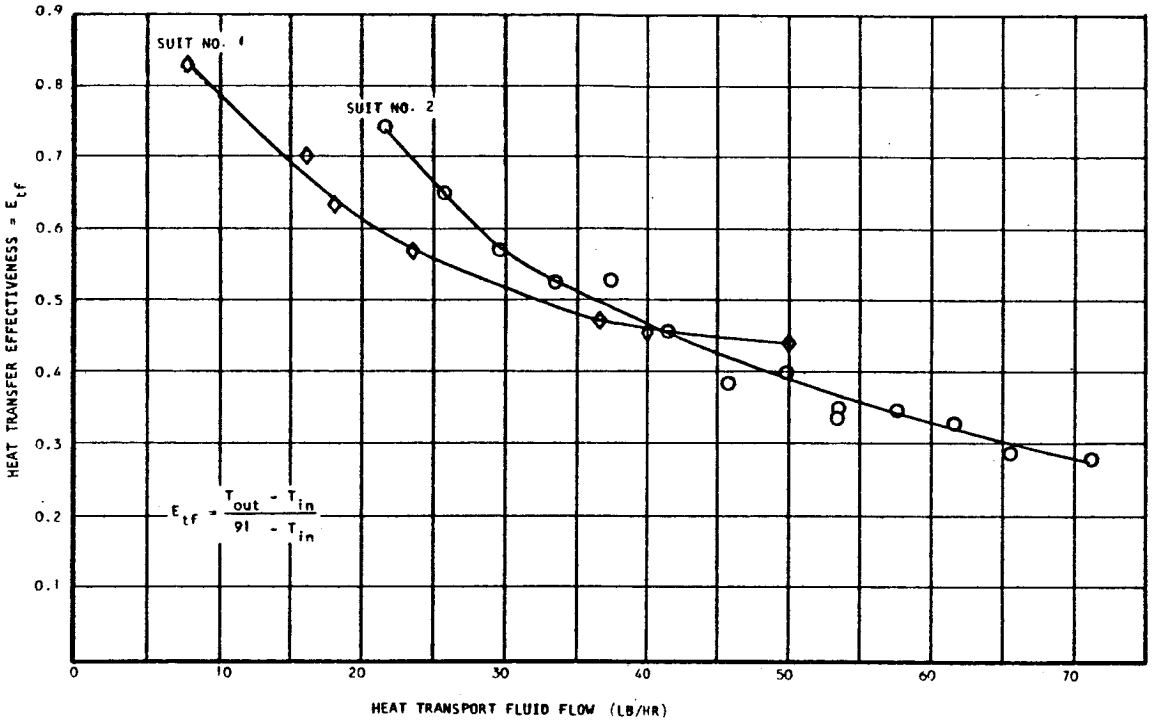

Figure 2-21. Liquid-Loop Suit Cooling Effectiveness

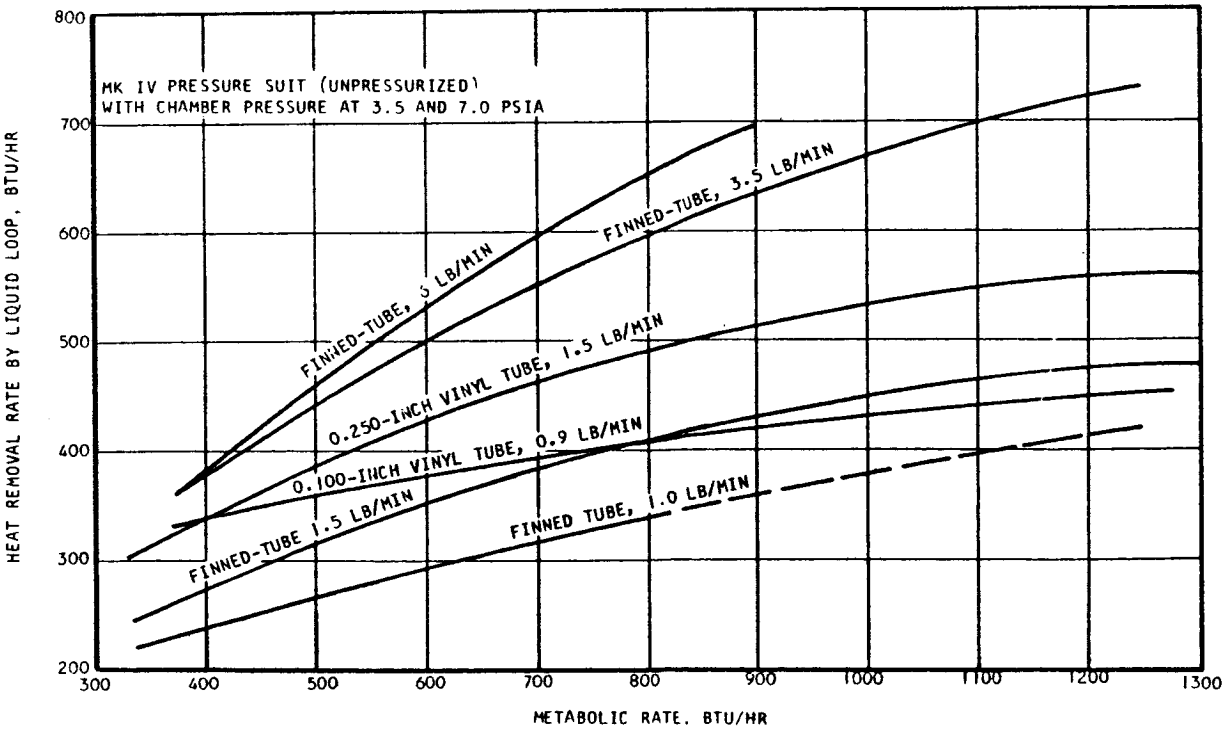

Figure 2-22. Liquid-Loop Suit Cooling Heat Removal Rate for Partial Coverage of the Body (Ref. 16)

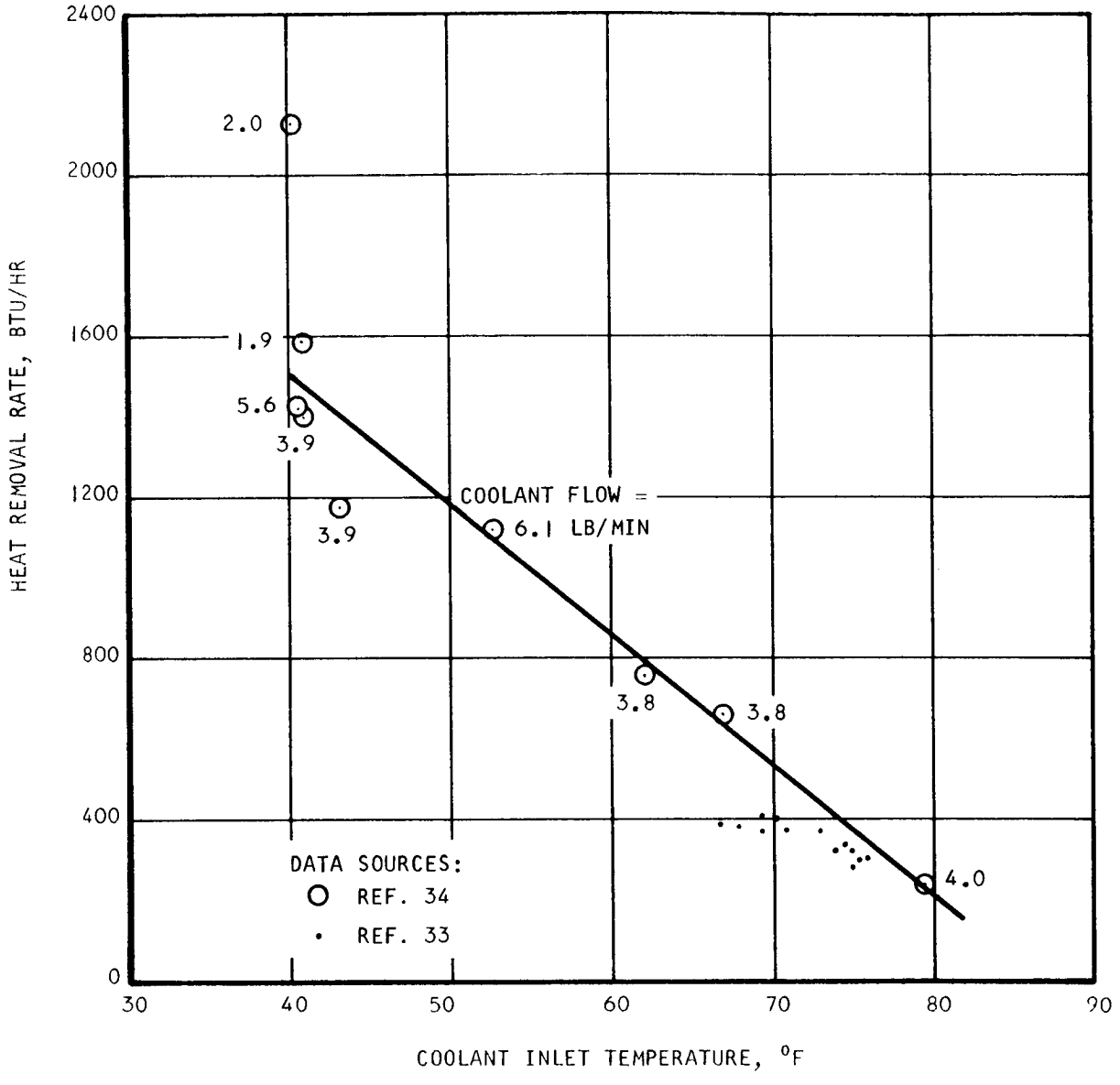

Figure 2-23. Coolant Inlet Temperature vs Heat Removal Rate

heat removal by the transport fluid. The difference between the rectal and skin temperatures increases with increasing metabolic rate to provide the temperature difference necessary for heat transport within the body.

Extravehicular Suit External Heat Balances

Extravehicular suit systems face somewhat different problems in various extraterrestrial environments. This is due to the significant differences in both the external environment and the internal requirements. For example, in the lunar surface environment, thermal radiation from the lunar surface (at a maximum temperature of about 710°R) requires careful design to avoid excessive heat loads. Also, the task of walking on the lunar surface in a pressurized suit may represent a high metabolic heat load. For a free-space environment, on the other hand, the metabolic rates may be somewhat lower because of the less strenuous nature of the tasks that will be performed. In addition, the external thermal environment will favor heat leak from the extravehicular suit. The Mars surface environment represents a special case with unique problems. The atmospheric pressure (approximately 1.7 psia at the surface) is not sufficient to adequately support a man without a pressure suit. This atmosphere complicates the problem of providing a heat sink for a portable environmental control system since water will boil at an excessively high temperature and other expendable evaporants have inferior characteristics. High wind velocities are anticipated for the Mars surface, requiring consideration of convective heat transfer in the extravehicular suit heat balances.

The principal extravehicular suit programs now in progress involve the Apollo and Gemini missions and use of fabric pressure suits. The limitations of these suit designs with respect to mobility and increased work rates have been established. At the present time, there is increasing interest in advanced suit designs, particularly the "hard" all-metal suit. One hard suit has reached an advanced prototype stage of development. This suit design appears to offer a number of potential advantages with respect to mobility characteristics.

Correale and Guy (Ref. 39) describe some of the Apollo extravehicular suit design considerations for the lunar environment. A design condition is indicated with a solar angle of 20 degrees from the normal at a 200-ft distance from a 14,000-ft-high crater wall that has a 20-degree slope relative to vertical. Suit thermal garment spectral characteristics are described as

$$\alpha = 0.10, \quad \epsilon = 0.05$$

Kincaide (Ref. 42) describes the original portable life-support system design used with the Apollo extravehicular suit. This system provides a ventilating flow of 15 cfm at a suit pressure of 3.7 psia for a 4-hour design duration. The Apollo extravehicular suit assembly program has been redirected to use a liquid cooling garment. The suit ventilating flow has been reduced to 5 cfm. A peak cooling requirement in excess of 2000 Btu/hr is provided by a coolant flow of approximately 240 lb/hr.

Cramer and Irvine (Ref. 41) analyzed geometrical models for the 50th-percentile man (total surface area = 20.6 ft^2). Figure 2-24 shows the geometrical models evolved during the study. The simplest cylindrical model was selected for the analysis of a passive thermal control. A spectral surface coating providing a low α/ε of 0.11 was recommended to provide the necessary low surface temperatures. Whether this performance is attainable in a fabric surface is unknown. In order to provide suitable thermal capacity to maintain a minimum temperature of 66°F during the cold condition, a 0.625-in. layer of water was proposed to be installed in the extravehicular suit.

Freedman (Ref. 40) presents test results involving a Gemini pressure suit equipped with an insulating coverall in a space environment simulator. The coverall insulation consisted of seven layers of 0.25-mil aluminized mylar with seven layers of 1.0-mil dacron spacer. Complete coverall weight was 5.7 lb, 1.4 lb of which was insulation. The heat balances obtained in unmanned tests in a space environment simulator are as follows:

Facing sun	-66 Btu/hr
Back to sun	-90 Btu/hr
Right side to sun	-96 Btu/hr
No sun	-132 Btu/hr

The overall heat transfer coefficient represented by the heat leaks above for the thermal coverall is 0.025 Btu/hr-ft^2-°F. Heat conduction through the seams is said to be the dominant mode of heat transfer through the coverall.

Table 2-6 shows results of NASA extravehicular suit heat balance studies for two different outer surface spectral characteristics. One of these represents a white, high-temperature-resistant nylon material. The second is a simple aluminum coating applied to the fabric.

Table 2-7 gives the spectral characteristics specified by NASA for the pressure suit used in Project Mercury.

Fejer and Seale (Ref. 38) report the results of thermal studies for protective suit systems for the lunar, martian, and venerian environments. The suit heat balance studies were based on use of an aluminized surfacr providing a solar absorptivity of 0.14 and a thermal emissivity of 0.47. Using a 0.125-in. layer of superinsulation ($k = 5 \times 10^{-4}$ Btu/hr ft), in the lunar thermal environment the night-time heat leak is reduced from -1590 Btu/hr (uninsulated suit) to -230 Btu/hr; the daytime heat gain is reduced from 1123 Btu/hr (uninsulated suit) to 89 Btu/hr. For the Mars surface, a convective heat transfer coefficient of 1.97 Btu/hr-ft^2-°F was estimated, assuming an ambient pressure of 1.25 psia and a wind velocity of 37 mph. Using a 0.125-in. layer of superinsulation ($k = 1.0 \times 10^{-2}$ Btu/hr ft °F at 1.25 psia), the night-time heat leak is reduced from -8400 Btu/hr to -2700 Btu/hr and the daytime heat leak is reduced from -300 Btu/hr to -120 Btu/hr.

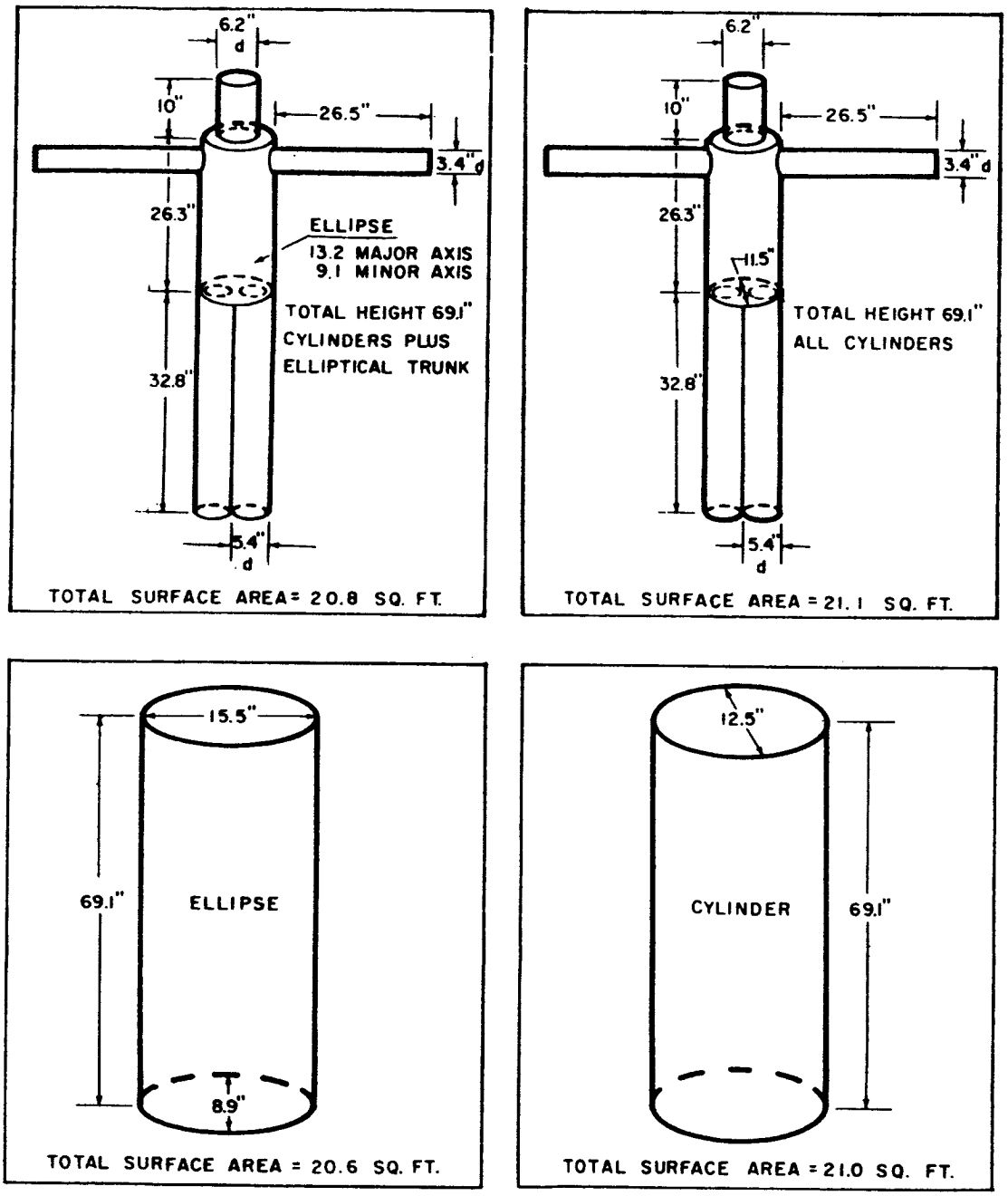

Figure 2-24. Geometric Models of Human Body (Ref. 41)

Because of the relatively high environmental temperatures (+800°F) then expected on Venus, use of an entirely different insulation concept using evacuated superinsulation in a double-wall protective vessel was proposed.

TABLE 2-6

COMPARISON OF SUIT AND COVERALL HEAT LEAKS FOR SURFACE CHARACTERISTICS (REF. 40)

Surface Spectral Characteristics	White Fabric	Aluminized Fabric
Solar absorptivity, α	0.36	0.09
Thermal emissivity, ϵ	0.85	0.30
Suit Alone (k/L = 15 Btu/hr-ft²-°F) Heat Leak (Btu/hr)		
Orbital day	511	-100
Orbital night	-1600	-600
Lunar surface day	2190	660
Lunar surface night	-4100	-1500
Coverall (k/L = 0.025 Btu/hr-ft²-°F) Heat Leak, (Btu/hr)		
Orbital day	10	-10
Orbital night	-74	-60
Lunar surface day	24	21
Lunar surface night	-180	-84

TABLE 2-7

MERCURY SUIT SPECTRAL CHARACTERISTICS (REF. 43)

Infrared spectral range emittance (spectral range 0 to 7μ with surface fabric at 25 to 600°F)	0.06
New Material Reflectivity	
a. Near infrared (2000 mμ)	0.88
b. Visible range (500 mμ)	0.84
c. Ultraviolet range (200 mμ)	0.87
Material Reflectivity After Abrasion and Wear	
a. Near infrared	0.82
b. Visible range	0.73
c. Ultraviolet range	0.715

Table 2-8 gives the Gemini suit thermal characteristics (Ref. 45). It should be emphasized that the thermal design of the extravehicular version of the Gemini suit has not been defined at the present time and the values listed in Table 2-8 should be considered to be representative of attainable performance. There is some doubt concerning the spectral characteristics of the outer garment since other measurements of the material indicate a solar absorptivity of 0.17 and a thermal emissivity of 0.88.

TABLE 2-8

GEMINI SUIT THERMAL CHARACTERISTICS (REF. 45)

	Outer Garment	Helmet Shell	Visor
Area, $in.^2$	4400*	264	71
Thermal conductivity, Btu/hr-ft-^{0}F	0.02	2.9	1.45
Material thickness, in.	0.35	0.09	0.13
Solar absorptivity	0.32	0.25	-
Thermal emissivity	0.56	0.88	-

*Torso area = 1650 $in.^2$, limb area = 2750 $in.^2$

The thermal design of the Apollo extravehicular suit has also apparently not yet been frozen. As a consequence of the uncertainty concerning the thermal and spectral characteristics of suits and suit materials, it will be necessary to conduct the extravehicular suit heat balances on a parametric basis using the thermal and spectral characteristics as variables.

The thermal characteristics of the Gemini suit will be used in the baseline studies, with various characteristics varied systematically to determine their effect on overall performance.

SECTION 3

THERMAL PROCESSES, SUIT ENVIRONMENT

INTRODUCTION

Cooling of the human body encased in an extravehicular pressure suit can be accomplished by a variety of processes, depending upon design of the suit. The initial approach, essentially an extension of aircraft full-pressure suit design, has involved use of a ventilating gas flow passed over the surface of the body. This method is satisfactory for the relatively low metabolic rates obtained in space cabins, where the pressure suit serves as a backup to the vehicle pressure shell. For extravehicular activities in pressurized suits, substantially higher metabolic rates are obtained. Increases in metabolic expenditure on the order of 150 to 300 percent are required for a pressurized state-of-the-art suit as compared with performance of the same task in a normal shirtsleeve environment. Therefore, it will be necessary to design extravehicular suit thermal control systems for metabolic rates as high as 1500 or 2000 Btu per hour.

It has not been possible to provide adequate cooling by ventilation without excessive power penalties for circulation of the ventilating gas. Also, with ventilating cooling, the predominant body cooling process is evaporation of moisture from the skin. The resultant high sweat rates and body temperatures impose an undesirable physiological stress. As a consequence of these factors, liquid-loop cooling methods have been adopted for extravehicular suits.

With the liquid-loop cooling method that has had the most detailed investigation to date, the heat is removed from the body by conduction to tubes containing a heat-transport fluid.

In addition to the ventilating-gas and liquid-loop suit cooling techniques, other methods, which involve use of radiation from the suit as the primary means of heat rejection, are possible. In one of these, a suit design is used in which the inner wall is in contact with the skin. Cooling in this case is done by conduction of heat from the body through the suit wall to the outer surface, where it is rejected by radiation to the environment. This situation would be represented by a tight "second-skin" suit concept. Another approach would provide a gas space between the skin and the suit inner wall. For low gas velocities, the body would be cooled primarily by radiation to the inner wall of the suit, conduction through the wall, and radiation from the outer wall to the environment. In the second case, the suit concept used might resemble a state-of-the-art pressure suit in which there was little or no circulation of the pressurizing gas.

The present study will be concerned with an analysis of thermal processes for extravehicular suits and will not attempt to evaluate suit concepts. Four principal cases will be considered:

a. Ventilation cooling

b. Liquid-loop cooling (conduction from body)

c. Radiation cooling (conduction from body)

d. Radiation cooling (radiation from body)

VENTILATION COOLING OF PRESSURE SUITS

As indicated in Section 2 of this report, a considerable amount of test data has recently been obtained for ventilation cooling of pressure suits (Ref. 26, 27, 28, 29, 30). Since ventilation cooling is used by all presently available full-pressure and extravehicular suits, it can be considered, in terms of development, the most advanced suit cooling method. Unlike methods in which heat conduction or radiation from the skin is the primary heat transfer mode, ventilation cooling is able to utilize the thermoregulatory mechanisms of the body for thermal control. Specifically, heat dissipation from the body is regulated by means of thermoregulatory control of the sweat mechanism. As mentioned previously, the physiological disadvantage of this dependence upon the sweat mechanism increases with metabolic rate. In addition, certain fundamental limitations on attainable heat removal rates have been observed. The thermodynamic processes and the heat- and mass-transfer processes will be analyzed to correlate observed performance and to determine ultimate performance capabilities for suit ventilation cooling methods.

Thermodynamic Analysis of Ventilation Cooling

It can be shown that in the use of ventilation cooling it will be necessary to depend upon dissipating much of the metabolic waste heat by evaporation of sweat from the skin, in order to avoid excessive penalties for circulation of ventilating gas. The latent cooling capacity of the ventilating gas flow is given by

$$Q_\ell = \dot{m}\, \Delta H h_{fg} \tag{3-1}$$

where ΔH represents the change in moisture content of the ventilating gas from the suit inlet to the suit outlet. The moisture content (mass ratio) is a function of the water vapor partial pressure, the total pressure, and the molecular weight of the ventilating gas, as follows:

$$H = \frac{P_{H_2O}\, M_{H_2O}}{(P - P_{H_2O}) M_a} \tag{3-2}$$

The sensible cooling capacity of the ventilating gas, represented in this case by convective heat transfer, is given by

$$Q_c = \dot{m} C_p\, \Delta T \tag{3-3}$$

where ΔT represents the rise in dry-bulb temperature of the ventilating gas as it flows through the suit. Since the specific heat of the ventilating gas will range from 0.22 to 0.24 Btu per lb ^{0}F and the suit outlet temperature will vary from approximately 85^0 to 90^{0}F, the total available sensible cooling

capacity will amount to only 8.8 to 10.8 Btu per lb of ventilating gas (for a suit inlet dry-bulb temperature of 45°F). The latent cooling capacity will be considerably greater. Figure 3-1 shows the total cooling capacity of the ventilating gas as a function of suit outlet dew-point temperature, assuming an outlet dry-bulb temperature of 90°F and an inlet dry-bulb temperature of 45°F. It will be noted that with dry ventilating gas at the suit inlet, the cooling capacity of the ventilating gas is increased significantly, for the same outlet conditions. In recirculating systems using water vapor removal by condensation, it will usually be impractical to provide ventilating gas inlet dew-point temperatures below about 45°F. Where desiccants are used for humidity control, very low dew points can be readily obtained. The gas obtained from cryogenic or gaseous storage containers will ordinarily have a very low moisture content, so that the vent flow in an open-cycle system will provide a substantial cooling capacity in the form of the moisture being dumped overboard.

Efficiency of Suit Ventilation

Suit ventilating performance is frequently given in terms of a suit efficiency, η_v, which relates the actual moisture pickup to that theoretically possible for the given suit inlet and outlet conditions.

$$\eta_v = \frac{(p_o - p_i)_{H_2O}}{(p_{os} - p_i)_{H_2O}} \tag{3-4}$$

where p_{os} represents the water vapor saturation partial pressure at the suit outlet dry-bulb temperature. Figure 3-2 gives the suit efficiency and outlet relative humidity as a function of the suit outlet dew-point temperature. Dew-point temperature is a somewhat more basic parameter than either relative humidity or suit efficiency, since it does not involve use of an arbitrary reference. Ventilating efficiency will vary somewhat with suit design, particularly with regard to the internal flow distribution. That is, not all of the ventilating flow passes over the same body area before returning to the suit outlet. The commonly specified suit outlet relative humidity of 70 percent corresponds to a suit efficiency of 60 percent and a suit outlet dew-point temperature of 79.5°F. This is somewhat higher than actually obtained in tests. For example, in the series of tests on the Gemini suit by Wortz et al. (Ref. 30, Table 2-5), suit outlet dew-points on the order of 67° to 70°F were obtained under conditions of severe heat storage at high metabolic rates (2000 to 2700 Btu per hour). Comparable performance has been obtained with the Apollo suit (Ref. 29).

Suit Ventilation Pressure Drop

The pressure drop characteristics of the Apollo and Gemini suits are approximately correlated by the following expression:

$$\sigma_d \Delta P_s = 0.018 \dot{m}^{1.67} \text{ inches of water} \tag{3-5}$$

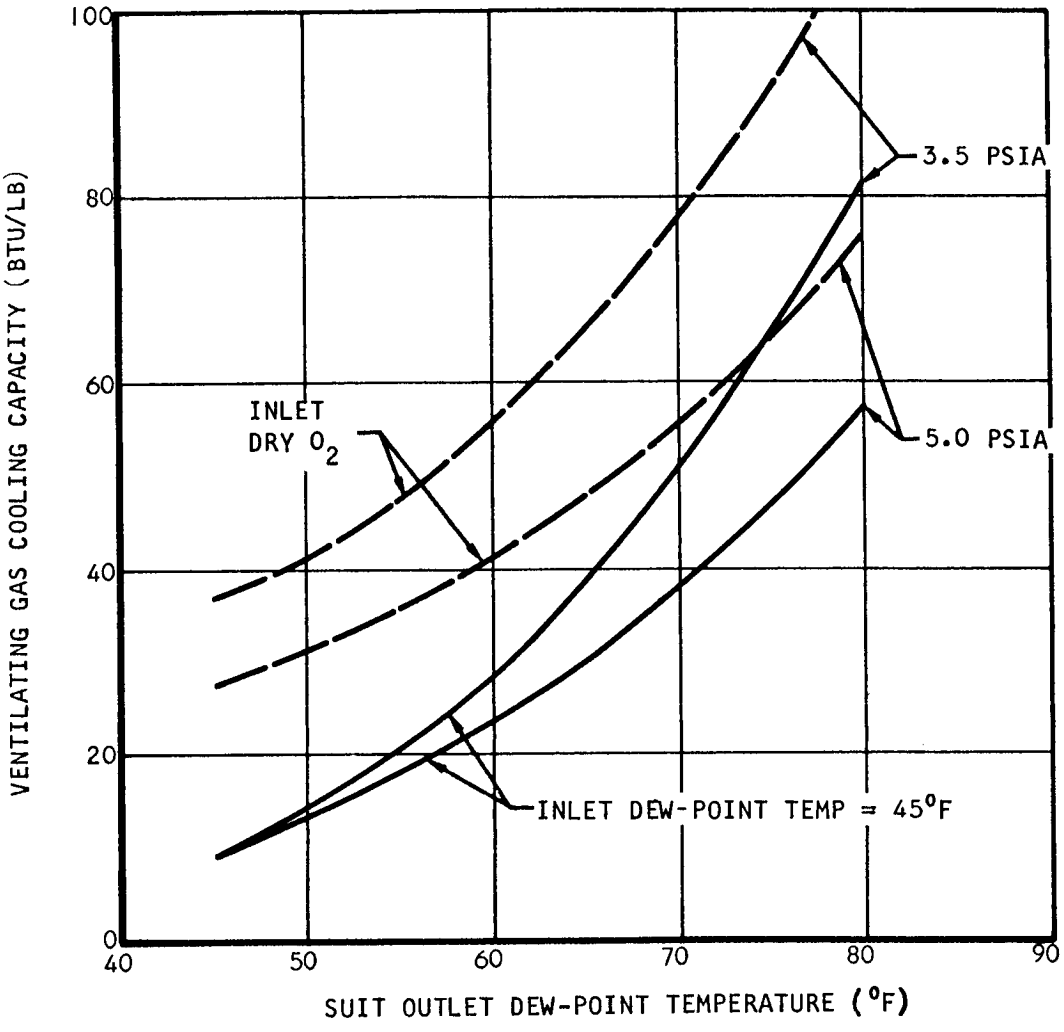

Figure 3-1. Cooling Capacity of Suit Ventilating Gas

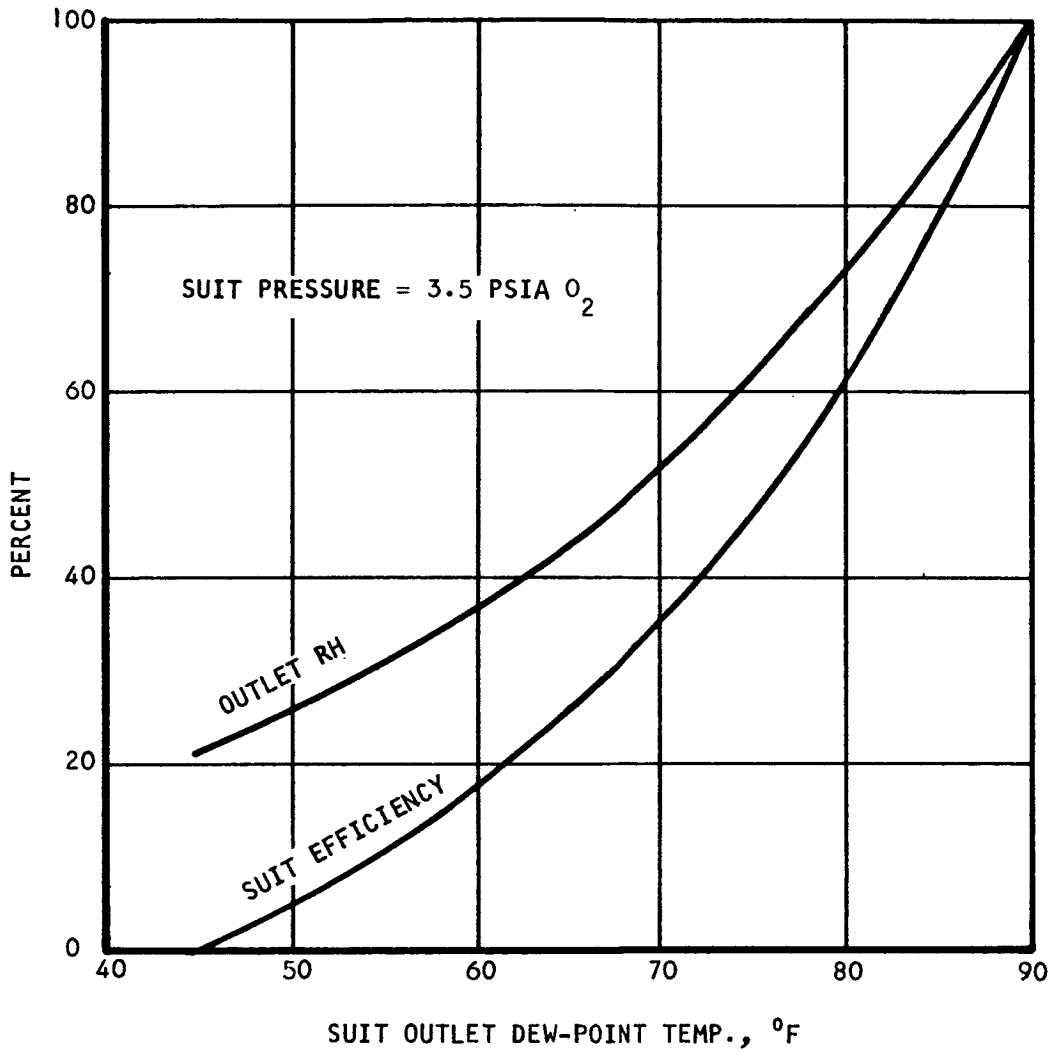

Figure 3-2. Suit Efficiency and Outlet Gas Relative Humidity vs Outlet Dew Point for 45°F Saturated Inlet Gas and 90°F Outlet Dry-Bulb Temperature

where the suit pressure drop, ΔP_s, is given in inches of water. Thus, the suit pressure drop depends upon the ventilating flow rate and gas density. The density ratio, σ_d, represents the ratio of the gas density to that for air at a reference condition (0.0765 lb per ft^3 at 14.7 psia and 59.6°F); it can be given in terms of the ventilating gas properties, as follows:

$$\sigma_d = 1.22 \frac{PM_a}{T_a} \tag{3-6}$$

The fan power requirement represented by the ventilating gas flow is given by the following expression:

$$W_f = 0.0256 \frac{\dot{m}\, \Delta P_T}{\eta_f\, \sigma_d} \text{ watts} \tag{3-7}$$

where η_f is the fan efficiency and ΔP_T is the total pressure drop in inches of water. Combining Equations (3-5), (3-6), and (3-7) and restricting consideration to a pure oxygen ventilating gas at 45°F results in the following expression for the fan power chargeable to suit ventilation alone:

$$W_s = 0.0770 \frac{\dot{m}^{2.67}}{\eta_f P^2} \text{ watts} \tag{3-8}$$

Equation (3-8) illustrates the sensitivity of the power requirement for suit ventilation to ventilating flow and pressure. Figure 3-3 shows the pumping power chargeable to suit pressure drop as a function of ventilating flow and pressure. If Equation (3-8) is given in terms of the ventilating gas volumetric flow rate, $\dot{q}$, the following expression is obtained:

$$W_s = 0.00477 \frac{\dot{q}^{2.67}\, P^{0.67}}{\eta_f} \tag{3-9}$$

Therefore, the power increases with increasing pressure for constant volumetric flow. Since the ventilating devices used in suit loop systems tend to provide constant volumetric flow with varying pressure, the characteristic represented by Equation (3-9) may be important where the system is required to function over a range of pressure.

Because of the pressure drop in accessories such as absorption beds, heat exchangers, and fittings, the total pressure drop will be somewhat higher than that given for the suit alone by Equation (3-4). In the various spacecraft suit loop systems designed to date, component design has varied (at the expense of size and weight) to provide an overall pressure drop of 3 to 6 inches of water (exclusive of suit pressure drop) at the design flow, which has ranged from 10 cfm for the one-man Mercury system to 36 cfm

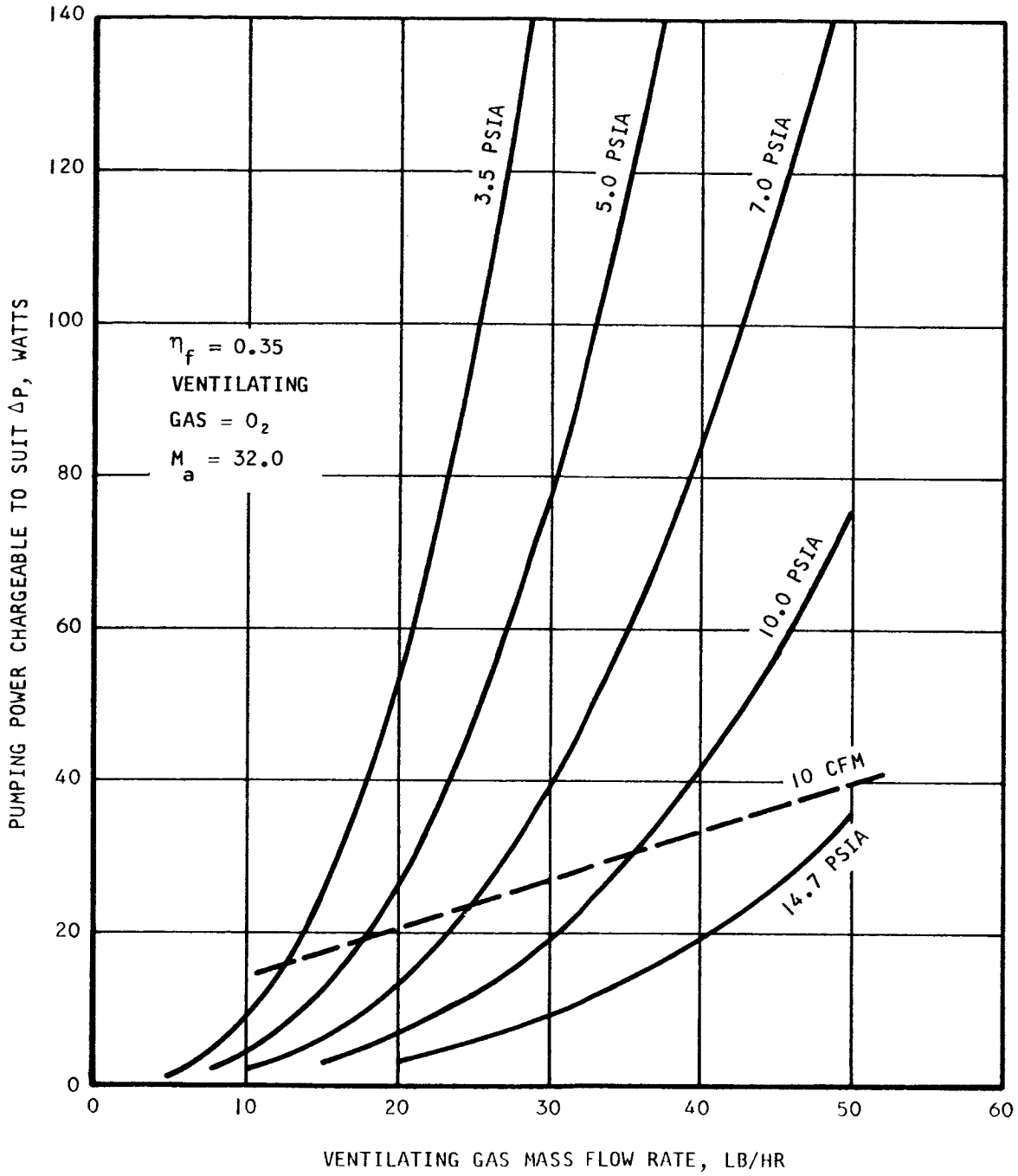

Figure 3-3. Suit Pressure Drop Ventilating Power

for the three-man Apollo system. Since the pressure drop characteristic obtained for most of the suit loop accessory equipment is that for laminar flow,

$$\sigma_d \Delta P_e = k_e \dot{m} \tag{3-10}$$

and the pumping power chargeable to the accessory equipment is given by

$$W_e = 4.26 \frac{k_e \dot{m}^2}{\eta_f P^2} \text{ watts} \tag{3-11}$$

Ventilation Cooling Energy Transfer Analysis

Present space and pressure suit assemblies vary to some extent in the internal ducting arrangement used to distribute the ventilating gas over the surface of the body. In most designs, the ventilating gas is brought into the suit at the waist or chest and is split into five parts, with a portion of the flow going to each of the extremities and to the head. Figure 3-4 shows a typical suit ventilation arrangement. Depending upon the suit design, the ventilating gas flow may be exhausted through the helmet or may be collected at the chest and exhaust there. The heat transfer analysis to follow will not be concerned with specific suit designs with particular ventilating gas flow splits but will involve a basic heat and mass transfer analysis to determine the ultimate capabilities of ventilating gas suit cooling methods. Figure 3-5 shows the ventilation gas distribution model to be used in the heat transfer analysis.

1. Sensible Heat Transfer

Suit cooling by ventilation provides heat removal from the body by sensible heat transfer and by evaporation of moisture from the skin. The ventilating gas thus serves as the instrument for both sensible and latent heat rejection. In order to minimize the pumping power associated with recirculation of the ventilating gas, it is customary to design for both low pressure drops and minimum ventilating gas flows. The heat- and mass-transfer processes take place within the laminar flow regime. If the transfer processes can be represented by laminar gas flow parallel to a flat plate and the effect of the mass transfer on heat transfer (by creation of convective currents) can be neglected, the heat transfer coefficient can be obtained from the following equation:

$$Nu = 0.664\ Pr^{0.33}\ Re^{0.50} \tag{3-12}$$

where Nu = Nusselt number $= \frac{hL}{k}$

Pr = Prandtl number $= \frac{C_p \mu}{k}$

Re = Reynolds number $= \frac{60\ V\rho L}{\mu}$

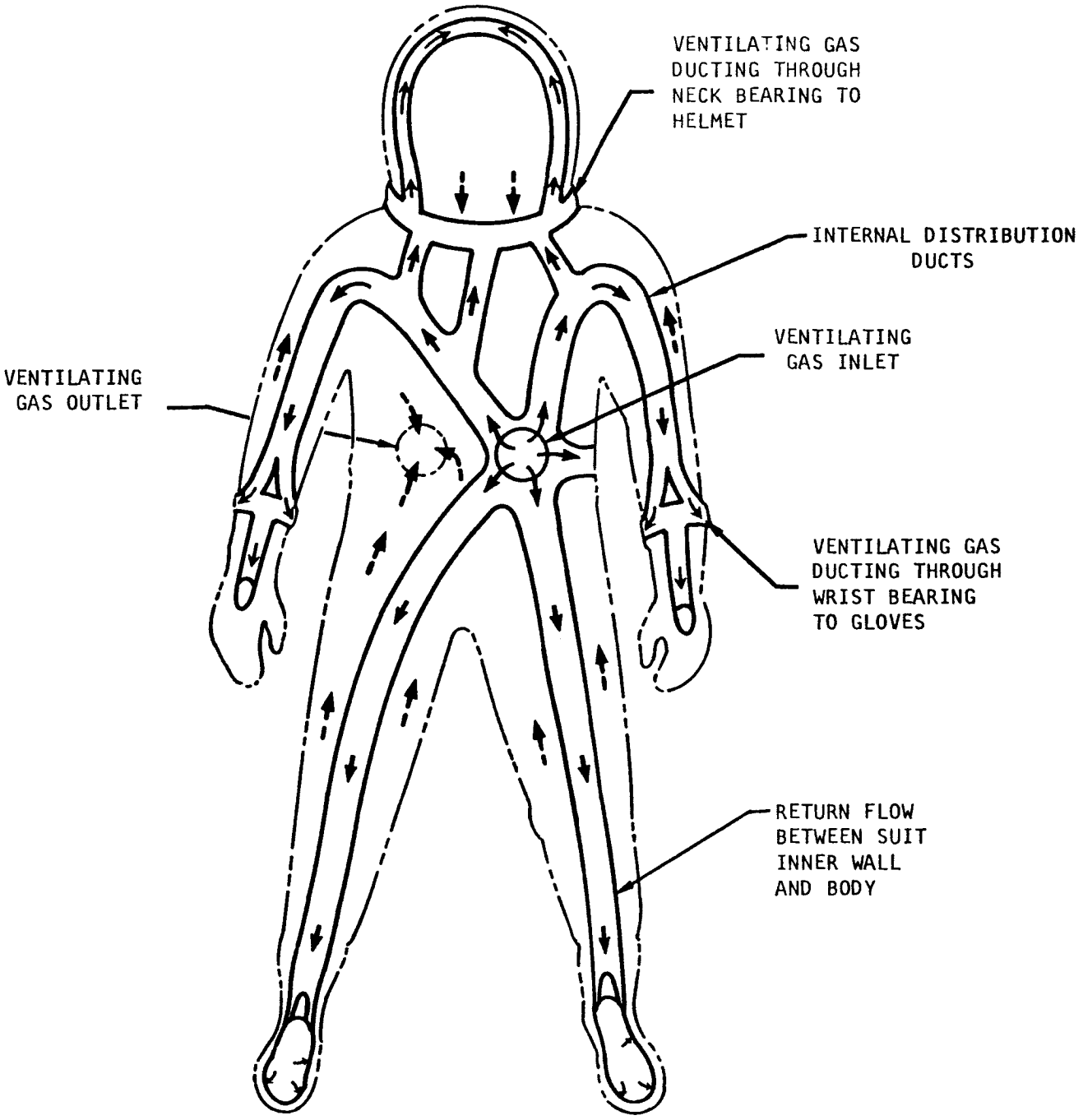

Figure 3-4. Typical Extravehicular Suit Ventilating Gas Distributing System

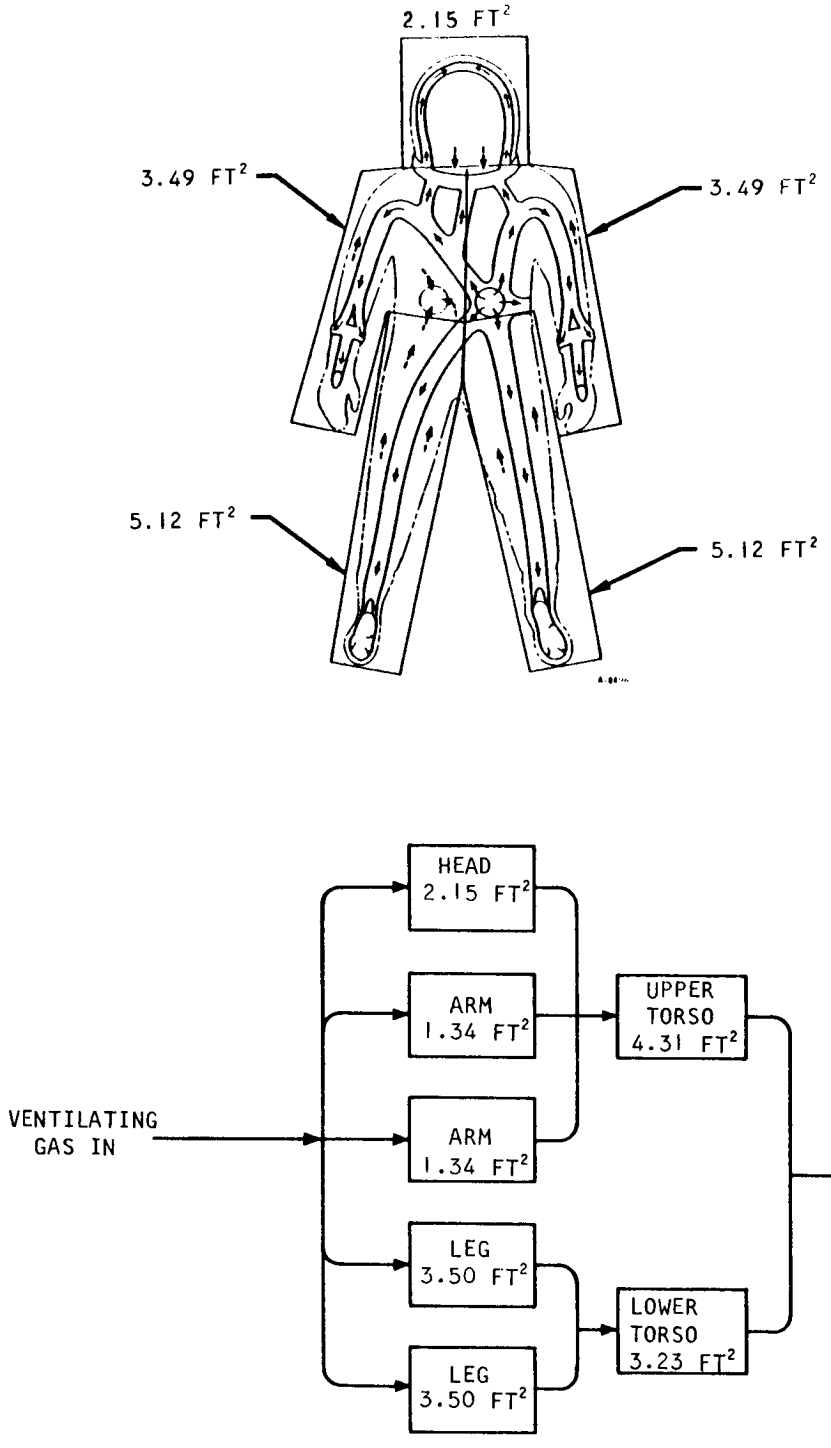

Figure 3-5. Suit Ventilation Gas Distribution Model

The Prandtl number is a function of the gas properties alone and will average close to 0.70 for the gas mixtures and temperature ranges of interest in the present application.

The ventilating gas velocity, V, is determined by the ventilating mass flow, the gas density, and the average internal ventilating gas flow area, e.g.,

$$V = \frac{\dot{m}}{60\ \rho A_v} \text{ ft/min} \tag{3-13}$$

On the basis of the geometric model shown in Figure 3-4, if there is a clearance of 0.75 in. between the body and the suit inner wall, there will be an approximately average flow area (A_v) of 0.196 ft^2 available for the passage of the ventilating gas. Assuming the ventilating gas is ducted to the extremities and exhausted at the waist, the characteristic flow dimension, L, is 3.5 ft. Using these geometric parameters, the expression for the Reynolds number becomes,

$$Re = 0.298\ \frac{\dot{m}}{\mu} \tag{3-14}$$

The Reynolds number is a correlating parameter for gas flow that is essentially independent of pressure when expressed in terms of mass flow as above.

Table 3-1 lists the thermal and transport properties of a number of gases that are possible constituents of ventilating gas systems. Special techniques are required for the estimation of the thermal conductivity and viscosity of gas mixtures.

The heat transfer coefficient, h, can be calculated from Equation (3-1), and is assumed to remain essentially constant for a particular set of operating conditions. Since the ventilating gas temperature will vary with time in the suit, it will be necessary to integrate the following energy balance expression:

$$h\ (T_s - T)\ dA = \dot{m}\ C_p\ dT \tag{3-15}$$

For the case where the body temperature is constant, the following expression is obtained for the heat transfer effectiveness:

$$E = \frac{T_o - T_i}{T_s - T_i} = \left[1 - \exp\ \left(-\frac{hA}{\dot{m}C_p}\right)\right] \tag{3-16}$$

where T_o and T_i are the ventilating gas outlet and inlet temperatures, respectively. The expression $\frac{hA}{\dot{m}\ C_p}$ is the number of transfer unit (NTU) for heat transfer.

Figure 3-6 shows the estimated heat transfer effectiveness as a function of ventilating gas flow.

TABLE 3-1

ATMOSPHERIC GAS THERMAL AND TRANSPORT PROPERTIES

	N_2	O_2	He	Ne	CO_2	H_2O	Air
Specific Heat at Const. Press (C_p), Btu/lb ^oF	0.249	0.220	1.26	0.25	0.203	0.445	0.240
Specific Heat Ratio	1.400	1.395	1.663	1.66	1.285	1.329	1.400
Molecular Weight (M)	28.02	32.00	4.003	20.18	44.01	18.02	28.96
Thermal Conductivity (k) Btu/hr/^oF/ft	0.0431	0.01546	0.0845	0.0277	0.00958	0.010	0.01516
Viscosity (μ), lb/hr/ft	0.01514	0.0499	0.0475	0.0750	0.0362	0.0242	0.0448
Prandtl Number (Pr)	0.713	0.709	0.710	0.678	0.770	1.078	0.708

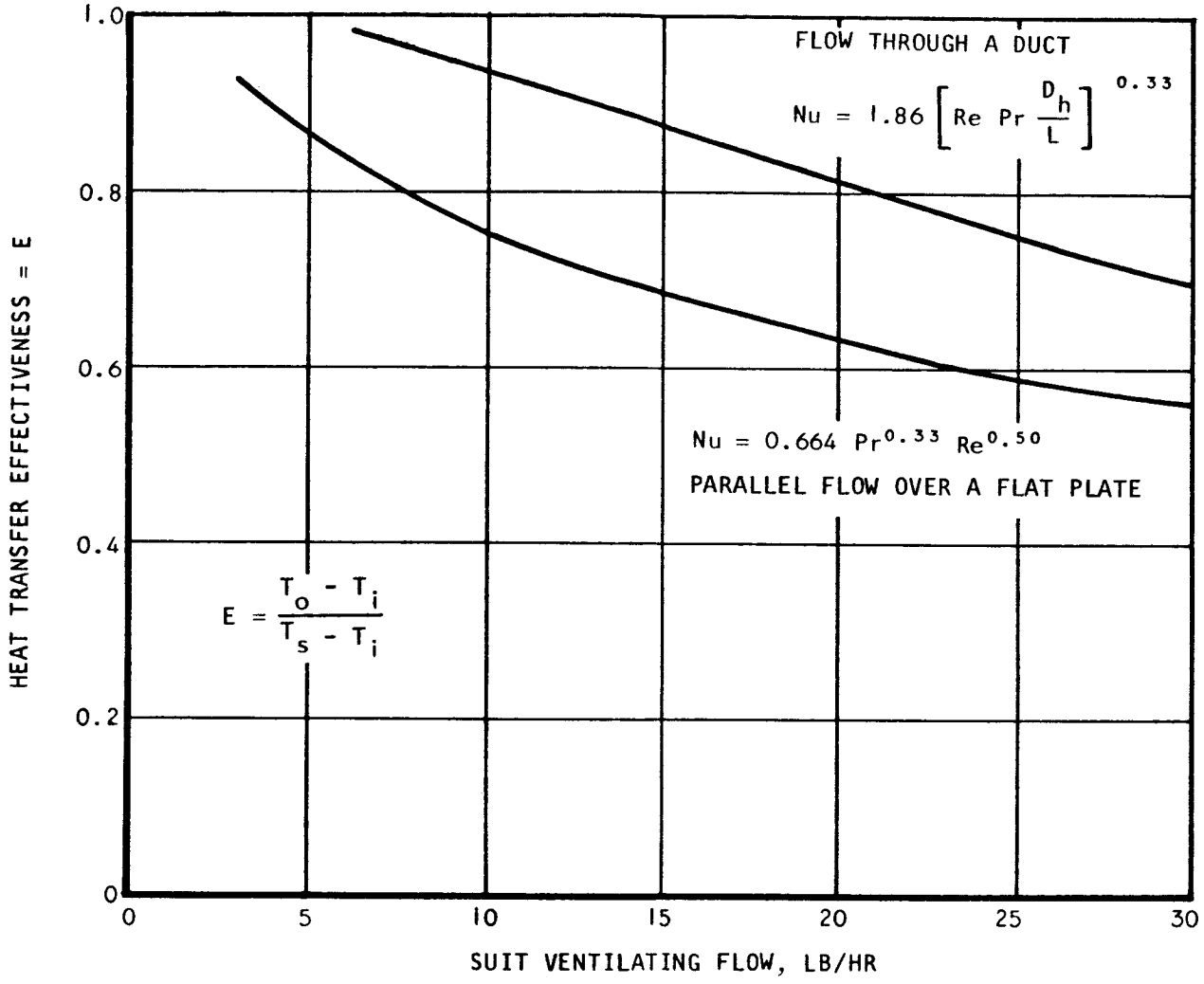

Figure 3-6. Estimated Heat Transfer Effectiveness for Suit Ventilating Gas Flow

Figure 3-7 shows the estimated suit outlet dry-bulb temperature as a function of ventilating flow for average body temperatures of 92 and 97°F. Comparison of the calculated suit outlet temperatures with those actually obtained for the Gemini suit (Ref. 27) (shown in Figure 3-8) discloses that the higher heat transfer effectiveness is realized than would be predicted by the simple heat transfer analysis presented here.

It can be demonstrated that the sensible heat rejection from the suit is better represented by the correlation applicable to heat transfer during laminar flow through ducts, namely,

$$Nu = 1.86\ Re^{0.33}\ Pr^{0.33} \left(\frac{D_h}{L}\right)^{0.33} \tag{3-17}$$

The Reynolds number and Nusselt number in this correlation are defined in terms of the hydraulic diameter, as follows:

$$Re = \frac{D_h\ \dot{m}}{A_v\ \mu} \tag{3-18}$$

$$Nu = \frac{h\ D_h}{k} \tag{3-19}$$

Assuming the same geometry as was used in the previous analysis, the hydraulic diameter, D_h, is equal to 0.222 ft. Therefore, the heat transfer model is represented by a duct 0.222 ft in diameter by 3.5 ft long. Figure 3-9 shows the predicted suit outlet dry-bulb temperature as a function of mass flow (given in terms of mass flow, the heat transfer model predicts that sensible heat removal will be independent of pressure level). Shown for comparison in Figure 3-9 is a correlation of test data for the Gemini suit. The difference between the theoretical values and the test data may be the result of heat transfer in the distribution ducting, which has been neglected in the present analysis.

Under the conditions obtained with high metabolic rates in ventilated suits, the test subject is under thermal stress with a high sweat rate, and an elevated skin temperature on the order of 97°F is representative of the test situation for the data shown in Figure 3-8. However, in the thermal design of future space suits, it will be undesirable to design for elevated body temperature. Since it will be desired in most instances to maintain the skin temperature below approximately 92°F to avoid active sweating, the previous heat transfer analysis can be used to estimate the sensible cooling to be obtained with a ventilating gas flow. Since this estimate does not allow for any heat transfer inside the gas distribution ducts, this estimate will be on the conservative side. With some suit designs, at low ventilating flow rates, it has been observed that the ventilating gas temperature approaches the suit outlet value before the gas leaves the distribution ducting.

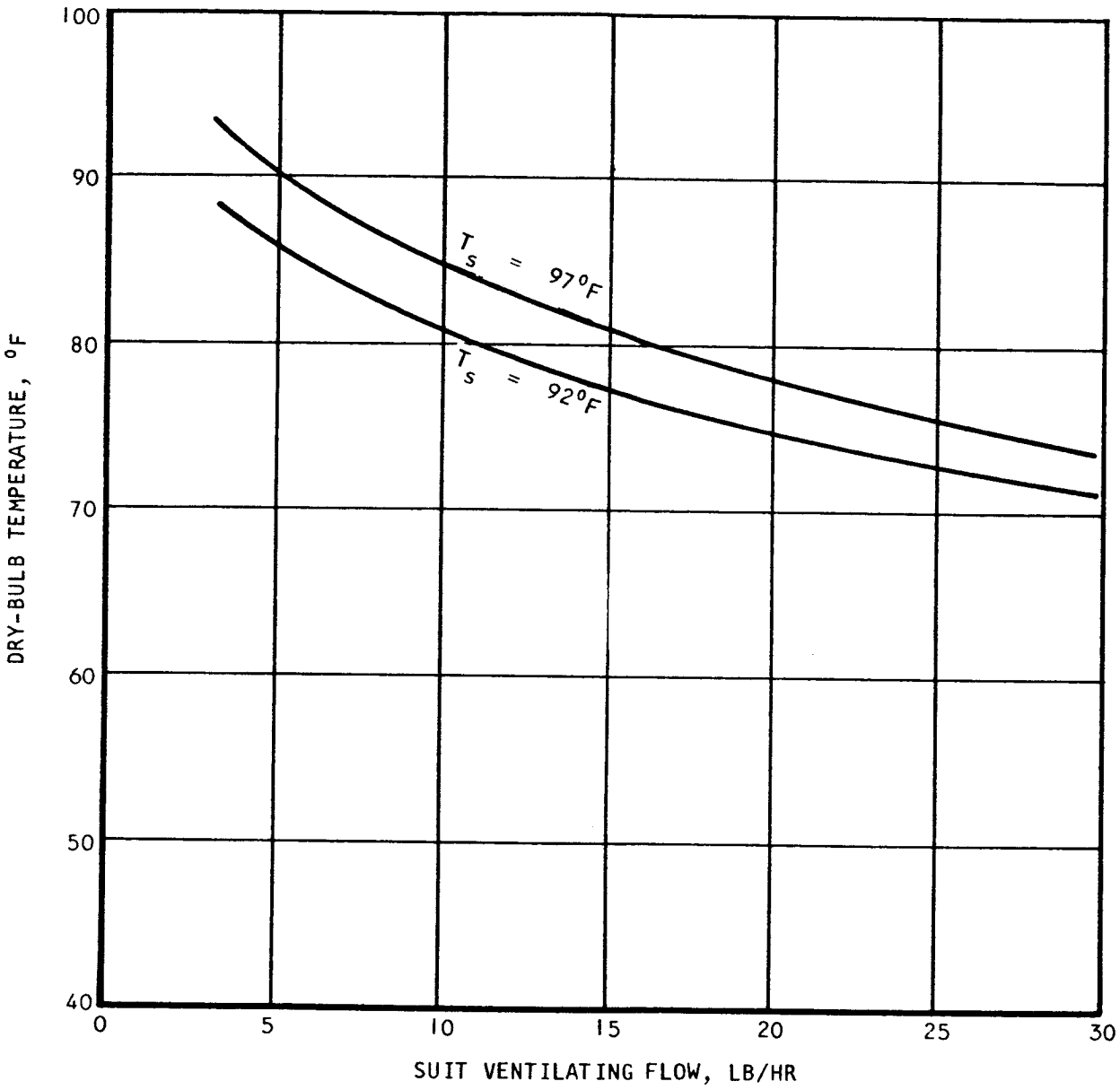

Figure 3-7. Estimated Suit Outlet Dry-Bulb Temperature for Inlet Temperature = 45°F

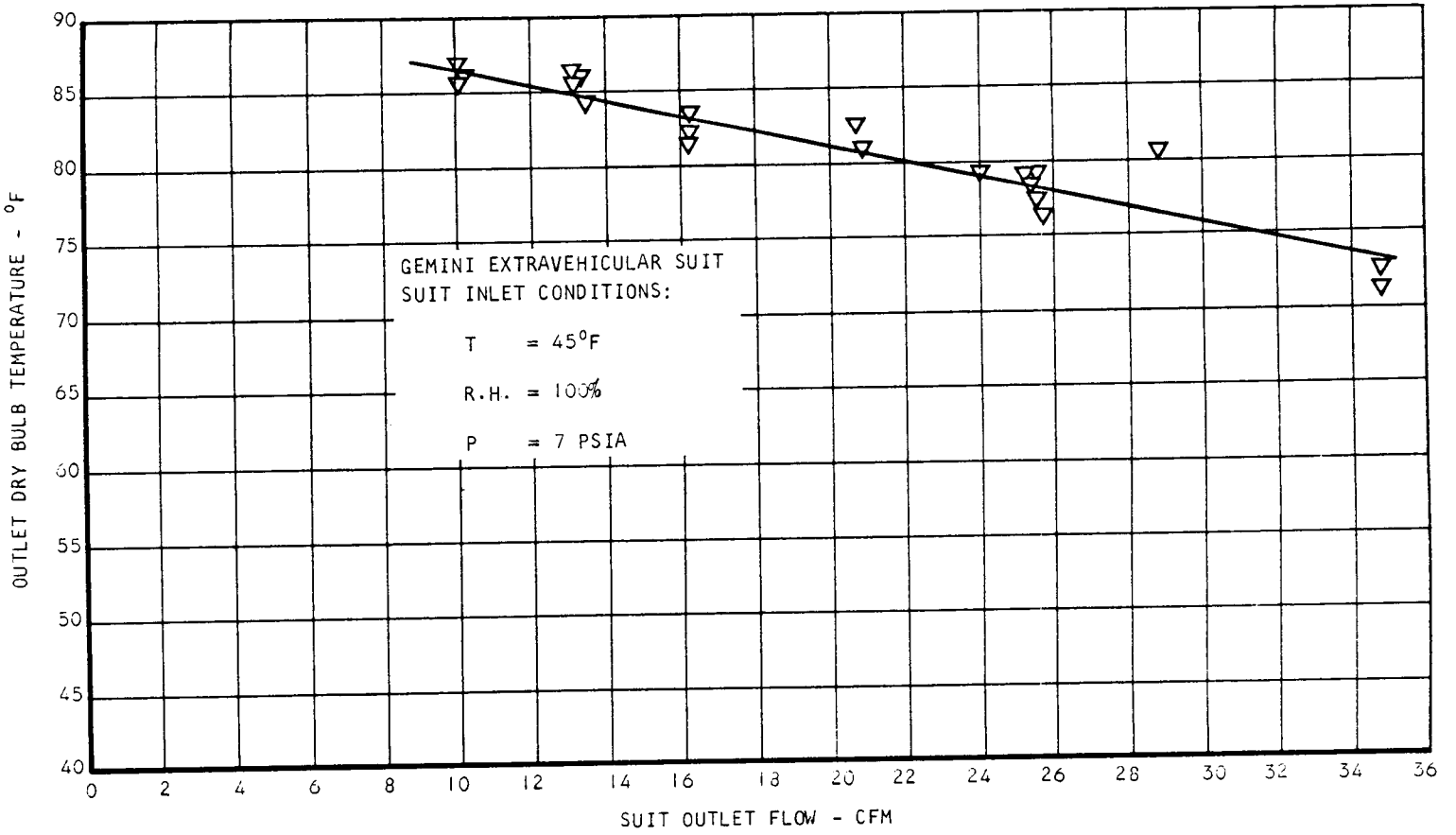

Figure 3-8. Measured Outlet Dry-Bulb Temperature vs Suit Outlet Volumetric Flow Rate

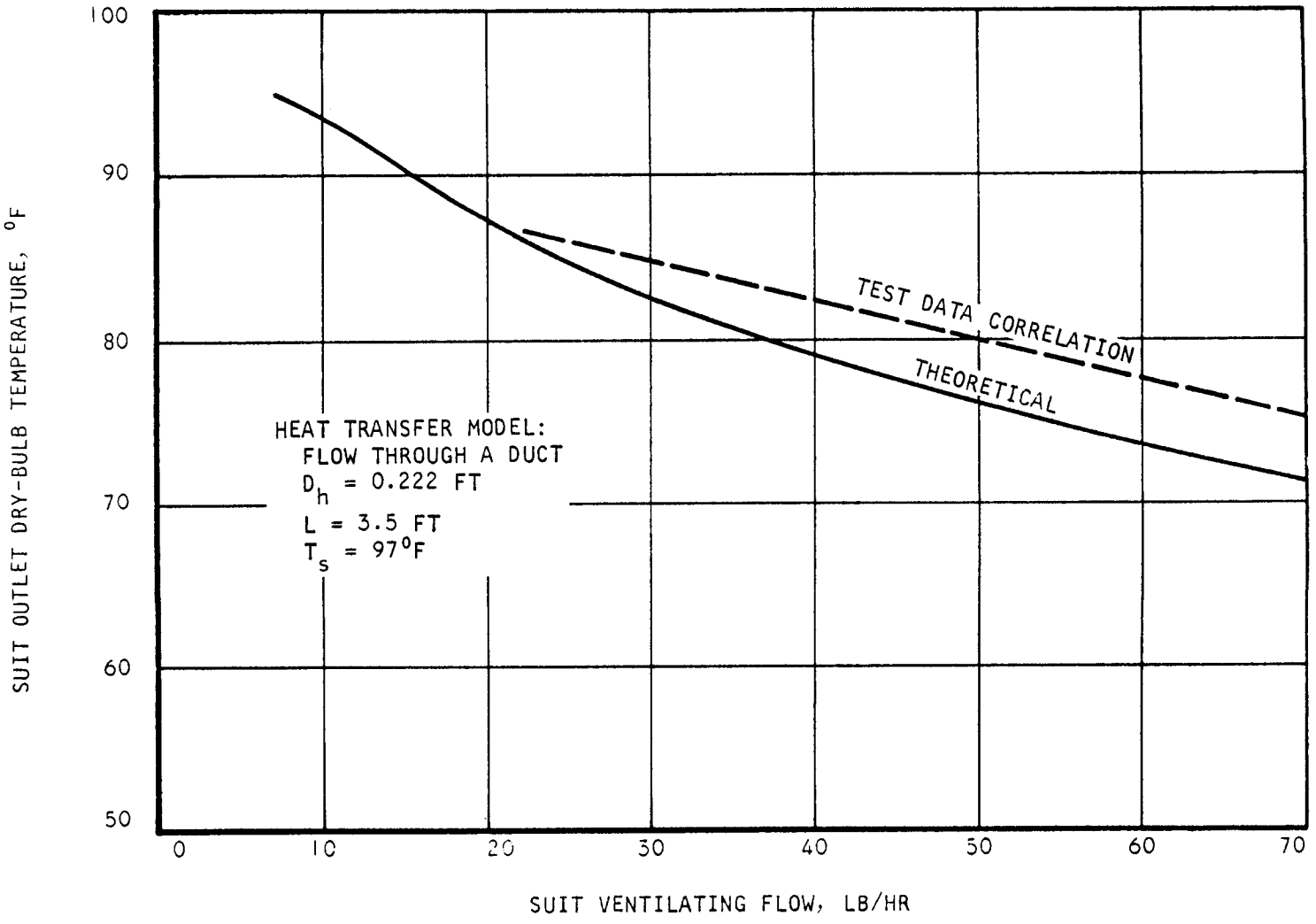

Figure 3-9. Comparison of Theoretical with Observed Suit Outlet Dry-Bulb Temperatures

2. Latent Heat Transfer

The mass transfer analog to Equation (3-12) (for laminar flow over a plane surface) is the following:

$$\frac{h_d L}{D} = 0.664\ Sc^{0.33}\ Re^{0.50} \qquad (3\text{-}20)$$

where h_d = mass transfer coefficient, ft per hour.

The characteristic length dimension, L, represents the length of the ventilating gas flow passage. The diffusion constant, D , is given by the following expression for diffusion of water vapor in air:

$$D = \frac{12.7}{P}\ \left(\frac{T}{460}\right)^{1.81}\ ft^2/hr \qquad (3\text{-}21)$$

The Schmidt number is then given by

$$Sc = \frac{\mu}{D\ \rho} = \frac{\mu RT}{P\ D} = \frac{\mu RT}{12.7}\ \left(\frac{T}{460}\right)^{-1.81} \qquad (3\text{-}22)$$

Therefore, the Schmidt number is independent of pressure and will be equal to approximately 0.523 for diffusion of water vapor in air at a temperature of $85^{0}F$.

The mass transfer coefficient, h_d, can be determined from Equation (3-20). Following is a material balance for an incremental section of the ventilating flow path:

$$h_d \rho_{H_2O}\ (m_{ws} - m_w)\ dA = \frac{\dot{m}\ M_{H_2O}}{M_a}\ dm_w \qquad (3\text{-}23)$$

where m_{ws} is the mole fraction of water vapor at the evaporating surface and m_w is the mole fraction of water vapor in the ventilating gas stream. By substitution, Equation (3-23) can be simplified and expressed in terms of water vapor partial pressures, as follows:

$$h_d\ [P_s - P_a]_{H_2O}\ dA = \frac{\dot{m}}{\rho}\ dp_{H_2O} \qquad (3\text{-}24)$$

Assuming constant water vapor partial pressure at the evaporating surface, the following expression can be obtained for the mass transfer effectiveness:

$$E_{mt} = \frac{[P_o - P_i]_{H_2O}}{[P_s - P_i]_{H_2O}} \left[1 - \exp\left(-\frac{h_d A\rho}{\dot{m}}\right)\right] \qquad (3\text{-}25)$$

The mass transfer effectiveness expression is analogous to that for heat transfer (Equation 3-16); the dimensionless group $\frac{h_d A\rho}{\dot{m}}$ represents the number of transfer units for mass transfer. The mass transfer coefficient, unlike the heat transfer coefficient, is dependent on pressure; Equation (3-25) together with Equations (3-20) and (3-21) show the mass transfer effectiveness, like heat transfer effectiveness, is independent of pressure when expressed as a function of mass flow.

Figure 3-10 shows the mass transfer effectiveness as a function of suit ventilating flow rate. The mass transfer effectiveness parameter is equivalent to the suit efficiency parameter given by Equation (3-4) and shown in Figure 3-2, if the suit outlet temperature is equal to the skin temperature. Since maximum suit efficiencies fall in the range from 40 to 60 percent, it is evident that the mass transfer effectiveness predicted by the material transport correlations will be somewhat high. Perhaps the most significant source of error in the analysis may be due to the assumption of uniform evaporation over the surface of the body. Because of the differing thermal characteristics of various areas of the body, this assumption is probably not valid even under conditions of severe thermal stress, where maximum sweat rates are obtained.

Figure 3-11 shows a correlation of the latent cooling capacity test data for the Gemini suit in terms of mass flow. This correlation is consistent with a mass transfer model based on flow through ducts, which is compatible with the previous correlation of sensible heat removal. The mass transfer analog of Equation (3-17) is the following:

$$\frac{h_d D_h}{D} = 1.86\, Sc^{0.33}\, Re^{0.33} \left(\frac{D_h}{L}\right)^{0.33} \qquad (3\text{-}26)$$

3. Combined Sensible and Latent Cooling

Based upon the previous analyses of sensible and latent heat transfer processes, estimates can be prepared for the total cooling effect to be obtained with suit ventilation. Figure 3-12 shows the maximum cooling to be obtained as a function of ventilating flow. It will be observed that a point of diminishing return is quickly reached with increasing ventilating flow, particularly when the increasing suit pressure drop is taken into consideration.

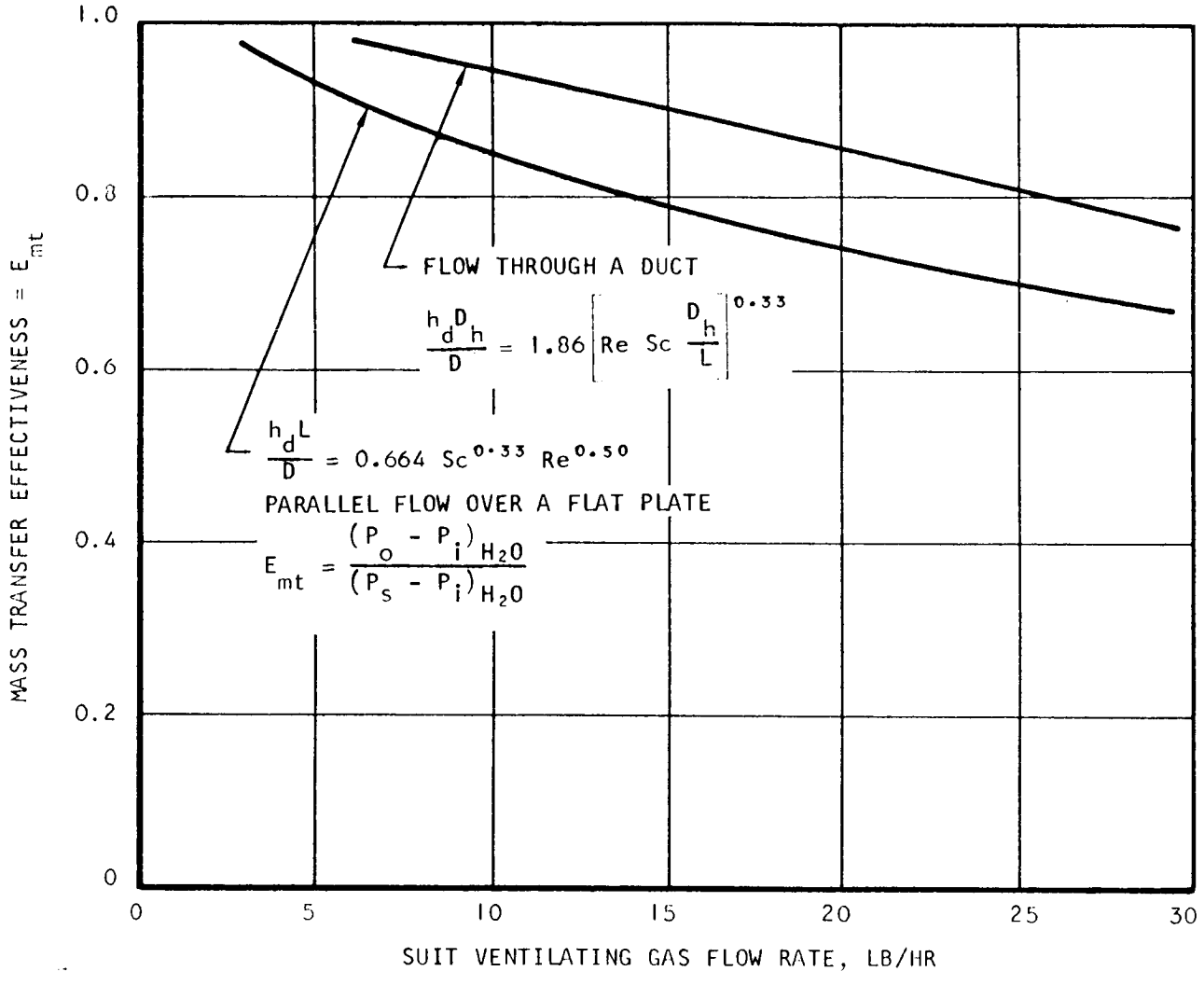

Figure 3-10. Estimated Mass Transfer Effectiveness for Suit Ventilating Gas Flow

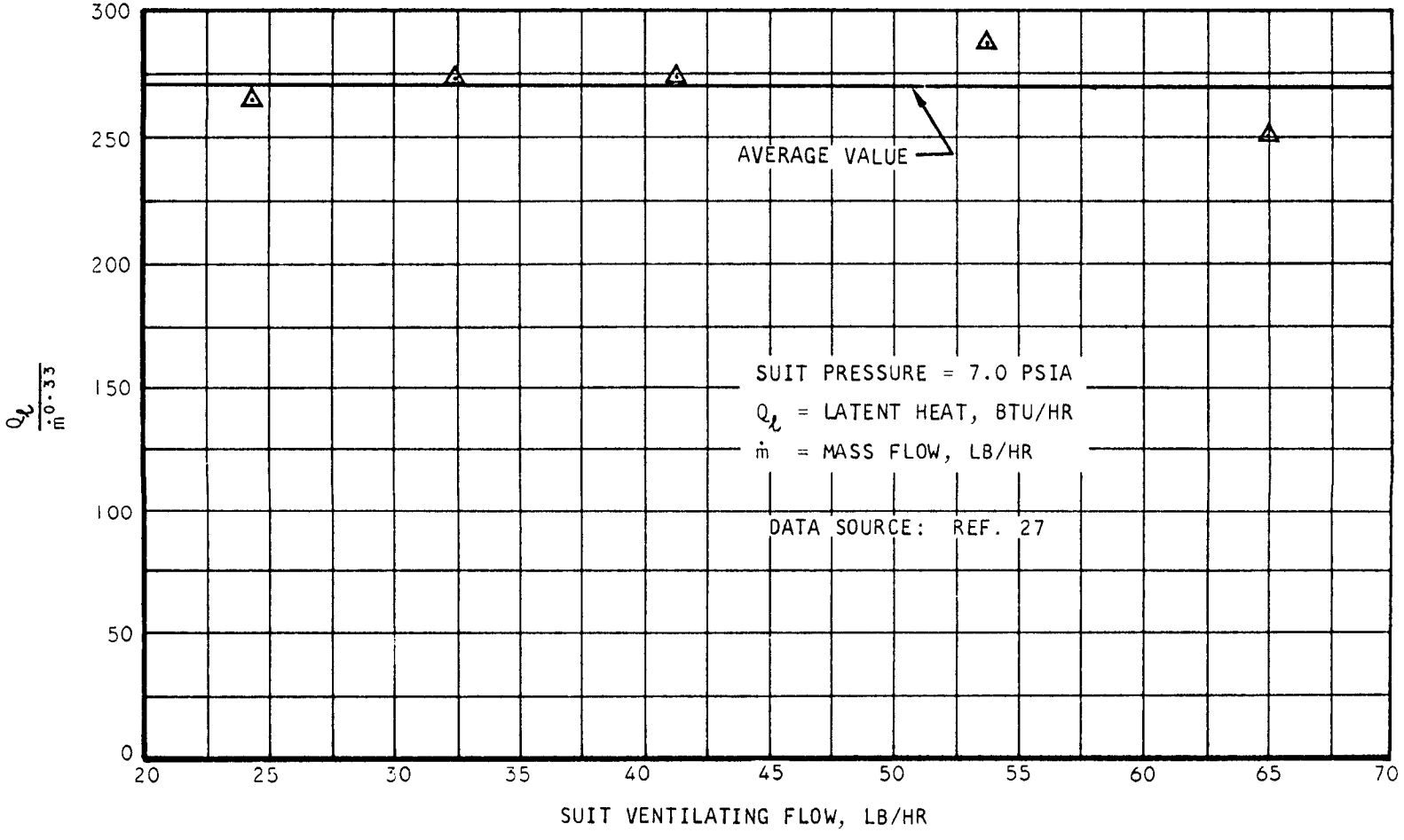

Figure 3-11. Mass Transfer Correlation of Suit Latent Cooling Data

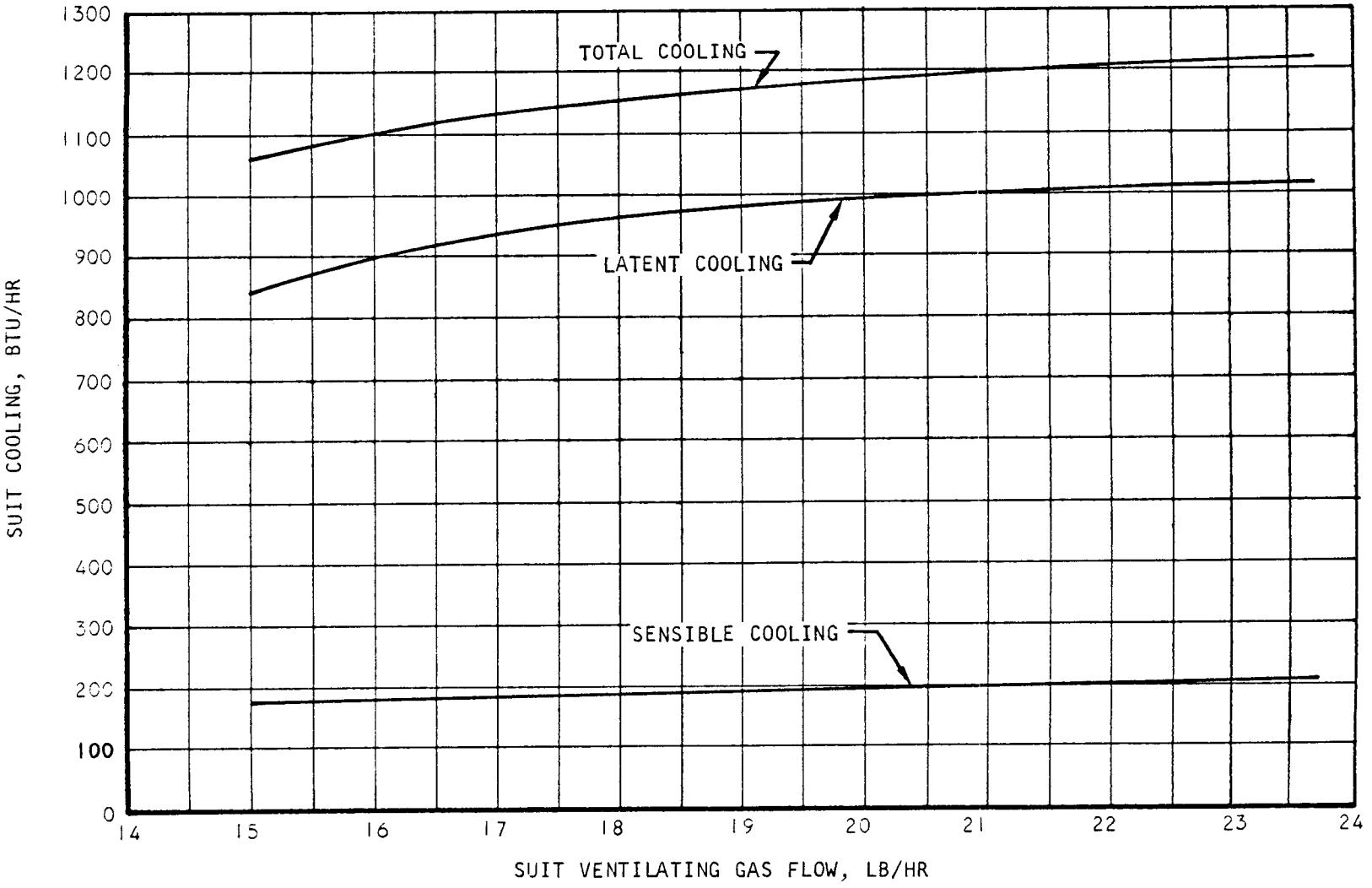

Figure 3-12. Estimated Maximum Cooling Capacity for Suit Ventilation at 3.5 psia

Therefore, it appears that ventilation cooling will be marginal with respect to performance for suit heat loads in excess of 1100 to 1200 Btu/hr. It will be noted from Figure 3-12 that the problem of high sweat rates will be alleviated only slightly by increasing the ventilating flow.

LIQUID-LOOP COOLING OF PRESSURE SUITS

Because of the relatively high density of liquid heat transport fluids compared with ventilating gases, liquid-loop suit cooling methods offer potential engineering advantage over suit ventilation, particularly at high metabolic rates, where large ventilating gas volume flows would be required to provide thermal adequacy. In addition, liquid-loop suit cooling provides a significant physiological advantage with respect to reduced sweat rates and reduced body temperatures under the high work rates obtained in pressurized suits.

Heat can be removed from the suit and transferred to the thermal transport loop by a number of different types of internal heat exchange device. These arrangements involve two basic principles: (1) conduction from the body by means of coolant tubes in contact with the skin and (2) evaporation of recycled water from the wicks in contact with the skin. The first arrangement involves use of full- or partial-coverage cooling garments inside the suit. The second scheme consists of a series of internal heat exchangers that condense water from the ventilating gas stream and return the condensate countercurrent to the ventilating flow (by means of wicks) for reevaporation. In this way, the water is repeatedly reevaporated at the same place and the cooling effect is obtained without eccrine sweating. The water that is recycled can be (1) introduced from an external supply, (2) provided in the original charge in the form of wet wicks, or (3) obtained from the body as perspiration.

Although the conduction methods are probably preferable from the standpoint of heat transfer efficiency, the reevaporative methods may offer advantage with respect to control simplicity, flexibility in handling varying heat loads, and ability to provide emergency cooling. Other internal heat exchange methods, such as those that depend upon radiation on to a liquid-cooled surface as the primary heat transfer process, do not appear to be competitive.

Conduction Cooling Heat Transfer Analysis

The liquid transport fluid will be distributed in a number of parallel small-diameter tubes covering all or part of the body surface area. For the case of streamline flow in small diameter tubes at low temperature differences, McAdams (Ref 52) gives the following heat transfer correlation

$$\frac{hd}{k} = 1.86 \left[\frac{4\dot{m}C_p}{\pi k L} \right]^{0.33} \qquad (3\text{-}27)$$

Following is a heat balance for heat transport fluid flowing through an element of tube length

$$h \pi \ (T_w - T) \, dL = \dot{m} \, C_p \, dT \qquad (3\text{-}28)$$

Integration of Equation (3-28) for constant tube wall temperature, T_w, results in the following expression for the transport fluid heat transfer effectiveness:

$$E_{tf} = \frac{T_o - T_i}{T_w - T_i} = \left[1 - \exp \left(- \frac{h \pi dL}{\dot{m} C_p} \right) \right] \qquad (3\text{-}29)$$

Figure 3-13 shows the heat transfer effectiveness as a function of coolant mass flow rate in terms of the heat transfer surface efficiency. Since not all of the tube area will be in contact with the skin, it would be expected that only a portion of the total surface area will be effective in removing heat from the body.

From comparison of the experimental data of Burton and Collier (Ref. 33) with the theoretical results in Figure 3-13, it would be estimated that the heat transfer surface efficiency is between 5 and 10 percent, averaging close to 8 percent for the first cooling garment configuration tested by Burton and Collier. For the second thermal garment, which involved a greater tube length, a somewhat lower surface efficiency is indicated in Figure 3-14. The reduction in performance, relative to theoretical performance, with increasing coolant flow may be explained by a decrease in skin temperature. Burton and Collier did not measure skin temperature, but assumed it to be constant at 91 ^{0}F in calculating thermal garment effectiveness. The data of Crocker, Webb, and Jennings (Ref. 34) indicate significant reduction in skin temperature with increasing heat removal rate. This would be expected, of course, if the body is assumed to offer a constant thermal resistance. Figure 3-15 shows the thermal conductance of the body as a function of liquid-loop heat removal rate. For the range of heat removal rate from 600 to 1600 Btu/hr, the thermal conductance appears to be essentially constant at an average value of approximately 75 Btu/hr-^{0}F. This corresponds to the lower limit on conductance obtained by other investigators under conditions of vasoconstriction (Ref. 3). Thermal conductances above this level represent the occurrence of vasodilation.

The liquid-cooled garment performance data reported in Ref. 33 and 34 were obtained with garments provided with approximately 240 ft (40 parallel tubes, each 6 ft in length) of tubing with a 0.125-in. outside diameter and a 0.060-in. inside diameter. The total heat transfer surface area is then 3.77 ft^2 (based on inside diameter) or 7.85 ft^2 (based on outside diameter). Burton and Collier calculated the tube surface area in contact with the body to be 0.45 ft^2 for the garment. This represents 5.7 percent of the total outside surface area of the cooling tubes which is in approximate agreement with the performance shown for this garment in Figure 3-14.

Conduction Cooling Comfort Analysis

Where the body is cooled by conduction, somewhat similar comfort considerations will be applicable. The inherent thermoregulatory mechanisms may be less effective in maintaining internal temperature in the desired range with conduction cooling of the body, since the sweat mechanism will not be used in the thermal control processes. Therefore, temperature control

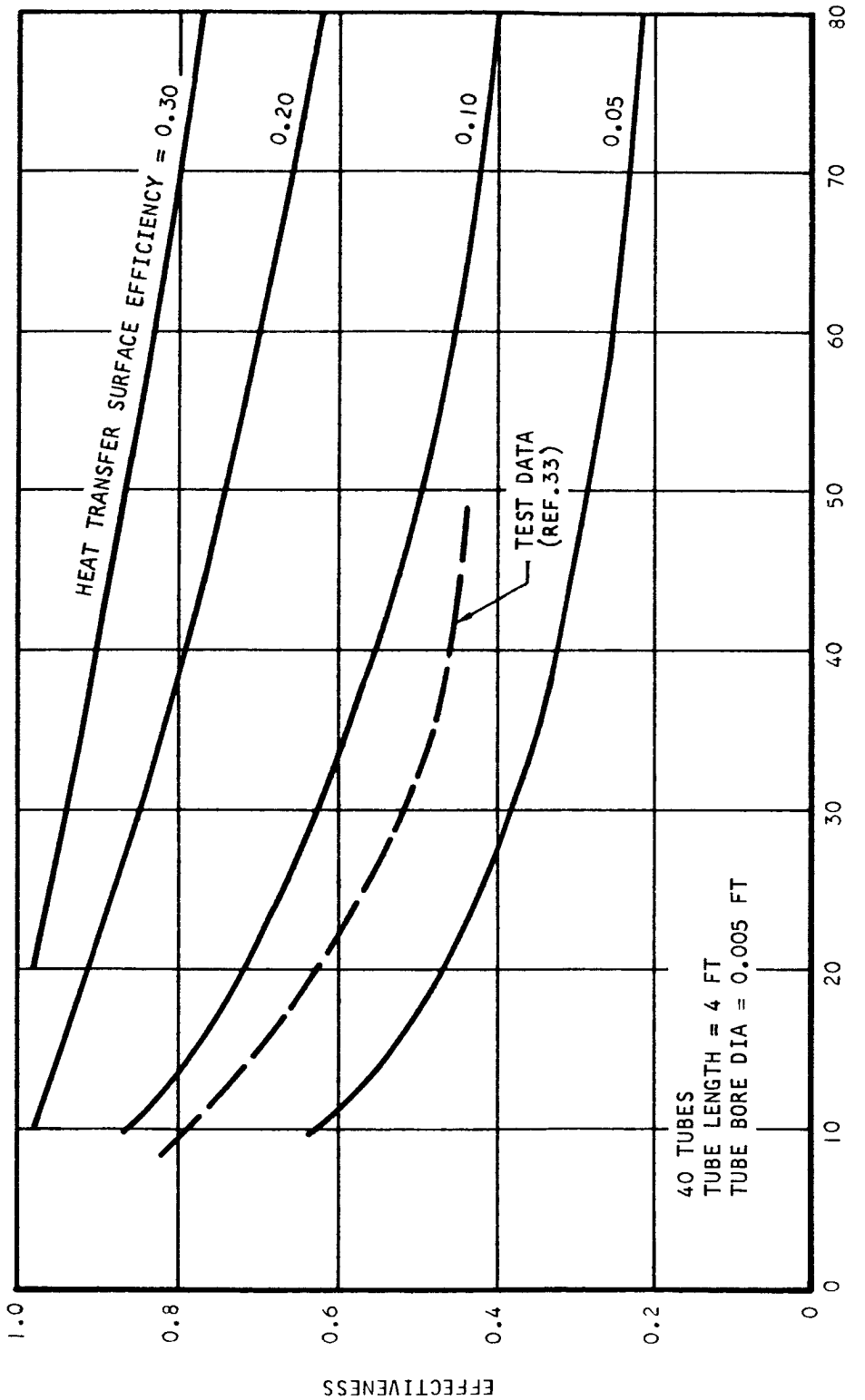

Figure 3-13. Estimated Effectiveness for Liquid-Loop Suit Cooling

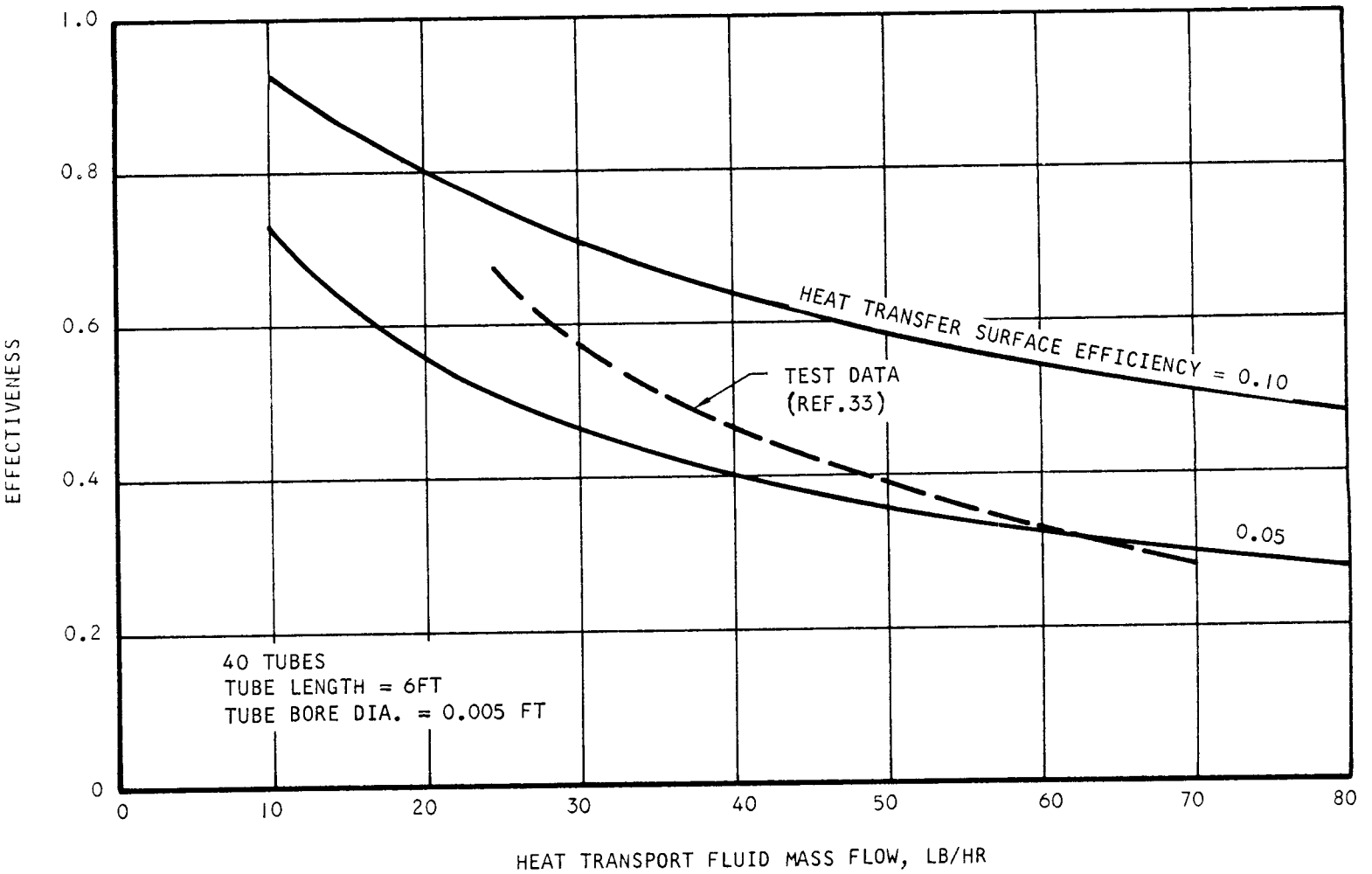

Figure 3-14. Estimated Effectiveness for Liquid-Loop Suit Cooling

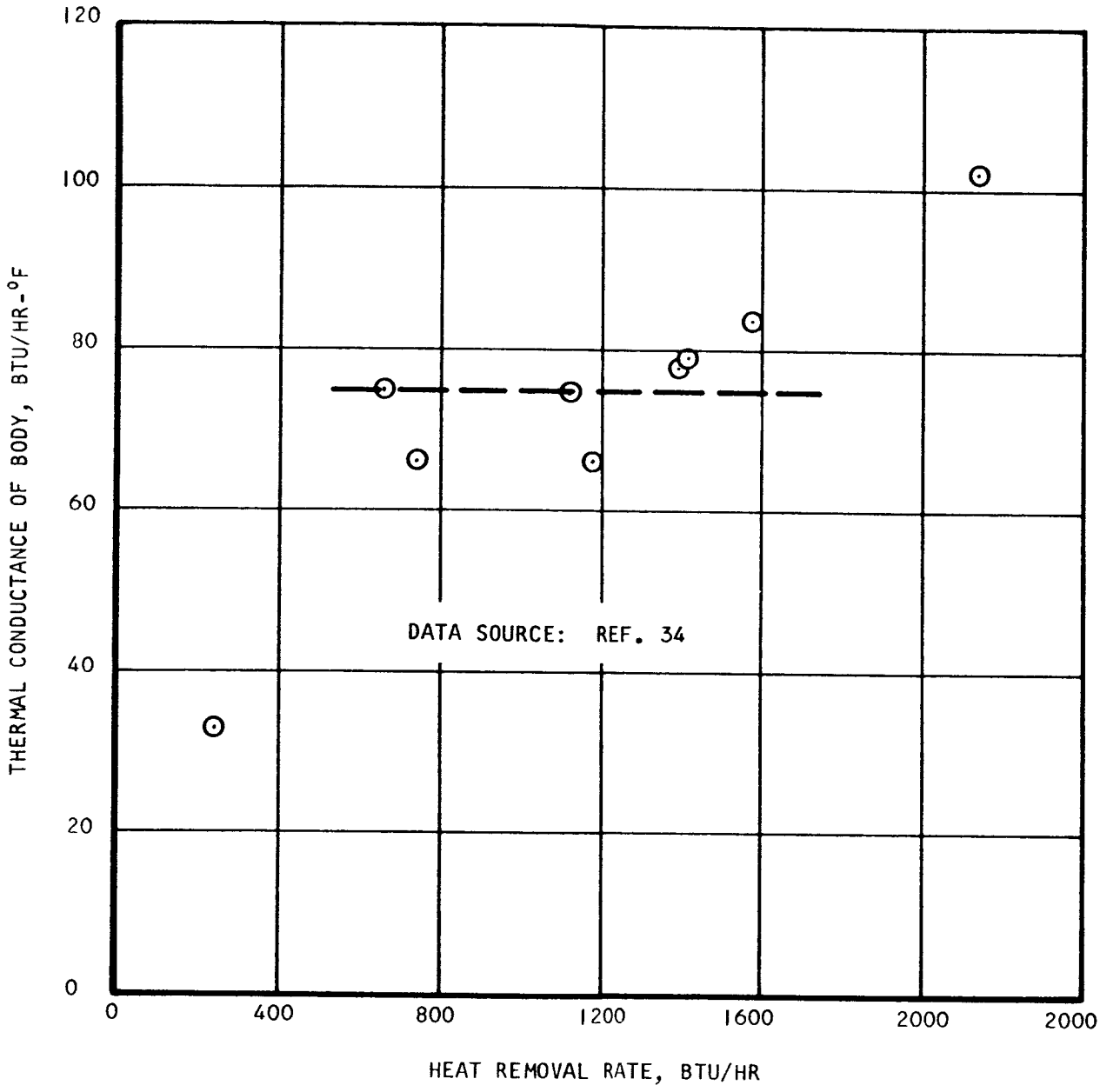

Figure 3-15. Thermal Conductance of Body with Liquid Loop Cooling

may be a more difficult problem, since metabolic rates can vary over a wide range, and conduction cooling tends to provide constant heat removal rates.

The approach to be used here for establishing comfort conditions for conduction cooling is based upon maintaining skin temperature within a specified range, bounded on the high side by the onset of active sweating and on the low side by the occurrence of shivering.

1. Zero Sweat Rate Criterion

The requirement for zero eccrine sweating has been specified for the liquid transport systems to be used with extravehicular suit assemblies. The previously cited physiological data of Kerslake (Ref. 7) and Benzinger (Ref. 1, 2, 3) can be analyzed to establish the conditions consistent with the requirement for zero eccrine sweat rate. For example, if the sweat rate is set equal to zero in Equation (2-5), the following expression is obtained for the skin temperature as a function of the body heat flux:

$$(T_s)_{Q_t = 0} = T_{so} - \frac{C_2 Q_t}{A} \qquad (3\text{-}30)$$

Using the range of C_2 obtained by Kerslake (from 0.065 to 0.085 Btu per hr-ft^2-^{0}F), it can be demonstrated that the skin temperature for zero sweat rate decreases with increasing metabolic rate and that the frequently cited sweating threshold of 91.4^{0}F is applicable to low metabolic rates only. This is illustrated in Figure 3-16. Benzinger's data (shown in Figure 2-2) indicate supression of the onset of vasodilation and active sweating with reduced skin temperature. These data can also be used as the basis of another zero sweat rate criterion, if the effective conductance of the body is known. Under the condition for no active sweating, it appears reasonable to assume occurrence of the minimum skin conductance (for full vasoconstriction) of 3.3 Btu per hr-ft^2-^{0}F. The zero sweat rate criterion developed from Benzinger's data is also shown in Figure 3-16. It will be noted that there is a significant difference between the zero sweat rate skin temperature correlations. This may be accounted for by differences in experimental conditions or in methods of calculating mean skin temperatures. Shown for comparison in Figure 3-16 are the skin temperature data of Crocker, Webb, and Jennings (Ref. 34) obtained with a liquid-cooled garment. Presumably, these tests were conducted under conditions where very low eccrine sweat rates were obtained. The liquid-loop cooling skin temperature data correlates fairly closely with the zero sweat skin temperature correlation derived from Benzinger's data. Therefore, it appears appropriate to base the zero sweat criterion for conduction cooling upon the liquid-loop data.

2. Shivering Limit Criterion

The commonly specified skin temperature limit of 84^0 to 86^{0}F for the onset of shivering applies to low metabolic rates. Like the skin temperature limit for onset of sweating, the skin temperature level representing the threshold for shivering decreases with increasing metabolic rate. Crocker,

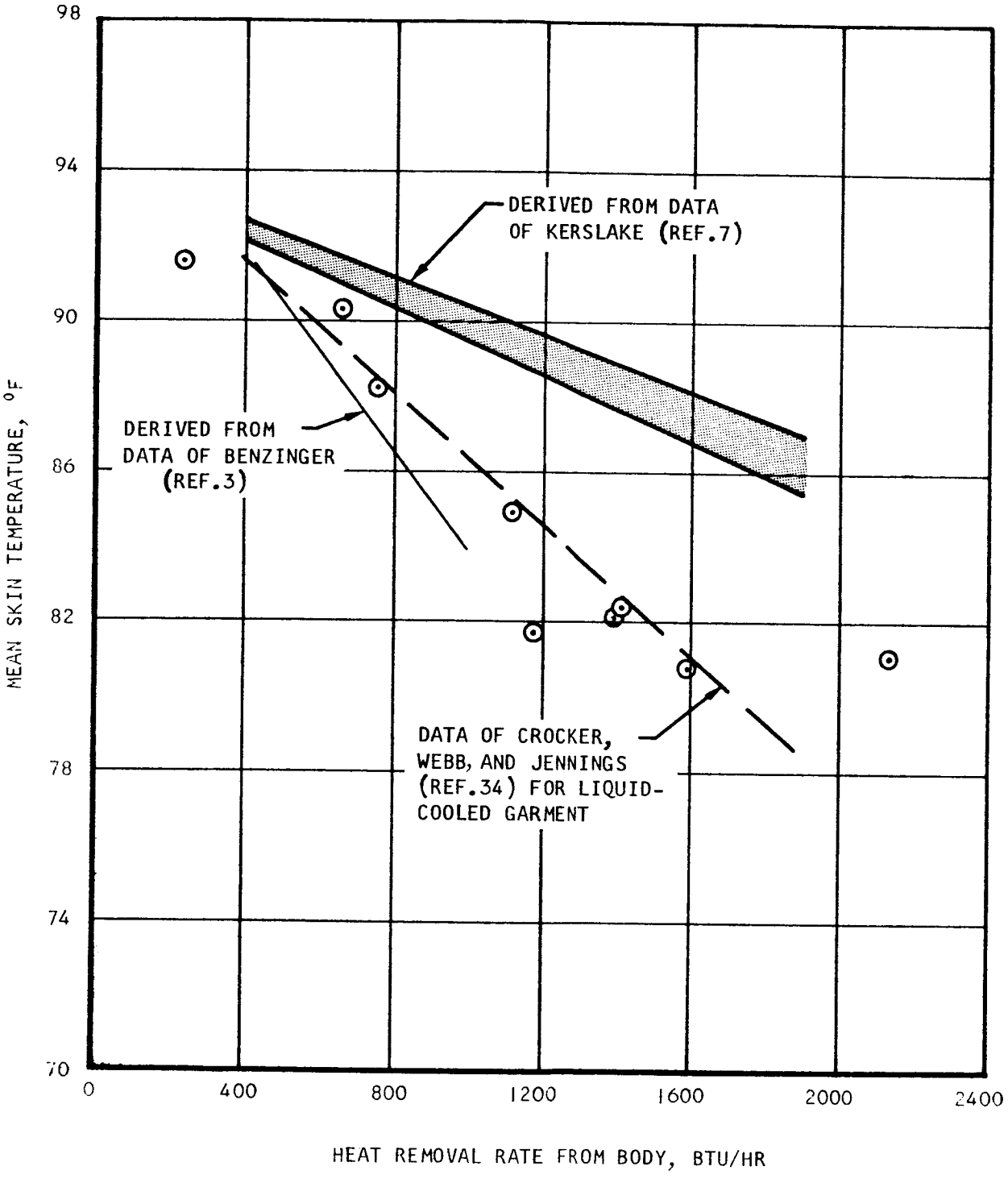

Figure 3-16. Mean Skin Temperature Correlation at Zero Sweat Rate

Webb, and Jennings (Ref. 34) cite the data of Cannon and Keatings (Ref. 55) (for the minimum skin temperature at which shivering provides a steady if depressed internal temperature level) to establish a minimum skin temperature level for conduction cooling of the body.

Another criterion for minimum skin temperature can be based upon heat loss from the body under conditions of vasoconstriction produced by cold conditions. Nielson (Ref. 56) obtained conductances ranging from 59 to 88 Btu per hr-^{0}F for a subject working at low skin temperatures. Assuming an internal temperature of 98.0^{0}F, the shaded area shown in Figure 3-17 represents the range of body heat loss predicted as a function of mean skin temperature from Nielson's data. Presumably, within this range it is possible to obtain a steady-state heat balance at internal temperature levels consistent with the thermoregulatory set-point. Consequently, thermal adaptation to this range of skin temperature should be possible without shivering. The limit defined by the body conductance of 3.3 Btu per hr-ft^{2}-^{0}F will be used as a lower boundary in the conduction cooling comfort zone.

3. Conduction Cooling Comfort Zone

Figure 3-18 shows the conduction cooling comfort zone, based upon the previous analyses of the skin temperature limits established on one side by sweating and on the other side by shivering. It is evident that the range of skin temperature indicated for thermal comfort is fairly narrow, particularly at the lower heat removal rates. The requirement for zero eccrine sweat rate is unnecessary from a comfort standpoint, since comfort conditions can be obtained at high sweat rates if adequate latent cooling capacity is provided. However, for reasons discussed previously, it is highly desirable to minimize sweat rates. It should be noted that the previous analysis did not consider the problem of thermal sensations. The available data indicate that at high work rates the reduced skin temperatures will be subjectively acceptable.

Comparison of Conduction and Radiation Liquid-Loop Cooling

It has been proposed to design a liquid transport suit cooling system that depends upon radiation from the skin to the coolant tube walls as the primary means of removing heat from the body. This approach can be shown to be much less efficient in terms of effective cooling capacity per unit tube area than removing the heat from the body by conduction to the tubes. Figure 3-19 shows the relative cooling capacity for radiation and conduction cooling of the body, as a function of the coolant temperature level. Although the effective area for conduction cooling is much less than that assumed for radiation (0.45 ft^{2} as compared with the total tube area of 7.85 ft^{2} assumed for radiation), the cooling rate for conduction cooling of the body (based upon the data of Ref. 34) is much greater. It should be emphasized that this comparison is based upon comparable garment designs; in one design, the tubes are maintained in close contact with the skin for conduction cooling, and in the other, the tubes are spaced from the body for radiation cooling. Even if the heat transport garment provided complete coverage of the body, it does not appear that radiation cooling would be competitive with the conduction

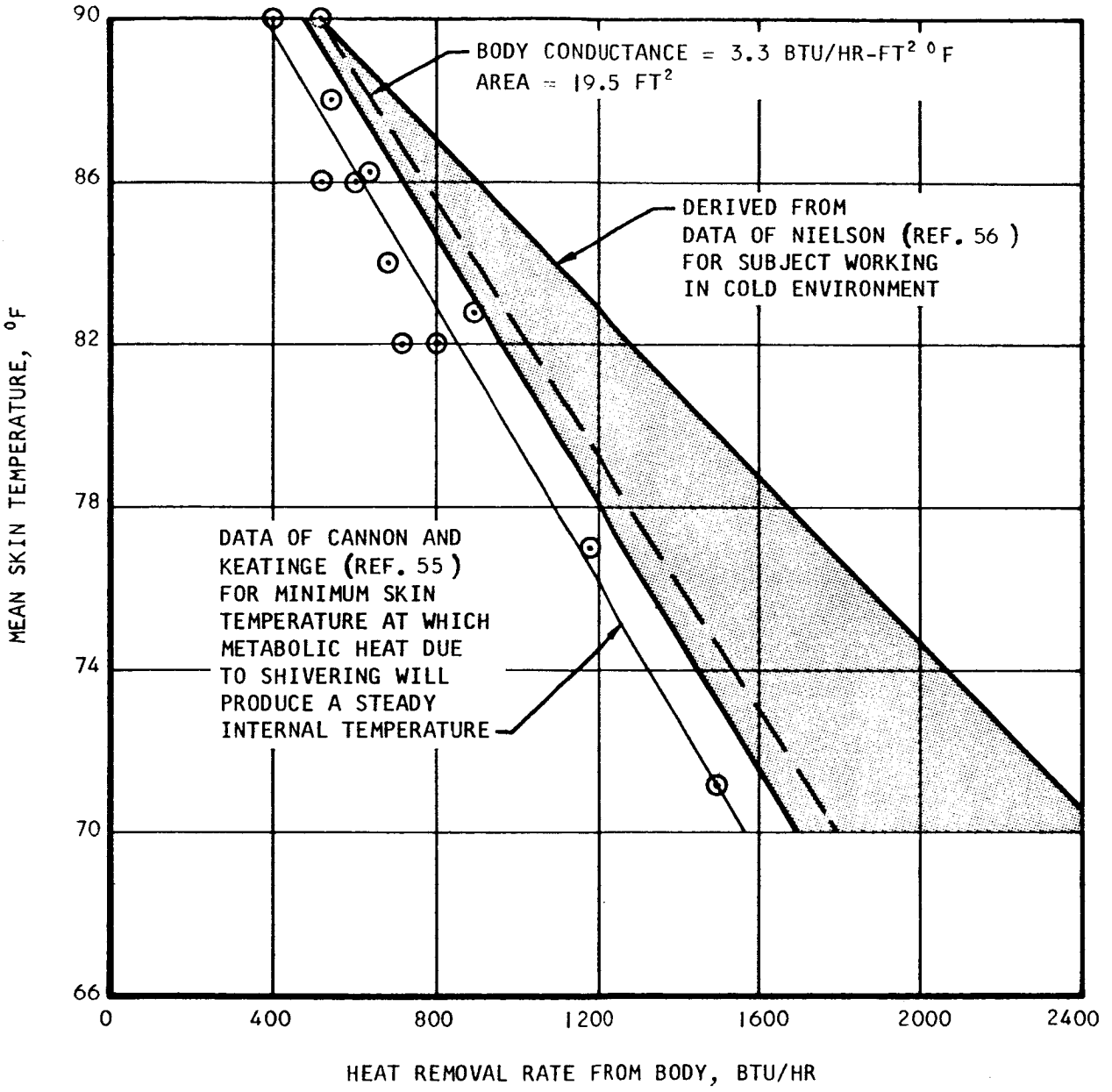

Figure 3-17. Mean Skin Temperature Correlation for Shivering

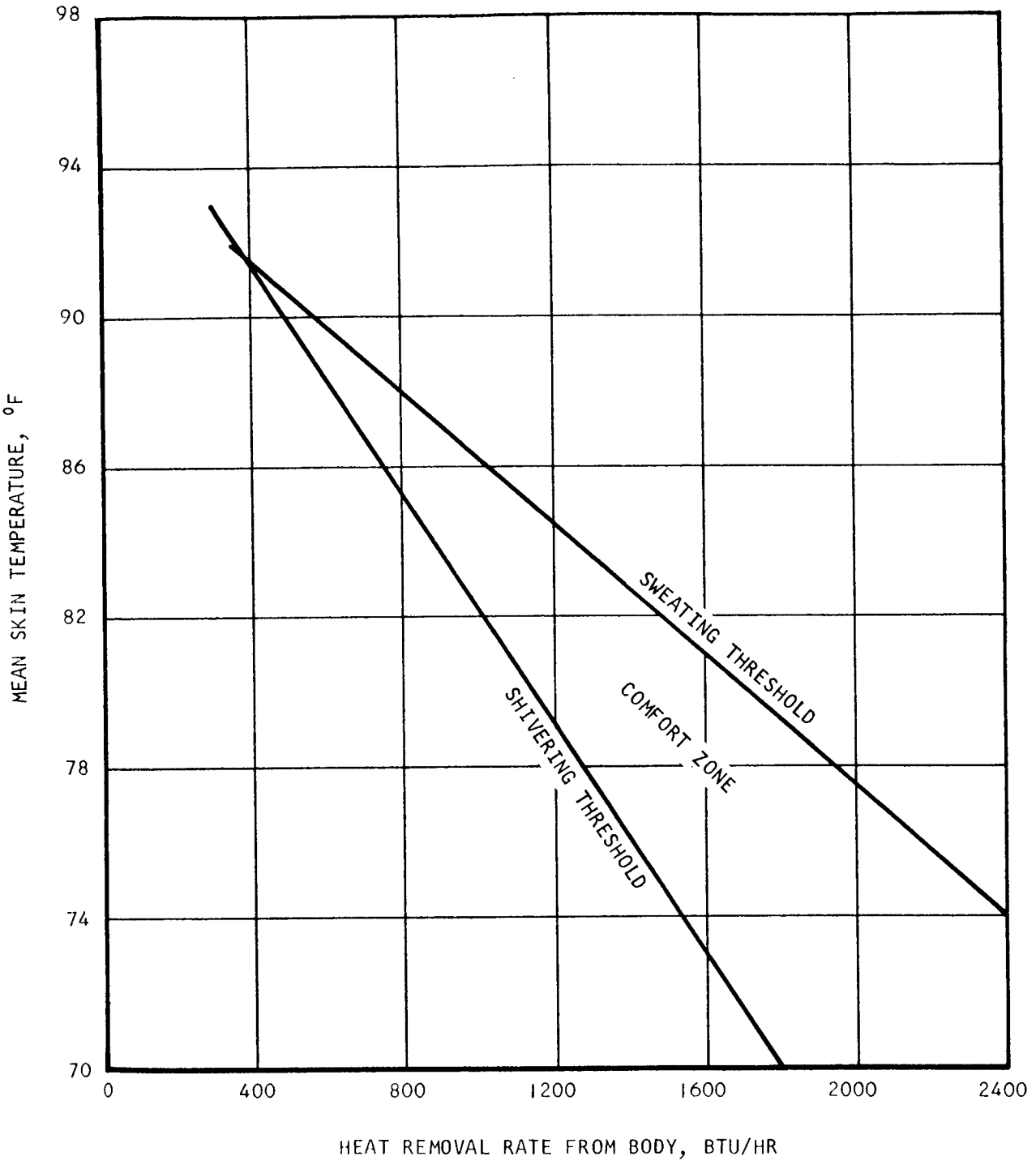

Figure 3-18. Conduction Cooling Comfort Zone

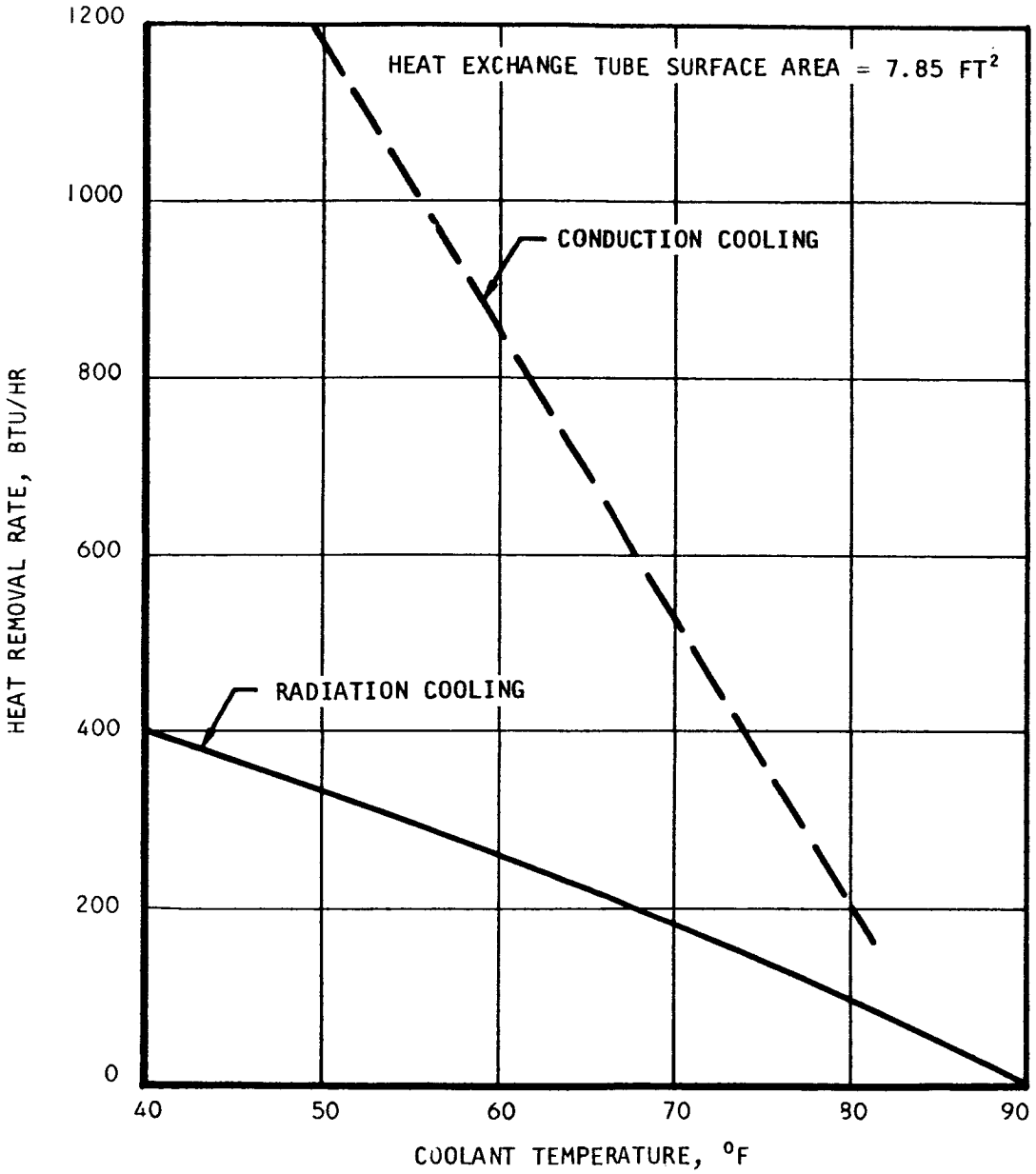

Figure 3-19. Comparison of Conduction and Radiation Suit Cooling with Liquid Transport Loop

cooling technique from a heat transfer standpoint. However, there may be other considerations involving crew acceptance resulting from the lack of physical constraint by skin contact that might favor the radiation cooling technique.

Estimated Liquid-Loop Performance

The previous heat transfer analysis for liquid-loop suit cooling can be used for performance predictions, if allowances are made for the temperature drop due to conduction through the coolant tube walls. Assuming the inner wall of the coolant passages to be at T_w and the outer wall to be at the mean skin temperature, T_s, the heat conduction through the tube wall with an effective area, A_{eff}, is given by

$$Q = \frac{k_t A_{eff}}{L_t} (T_s - T_w) \tag{3-31}$$

where k_t and L_t represent the thermal conductivity and the thickness of the tube wall, respectively. The heat transfer to the coolant is given by

$$Q = E_{tf} \dot{m} C_p (T_w - T_i) \tag{3-32}$$

Combination of Equations (3-31) and (3-32) with elimination of T_w results in the following expression for the heat transport through the coolant tubes:

$$Q = \frac{\dot{m} C_p E_{tf} (T_s - T_i)}{1 + \frac{\dot{m} C_p E_{tf} L_t}{k_t A_{eff}}} \tag{3-33}$$

By differentiation of Equation (3-33) with respect to T_i for constant T_s, E_{tf}, and $\dot{m}$, an expression can be obtained for evaluation of the parameter $\frac{k_t A_{eff}}{L_t}$ in terms of the variation of the heat removal rate with coolant inlet temperature. From the data given in Figure 2-23,

$$\frac{k_t A_{eff}}{L_t} = 58.8 \text{ Btu/hr-}^{\circ}\text{F} \tag{3-34}$$

Figure 3-20a shows the results of heat transfer calculations using heat transfer surface efficiencies comparable to those obtained by Burton and Collier (Ref. 33) while neglecting the tube wall temperature drop. Figure 3-20b gives equivalent performance after allowing for the tube wall temperature drop represented by the value of the heat conduction parameter given by Equation (3-34). It will be noted that the thermal resistance of the tube wall will significantly affect performance, particularly at high heat fluxes. Shown for comparison in Figure 3-20b are the performance data obtained from References 33 and 34. It appears that a reasonable correlation is obtained for the data obtained by two different investigators using liquid-cooled garments of similar design characteristics. Attainment of higher performance will require increased effective area coverage of the body or reduction in the tube wall thermal resistance (by increased thermal conductivity or reduced wall thickness).

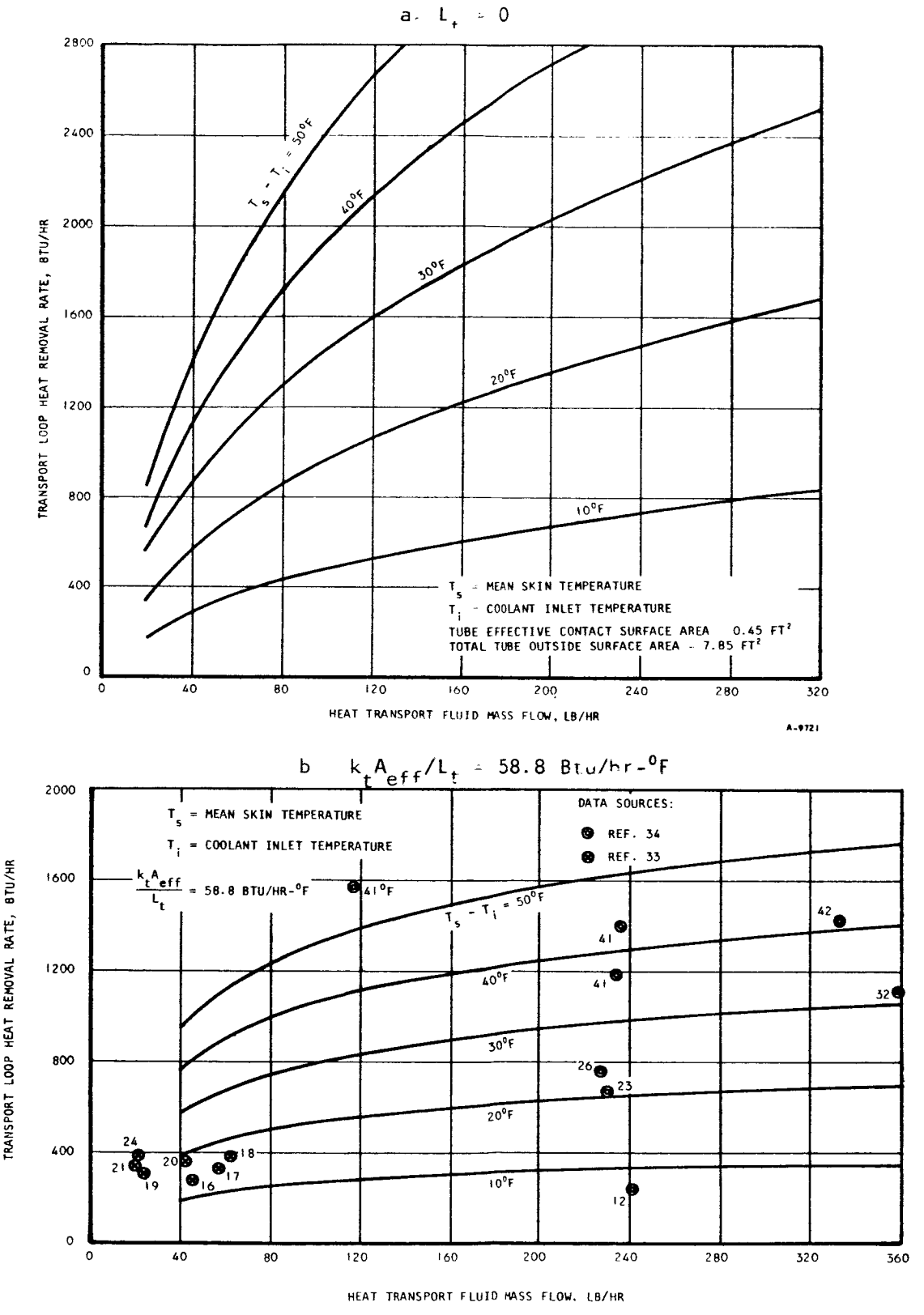

Figure 3-20. Estimated Extravehicular Suit Heat Removal Rates for Liquid-Loop Cooling

RADIATION COOLING (CONDUCTION FROM BODY)

In order to evaluate the possibility of a passive thermal control system for an extravehicular suit based upon the principle of heat conduction from the skin to the suit outer wall, computations were made based upon the thermal properties of an existing suit design (the Gemini suit). It should be recognized that an extravehicular suit designed for passive thermal control would have thermal properties tailored for that purpose. Figure 3-21 shows the heat balance used for the extravehicular suit heat balance studies. Section 5 of this report describes the extravehicular heat balance calculation methods.

When heat conduction through the walls of the extravehicular suit is taken into account, the surface temperature distribution will be substantially different from the equilibrium temperatures with zero heat leak. Figure 3-22, for example, shows the surface temperature distribution for the case where the skin is in contact with the inner wall of the suit. In this case, the composite suit thermal characteristics are represented by an equivalent thermal conductivity of 0.02 Btu/hr-ft with a wall thickness of 0.35 in. (Ref. 45). For the conditions shown, the temperature gradient around the body is reduced from 300°F to approximately 100°F. The corresponding heat leak represents a net loss of 337 Btu/hr. Figure 3-23 shows the heat flux distribution. The portion of the suit facing the sun has a maximum input heat flux of 35 Btu/hr-ft^2, while the dark-side portion of the suit has an output heat flux of between 30 and 40 Btu/hr-ft^2. The heat flux integrated over the area of the body leads to a net heat loss of 337 Btu/hr for the conditions specified.

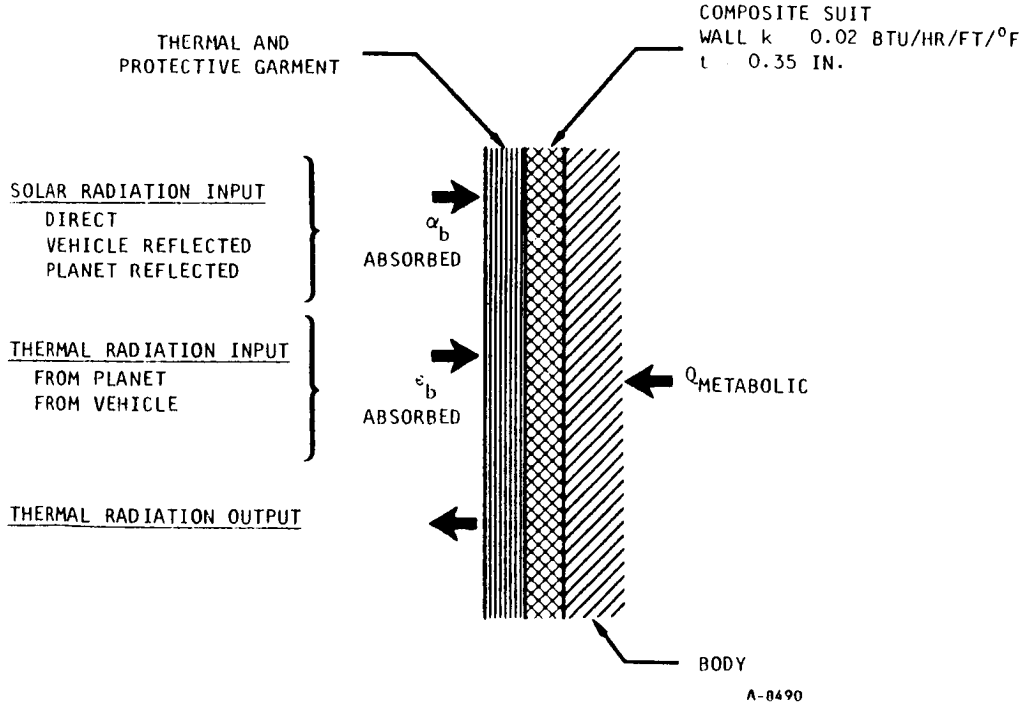

Figure 3-21. Heat Transfer Model for Radiation Cooling of the Extravehicular Suit with Heat Conduction from the Skin through the Suit Wall

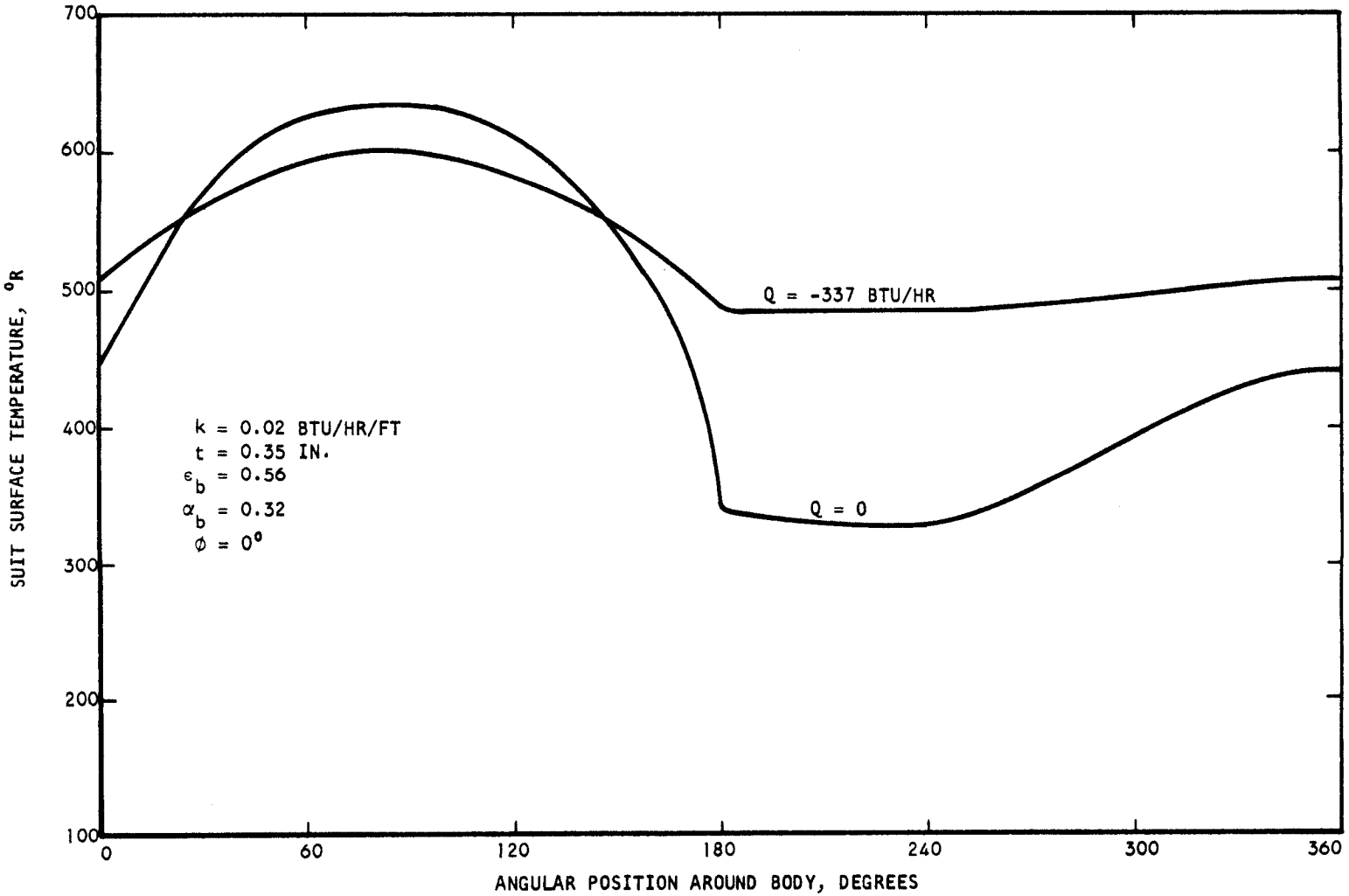

Figure 3-22. Effect of Heat Transfer on Extravehicular Suit Surface Temperature (160-nm Earth Orbit)

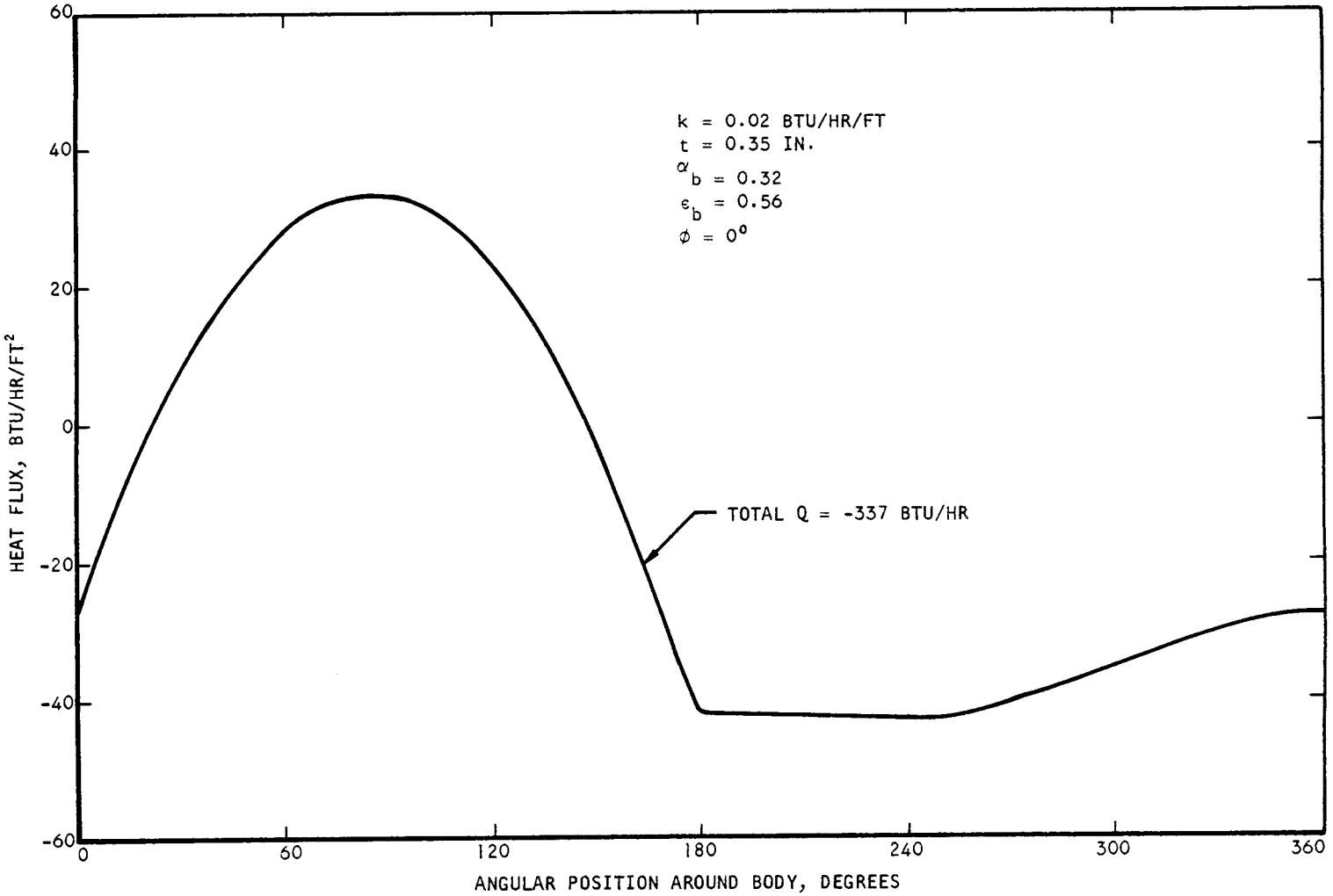

Figure 3-23. Typical Heat Flux Distribution for Radiation-Conduction Cooling in Extravehicular Suit

The variation in the total heat leak from the extravehicular suit with the orbital parameters is given in Figure 3-24. For the extravehicular suit characteristics used here, the suit heat leak will range from 200 to 700 Btu/hr.

It should be emphasized that the values shown in this study are based upon the assumptions that equilibrium conditions will be attained and that peripheral heat conduction in the garment will be negligible. Thermal inertia will substantially modify these curves, although cursory calculations indicate that the extremes indicated will be attained, unless special provisions in the form of heat storage materials are added to the suit. The short-duration peaks, however, will be reduced, both by system thermal capacity and the ability of the body to adjust to varying environmental conditions. Where the orbital plane is normal to solar radiation ($\phi = 0^0$), the heat leak from the suit remains constant at -340 Btu/hr. Where the orbital plane is parallel to the solar radiation, an average heat leak rate of approximately -600 Btu/hr is obtained.

Other methods of modifying the heat rejection rate from the suit involve use of thermal insulation and of different spectral characteristics for the outer surface. Addition of insulation and use of an outer surface with a higher thermal emissivity would serve to maintain heat rejection rate while reducing its range of fluctuation.

One of the problems with the concept considered here results from collection of insensible perspiration on the inner wall of the suit. This could be accommodated by use of porous wall materials permitting diffusion of water vapor overboard or by use of an inner garment that collects the moisture. An inner garment would serve the additional purpose of providing thermal insulation to assist in thermal regulation.

RADIATION COOLING (RADIATION FROM BODY)

A passive cooling system in which an air gap is located between the body and the suit inner wall requires a less radical new extravehicular suit concept than the previous case where the suit wall provides conduction cooling of the body. Figure 3-25 shows the heat transfer model used in system thermal analysis. As before, the baseline suit thermal characteristics are based on a state-of-the-art suit assembly (the Gemini suit). In this case, different characteristics of the suit will be varied parametrically to determine what effect they have on suit heat leak.

For the case where an air gap separates the inner wall of the suit from the body, an additional thermal resistance, represented by the air gap, appears in the heat transfer path. If the gas is essentially stagnant or it flows through the gap at relatively low velocities, the thermal resistance is primarily determined by radiative heat transfer. The addition of the internal air gap significantly reduces the heat loss from the extravehicular suit. Figure 3-26, for example, shows the heat flux distribution for the case with the air gap. (Figure 3-27 shows the heat flux for equivalent conditions without the air gap). Comparison of the two figures shows that the maximum

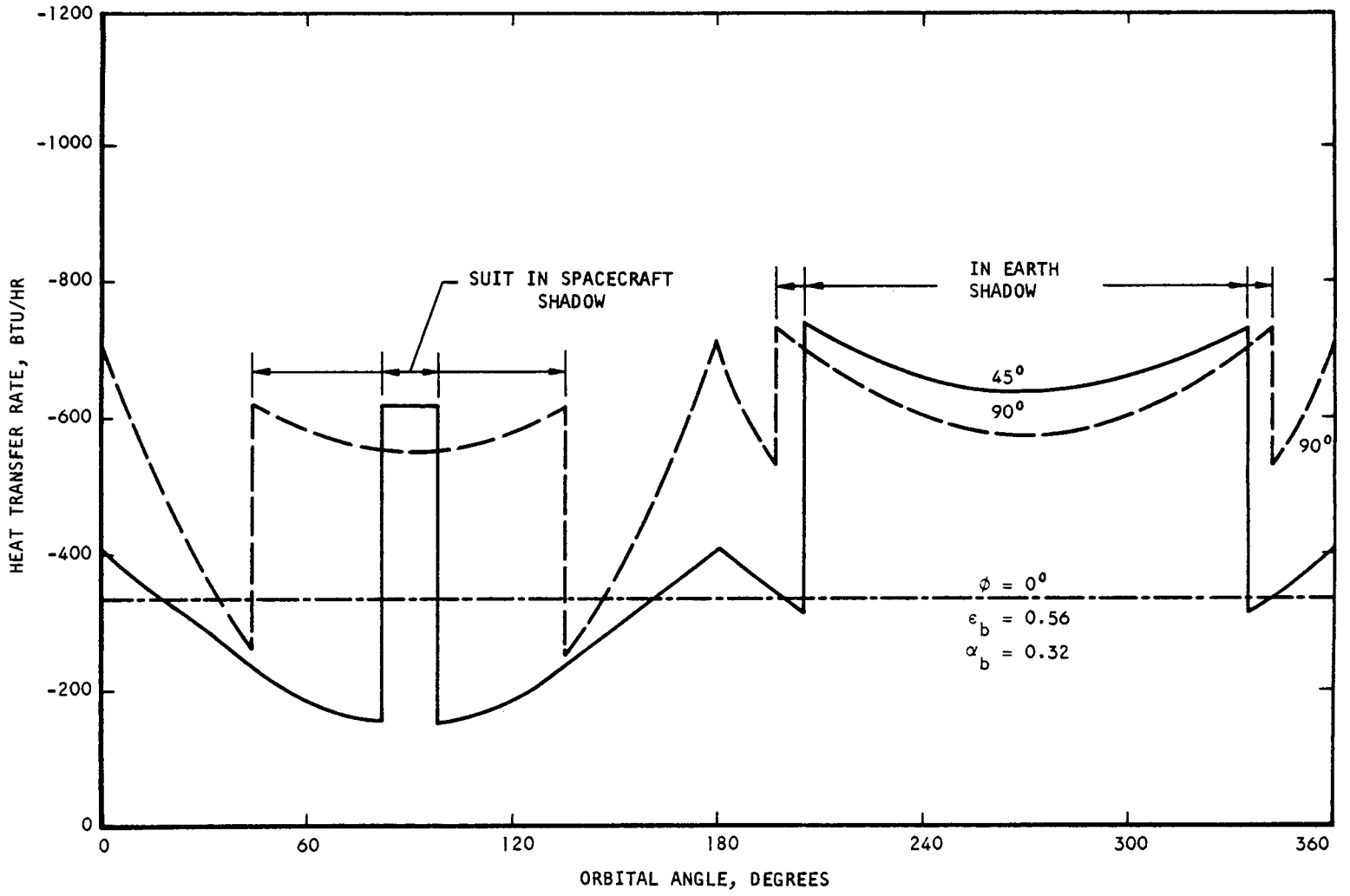

Figure 3-24. Heat Rejection Variation with Position in 160-nm Earth Orbit

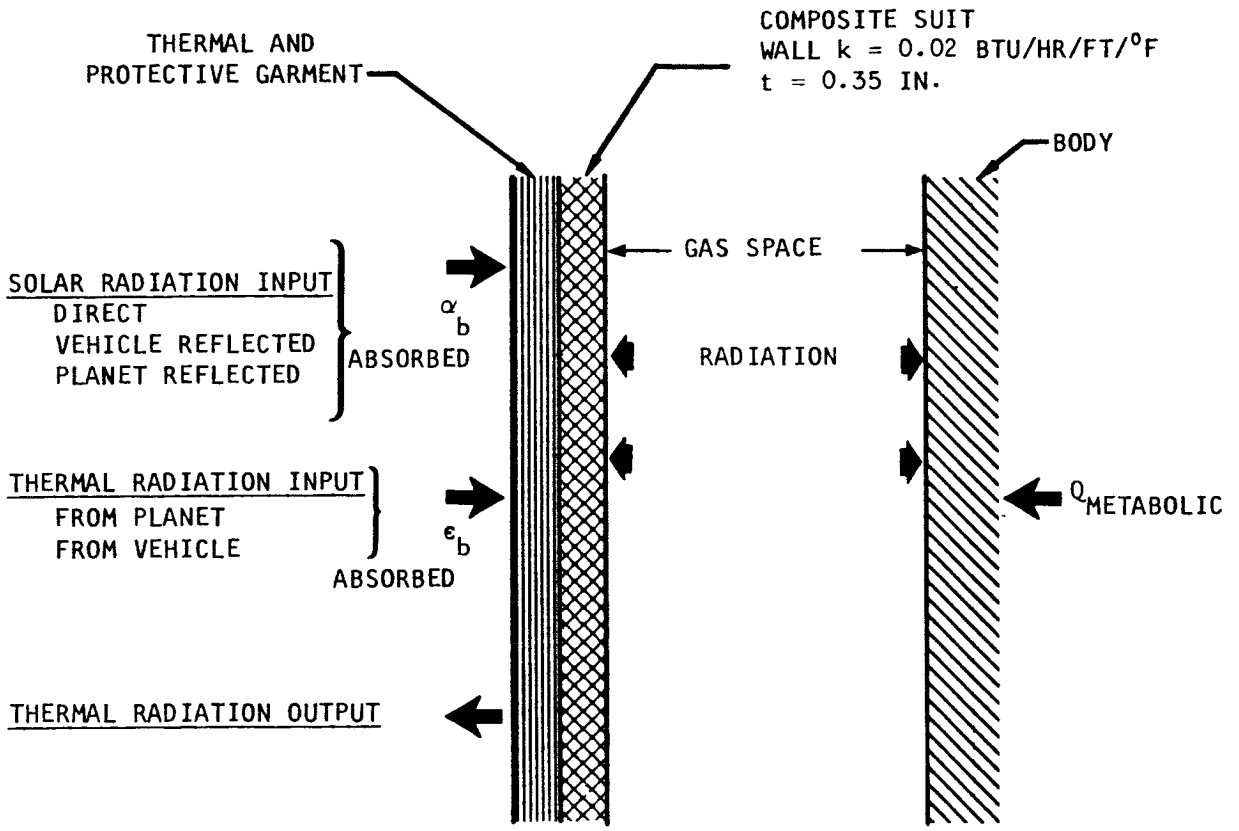

Figure 3-25. Heat Transfer Model for Radiation Cooling of the Extravehicular Suit with Radiation from the Skin to the Inner Wall

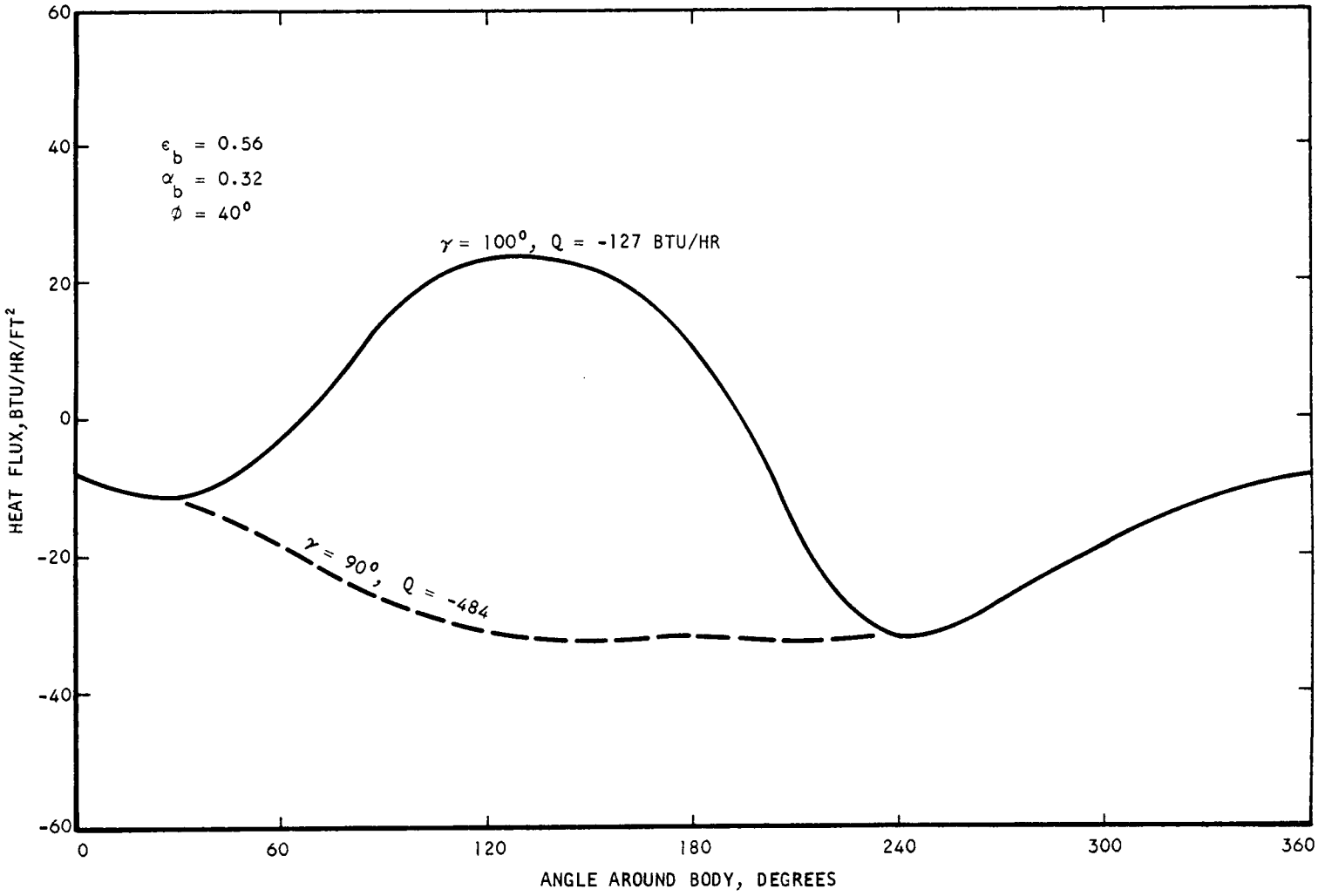

Figure 3-26. Typical Heat Flux Distribution for Radiation Cooling with Air Gap in Extravehicular Suit

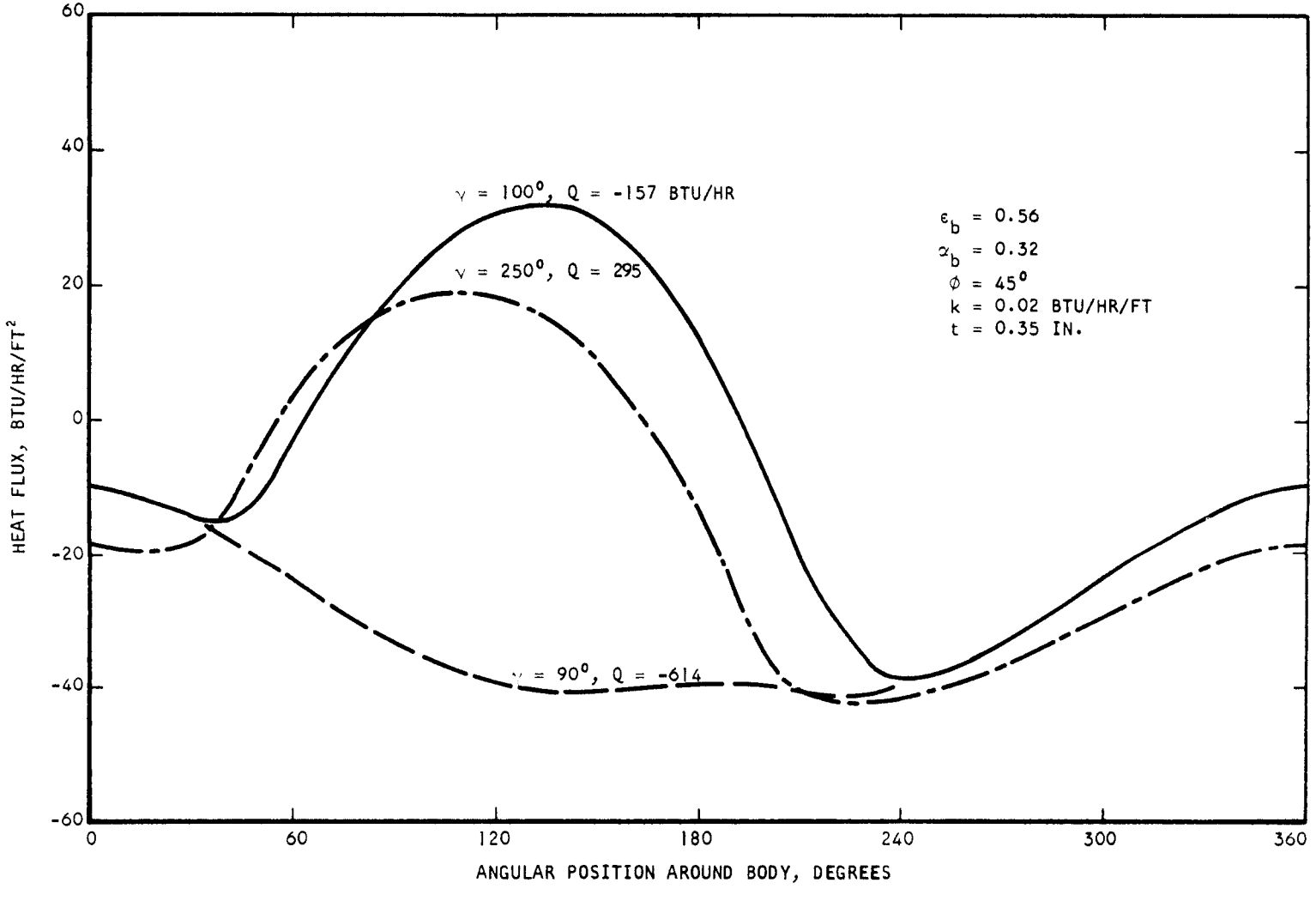

Figure 3-27. Typical Heat Flux Distribution for Radiation Cooling without Air Gap in Extravehicular Suit

heat flux input is reduced from 34 Btu/hr-ft^2 to 25 Btu/hr-ft^2 and the maximum heat loss is reduced from -40 Btu/hr-ft^2 to -32 Btu/hr-ft^2. Corresponding total heat leaks are reduced from a maximum of -614 Btu/hr to -484 Btu/hr. Therefore, from a thermal standpoint, whether or not the air gap is desirable depends upon the design objectives concerning heat dissipation.

Figure 3-28 shows the total heat leak for the extravehicular suit with an internal air gap as a function of the orbital parameters. It can be shown by comparison with Figure 3-24 that the air gap reduces the range over which heat loss will vary. This is probably desirable as a means of passive temperature control. Other means of providing passive thermal control to be investigated involve use of thermal insulation and special surface coatings.

Figure 3-29 shows the effect on heat leak of varying the thickness of the suit wall. Relatively little change is obtained when the suit is exposed to sunlight; greater reduction in heat leak is obtained during dark-side operation or when the suit is in the shadow of the vehicle.

The previous heat leak calculations have been based upon an extravehicular suit in the immediate vicinity of a spacecraft, the suit maintaining a fixed orientation relative to the earth-spacecraft vector. Figure 3-30 shows the heat leak as a function of extravehicular suit orientation where the suit is remote from the spacecraft. It will be observed that the heat leaks are somewhat greater than those described previously for comparable conditions. The maximum heat leak increases from -484 Btu/hr to -660 Btu/hr. Therefore, if the extravehicular excursion involves moving a significant distance from the spacecraft, it will be necessary to allow for a greater heat leak from the suit. It can be seen that suit orientation will have relatively little effect, although it may be necessary to consider this factor in designing passive thermal control systems for extravehicular suits.

As shown in Figure 3-31, the spectral characteristics of the outer surface of the extravehicular suit will exert an important effect on the suit heat leak. For the spectrally selective surface (ϵ_b = 0.80, α_b = 0.20), an average heat leak of approximately -584 Btu/hr is obtained. For a reflective surface coating (ϵ_b, = 0.05, α_b = 0.10), an average heat leak into the suit of approximately +78 Btu/hr is obtained. For typical suit surface characteristics (ϵ_b = 0.56, α_b = 0.32), the heat leak will be approximately -342 Btu/hr. Therefore, the suit surface characteristics can be selected either to minimize or to maximize the radiative heat loss.

It can be concluded that selection of the suit surface spectral characteristics will be an important factor in the thermal design of extravehicular suit systems. However, practical considerations based upon material availavility and durability may limit selection. For example, it has been found that aluminized mylar, which has good performance if minimum heat leak is desired, is not sufficiently durable. A high-temperature-resistant nylon fabric is presently favored as the outer material for space suit assemblies. Performance approaching that given for the spectrally selective surface can be obtained at the present time.

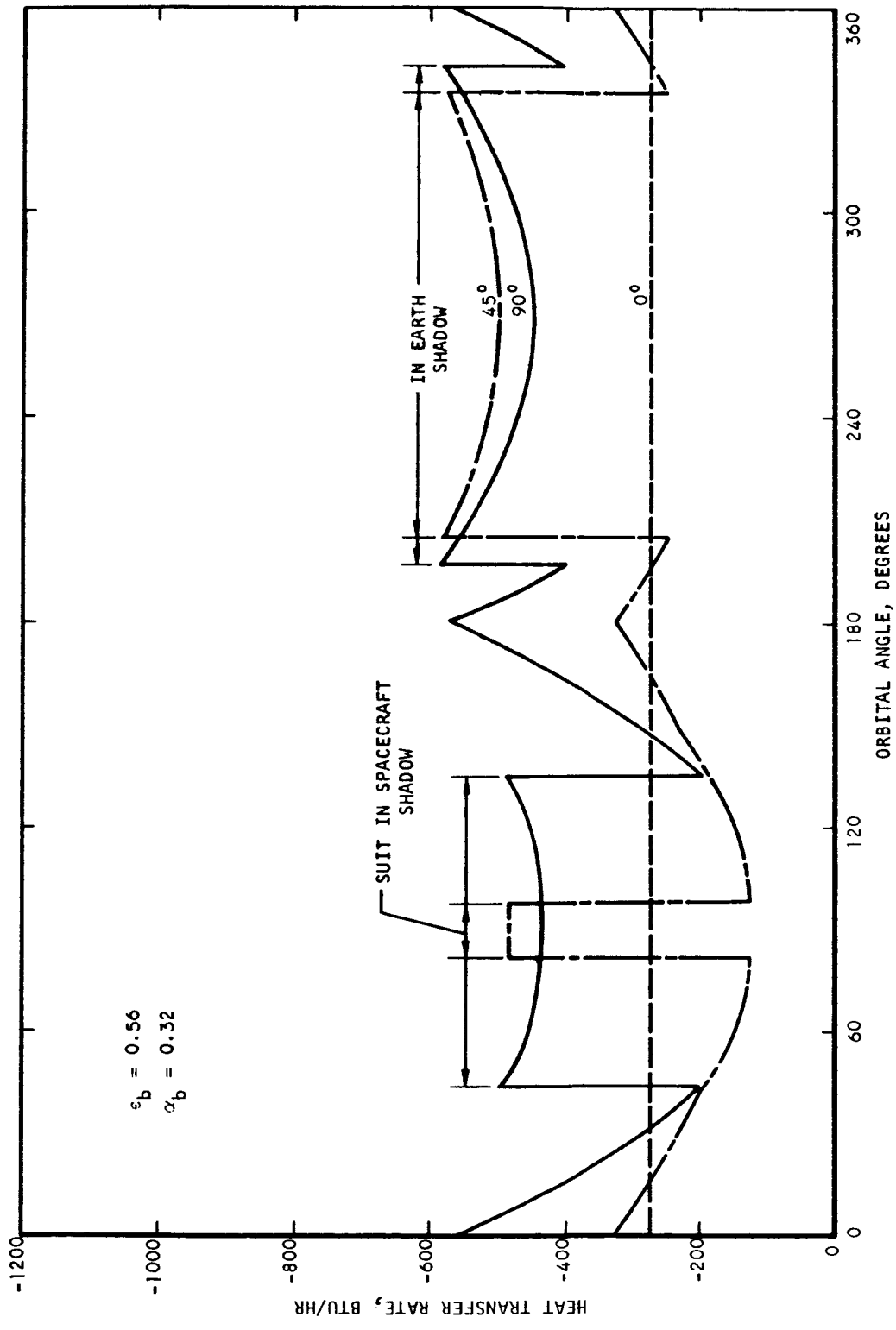

Figure 3-28. Heat Rejection Variation with Position in a 160-nm Earth Orbit (Extravehicular Suit with Air Gap)

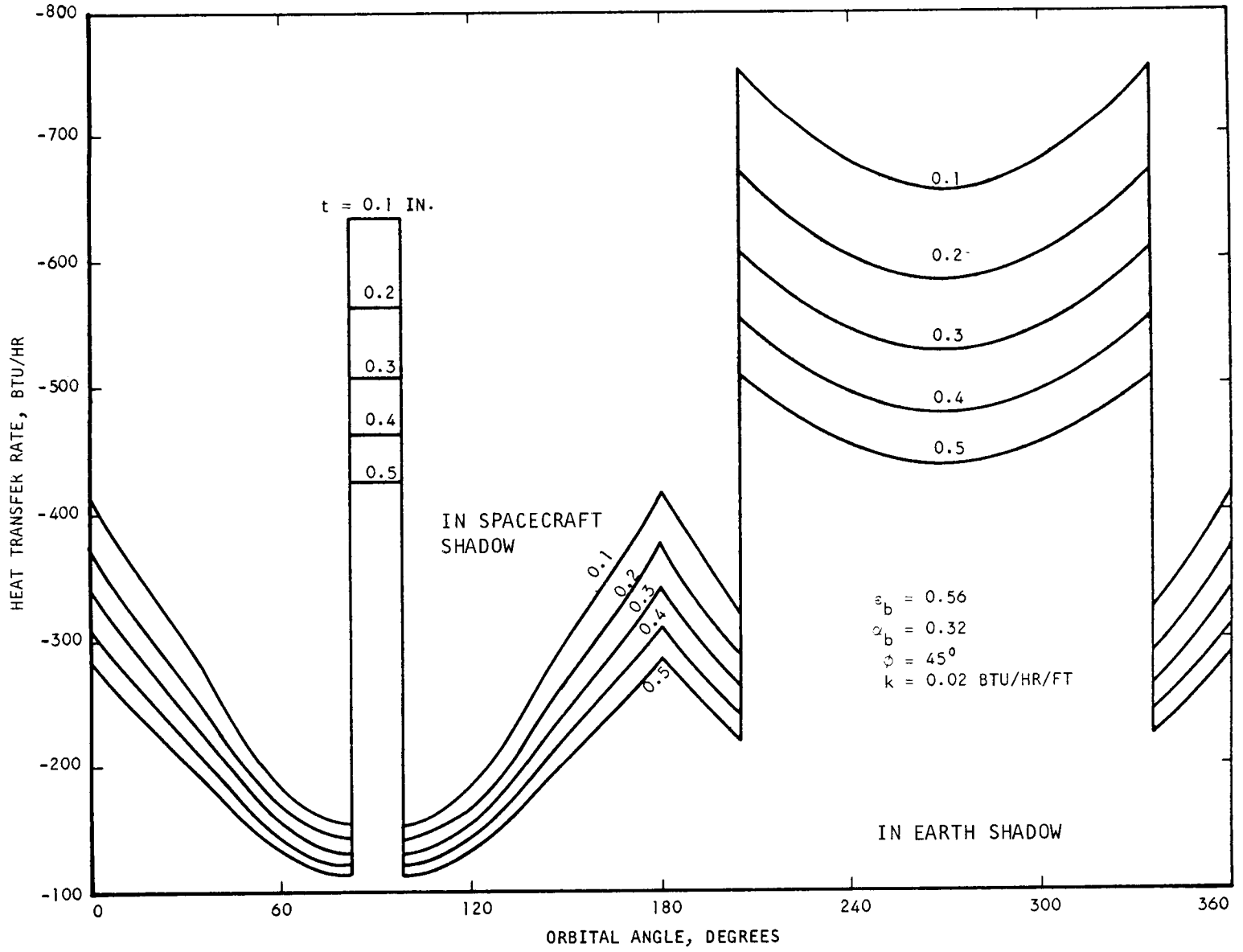

Figure 3-29. Effect of Suit Wall Thickness on Heat Loss from Extravehicular Suit

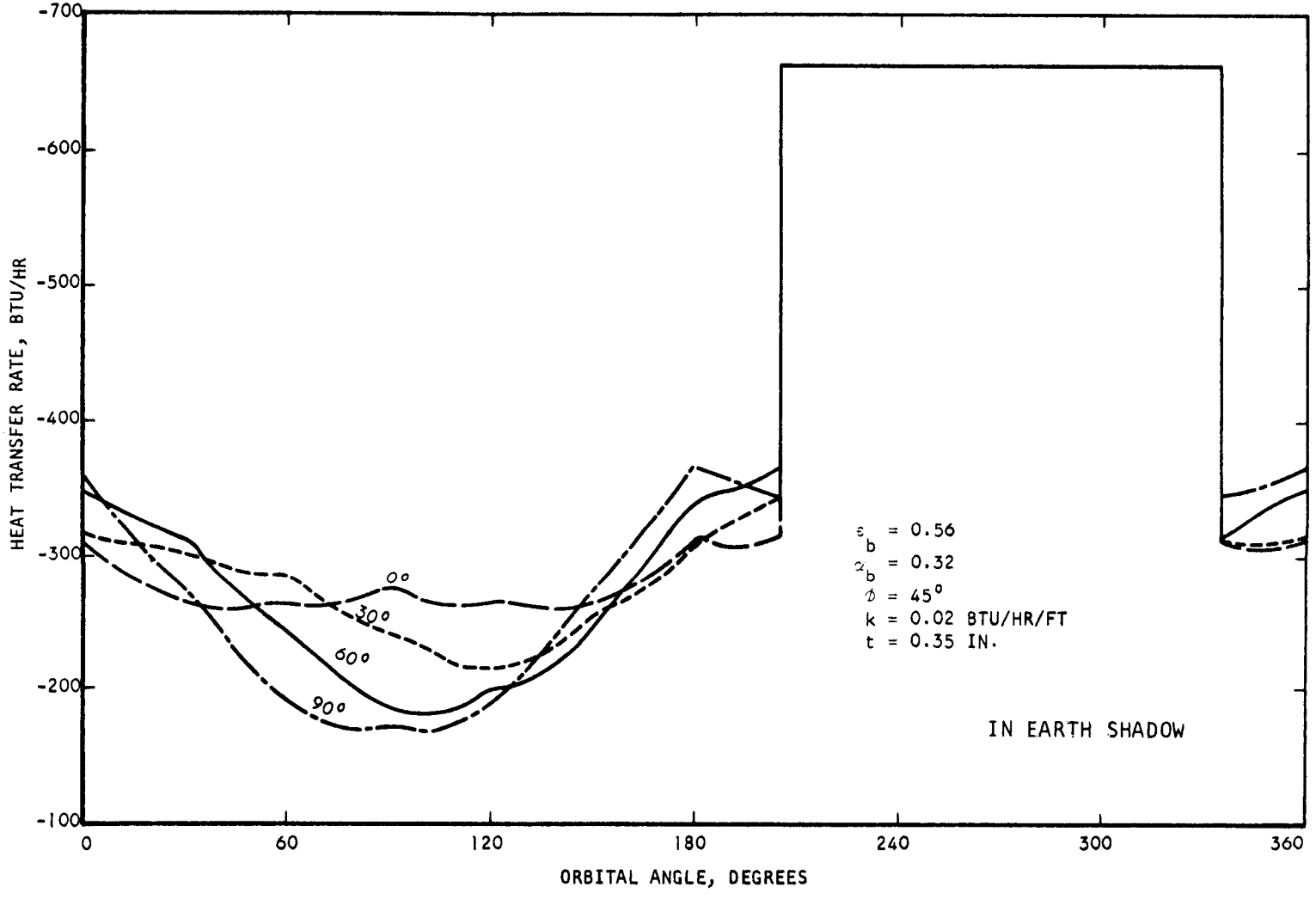

Figure 3-30. Effect of Orientation on Heat Loss from Extravehicular Suit

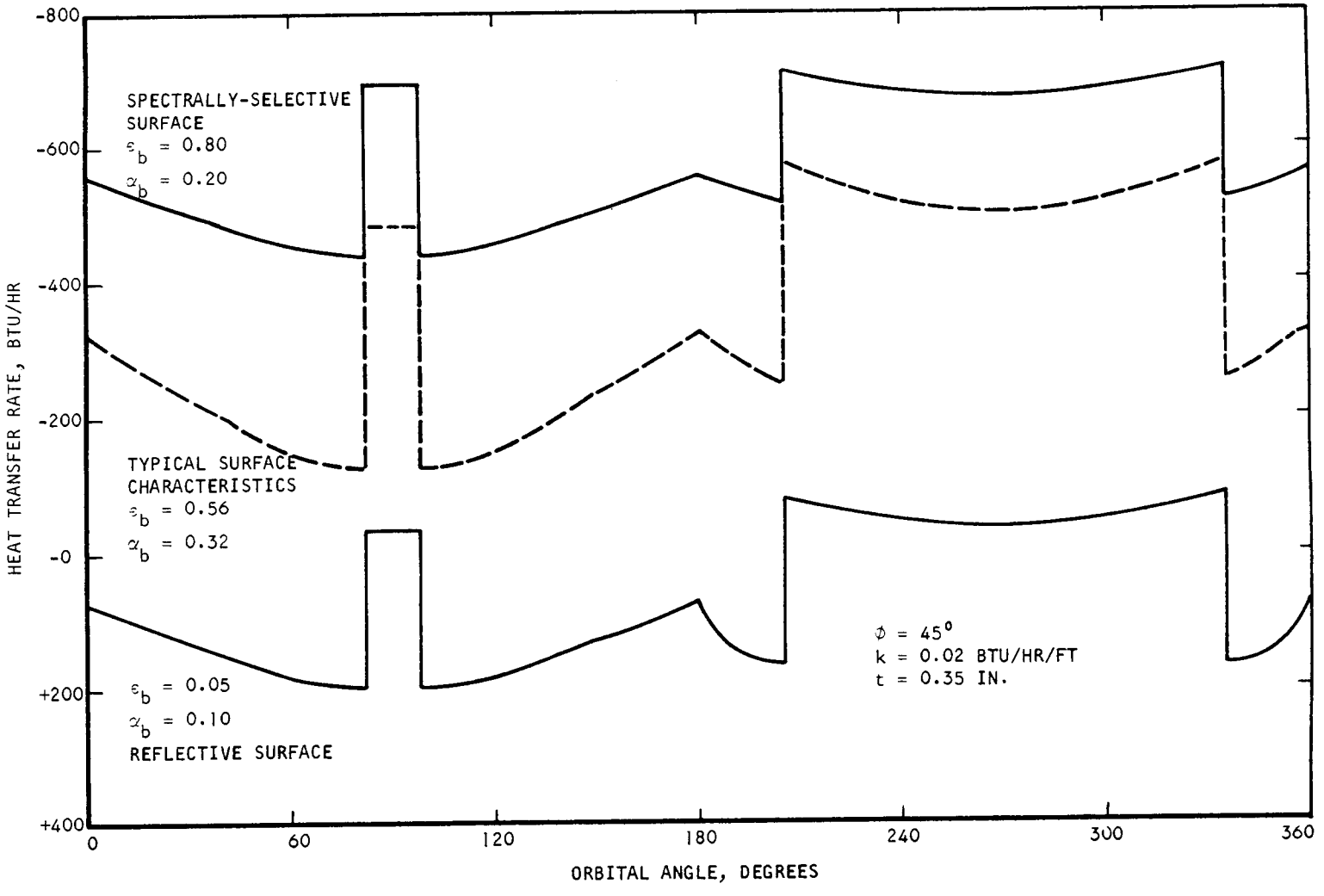

Figure 3-31. Effect of Surface Spectral Characteristics on Extravehicular Suit Heat Balance

Since there is considerable uncertainty at the present time concerning attainable performance with materials suitable for extravehicular suit outer surfaces, additional extravehicular suit heat balance computations were made using suit spectral characteristics obtained from the literature cited in Section 2 of this report. The results of these studies are given in Figures 3-32 and 3-33 and are summarized in Table 3-2. If the solar absorptivity can be reduced to values less than 0.1, the difference between the maximum and minimum heat leak (between day and night conditions) can be reduced to less than 200 Btu/hr, for the assumed suit insulating properties. Of course, this variation can also be reduced by addition of thermal insulation which would additionally serve to decrease overall heat rejection, which, in this case, would be a disadvantage. However, increase of the thermal emissivity to approximately 0.9 will increase the maximum heat rejec tion rate to approximately 800 Btu/hr. Therefore, it can be concluded that if a thermal emissivity of 0.9 and a solar absorptivity of approximately 0.05 are attainable, the extravehicular suit heat rejection rate will be approximately 750 ±50 Btu/hr in an earth orbit.

The theoretical limit for radiation cooling of the body can be determined by means of a simple calculation assuming, (1) the entire surface of the body (19.5 ft^2) to be available for radiation, (2) the skin temperature to be 91°F, and (3) the inner wall temperature of the suit to be 32°F (established by the freezing point of water). The maximum theoretical heat transfer rate determined by this computation amounts to 1100 Btu/hr. It can be concluded from this that any suit cooling scheme using a radiation gap between the body and the inner wall will not dissipate heat at higher rates, without buildup of ice on the inner wall of the suit. If only 80 percent of the area of the body is available for radiation, which is the usual value assumed in estimating radiative heat loss from the body, the theoretical maximum heat removal rate is reduced to 880 Btu/hr. This is rather close to the value determined by the heat transfer analysis. Consequently, it can be concluded that the attainable heat rejection rate will not be increased by any combination of suit thermal or spectral characteristics, where the body is cooled by a radiation through an air gap. With any type of cold wall radiation cooling scheme, condensation of moisture on the cold surface will represent a design problem. It may be possible to use wicks or membranes to remove the condensate.

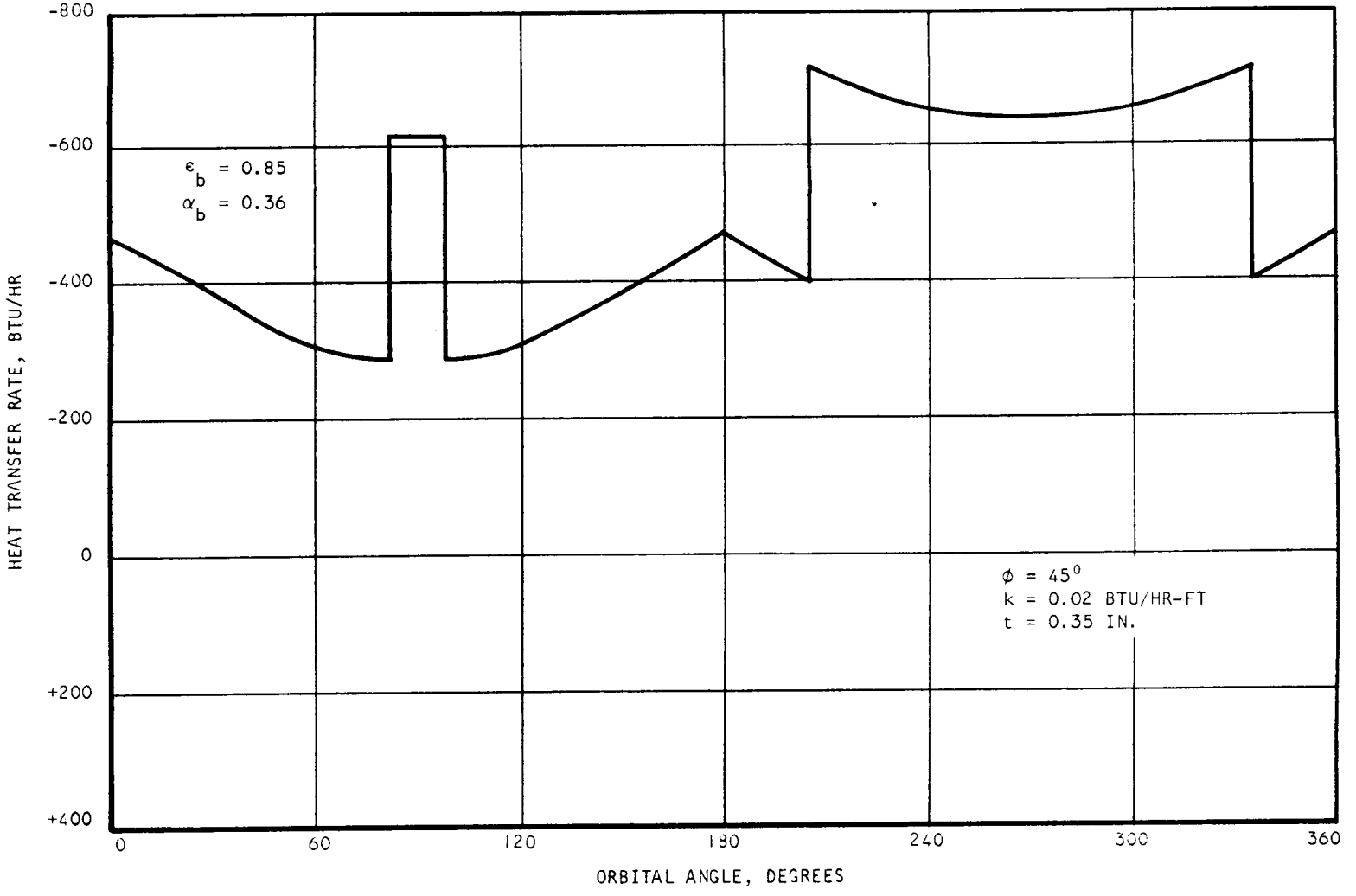

Figure 3-32. Effect of Surface Spectral Characteristics on Extravehicular Suit Heat Leak

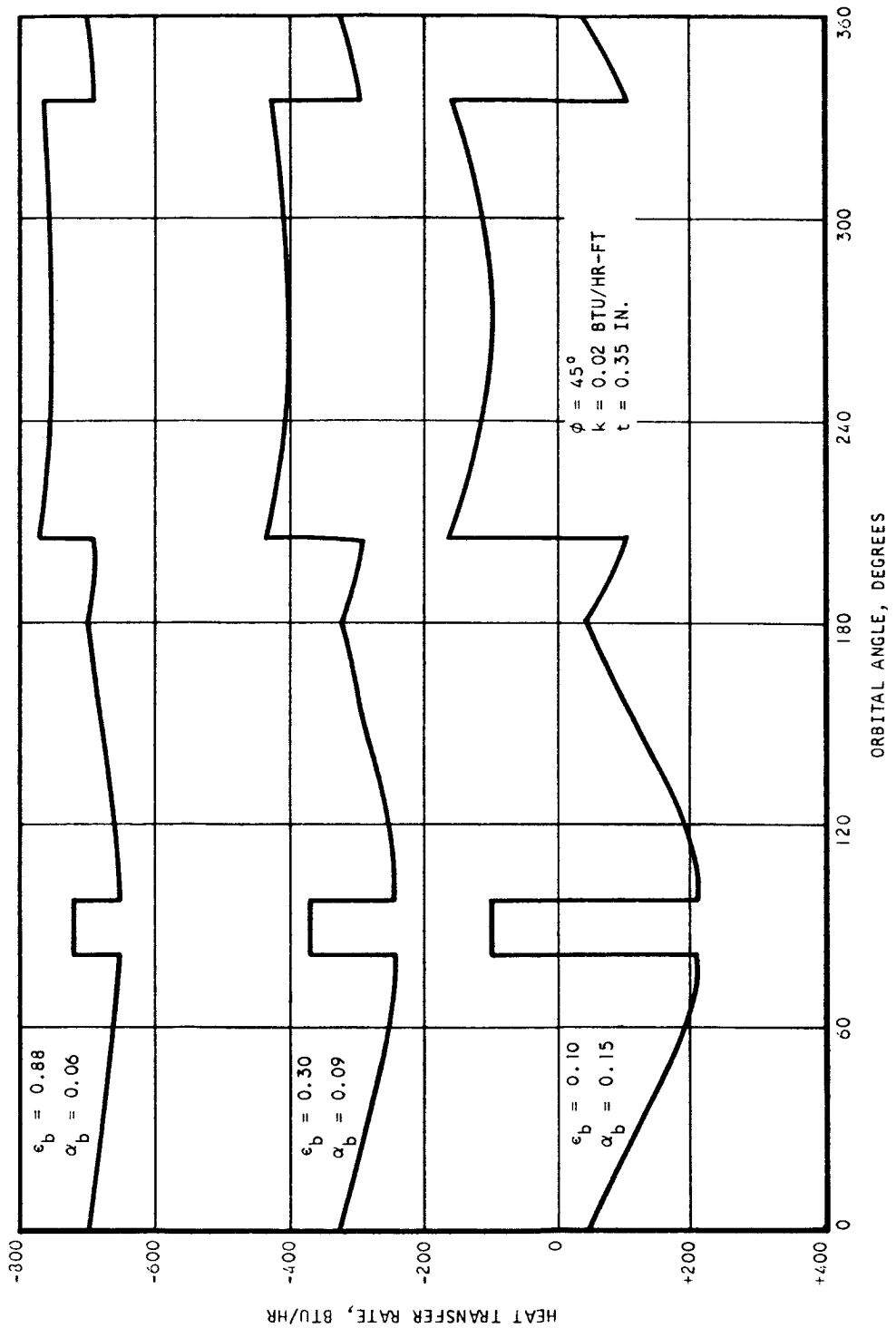

Figure 3-33. Effect of Surface Spectral Characteristics on Extravehicular Suit Heat Leak

TABLE 3-2

EFFECT OF SUIT OUTER SURFACE SPECTRAL CHARACTERISTICS ON EXTRAVEHICULAR HEAT BALANCE FOR 160-NM EARTH ORBIT

Suit Outer Surface Spectral Characteristics		Ref.	Heat Transfer Rate (Btu/hr)		
			Maximum	Minimum	Average
α_b	ϵ_b				
0.20	0.80		-715	-440	-584
0.32	0.56	45	-575	-125	-342
0.10	0.05	39	+197	- 80	+ 78
0.06	0.88	43	-770	-655	-708
0.09	0.30	40	-430	-242	-333
0.15	0.10		+210	-162	+ 25
0.36	0.85	40	-750	-390	-489

DISCUSSION AND CONCLUSIONS

Extravehicular suit cooling by ventilation appears to be limited to heat removal rates of about 1300 Btu/hr for ventilating gas flow rates up to 15 cfm at 3.7 psia. Most of this heat removal will be accomplished by evaporation of sweat from the body. At high metabolic rates, the high sweat rates obtained with ventilation cooling will be accompanied by high skin and internal temperatures, which are undersirable from both comfort and physiological standpoints. Increasing ventilating flow beyond approximately 15 cfm results in relatively small gains in cooling rate while greatly increasing the power requirement for suit ventilation.

Suit ventilation performance data can be correlated by the heat and mass transfer equations developed for flow through ducts. If the ventilating flow is expressed in terms of mass flow rate, the heat transfer effectiveness and mass transfer effectiveness (as well as the corresponding dry-bulb and dew-point temperatures) can be correlated as a function of flow, independent of pressure. The mass transfer effectiveness applicable for flow through equivalent ducts correlates with the observed suit performance if a water-vapor partial pressure at the skin, $(P_s)_{H_2O}$, less than that given for the skin temperature is assumed. A water vapor partial pressure at the skin of approximately 0.50 psi has been found to provide the best correlation of the test data with the calculated performance. The water vapor partial pressure at the mean skin temperature of 96°F is 0.84 psi. Part of the difference can be explained by vapor pressure lowering due to dissolved electrolytes in the sweat that evaporates from the skin.

Extravehicular suit thermal control by liquid-loop cooling methods involving conduction of heat from the body appears to be capable of removing essentially any internal heat load within the capability of man to generate, without active sweating. Liquid-loop conduction cooling of relatively small prime heat transfer surface areas of the body has provided heat removal rates in excess of 2000 Btu/hr under conditions where essentially no sweating is obtained.

Liquid-cooled garment performance is correlated by a simple heat transfer analysis that considers only the transfer coefficient on the liquid side and the thermal resistance of the tube wall. For high heat removal rates, it is necessary to consider the reduction in mean skin temperature, which is given approximately by heat flow through a constant conductance (at a minimum value of 3.3 Btu/hr-ft^2-^{0}F for full vasoconstriction) from a constant internal temperature heat source.

Comfort design criteria have been developed for conduction cooling of the body, based upon maintaining skin temperature within limits represented by thresholds for onset of sweating and shivering, respectively. Conduction cooling tends to provide constant heat removal from the body for constant skin temperature and consequently is not subject to thermoregulatory control. Therefore, it will be essential to provide some means of matching cooling capacity with metabolic rate, where conduction heat transfer provides the major mechanism for cooling of the body.

The temperature control requirements depend to a large extent upon the thermal control methods used with the extravehicular suit. The temperature control used with the extravehicular suit thermal transport assembly can be either active or passive. If active, it can be either automatic or manual. Passive control schemes may involve use of the thermoregulatory mechanisms of the body to maintain suitable conditions. An example of this is the conventional suit ventilating loop where sweat rate varies to provide a thermal balance. The suit cooling concepts involving conduction of heat from the skin will probably require some type of active temperature control. Control systems based upon the following principles are possible.

- Suit Outlet Humidity: increase in suit outlet humidity indicates occurence of sweating and requirement for additional cooling.
- Tympanic membrane temperature: can be measured by thermocouple or microbolometer for direct indication of cranial internal temperature.
- Skin temperature: increase in skin temperature above predetermined temperature level (91 to 94^{0}F) indicates onset of sweating.
- Galvanic Skin Resistance: substantial increase in skin conductivity is observed at sweat point.
- Subjective control: manual control in response to comfort sensations.
- Rectal or oral temperatures
- Metabolic rate: respiration rate or pulse rate can be monitored to given an approximate indication of metabolic rate.

Since there are major problem areas beyond the scope of the present discussion associated with application of any of these techniques, temperature control can be considered to be a major problem area in application of conduction cooling methods to extravehicular suit systems.

Liquid-loop cooling methods employing radiative heat transfer between the skin and the cooled surfaces have been found to be noncompetitive with liquid-loop systems using condution cooling of the body. For example, a thermal transport garment design capable of removing over 2000 Btu/hr by conduction from the skin will remove less than 400 Btu/hr by radiation.

Cooling of the body by conduction directly through the suit wall to the outer surface where the heat is dissipated by radiation was studied, assuming the skin temperature to be maintained at an average value of 90^{0}F. In the earth orbital case analyzed in this section of the report, a net heat loss from the suit was obtained for the proper suit spectral characteristics, although a relatively high heat flux input might be obtained on one side of the suit (facing the sun) while the other side (facing space) would have a correspondingly high heat flux output. By proper selection of suit spectral characteristics (high thermal emissivity, low solar absorptivity), the range of heat flux can be reduced.

If it is necessary to provide an air gap between the body and the inner wall of the suit, as it appears probable, the thermal resistance imposed by radiation through the air gap will reduce the total heat rejection rate by approximately 230 Btu/hr (for one set of conditions). The maximum heat rejection from the body by means of radiation from an extravehicular suit appears to be limited by ice formation on the inner wall to rates less than 1100 Btu/hr. It has been shown to be possible to achieve, in practice, a heat rejection rate of 750 Btu/hr from an extravehicular suit (in an earth orbit) with a variation of ±50 Btu/hr with variation in orbital position, by proper selection of suit spectral characteristics.

Development of an extravehicular suit assembly using purely passive thermal control methods appears to be remote because of the complexity of man's requirements, the range of metabolic rates that will be obtained, and the variation in the external environments. However, it is evident that for certain space environments it will be possible to dissipate a considerable part of the internal heat load by radiation as a means of reducing the size and weight of the portable environmental control system. For example, assuming an average design heat rejection rate of 1500 Btu/hr, approximately 50 percent of the heat sink can be provided by radiation (in an earth orbit), thereby effecting an evaporant saving of 0.72 lb/hr of operation and a fixed weight saving in equipment of from 4 to 7 lb. It can be concluded, therefore, that there is incentive for use of radiation cooling of extravehicular suits in conjunction with conventional liquid-loop or ventilating-gas suit cooling systems, although it appears unlikely that it will be possible to provide all of the thermal control requirements by passive radiative methods.

SECTION 4

THERMAL PROCESSES, SHIRTSLEEVE ENVIRONMENT

Until recently, studies of atmosphere conditioning of spacecraft have been concerned almost exclusively with the requirements for pressure suit operation. In the Gemini missions, as in the previous Mercury flights, the crew is maintained in ventilated pressure suits (unpressurized during normal operation). The Apollo spacecraft will have provisions for removing the pressure suits for much of the mission, although the basic environmental control system is optimized for suit operation.

Long-duration missions require extended capability for shirtsleeve operation. Unfortunately, some of the design criteria applicable to a spacecraft shirtsleeve cabin are incompletely known. For example, comfort zone conditions of temperature, humidity, and ventilation rate are commonly based on experience in the earth environment. The data obtained from such experience may not be directly applicable to spacecraft, where the normal gravity field is lacking and an artificial low-pressure atmosphere will be used. In Section 2, comfort criteria are analyzed to determine design methods applicable to space environments.

The heat transfer model to be used in the analysis of the shirtsleeve environment consists of a vertical cylinder with an average diameter of 1.0 ft and a surface area of 19.5 ft^2. The metabolic heat load is to be dissipated by a combination of sensible and latent heat removal processes. Sensible heat removal is represented by radiation and forced convection at the outer surface of the clothing. It is assumed here that latent heat transfer occurs with the evaporation of moisture on the skin with the water vapor diffusing through the clothing with negligible resistance to be swept away by the ventilating flow. Natural convection is neglected for the free-space environment because of the absence of gravity, although it is considered for the lunar surface environments. The purpose of the analysis is to parametrically establish the effects of ventilating gas flow, wall temperature, clothing, and atmospheric composition and pressure on heat removal rates from the body in a shirtsleeve space cabin.

ENERGY TRANSFER ANALYSIS

Energy Balance Criterion

Body temperature and sweat rate depend upon a balance between metabolic energy production, work output, and energy transfer to the atmosphere. Man normally dissipates waste energy by a combination of radiation and convection heat transfer, and evaporation mass transfer. Any deficit in the energy balance is accompanied by heat storage in the body, which requires a change in the average body temperature. Although heat storage up to 600 Btu can be tolerated before physical collapse occurs (Ref. 15), it was assumed to be zero in order to generate comfort zone predictions valid for long-duration

conditions. In addition, the energy dissipation due to human work output was assumed to be negligible. Therefore, the heat balance which must be satisfied for the body is

$$M = Q_r + Q_c + Q_\ell \tag{4-1}$$

To achieve minimum sweat rates, most body cooling must be accomplished by sensible heat transfer with either free or forced convection. The above heat balance must be achieved at atmospheric temperatures and velocities consistent with the interrelated factors of skin temperature, physiology, comfort, and minimum sweat rate discussed previously in this report.

Thermal Parameters

The factors that influence the thermal analysis are shown schematically in Figure 4-1; the equations are developed in detail below. The geometrical model of man shown in the figure is the same as that used by Jannsen (Ref. 22), although in the analysis to follow the model was assumed to be in a sitting position. The boundaries of the comfort zones were predicted using Equation (4-1) by setting the fraction of maximum evaporative capacity, C, equal to 0.10, 0.25, and 0.70, and evaluating the three cooling terms with a comfortable skin temperature of 91.4 ^{0}F.

Effect of Clothing

All the sensible heat is assumed to pass through the clothing by conduction, and the clothing heat transfer area is assumed to be equal to the surface area of the man. Both of these assumptions are somewhat conservative, since some sensible heat transfer occurs from unclothed portions of the body; in addition, the clothing surface area may be 40 percent greater than that of man (Ref. 12), although probably not all of the increased area is available for heat transfer.

The relationship between clothing surface temperature, T_c, and skin temperature, T_s, obtained by considering a simple conduction process through clothing of thickness, L, is as follows:

$$Q_r + Q_c = \frac{kA}{L} (T_s - T_c)$$

or

$$T_c = T_s - \frac{L}{k} \frac{(Q_c + Q_r)}{A} \tag{4-2}$$

The value L/k is known as the clothing or CLO value. The reference point for the CLO value is taken as a man in a suit with no gloves, or light gloves, and leather footgear with light socks. This is known as 1 CLO and corresponds to a value for L/k of 0.88 ^{0}F-sq ft-hr/Btu. The CLO value ranges from four for artic equipment to zero for the unclothed

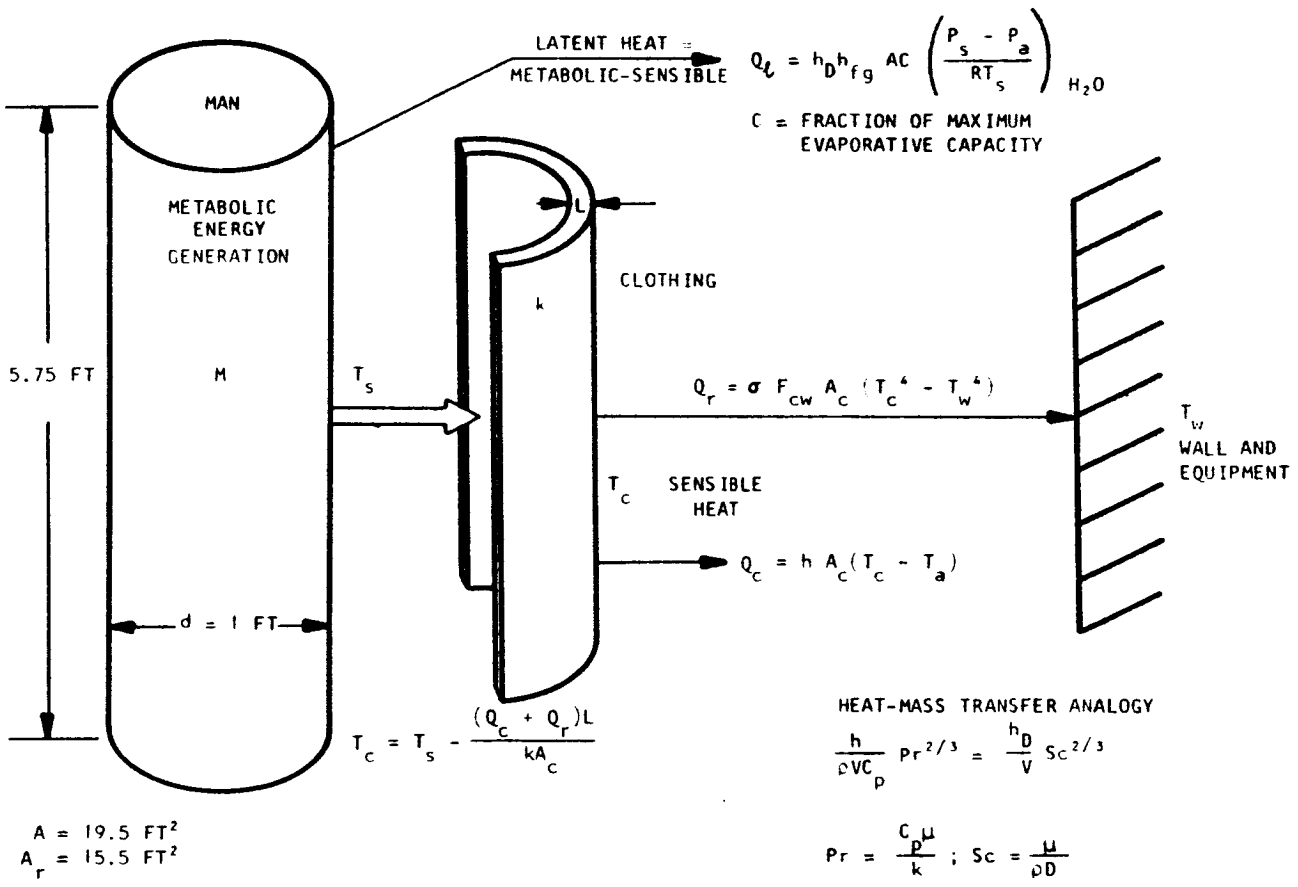

Figure 4-1. Thermal Analysis Parameters

subject. A value of 0.5 CLO is often used, as it is typical of light indoor clothing. Figure 4-2 shows the temperature decrease across the clothing for different CLO values and sensible heat rates.

Radiation

Thermal radiation that normally occurs between the numerous equipments, structures, and man is an appreciable fraction of the heat lost in most cases. Therefore, radiation heat transfer must be considered in the heat balance considerations for man.

The actual radiation heat transfer problem is a complex one involving numerous thermal radiation sources at different temperatures and geometries. The problem can be greatly simplified by theoretically collecting all equipment and structures into an equivalent enclosure at a mean radiation temperature. This procedure must be followed since equipment and structure cannot be represented parametrically. Therefore, the mathematical model used in the following analysis is based upon a man in an enclosure at a single mean radiation temperature. The crewman is also assumed to be at a single mean temperature, equal to the temperature of the outer surface of the clothing.

The basic equation for radiation heat transfer between the man and the enclosure is

$$Q_r = \sigma F_{cw}(T_c^4 - T_w^4)A_r \qquad (4\text{-}3)$$

Values of the gray-body view factor can be calculated with the following equation (Ref. 47):

$$F_{cw} = \frac{1}{\frac{1}{\epsilon_c} + \frac{A_r}{A_w}\left(\frac{1}{\epsilon_w} - 1\right)} \qquad (4\text{-}4)$$

If man is in an enclosure much larger than himself, the ratio A_r/A_w is small, and $F_{cw} = \epsilon_c$. Therefore, Equation (4-3) generally can be written as

$$Q_r = \sigma \epsilon_c A_r (T_c^4 - T_w^4) \qquad (4\text{-}5)$$

Substituting the assumed value of the radiation area (15.5 sq ft) and the value of the Stefan-Boltzman constant, σ, into Equation (4-5) yields the final simplified radiation cooling equation for man.

$$Q_r = 2.65 \times 10^{-8} \epsilon_c (T_c^4 - T_w^4) \qquad (4\text{-}6)$$

Figure 4-3 shows the radiation cooling rate as a function of clothing surface and mean wall temperature.

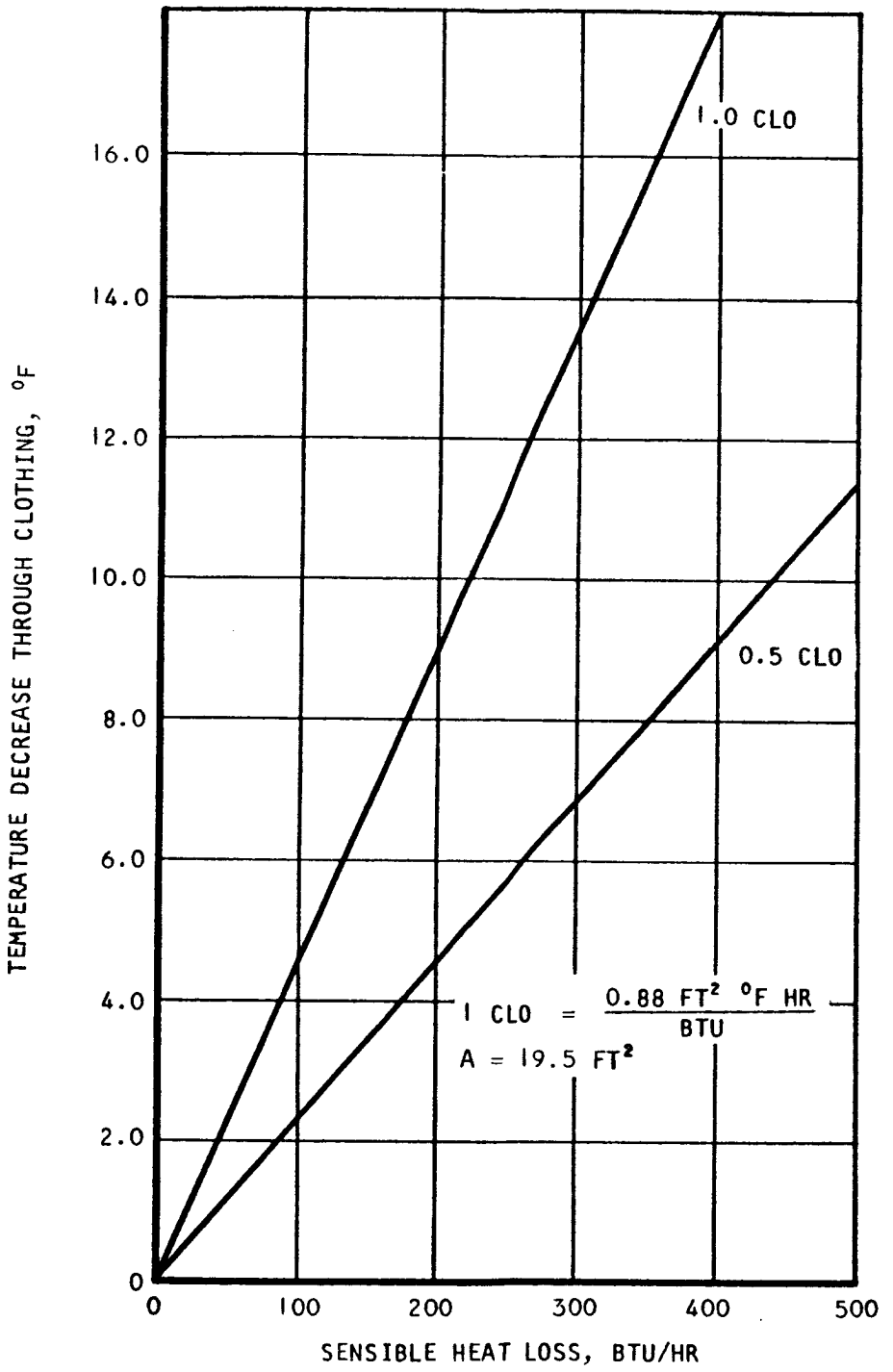

Figure 4-2. Temperature Decrease Across Clothing for Various Amounts of Sensible Heat and CLO Values

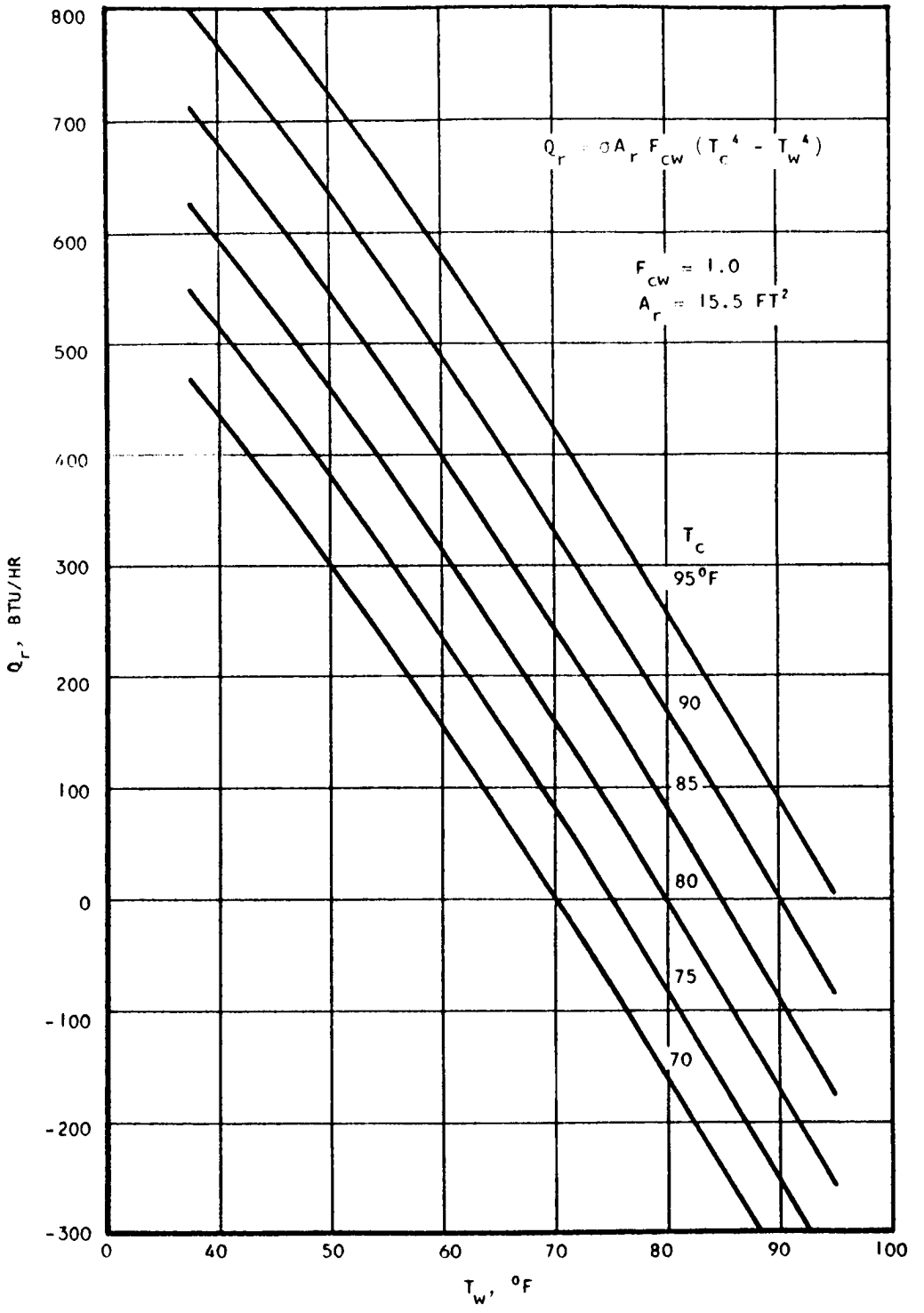

Figure 4-3. Radiation Cooling Rate

Heat-Mass Transfer Analogy

Latent cooling is the result of a mass-transfer process which occurs when the density of water vapor at the skin surface is greater than the water-vapor density in the atmosphere. The cooling capacity equals the rate of water-vapor mass transfer multiplied by the heat of vaporization of water at skin temperature. The prediction of mass transfer rates for small mass-fraction components is greatly simplified by the use of the Heat-Mass Transfer Analogy, as described by Eckert (Ref. 48), in conjunction with heat transfer similarity relations.

A mass transfer coefficient, h_D, can be defined as follows:

$$\left(\frac{dm}{dt}\right)_{H_2O} = -DA\left(\frac{\partial \rho}{\partial x}\right)_s = h_D A(P_s - P_a)_{H_2O} \qquad (4\text{-}7)$$

The similarity between Equation (4-7) and the corresponding heat transfer equations is obvious. Dimensional analysis of mass-transfer differential equations reveals the dimensionless property ratio defined by Equation (4-8) which is referred to as the Schmidt number, Sc.

$$Sc = \frac{\mu}{\rho D} \qquad (4\text{-}8)$$

The significance of the Schmidt number in mass transfer is similar to the significance of the Prandtl number in heat transfer; in particular, the mass-fraction and temperature profiles are similar when Sc = Pr (Ref. 48). Extending the analogy further, a dimensionless mass transfer coefficient, $h_D L/D$, can be defined by nondimensionalizing Equation (4-7) in the same way that the dimensionless heat transfer coefficient, hL/k, was developed.

The general statement of the Heat-Mass Transfer Analogy revealed by detailed analysis is that the solution of a mass-transfer problem can be obtained from the equations for the corresponding heat transfer problem if the Nusselt number, hL/k, is replaced by the dimensionless mass-transfer coefficient $h_D L/D$; and the Prandtl number, $C_p\mu/k$ is replaced by the Schmidt number $\mu/\rho D$. This law has been verified for laminar and turbulent flow over a flat plate, through a tube, and around cylinders and spheres (Ref. 48).

Forced Convection

A fan that blows air toward a sitting man to provide adequate cooling does not yield a simple, well-defined heat transfer geometry. Some of the flow may be parallel to the axis of the cylinder, while the rest is perpendicular; and the flow may be either laminar or turbulent. After considering the equations which apply to each of these cases, the geometrical model that generally covers the situations of interest most accurately will be selected.

The value of the dimensionless Reynolds number, $\rho VL/\mu$, determines whether the flow will be laminar or turbulent in forced-convection problems. The flow will be laminar if the Reynolds number is less than approximately 10^5 for flow both parallel and perpendicular to a cylinder (Ref. 48). For the velocities, characteristic lengths, and fluid properties of interest, the Reynolds number will be less than 10^5; therefore only laminar flow correlations will be used.

Theoretical analysis of laminar flow parallel to a surface has yielded the following experimentally verified equation, which is valid for Prandtl numbers from 0.6 to 15.0 (Ref. 48).

$$\frac{hL}{k} = 0.664 \left(\frac{\rho VL}{\mu}\right)^{0.5} \left(\frac{C_p \mu}{k}\right)^{0.33} \qquad (4\text{-}9)$$

The fluid properties in Equation (4-9) should be evaluated at a film temperature equal to the average of the wall and the fluid bulk temperature. Empirical development of dimensionless heat transfer correlations from a large mass of data obtained with many gases and liquids in laminar flow perpendicular to a cylinder provided Equation (4-10), which is valid for Reynolds numbers between 100 and 10,000 (Ref. 51).

$$\frac{hd}{k} = 0.60 \left(\frac{\rho Vd}{\mu}\right)^{0.5} \left(\frac{C_p \mu}{k}\right)^{0.33} \qquad (4\text{-}10)$$

There is a distinct similarity between Equations (4-9) and (4-10); the major difference in this case is the fact that the length of the flow path parallel to man will generally be double the effective cylinder diameter. The difference in the heat transfer coefficients calculated with these two equations, however, is only 25 percent. Because flow perpendicular to man requires a lower forced-convection velocity to provide a given amount of cooling, Equation (4-10) was selected for further use.

The forced-convection mass transfer equation, which will be used to estimate the latent cooling by evaporation, was obtained by making the modifications to Equation (4-10) called for by the Heat-Mass Transfer Analogy, with the following result:

$$\frac{h_D d}{D} = 0.60 \left(\frac{\rho Vd}{\mu}\right)^{0.50} \left(\frac{\mu}{\rho D}\right)^{0.33} \qquad (4\text{-}11)$$

The preceding equations are applicable to any fluid, at any pressure within the stated restrictions on Reynolds and Prandtl numbers. The development of simplified equations for air (oxygen-nitrogen mixtures) is described below.

Simplified Forced-Convection Equations for Oxygen-Nitrogen Mixtures

Over the range of atmospheric temperatures of interest for human thermal comfort ($40^{\circ}F$ to $100^{\circ}F$), the combination of fluid transport properties that appears in the above equations has a negligible variation for air. Inserting the properties of air into Equation (4-10), and combining the resulting equation for the heat transfer coefficient with the pertinent information in Figure 4-1 gives the following equation:

$$Q_c = 0.407 \sqrt{PV} \ (T_c - T_a) \qquad (4\text{-}12)$$

Since the properties of oxygen-nitrogen mixtures are approximately independent of the fraction of each component, Equation (4-12) is applicable to any oxygen-nitrogen mixture, for all total pressures. Figure 4-4 shows the range of forced-convection cooling rates achievable with reasonable velocities and temperature differences, for a total pressure of 6 psia.

A simplified equation for latent cooling is obtained in a similar way. Eckert reports a correlation for the diffusion coefficient of water in air as follows:

$$D = \frac{12.7}{P \ (psia)} \left(\frac{T}{460}\right)^{1.8} \frac{ft^2}{hr} \qquad (4\text{-}13)$$

Substituting Equation (4-13) and the transport properties of air into Equation (4-11), and combining the result with the pertinent information in Figure 4-5 gives the following simplified latent cooling equation.

$$Q_{\ell} = 2.46 \ C \ T_a \sqrt{V/P} \ (P_s - P_a)_{H_2O} \qquad (4\text{-}14)$$

Equation (4-14) applies to all oxygen-nitrogen mixtures, for all values of pressure and relative humidity. With C = 1, the results predicted by the above equation are 15 percent higher than the maximum evaporation rates tabulated by Kranz (Ref. 23) and 10 percent higher than the measurements of Clifford et. al. (Ref. 40). The maximum evaporative capacity predicted by Equation (4-14) with C = 1 is presented in Figure 4-5 as a function of pressure, velocity, and dew point; atmospheric temperature and dew point have a relatively small effect on latent cooling for the practical range of these parameters. These calculations indicate that latent cooling increases with decreasing pressure, primarily because the diffusion coefficient is inversely proportional to pressure.

The appropriate conversion factors have been incorporated in developing Equations (4-12) and (4-14) so that the velocity can be expressed in ft per min and the pressures in psia.

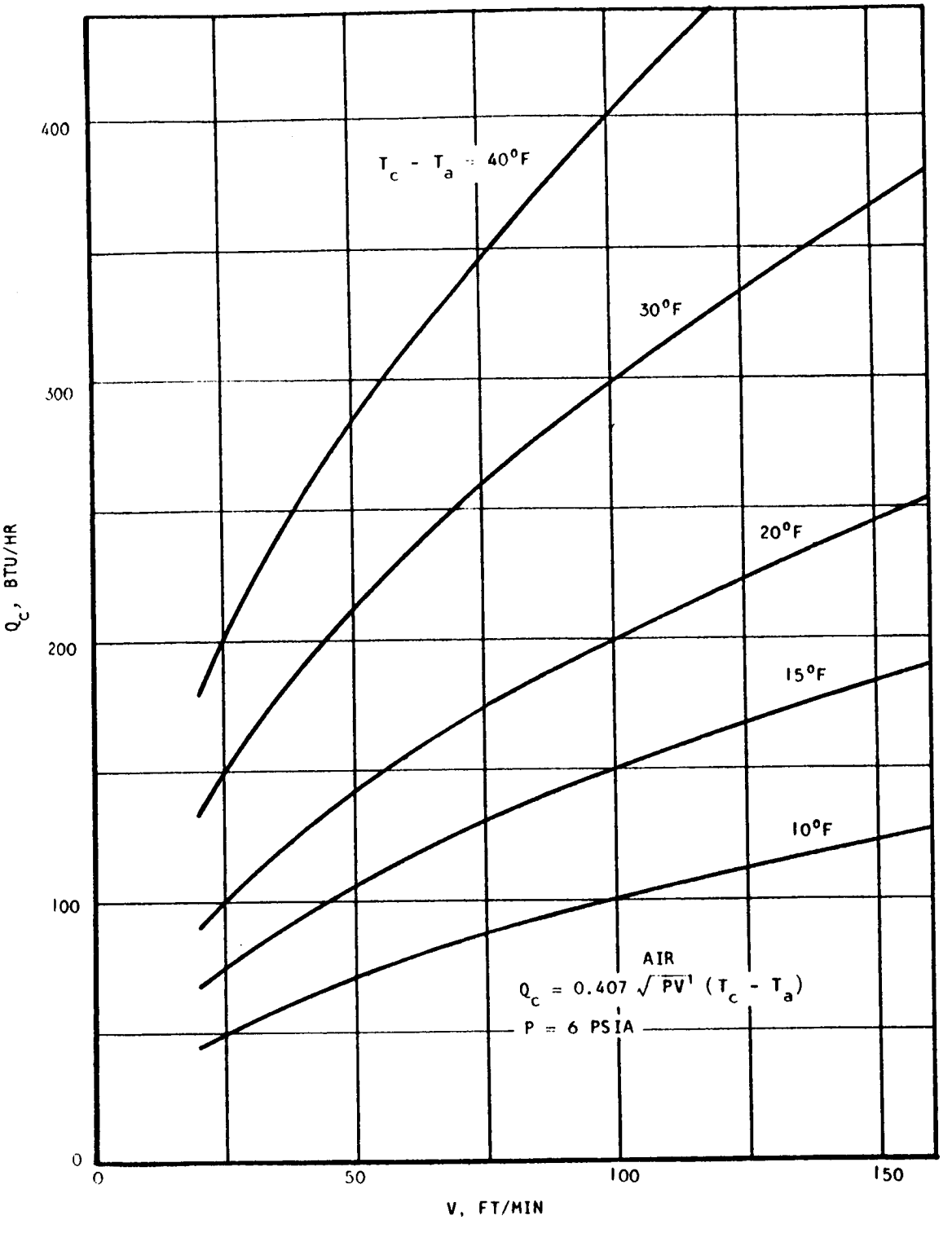

Figure 4-4. Forced-Convection Cooling

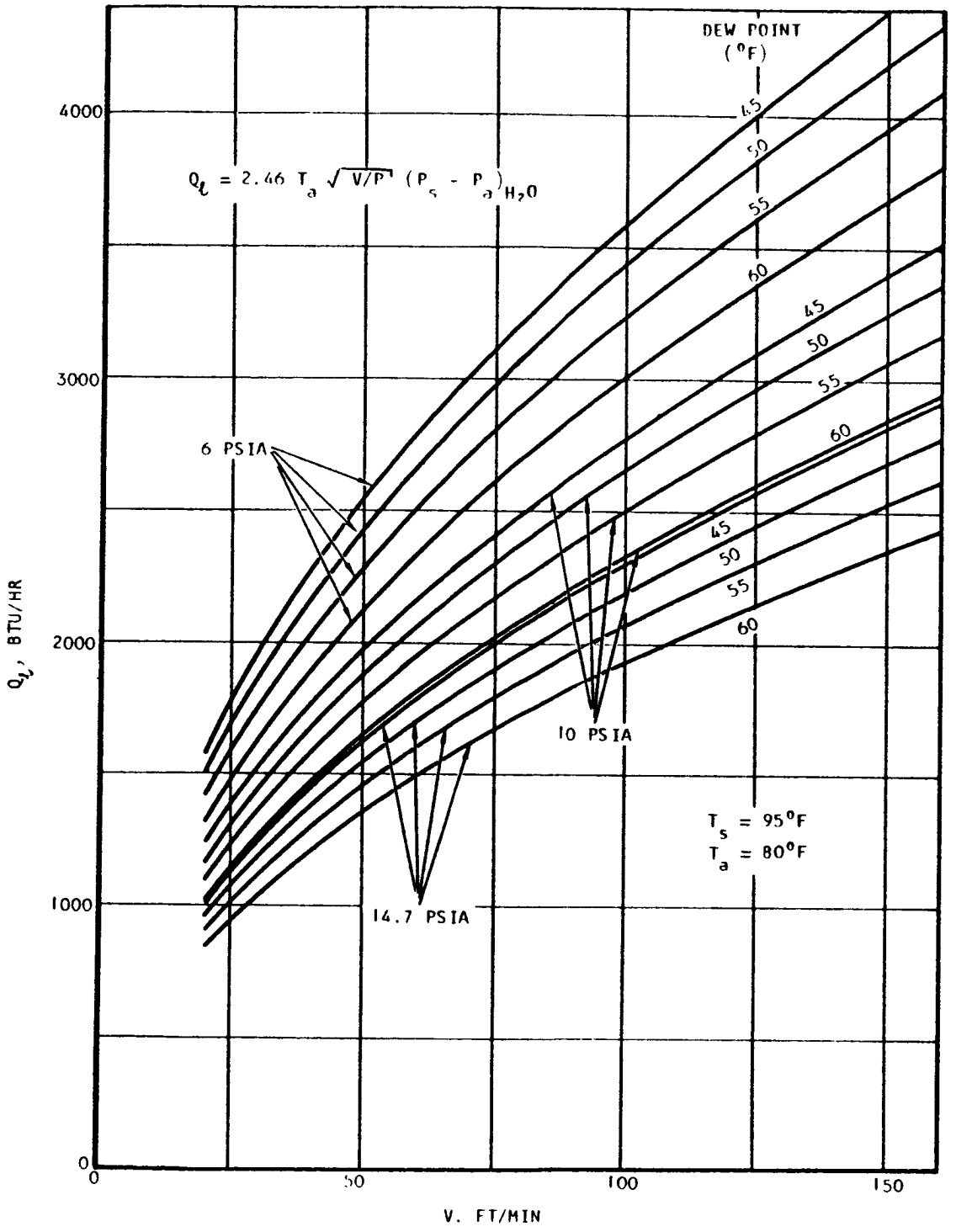

Figure 4-5. Maximum Evaporative Capacity in Air

Free Convection

Free-convection flow in a gravitational field, which occurs because of the buoyancy forces resulting from density differences, is a preferred method for cooling man, because it requires no additional power and equipment. This mode of heat transfer is generally adequate for normal activities on earth, and may provide adequate cooling on the moon even though the gravitational field is only 1/6 that of earth; zero-gravity environments require forced convection.

The dimensionless parameter which characterizes free-convection processes is the Grashof number, Gr, which is defined as follows:

$$Gr = \frac{g \, L^3 \, \rho \Delta \rho}{\mu^2} \tag{4-15}$$

For values of $Gr \cdot Pr$ less than 10^9, the flow is laminar; this will generally be the case in human body cooling.

Theoretical analysis of laminar free convection yields the following experimentally verified equation, which is valid for all Prandtl numbers (Ref. 48).

$$\frac{hL}{k} = 0.67 \left[\frac{Pr}{0.952 + Pr}\right]^{0.25} (Gr \cdot Pr)^{0.25} \tag{4-16}$$

The fluid properties in Equation (4-16) should also be evaluated at an average film temperature. Equation (4-16) applies to a vertical cylinder if the cylinder length is used for the characteristic length, and to a horizontal cylinder if 2.5 times the diameter is used (Ref. 48). Since the length of the vertical cylinder for a sitting man is approximately equal to 2.5 times the cylinder diameter, the results for free-convection cooling are essentially independent of the body orientation.

Free convection with combined heat and mass transfer is complicated by the effect of the water vapor on the density difference (Ref. 48). For this case, the following equation for the density difference was derived using the perfect gas equations.

$$\Delta\rho = \rho_a \frac{(T_c - T_a)}{T} + \frac{(P_c - P_a)_{H_2O}}{T \, R_{H_2O}} \left(\frac{R_{H_2O}}{R_a} - 1\right) \tag{4-17}$$

Finally, the free-convection mas transfer equation obtained by modifying Equation (4-16) is

$$\frac{h_D L}{D} = 0.67 \left[\frac{Sc}{0.952 + Sc}\right]^{0.25} (Gr \cdot Sc)^{0.25} \tag{4-18}$$

The preceding equations are applicable to any fluid, at any pressure, provided Gr·Pr and Gr·Sc are less than 10^9. The development of simplified equations for an oxygen-nitrogen atmosphere is described below.

Simplified Free-Convection Equations for Oxygen-Nitrogen Mixtures

Combining Equations (4-15), (4-16), and (4-17), and the transport properties of air, with the pertinent information in Figure 4-1 gives the following equation:

$$Q_c = 4.4 (T_c - T_a) \left\{ \rho g \left[0.005 P (T_c - T_a) + 1.02 (P_c - P_a)_{H_2O} \right] \right\}^{0.25} \quad (4\text{-}19)$$

With comfortable conditions, $(P_c - P_a)_{H_2O}$ is much less than the maximum value over most of the body and has a small effect on the buoyancy force. It was therefore neglected, which simplified Equation (4-19) further to provide the following final result for free-convection cooling in air.

$$Q_c = 1.17 \rho^2 g (T_c - T_a)^{0.25} (T_c - T_a) \quad (4\text{-}20)$$

The free-convection cooling calculated to be available on the moon is presented in Figure 4-6 as a function of pressure and temperature difference.

Combining Equations (4-13), (4-15), (4-17), and (4-18) and the transport properties of air, with the pertinent information in Figure 4-1 provided the following simplified latent cooling equation:

$$Q_\ell = 25.7 \frac{C T_a}{P} (P_s - P_a)_{H_2O} \left\{ \rho g \left[0.005 P (T_c - T_a) + 1.02 (P_s - P_a)_{H_2O} \right] \right\}^{0.25} \quad (4\text{-}21)$$

The second term in the brackets was not deleted from the latent cooling equation as it was from Equation (4-19) because, over the 10 to 25 percent of the body area where most of the latent cooling is occurring under comfortable conditions, this term will be close to the value given in Equation (4-21). With C = 1 in Equation (4-21), the free-convection maximum evaporative capacity was calculated as a function of dew point and of atmospheric pressure and temperature; the results are shown in Figure 4-7.

Combined Free and Forced Convection

The simplest method for treating problems of combined free and forced convection involves the use of a rule proposed by McAdams (Ref. 52): calculate both the free and forced convection heat transfer coefficients using the appropriate equations and use the higher of the two values. The accuracy of this approach has been found to be within 25 percent of the measured results. In the problem of interest here, forced convection would probably be used only under conditions where the required heat transfer rate is much greater

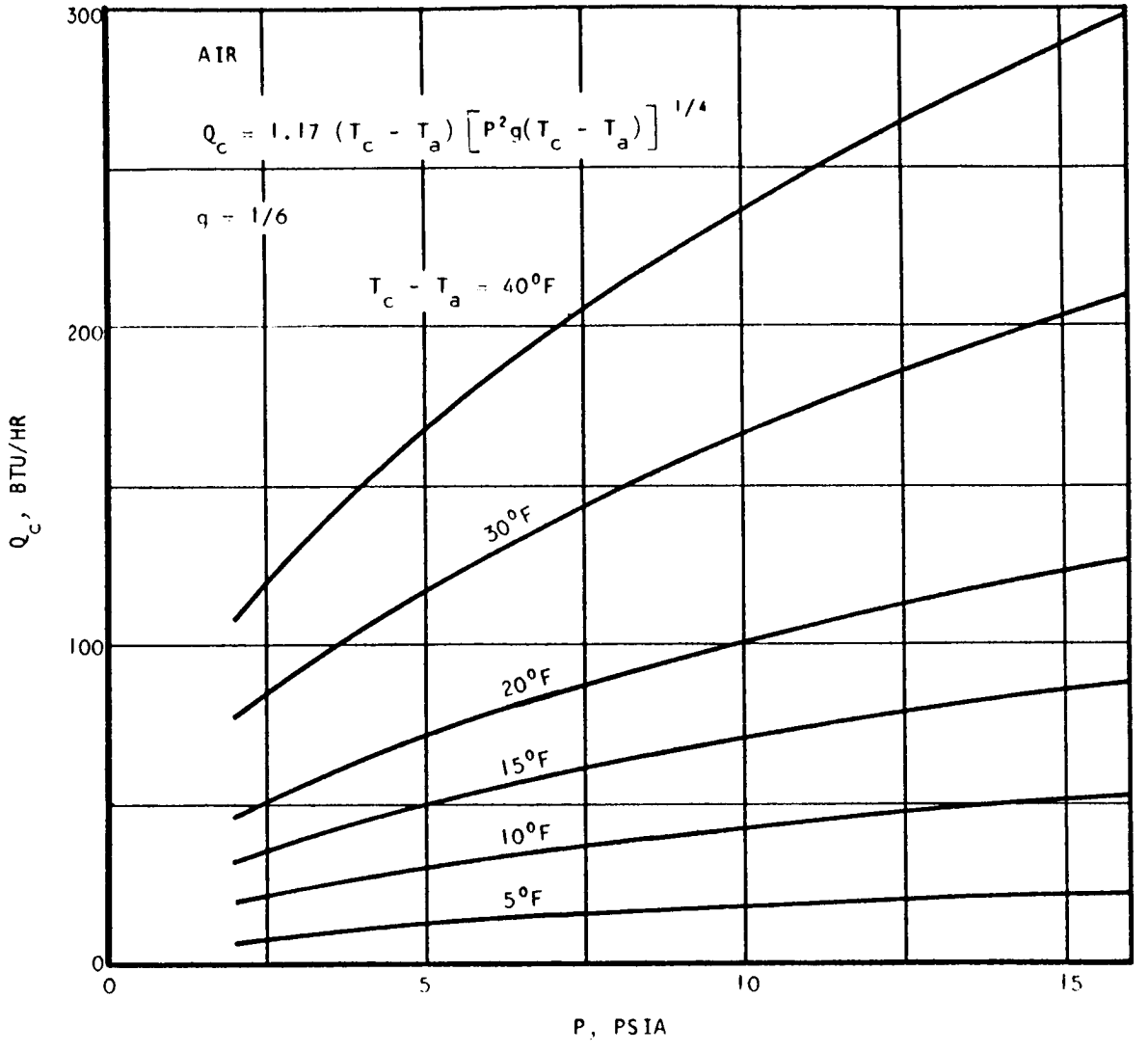

Figure 4-6. Lunar Free-Convection Cooling

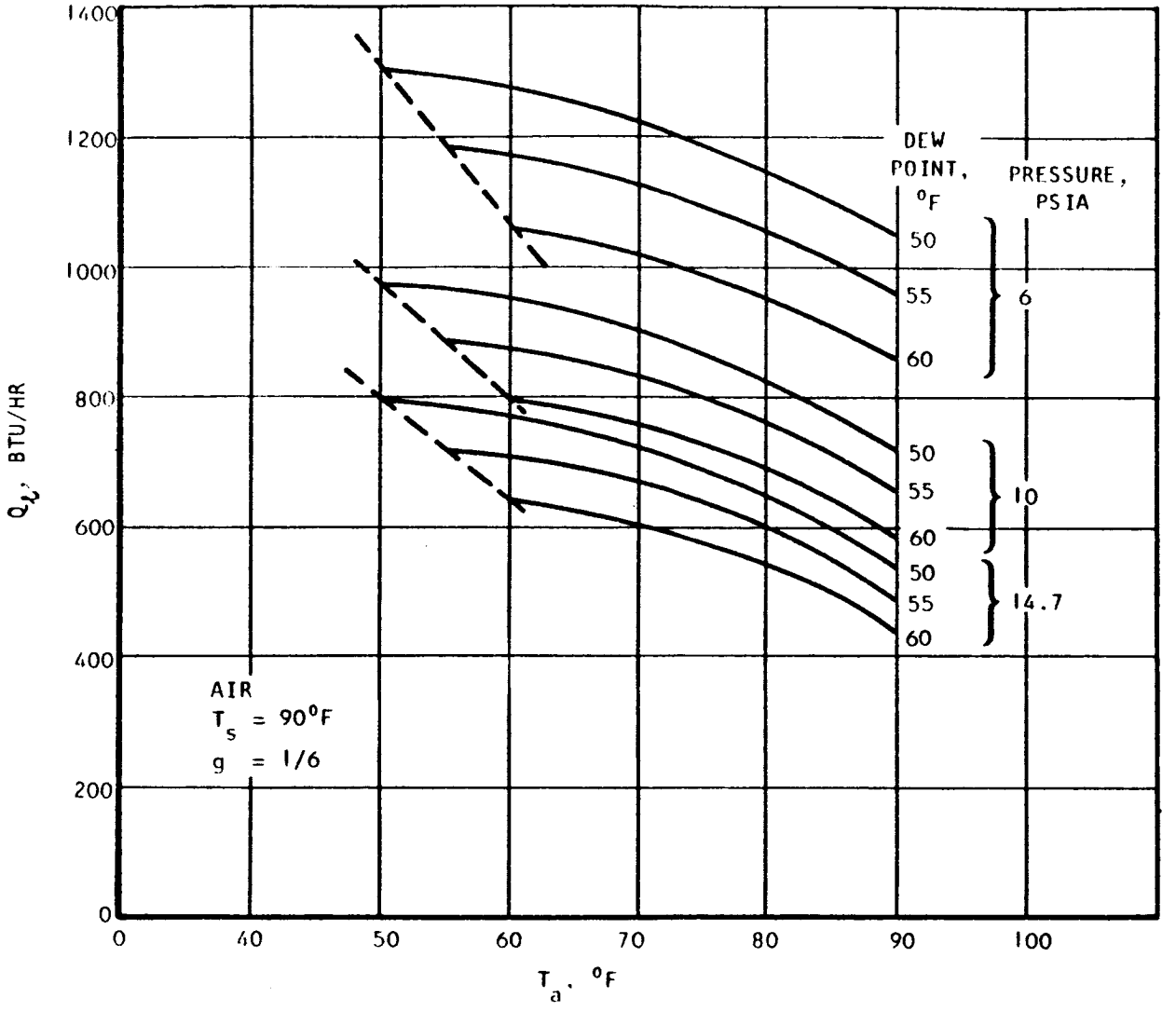

Figure 4-7. Lunar Free-Convection Maximum Evaporation Rate

than that provided by free convection. It is of interest to know, however, the forced-convection velocity at which the forced-convection heat transfer coefficient is equal to the free-convection heat transfer coefficient. The following approximate equation for this critical velocity in air was developed by setting Equations (4-12) and (4-20) equal to each other:

$$V_{crit} = 8.3 \left[g \, (T_c - T_a) \right]^{0.50} \text{ ft/min} \qquad (4\text{-}22)$$

With a 10°F temperature difference between the clothing surface and the atmospheric temperature, the critical velocity is 26 ft per min on earth and 10.5 ft per min on the moon.

COMFORT ZONE ANALYSIS

General

The information presented in the previous sections on physiological characteristics, comfort criteria, and energy transfer analysis are combined in this section to yield predictions for the boundaries of comfort zones in an oxygen-nitrogen atmosphere as a function of gravity, forced-convection velocity, metabolism, and atmospheric temperature and pressure. The requirements to be satisfied are: the energy balance stated in Equation (4-1); a skin temperature between 90°F and 93°F, with 91.4°F being a preferred value; and a required evaporation rate between 10 and 25 percent of the maximum evaporative capacity for the comfortable zone, and 25 to 70 percent in the tolerable zone. The energy transfer equations for oxygen-nitrogen mixtures are summarized in Table 4-1.

The development of the comfort zone boundaries is straightforward for a nude body. The added heat transfer resistance of clothing requires a trial-and-error solution for the clothing surface temperature, using Equation (4-2) in addition to the equations in Table 4-1. The calculation procedure is summarized below for both free and forced convection, and results are shown for 1/2 CLO as well as for a nude body.

Free-Convection Comfort Zones

The parameters that affect free convection are apparent from an examination of Table 4-1. In order to present the results as compactly as possible, some simplifying assumptions are adopted. It is assumed first that the mean radiation temperature of the walls and equipment is equal to the atmospheric air temperature. Also, because in practice the dew-point temperature under long-term comfortable conditions is allowed to vary only within narrow bounds and therefore has a small effect on maximum evaporative capacity, the water-vapor partial pressure in the atmosphere, P_{aH_2O}, is assumed to be constant. The remaining variables are gravity and atmospheric pressure and temperature. Therefore, the total free-convection cooling, which is equal to the metabolism, can be plotted versus atmospheric temperature for various combinations for gravity and pressure.

TABLE 4-I

HUMAN BODY ENERGY TRANSFER EQUATIONS IN OXYGEN-NITROGEN MIXTURES

Mode of Energy Transfer	Free Convection	Forced Convection
Radiation, Q_r	$2.65 \times 10^{-8}\ \varepsilon(T_c^4 - T_w^4)$	$2.65 \times 10^{-8}\ \varepsilon(T_c^4 - T_w^4)$
Convection Heat Transfer, Q_c	$1.17\ [P^2 g]^{0.25}\ (T_c - T_a)^{1.25}$	$0.407\ \sqrt{PV}\ (T_c - T_a)$
Latent Cooling of Evaporation, Q_ℓ	$25.7\ \frac{CT_a}{P}\ (P_s - P_a)_{H_2O} \left\{ Pg\ [0.005P(T_s - T_a) + 1.02(P_s - P_a)_{H_2O}] \right\}^{0.25}$	$2.46\ CT_a\ \sqrt{V/P}\ (P_s - P_a)_{H_2O}$

Q - Btu/hr

V - ft/min

T - ^{o}R

P - psia

g - fraction of earth gravity

C - fraction of maximum evaporation rate

The calculation procedure is summarized in Table 4-2 for lightly clothed, earth conditions.

TABLE 4-2

FREE-CONVECTION COMFORT ZONE CALCULATION PROCEDURE*

T_a	T_c	Q_r	Q_c	T_c	Q_ℓ (C = 1)	$M = Q_r + Q_c + Q_\ell$		
						C = 0.10	0.25	0.70
60	81	269	202	80.9	1192	590	769	1306
70	84.5	191	127	84.4	1130	431	600	1109

* $p = 14.7$ psia; $g = 1$; CLO = 1/2; $\epsilon = 0.8$

The trial and error solution for T_c requires an arbitrary selection of a value for T_c, calculation of Q_r and Q_c using the equations in Table 4-1, and then calculation of T_c using Equation (4-2). When the assumed and calculated value of T_c agree, the calculation proceeds as shown in Table 4-2.

Free-convection comfort zones were predicted for the gravity and atmospheric pressure existing on earth; the results are shown in Figures 4-8 and 4-9 for nude and 1/2 CLO conditions, respectively. The results shown in Figure 4-9 were calculated with clothing and dew point values corresponding to those used in developing the comfort zone boundaries shown in the ASHRAE Comfort Chart presented as Figure 2-4. The seated, at-rest activity used to develop Figure 2-4 corresponds to a metabolism of approximately 400 Btu/hr. The circles shown on Figure 4-9 at a metabolism of 400 Btu/hr represent the ASHRAE data. The agreement with the prediction is significant; the slightly cool and slightly warm temperatures, which would define the boundaries of the comfortable range, are within 1^0F of the predicted values. The comfortable temperature is in the middle of the comfortable zone, and the warm temperature is 5^0F greater than the upper limit for the comfortable zone. The excellent agreement between the comfort zone predictions presented in Figure 4-9, which is based upon the general analysis described above, and the ASHRAE data provides considerable confidence in the validity of the correlations and methods used.

Comfort zone predictions were also made for a lunar gravity of 1/6 earth gravity, and a pressure of 6 psia, which is contemplated for some lunar shelters, with the results shown in Figures 4-10 and 4-11. Free-convection comfort zone predictions, similar to those shown, can be made for any set of conditions and can be used to determine if free convection will provide comfortable conditions, and the atmospheric temperature required for the metabolisms that will exist.

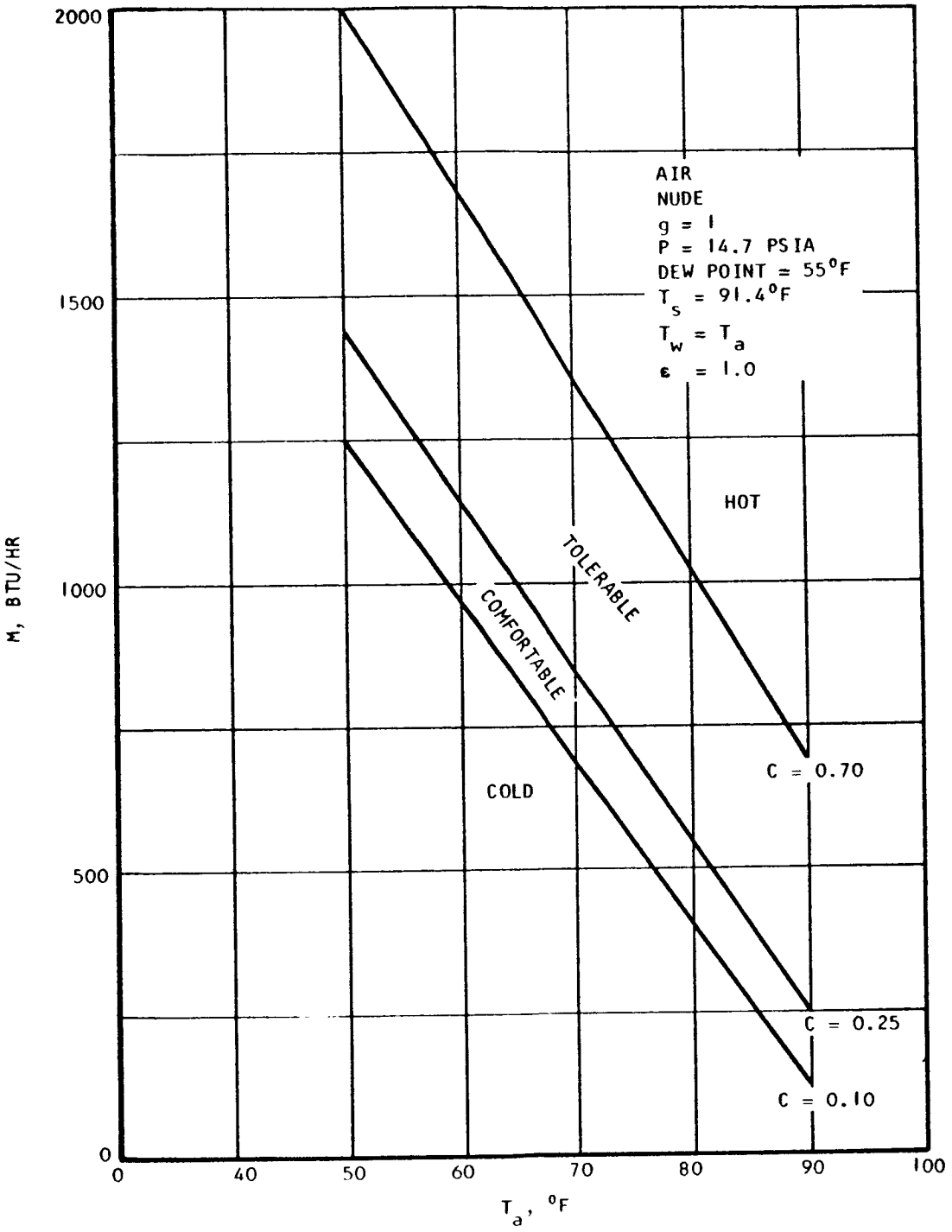

Figure 4-8. Earth Free-Convection Comfort Zones

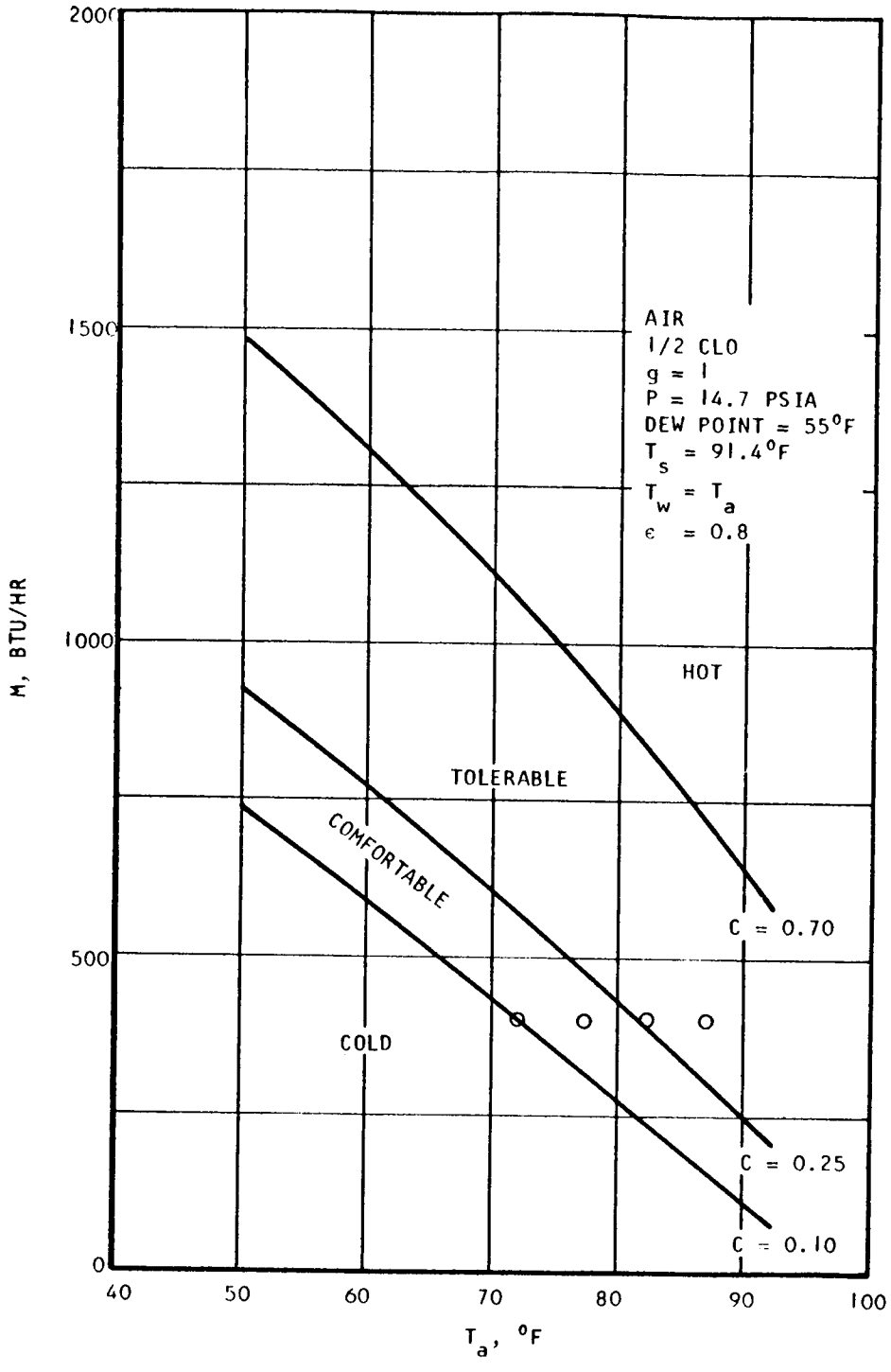

Figure 4-9. Earth Free-Convection Comfort Zones

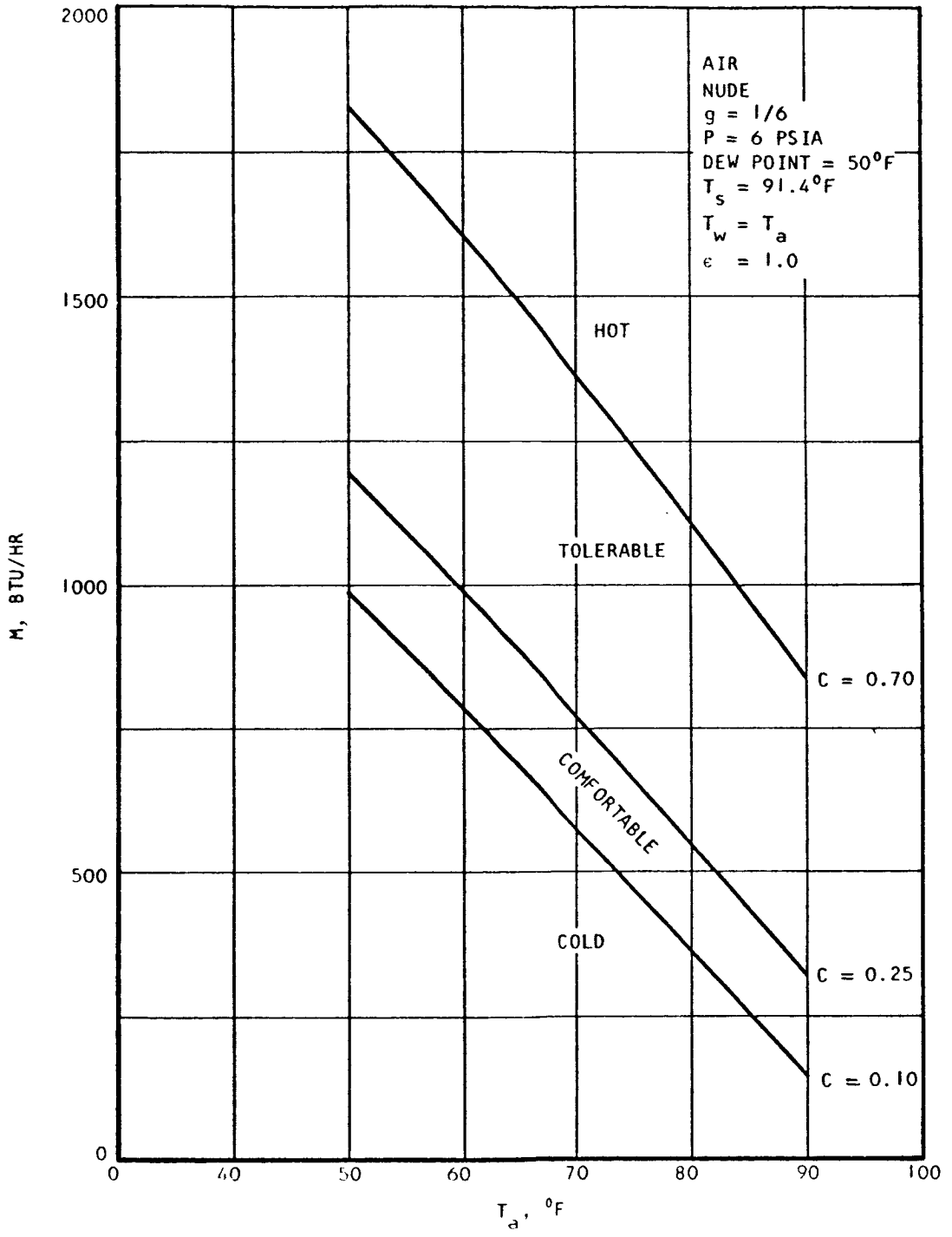

Figure 4-10. Lunar Free-Convection Comfort Zones

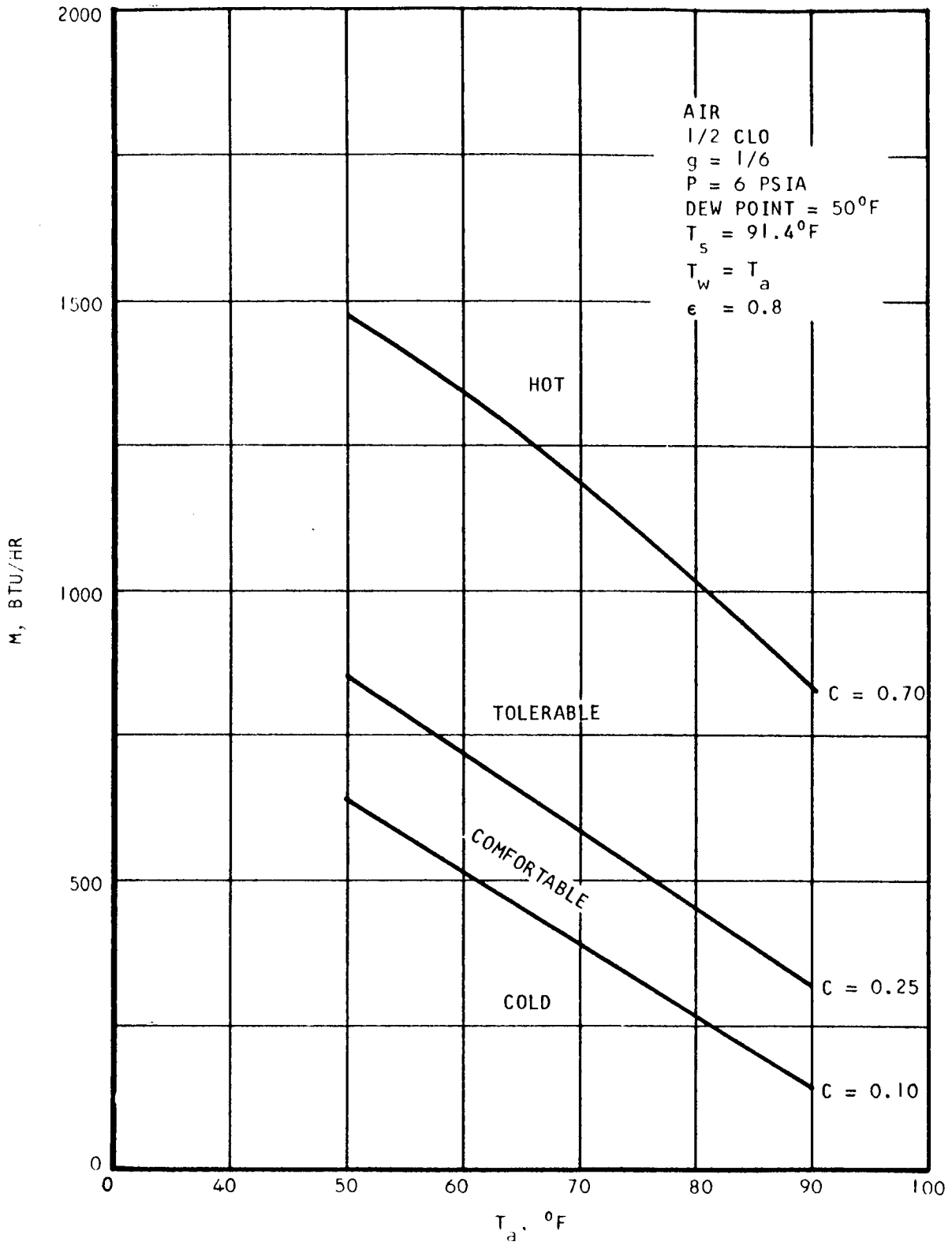

Figure 4-11. Lunar Free-Convection Comfort Zones

Forced-Convection Comfort Zones

Velocity is an important parameter in forced-convection cooling problems, in addition to all the parameters that affect free convection. It is therefore impossible to present the forced-convection comfort zone information in as compact a way as was possible with free convection. The same simplifying assumptions about wall temperature and dew point are useful, but a separate figure showing the comfort zone boundaries as a function of velocity and atmospheric temperature must be prepared for each metabolism and atmospheric pressure.

The first step in the preparation of forced-convection comfort zones is to insert Equations (4-6), (4-12), and (4-14) into Equation (4-1) and to solve for the velocity; this provides the following result:

$$V = \left[\frac{M - 2.65 \times 10^{-8} \epsilon \left(T_c^4 - T_w^4\right)}{0.407 \sqrt{P}\ (T_c - T_a) + 2.46 \frac{C\,T_a}{\sqrt{P}} (P_s - P_a)_{H_2O}} \right]^2 \qquad (4\text{-}23)$$

The calculation for a nude body is straightforward, as T_c is equal to the skin temperature. Then, for each combination of metabolism and atmospheric pressure, Equation (4-23) can be solved for velocity as a function of atmospheric temperature, while C takes on the comfort zone boundary values of 0.10, 0.25, and 0.70. The results of this calculation for a pressure of 14.7 psia and a metabolism of 500 Btu/hr is shown in Figure 4-12.

The trial-and-error calculation required to establish clothed, forced-convection comfort zones is illustrated in Table 4-3.

TABLE 4-3

FORCED CONVECTION COMFORT ZONE CALCULATION PROCEDURE*

T_a	T_c	Q_r	$M-Q_r$	$Q_c/\sqrt{V}$	$0.1\ Q_\ell/\sqrt{V}$	V	Q_c	T_c
60	82	276	224	34.3	18.4	18.1	146	82
70	83.5	178	322	21	18.8	65	170	83.7

*M = 500; CLO = 1/2; ϵ = 0.8; P = 14.7 psia; C = 0.10

For each value of C and T_a, a value of T_c is assumed. With the assumed value of clothing temperature, the radiation cooling and velocity is calculated; and with the calculated velocity value, Q_c is calculated. The clothing surface temperature is then calculated using the calculated values of Q_c and Q_r in Equation (4-2). When the assumed and calculated value of T_c agree, one

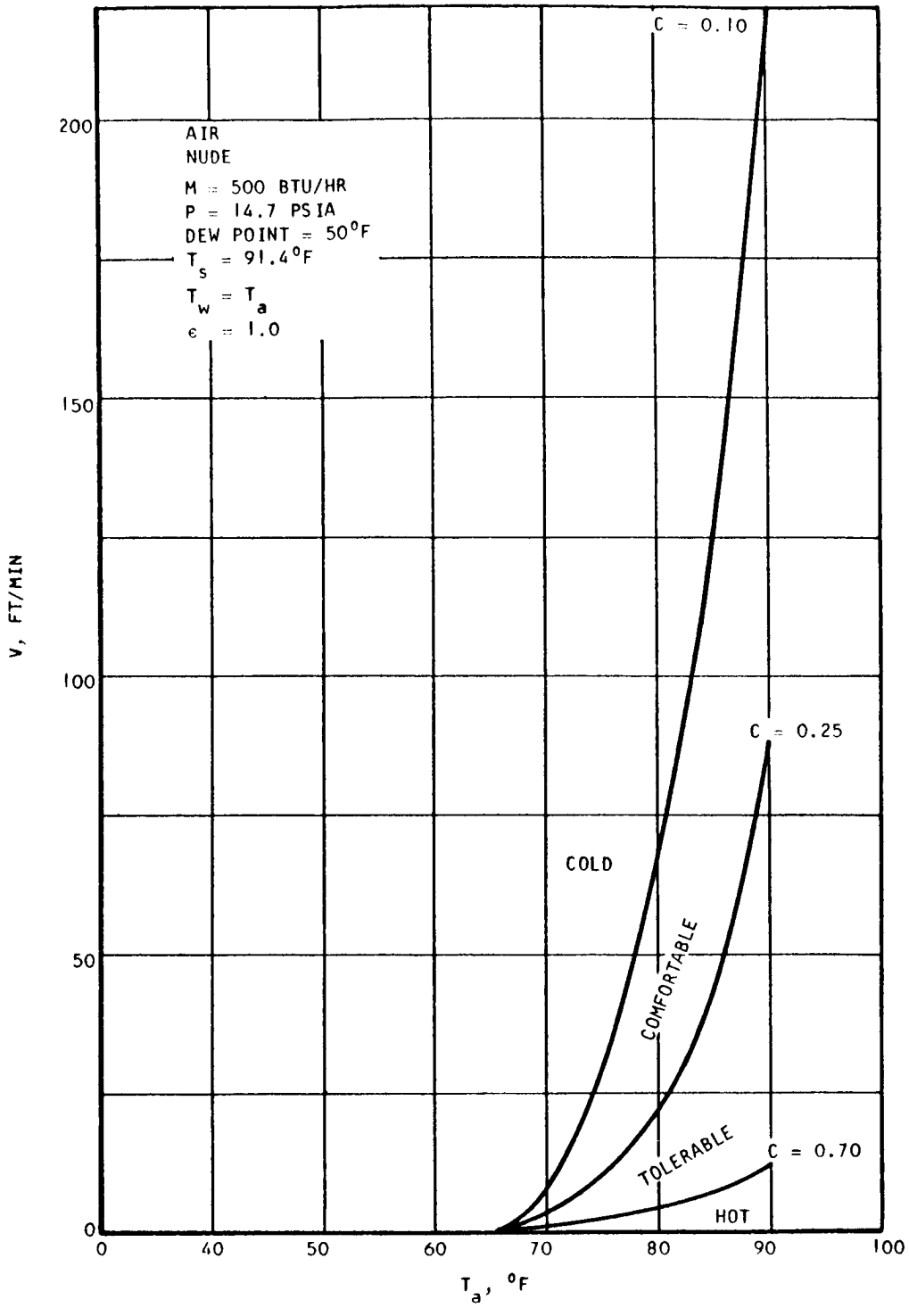

Figure 4-12. Forced-Convection Comfort Zones

point has been established. The results of this calculation for the conditions given in Table 4-3 are shown in Figure 4-13. Figures 4-14 through 4-17 were prepared to show the effect of metabolism and clothing on forced-convection comfort zones for a pressure typical of those recommended for various long-term, shirtsleeve-environment space missions. Increases in both metabolism and clothing tend to increase the velocity required at a given temperature and broaden the comfortable zone.

DISCUSSION AND CONCLUSION

While the equations, criteria, and calculation procedures described above provided predictions that were in substantial agreement with empirical information, in some cases it may be necessary to refine the analysis to eliminate some of the simplifying assumptions and uncertainties. For this reason a brief discussion of some of these details is presented below.

The comfort zone charts were prepared assuming a constant skin temperature of 91.4°F. Skin temperatures between 90°F and 93°F are comfortable, however, and values as high as 95°F tolerable. It is possible, therefore, that a skin temperature of 90°F should be used to evaluate the lower boundary of the comfortable zone at 10 percent of maximum evaporative capacity, while values of 93°F and 95°F should be used to evaluate the boundaries at 25 and 70 percent of maximum evaporative capacity, respectively. This would have the effect of broadening both the comfortable and tolerable zones. While the results of Fahnestock, et al., (Ref. 5) indicate that this may be a better approach, additional comfort data are required before a final decision can be made.

The assumption that the mean radiation temperature of the walls and equipment is approximately equal to the atmospheric gas temperature is very useful for general parametric studies, but may be seriously in error. It will, therefore, be necessary in many cases to perform a more rigorous radiation heat transfer analysis once the enclosure geometry and temperature distribution have been established in some detail.

The effect of clothing was greatly simplified; the heat transfer resistance of the clothing was assumed to be uniform over the entire body, and the heat transfer area and the evaporative cooling capacity were assumed to be unaffected by the presence of clothing. It is difficult to improve upon these assumptions due to the lack of detailed information about clothing heat transfer resistance and area. Also, until these assumptions are shown to cause significant error in the results there is little motivation to improve them. However, these clothing assumptions should be considered for each case to determine if the rationale used to justify their use is valid.

The regional variation in body temperature, heat rejection, and sweat rate shown in Figure 2-3 was used to justify some of the assumptions in the analysis, but was not directly applied in detail. Once again, until it has been shown that using a uniform skin temperature leads to a significant error in the results, there is little justification for analyzing the body as a number of separate regions.

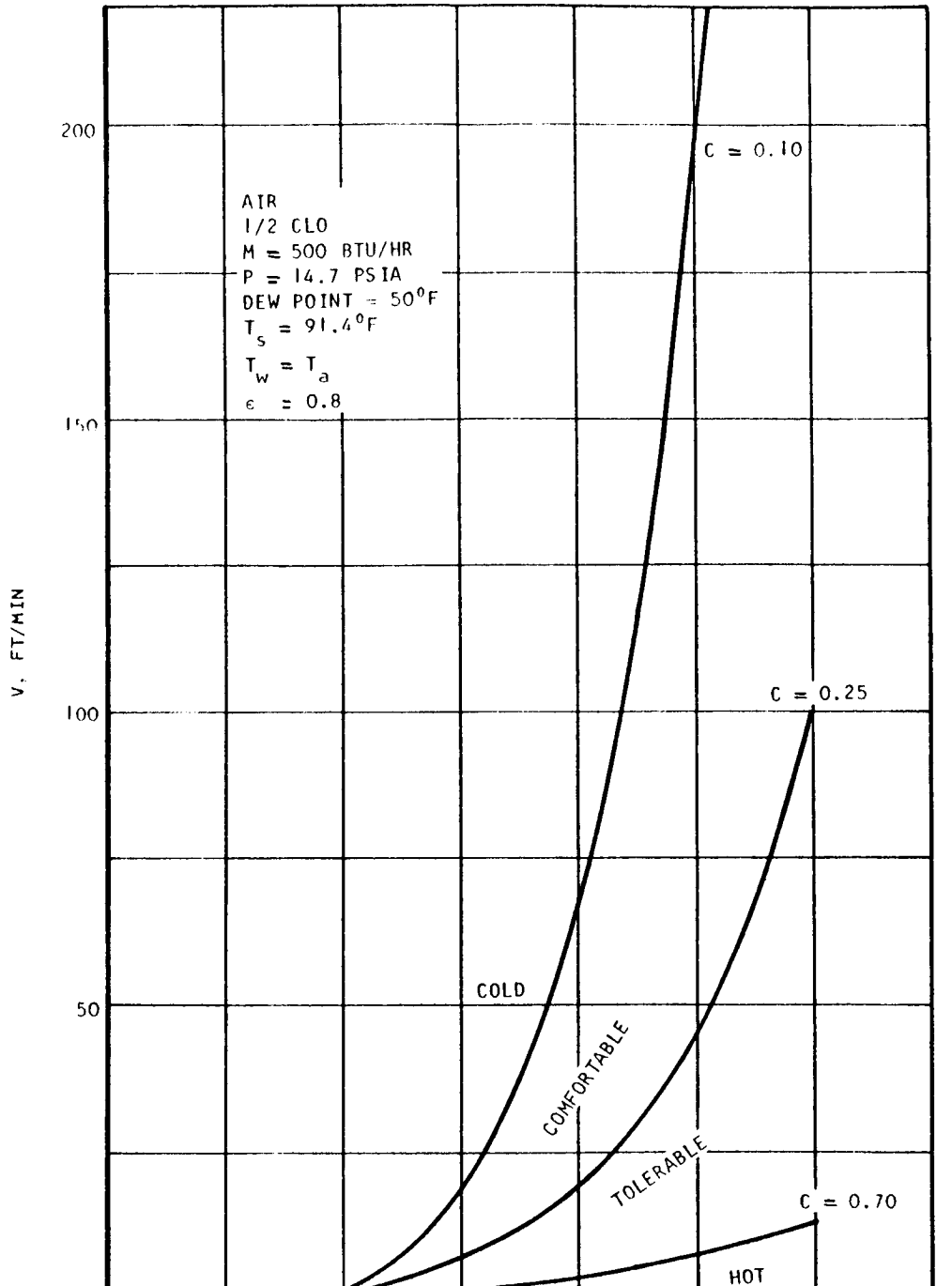

Figure 4-13. Forced-Convection Comfort Zones

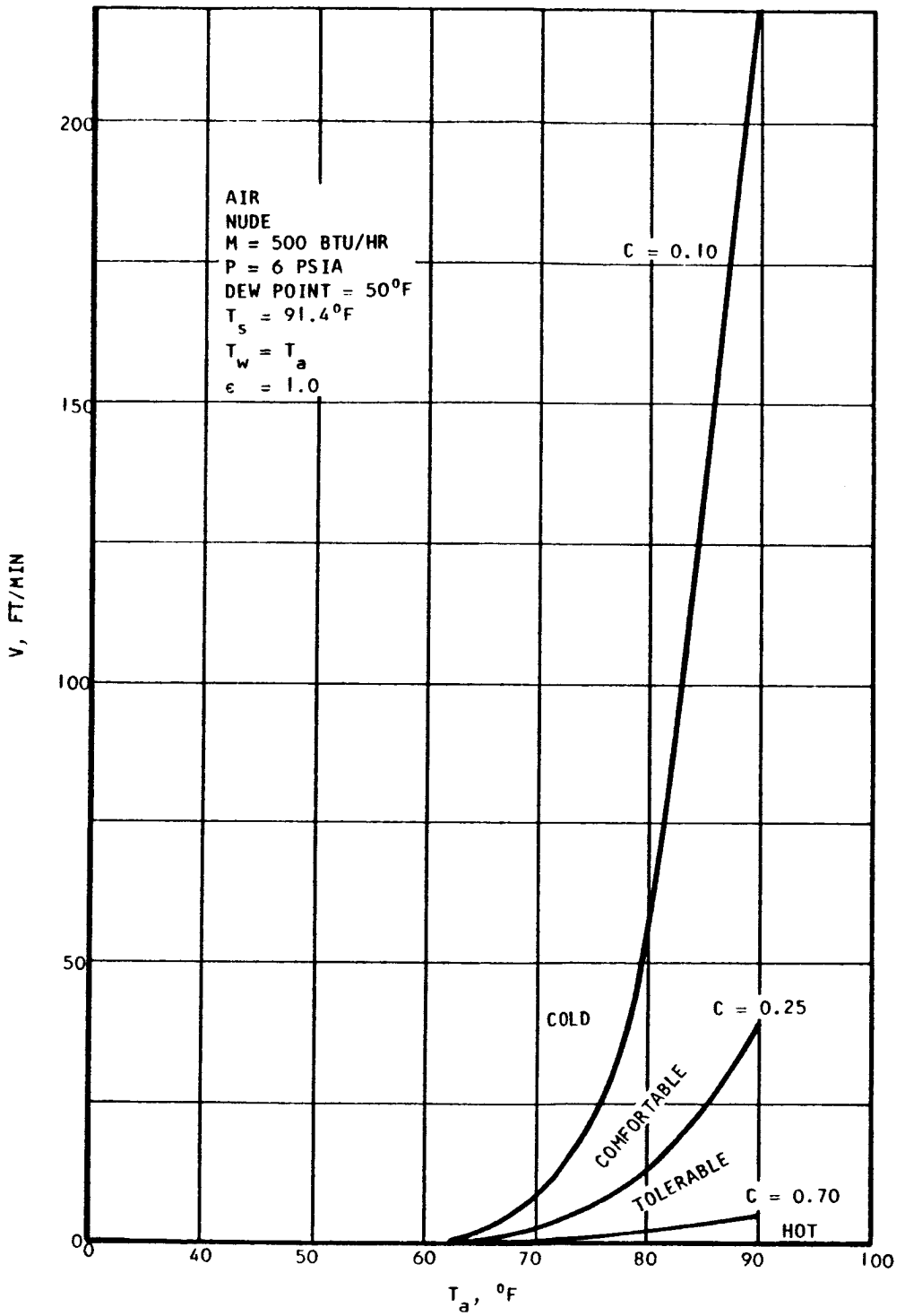

Figure 4-14. Forced-Convection Comfort Zones

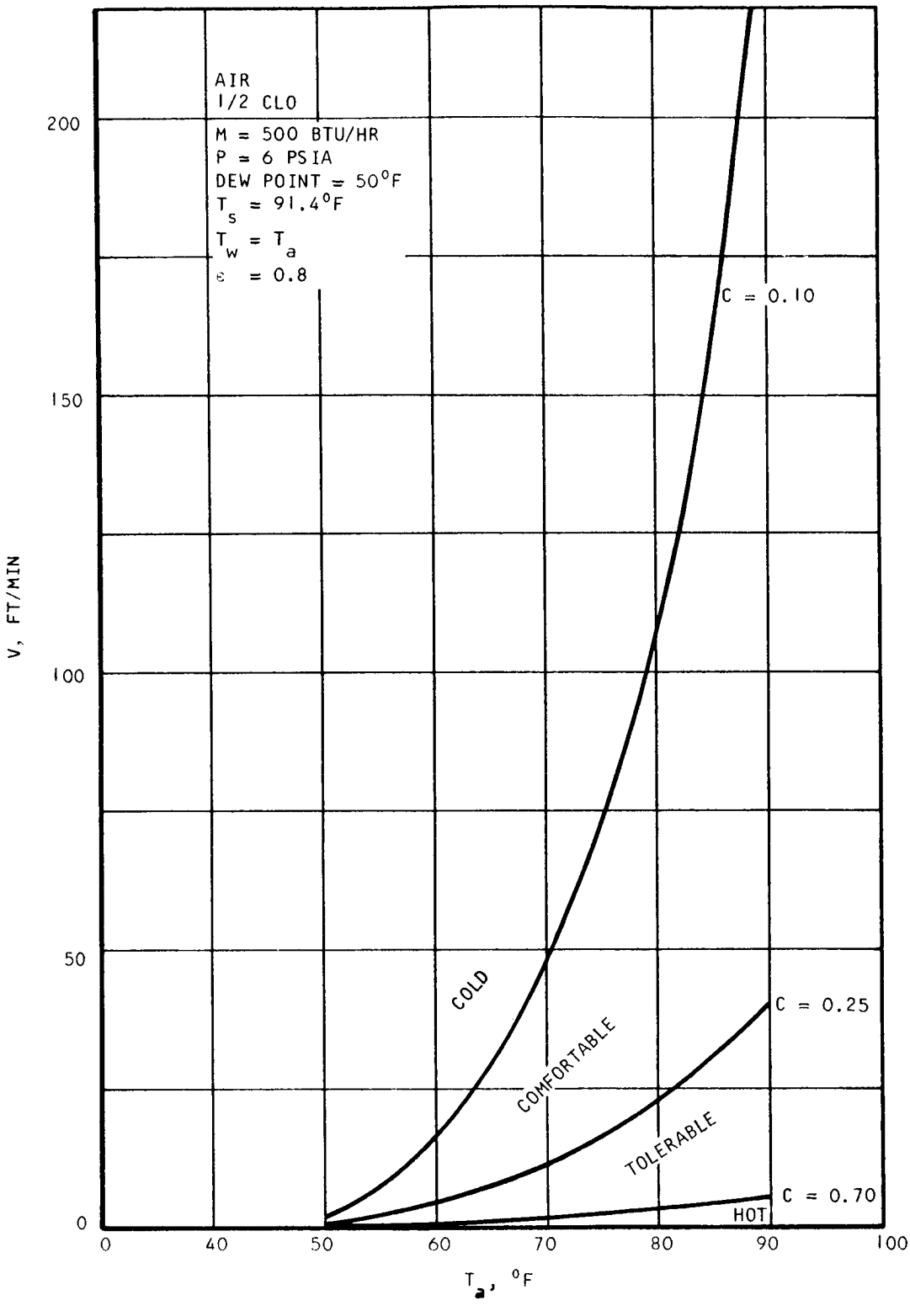

Figure 4-15. Forced-Convection Comfort Zones

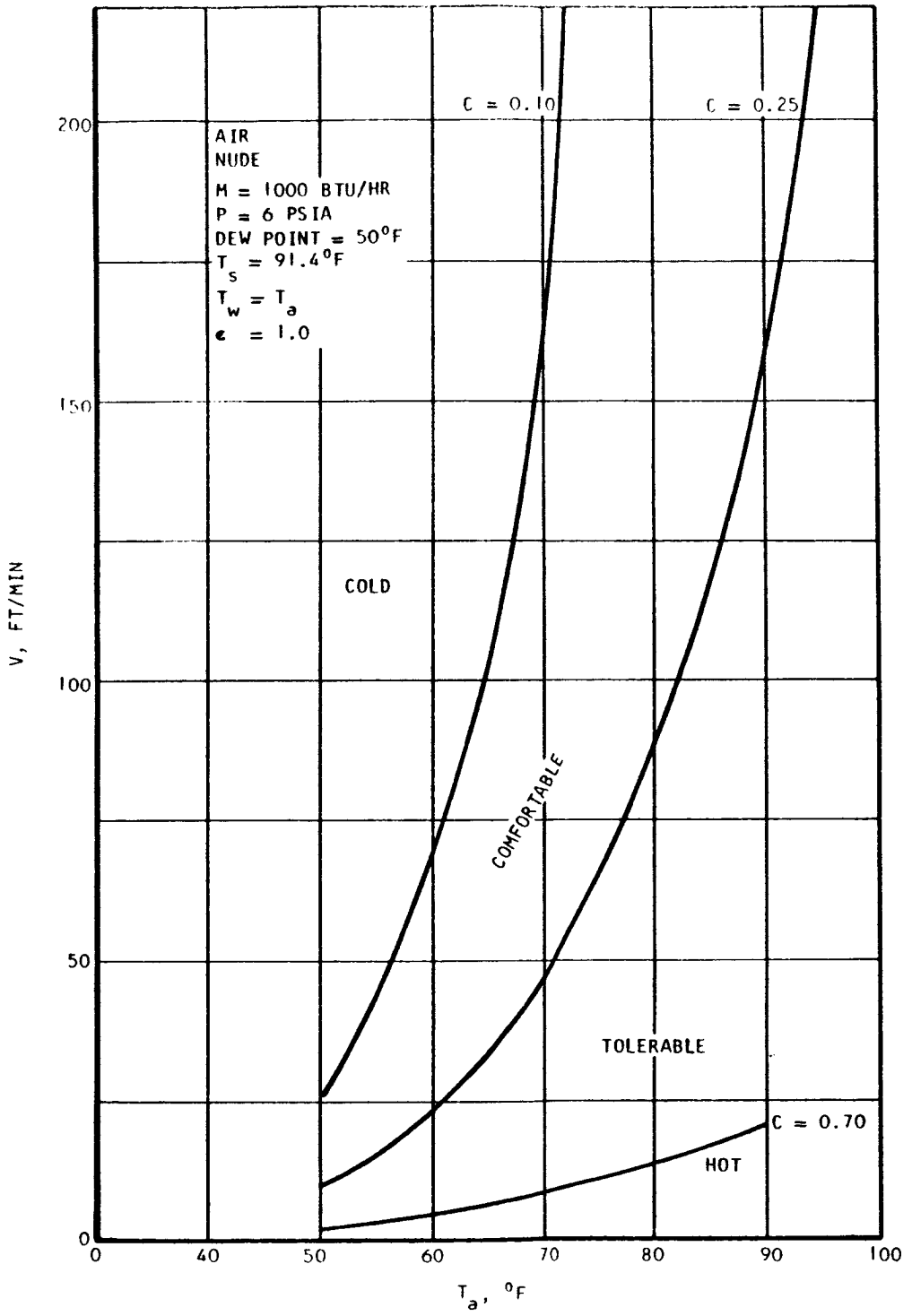

Figure 4-16. Forced-Convection Comfort Zones

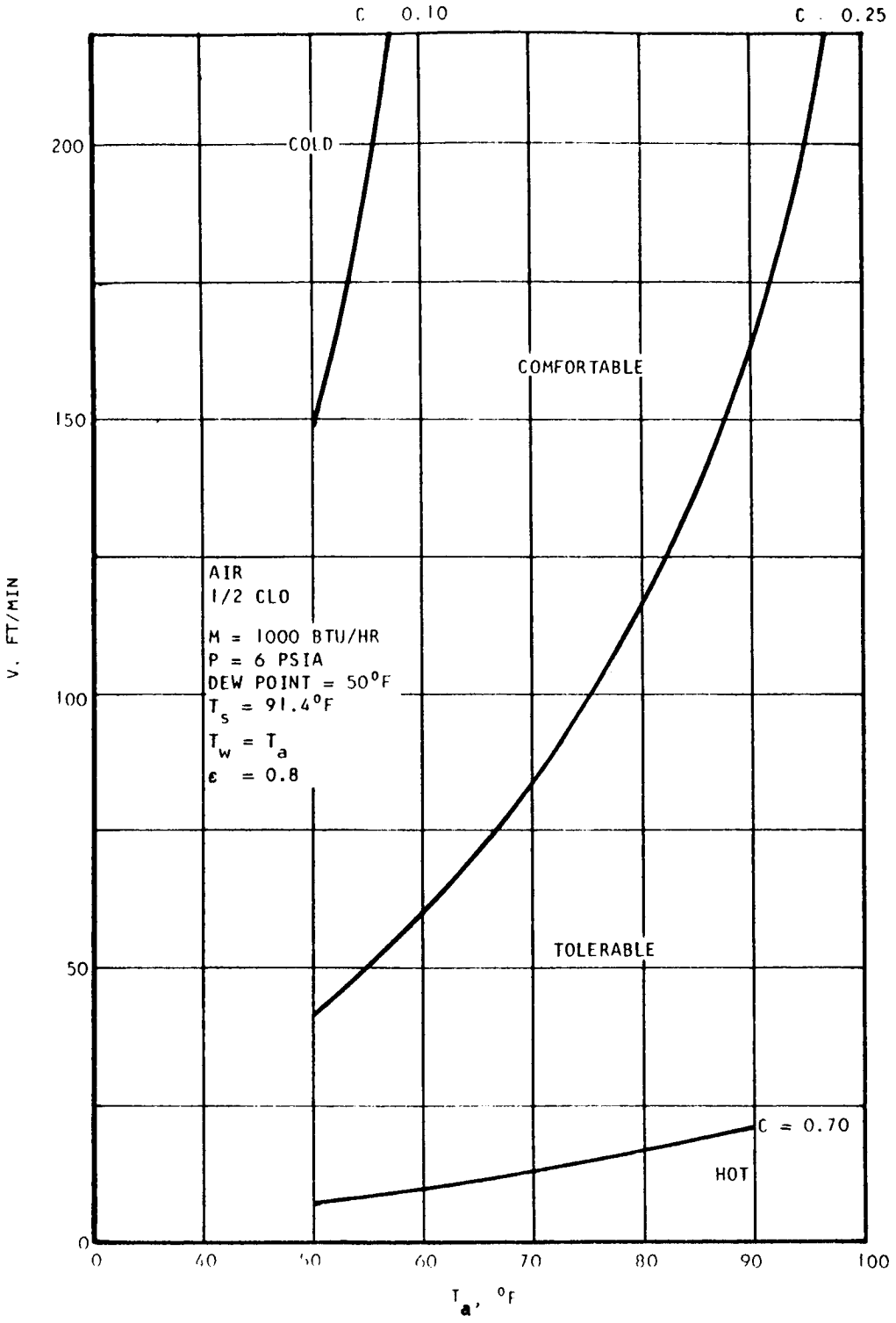

Figure 4-17. Forced-Convection Comfort Zones

Average heat and mass transfer coefficients were used to calculate the cooling rates. In fact, there may be substantial variation of these coefficients with position (Ref. 53). The discussion of this feature in the referenced paper may, therefore, be of interest.

It was assumed that the maximum water-vapor partial pressure on the skin is equal to the saturation pressure of water corresponding to the skin temperature. Due to the presence of oils and salts in sweat, however, the actual maximum water-vapor partial pressure may be only 90 percent of the saturation pressure (Ref. 54). The value of this uncertainty is consistent with those of the other simplifying assumptions.

In much previous work, the importance of relative humidity has been exaggerated. The latest ASHRAE data, which are presented in Figure 2-4, shows a much smaller effect. This is in agreement with results predicted by the equations contained in this report. which show that relative humidity becomes important only at relatively high atmospheric temperatures, where the atmospheric water-vapor partial pressure can become a significant fraction of the water-vapor saturation pressure corresponding to skin temperature.

Latent cooling by evaporation has a minimum value due to respiratory water loss and diffusion of water vapor through the skin; the latter provides much the larger contribution. The comfort criterion adopted states that this minimum value is 10 percent of the maximum evaporation rate (Ref. 25). While this may have been true for the test conditions under which the comfort criterion was developed, the general validity of this statement is questionable; this is because respiratory water loss is primarily a function of metabolism, and diffusion of water through the skin would be much more independent of atmospheric conditions than maximum evaporation rate. Additional testing is therefore recommended to determine the important relation for the minimum quantity of latent cooling.

The heat and mass transfer analysis described above assumed a constant value for the temperature and water vapor content of the air flowing by the body. In fact, the temperature will tend to increase due to convective heat transfer and the water content due to evaporative cooling. Approximate estimates of the magnitude of these effects have shown that, in general, they cause less than a 10 percent decrease in cooling. For example, the air temperature rise associated with 100 Btu/hr of convective cooling in a 6 psia atmosphere, assuming an air velocity of 40 ft/min intercepts a body cross-sectional area of 3 sq ft, is only 2^{0}F. Similar estimates can be made in any particular case to determine if the uniform temperature and water content assumption is justified.

The equations given in Table 4-1, which were used to develop the comfort zones presented in Figures 4-10 to 4-17, apply only to oxygen-nitrogen atmospheres. While this is the conventional atmosphere for man, others (for example, oxygen-helium) are being considered for some space missions. The

development of the comfort zones for these unconventional atmospheres proceeds in the same way as for air. However, it will be necessary to develop a separate set of simplified equations by inserting the fluid properties for each composition into the general energy transfer equations presented in this report.

The general approach described in this report for predicting conditions for human comfort accounts for the interrelated factors of physiology, comfort, and energy transfer. The approach appears to be valid, based upon comparison with limited experimental data, even though many simplifying assumptions were incorporated in the analysis. Final confirmation of the general validity of this approach requires additional comfort data at reduced pressure and more than one metabolism.

SECTION 5

EXTRAVEHICULAR SUIT HEAT BALANCES

INTRODUCTION

Results of some of the earth-orbital extravehicular suit heat balance studies were presented in Section 3 of this report to illustrate the effects of two different radiative suit cooling concepts. Both of these involved radiation from the outer surface of the suit as the primary means of cooling. The difference between the two concepts is that in one method, the body is cooled by conduction through the suit wall, and in the other method, the body is cooled by radiation to the inner wall of the suit through an air gap.

Environmental Parameters

This section of the report is devoted to a more extensive discussion of computation methods and presentation of results applicable to environments other than earth-orbital. Extravehicular heat balance studies have been made for the following environments:

Earth orbit, 160 nm, in proximity to spacecraft and remote from spacecraft

Lunar orbit, 50 nm, in proximity to spacecraft and remote from spacecraft

Mars orbit, 600 nm, in proximity to spacecraft and remote from spacecraft

Lunar planes

Lunar craters, 20-degree wall (from normal)

Mars surface

For purposes of discussion and description, the environments can be classified as planetary orbital, lunar surface, lunar craters, and Mars surface. Table 5-I lists some of the relevant thermal parameters for the extravehicular heat balances.

Earth and Mars thermal radiation fluxes for orbital heat balances were calculated from planetary heat balances. Thus, the average thermal radiation flux for earth and Mars orbits is 25 percent of the solar constant. For computation of the planetary thermal heat flux in a lunar orbit, it was necessary to consider the surface temperature variation with position, which is given approximately by the cosine law.

TABLE 5-I

PLANETARY THERMAL PARAMETERS

	Planet		
	Earth	Moon	Mars
Radius, nm	3441	938	1799
Albedo	0.35	0.07	0.15
Solar constant, Btu/hr-ft^2	443	443	190.5

Extravehicular Suit Thermal Parameters

The man in a pressurized extravehicular suit was assumed to have an effective surface area for radiant interchange of 21.8 ft^2 in the form of a cylinder 13.2 in. in diameter and 69.1 in. long. The spectral characteristics of the outer surface of the suit were varied over the range shown in Table 5-2 to demonstrate the effect of these parameters.

TABLE 5-2

ASSUMED SUIT SPECTRAL CHARACTERISTICS

Surface Type	Solar Absorptivity	Thermal Emissivity	Typical Material
Reflective	0.10	0.05	Aluminized mylar
Suit material	0.32	0.56	Gemini suit
Spectrally selective	0.20	0.80	Nylon, dacron

It is believed that this range of spectral properties will adequately cover the performance that can be anticipated.

Figure 5-I shows a typical wall construction for fabric suits. In order to make the study as realistic as possible, a composite thermal conductivity of 0.02 Btu/hr-ft-^{0}F was used with a composite wall thickness of 0.35 in. This performance is representative of state-of-the-art (Gemini) pressure suits. In severe thermal environments, such as that on the lunar surface, the addition of an outer thermal garment using "superinsulation" (multiple

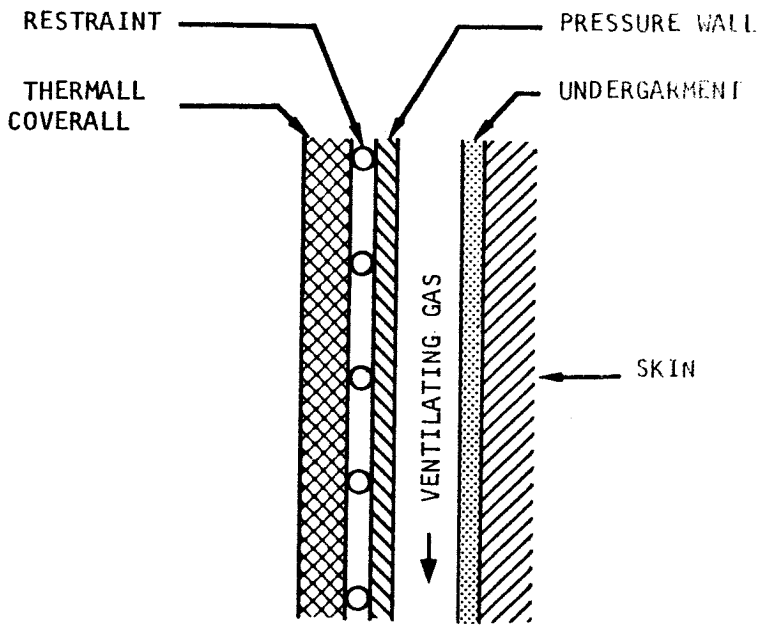

Figure 5-1. Typical Suit Wall Construction

layers of aluminized mylar) with an effective thermal conductivity of 5×10^{-4} Btu/hr-ft-^{0}F was assumed. The implication of meteoroid protection provisions on system thermal design were not considered.

In the extravehicular suit heat balances discussed in this section of the report, the extravehicular suit is assumed to have ventilating gas gap between the suit inner wall and the body. The effect of the ventilating gas velocity on heat transfer was neglected; it was assumed that the predominant heat transfer process between the suit and the body was radiation from a mean skin temperature of 90^{0}F.

Heat Balance Computation Methods

In determination of the extravehicular heat balances, the effective sink temperature is an important parameter that characterizes the external thermal environment and a surface in that environment. The effective sink temperature represents the equilibrium temperature of a surface with no heat transmission other than by radiant interchange with the surroundings. The effective sink temperature is calculated from an energy balance that considers the energy flux represented by the radiant source (Q_x), the absorptivity of the surface to that radiation (α_{bx}), and the view factor of the surface to the source of radiation (F_x):

$$\sigma \epsilon_b T_{es}^4 = \Sigma Q_x \alpha_{bx} F_x \qquad (5\text{-}1)$$

Because of the complexity of the view factor equations for the cases treated in the present study program, detailed listing of the heat balance relationships will not be given here. Rather, reference is made to the three computer program tabulations contained in the appendixes. The discussion in this section of the report will be concerned primarily with results of the computer studies and with the assumptions forming the basis for the analysis.

The extravehicular suit heat balance computations were made on the basis of attainment of equilibrium conditions. Thermal inertia will tend to reduce some of the peaks and valleys shown in the temperature and heat flux distributions. Since the study was intended to be of a parametric nature with extravehicular suits of an undefined design, this approach should be valid in establishing the scope of the problem. In the performance analysis of extravehicular systems for specific missions, the extravehicular assembly design, the spacecraft thermal parameters, and the mission parameters should be defined in sufficient detail to permit a transient-state analysis.

PLANET ORBITAL

Figure 5-2 shows the geometry assumed in the orbital extravehicular studies. The computer program developed for this study, tabulated in Appendix A for reference, is applicable to a man in an extravehicular suit with arbitrary surface properties and insulating characteristics in variable proximity to a spacecraft of arbitrary diameter, internal heat generation,

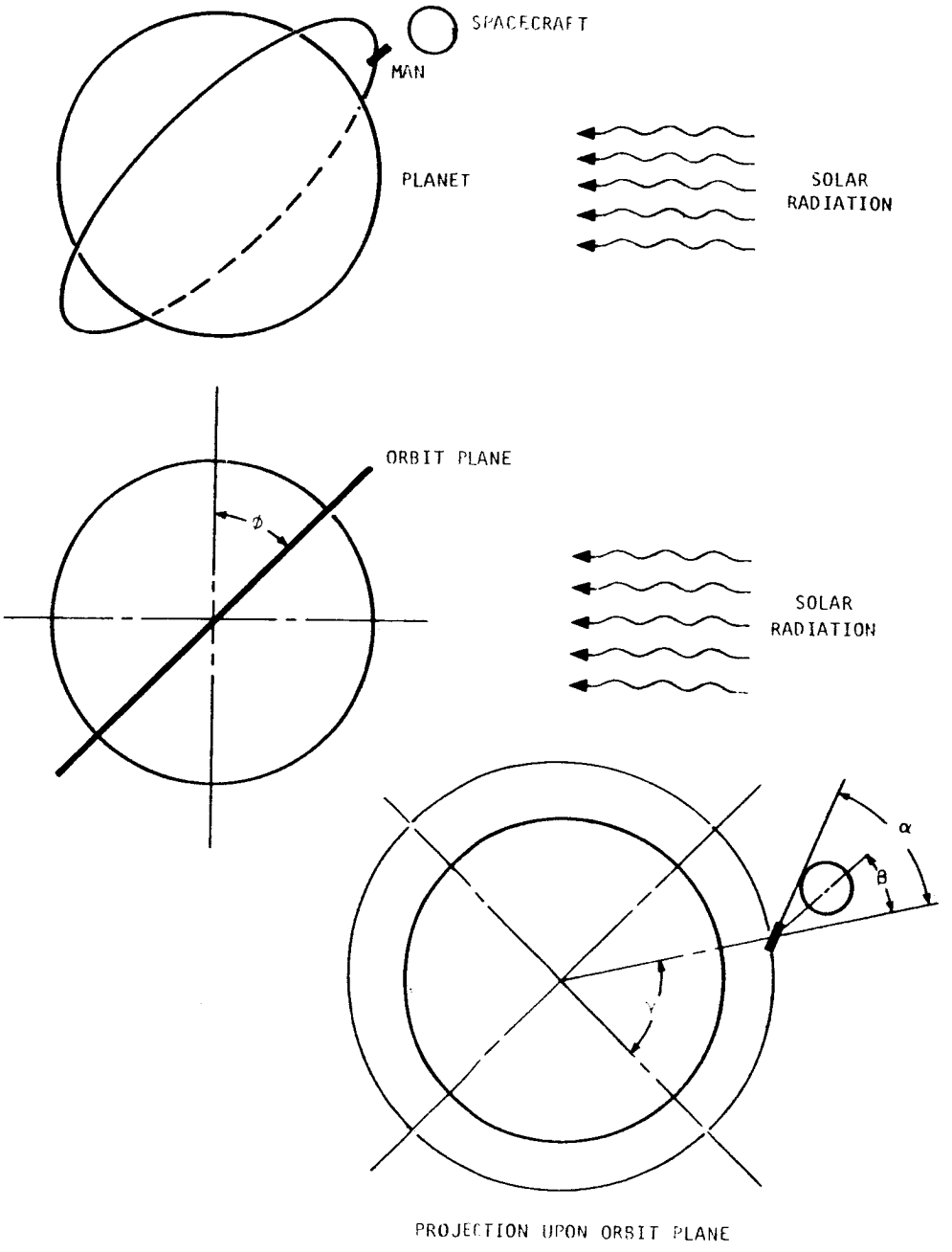

Figure 5-2. Planet Orbit Extravehicular Heat Balance Geometry

and surface characteristics. The orbit height and inclination, vehicle anomaly, planet diameter and albedo, and solar constant are all variable. The computer program assumes circular orbits and spherical spacecraft.

Table 5-3 shows a typical tabulation for an earth-orbital extravehicular heat balance. In this case, the orbital plane was inclined at a 45-degree angle relative to solar radiation. For convenience in the heat balance studies, the orbital plane was referenced at an angle ($\emptyset$) relative to solar radiation. Since in an actual orbit this angle will be continually changing, the data presented do not represent orbital histories but give the variation that can be anticipated with varying orbital parameters.

Earth Orbit

Figures 5-3, 5-4, and 5-5 present the effective sink temperatures obtained by extravehicular suits in 160-nm earth orbits. Figures 5-3 and 5-4 are applicable to a suit with a spectrally selective surface coating (ϵ_b = 0.80 and α_b = 0.20) and Figure 5-5 is applicable to a suit with a reflective coating (ϵ_b = 0.05 and α_b = 0.10). Figure 5-4 demonstrates the effect obtained when the extravehicular suit moves away from the spacecraft to a distance where the thermal inputs from the spacecraft to the suit are negligible. As might be expected, the result of this is an increase in the temperature gradient obtained around the body.

As previously mentioned, the effective sink temperature parameter represents the equilibrium suit surface temperature with no heat conduction through the suit wall. Heat conduction will drastically modify the surface temperature distribution. This is illustrated by Figure 3-22 for a typical earth-orbital case.

Lunar Orbit

Because of the lack of atmosphere on the moon, the lunar surface temperature varies greatly with position of the sun relative to the surface. Therefore, in the lunar orbital heat balances, variation in the thermal radiation with orbital position was taken into account. Figures 5-6, 5-7, and 5-8 show the effective sink temperature for extravehicular suits in 50-nm lunar orbits. Figures 5-6 and 5-7 are applicable to suits with spectrally selective surfaces (ϵ_b = 0.80 and α_b = 0.20); Figure 5-8 gives the effective sink temperature obtained with a reflective surface (ϵ_b = 0.05 and α_b = 0.10). As can be deduced from these curves, the lunar orbital mission vehicle has a relatively low-temperature environment relative to an earth orbit.

Mars Orbit

A Mars orbit will provide a relatively low-temperature environment because of the reduced solar constant obtained in the vicinity of Mars.

TABLE 5-3

EARTH ORBITAL EXTRAVEHICULAR HEAT BALANCE COMPUTATION

HEAT TRANSFER COMPUTATION FOR MAN IN EARTH ORBIT (45) SEPT. 22, 1964 PAGE 1

PLANET (SPHERICAL)
3441.000 = RADIUS (N.M.)
0.350 = ALBEDO
443.000 = SOLAR CONSTANT (BTU/HR-SQFT)

SPACECRAFT (SPHERICAL)
5.000 = RADIUS (FEET)
0.200 = SOLAR ABSORPTIVITY
0.900 = INFRARED ABSORPTIVITY
0.000 = INTERNAL HEAT LOAD (BTU/HR)

SUIT (CYLINDRICAL)
6.250 = RADIUS (INCHES)
69.100 = HEIGHT (INCHES)
0.350 = THICKNESS (INCHES)
160.000 = DISTANCE FROM PLANET SURFACE (N.M.)
2.000 = DISTANCE FROM VEHICLE SURFACE (FEET)
0.320 = SOLAR ABSORPTIBITY
0.560 = INFRARED ABSORPTIVITY
0.020 = THERMAL CONDUCTIVITY (BTU/HR-FT-R)
1.000 = INTERCHANGE FACTOR E(B-I)
550.000 = SKIN TEMPERATURE OF CREW (R)

ANGLES IN DEGREES
45.000 = ORBIT PLANE INCLINATION ANGLE
(W.R.T. PLANE PERPENDICULAR TO SUN DIRECTION)
90.000 = ANGLE BETWEEN BODY AXIS AND
BODY POSITION VECTOR
0.000 = ANGLE BETWEEN BODY-VEHICLE VECTOR AND
BODY POSITION VECTOR

SHADOW ANGLE INTERCEPTS	ENTER	EXIT
SUIT IN SHADOWS (PLANET)	204.637	335.363
(VEHICLE)	81.787	98.213
VEHICLE IN SHADOW (PLANET)	204.637	335.363

TABLE 5-3 (Continued)

HEAT TRANSFER COMPUTATION FOR MAN IN EARTH ORBIT (45) SEPT. 22, 1964 PAGE 2

γ (DEG)	-ABSORBED HEAT FLUXES (BTU/HR-SQFT)-SPACECRAFT DIRECT SOLAR	REFTD. SOLAR	PLANET EMISSN	INSIDE HEAT	TOTAL	TS**4 (E-08)	TS (R)
90.00	22.15	7.73	22.85	0.00	52.73	342.01	430.04
100.00	22.15	7.61	22.85	0.00	52.61	341.25	429.80
110.00	22.15	7.27	22.85	0.00	52.26	338.98	429.09
120.00	22.15	6.70	22.85	0.00	51.69	335.29	427.91
130.00	22.15	5.92	22.85	0.00	50.92	330.27	426.30
140.00	22.15	4.97	22.85	0.00	49.97	324.09	424.29
150.00	22.15	3.87	22.85	0.00	48.86	316.93	421.93
160.00	22.15	2.64	22.85	0.00	47.64	309.01	419.27
170.00	22.15	1.34	22.85	0.00	46.34	300.56	416.37
180.00	22.15	0.00	22.85	0.00	45.00	291.86	413.33
190.00	22.15	0.00	22.85	0.00	45.00	291.86	413.33
200.00	22.15	0.00	22.85	0.00	45.00	291.86	413.33
210.00	0.00	0.00	22.85	0.00	22.85	148.18	348.90
220.00	0.00	0.00	22.85	0.00	22.85	148.18	348.90
230.00	0.00	0.00	22.85	0.00	22.85	148.18	348.90
240.00	0.00	0.00	22.85	0.00	22.85	148.18	348.90
250.00	0.00	0.00	22.85	0.00	22.85	148.18	348.90
260.00	0.00	0.00	22.85	0.00	22.85	148.18	348.90
270.00	0.00	0.00	22.85	0.00	22.85	148.18	348.90

Fourth-Power Average Effective Sink Temperature, ^{0}R

Effective Sink Temperature, ^{0}R

γ (DEG)	ω (DEG)	ABSORBED HEAT FLUXES (BTU/HR-SQFT)-SPACE SUIT- DIRECT SOLAR	REFLECTED SOLAR PLANET	REFLECTED SOLAR VEHICLE	THERMAL EMISS. PLANET	THERMAL EMISS. VEHICLE	TOTAL	TS (R)	T(OUT) (R)	QRATE B/H-SF	AVERAGE VALUES TS (R)	AVERAGE VALUES T(OUT) (R)	AVERAGE VALUES Q(IN) BTU/HR
90.00													
	0.00	0.00	32.04	0.00	36.81	0.00	68.85	517.59	531.35	-7.62			
	30.00	0.00	28.02	0.00	32.20	0.00	60.22	500.55	522.40	-11.23			
	60.00	0.00	19.90	0.00	22.87	0.24	43.02	460.17	503.64	-18.71			
	90.00	0.00	11.05	0.00	12.70	2.78	26.54	407.83	484.36	-26.27			
	120.00	0.00	3.89	0.00	4.47	7.77	16.13	360.07	471.43	-31.25			
	150.00	0.00	0.28	0.00	0.32	13.05	13.64	345.34	468.24	-32.47			
	180.00	0.00	0.00	0.00	0.00	15.06	15.06	354.00	470.07	-31.77			
	210.00	0.00	0.28	0.00	0.32	13.05	13.64	345.34	468.24	-32.47			
	240.00	0.00	3.89	0.00	4.47	7.77	16.13	360.07	471.43	-31.25			
	270.00	0.00	11.05	0.00	12.70	2.78	26.54	407.83	484.36	-26.27			
	300.00	0.00	19.90	0.00	22.87	0.24	43.02	460.17	503.64	-18.71			
	330.00	0.00	28.02	0.00	32.20	0.00	60.22	500.55	522.40	-11.23			
	END	0.00	11.05	0.00	12.70	2.78	26.54	407.83	485.66	-26.83			
	END	0.00	11.05	0.00	12.70	2.78	26.54	407.83	485.66	-26.83	430.66	492.77	-484.2
100.00													
	0.00	0.00	31.55	0.00	36.81	0.00	68.36	516.67	530.85	-7.82			
	30.00	0.00	27.60	0.00	32.20	0.00	59.79	499.66	521.95	-11.41			
	60.00	37.45	19.60	0.00	22.87	0.24	80.16	537.66	542.65	-3.02			
	90.00	100.24	10.89	0.00	12.70	2.77	126.60	602.73	584.71	14.47			
	120.00	136.17	3.83	0.00	4.47	7.75	152.22	631.15	605.46	23.31			
	150.00	135.61	0.27	0.00	0.32	13.02	149.22	628.02	603.12	22.30			
	180.00	98.72	0.00	0.00	0.00	15.03	113.75	586.81	573.69	9.84			
	210.00	35.37	0.27	0.00	0.32	13.02	48.98	475.36	510.30	-16.07			
	240.00	0.00	3.83	0.00	4.47	7.75	16.05	359.64	471.32	-31.29			
	270.00	0.00	10.89	0.00	12.70	2.77	26.36	407.16	484.14	-26.35			
	300.00	0.00	19.60	0.00	22.87	0.24	42.71	459.36	503.31	-18.84			
	330.00	0.00	27.60	0.00	32.20	0.00	59.79	499.66	521.95	-11.41			
	END	0.00	10.89	0.00	12.70	2.77	26.36	407.16	485.45	-26.91			
	END	17.41	10.89	0.00	12.70	2.77	43.77	462.17	505.34	-18.78	528.87	539.47	-127.3
110.00													
	0.00	0.00	30.10	0.00	36.81	0.00	66.91	513.92	529.36	-8.42			
	30.00	0.00	26.33	0.00	32.20	0.00	58.53	497.00	520.62	-11.94			
	60.00	39.71	18.70	0.00	22.87	0.24	81.53	539.93	543.98	-2.47			
	90.00	100.24	10.39	0.00	12.70	2.75	126.08	602.11	584.27	14.29			
	120.00	133.91	3.65	0.00	4.47	7.70	149.73	628.55	603.51	22.47			
	150.00	131.69	0.26	0.00	0.32	12.93	145.21	623.75	599.93	20.94			
	180.00	94.19	0.00	0.00	0.00	14.93	109.13	580.76	569.63	8.14			
	210.00	31.45	0.26	0.00	0.32	12.93	44.97	465.30	505.85	-17.84			
	240.00	0.00	3.65	0.00	4.47	7.70	15.82	358.37	471.04	-31.40			
	270.00	0.00	10.39	0.00	12.70	2.75	25.85	405.14	483.53	-26.59			
	300.00	0.00	18.70	0.00	22.87	0.24	41.81	456.92	502.29	-19.24			
	330.00	0.00	26.33	0.00	32.20	0.00	58.53	497.00	520.62	-11.94			
	END	0.00	10.39	0.00	12.70	2.75	25.85	405.14	484.84	-27.16			
	END	34.28	10.39	0.00	12.70	2.75	60.13	500.36	522.78	-11.53	527.34	538.53	-133.5

HEAT TRANSFER COMPUTATION FOR MAN IN EARTH ORBIT (45) SEPT. 22, 1964 PAGE 4

γ (DEG)	ω (DEG)	ABSORBED HEAT FLUXES (BTU/HR-SQFT)-SPACE SUIT- DIRECT SOLAR	REFLECTED SOLAR PLANET	REFLECTED SOLAR VEHICLE	THERMAL EMISS. PLANET	THERMAL EMISS. VEHICLE	TOTAL	TS (R)	T(OUT) (R)	QRATE B/H-SF	AVERAGE VALUES TS (R)	AVERAGE VALUES T(OUT) (R)	AVERAGE VALUES Q(IN) BTU/HR
120.00													
	0.00	0.00	27.74	0.00	36.81	0.00	64.55	509.32	526.94	-9.40			
	30.00	0.00	24.27	0.00	32.20	0.00	56.46	492.56	518.42	-12.83			
	60.00	43.40	17.24	0.00	22.87	0.24	83.75	543.57	546.14	-1.59			
	90.00	100.24	9.57	0.00	12.70	2.72	125.24	601.10	583.56	13.99			
	120.00	130.21	3.37	0.00	4.47	7.62	145.67	624.24	600.29	21.09			
	150.00	125.30	0.24	0.00	0.32	12.79	138.65	616.58	594.66	18.70			
	180.00	86.81	0.00	0.00	0.00	14.77	101.58	570.45	562.85	5.31			
	210.00	25.06	0.24	0.00	0.32	12.79	38.41	447.32	498.40	-20.78			
	240.00	0.00	3.37	0.00	4.47	7.62	15.45	356.25	470.57	-31.58			
	270.00	0.00	9.57	0.00	12.70	2.72	25.00	401.79	482.50	-26.99			
	300.00	0.00	17.24	0.00	22.87	0.24	40.34	452.85	500.62	-19.90			
	330.00	0.00	24.27	0.00	32.20	0.00	56.46	492.56	518.42	-12.83			
	END	0.00	9.57	0.00	12.70	2.72	25.00	401.79	483.84	-27.57			
	END	50.12	9.57	0.00	12.70	2.72	75.12	529.00	537.86	-5.17	523.94	536.57	-148.5
130.00													
	0.00	0.00	24.54	0.00	36.81	0.00	61.35	502.88	523.60	-10.75			
	30.00	0.00	21.47	0.00	32.20	0.00	53.66	486.33	515.41	-14.03			
	60.00	48.42	15.25	0.00	22.87	0.23	86.77	548.41	549.04	-0.40			
	90.00	100.24	8.47	0.00	12.70	2.68	124.09	599.72	582.59	13.58			
	120.00	125.20	2.98	0.00	4.47	7.51	140.15	618.25	595.88	19.21			
	150.00	116.62	0.21	0.00	0.32	12.60	129.75	606.44	587.34	15.59			
	180.00	76.79	0.00	0.00	0.00	14.55	91.34	555.49	553.37	1.39			
	210.00	16.38	0.21	0.00	0.32	12.60	29.51	418.80	487.95	-24.87			
	240.00	0.00	2.98	0.00	4.47	7.51	14.95	353.32	469.91	-31.83			
	270.00	0.00	8.47	0.00	12.70	2.68	23.85	397.11	481.08	-27.53			
	300.00	0.00	15.25	0.00	22.87	0.23	38.35	447.15	498.33	-20.81			
	330.00	0.00	21.47	0.00	32.20	0.00	53.66	486.33	515.41	-14.03			
	END	0.00	8.47	0.00	12.70	2.68	23.85	397.11	482.48	-28.12			
	END	64.43	8.47	0.00	12.70	2.68	88.29	550.79	550.48	0.20	518.65	533.64	-172.2
140.00													
	0.00	0.00	20.59	0.00	36.81	0.00	57.40	494.59	519.42	-12.43			
	30.00	0.00	18.01	0.00	32.20	0.00	50.21	478.31	511.66	-15.53			
	60.00	54.59	12.79	0.00	22.87	0.23	90.49	554.19	552.57	1.06			
	90.00	100.24	7.11	0.00	12.70	2.63	122.68	598.01	581.39	13.08			
	120.00	119.03	2.50	0.00	4.47	7.37	133.36	610.61	590.33	16.86			
	150.00	105.92	0.18	0.00	0.32	12.36	118.78	593.20	578.06	11.67			
	180.00	64.43	0.00	0.00	0.00	14.28	78.71	535.20	541.23	-3.60			
	210.00	5.68	0.18	0.00	0.32	12.36	18.54	372.86	474.47	-30.08			
	240.00	0.00	2.50	0.00	4.47	7.37	14.33	349.60	469.11	-32.14			
	270.00	0.00	7.11	0.00	12.70	2.63	22.44	391.09	479.35	-28.20			
	300.00	0.00	12.79	0.00	22.87	0.23	35.89	439.81	495.48	-21.93			
	330.00	0.00	18.01	0.00	32.20	0.00	50.21	478.31	511.66	-15.53			
	END	0.00	7.11	0.00	12.70	2.63	22.44	391.09	480.76	-28.81			
	END	76.79	7.11	0.00	12.70	2.63	99.23	567.12	560.53	4.53	511.47	529.81	-204.1

γ (DEG)	ω (DEG)	ABSORBED HEAT FLUXES (BTU/HR-SQFT)-SPACE SUIT- DIRECT SOLAR	REFLECTED SOLAR PLANET	REFLECTED SOLAR VEHICLE	THERMAL EMISS. PLANET	THERMAL EMISS. VEHICLE	TOTAL	TS (R)	T(OUT) (R)	QRATE B/H-SF	AVERAGE VALUES TS (R)	AVERAGE VALUES T(OUT) (R)	AVERAGE VALUES Q(IN) BTU/HR
150.00													
	0.00	0.00	16.02	0.00	36.81	0.00	52.83	484.43	514.50	-14.40			
	30.00	6.71	14.01	0.00	32.20	0.00	52.92	484.65	514.61	-14.35			
	60.00	61.75	9.95	0.00	22.87	0.22	94.80	560.67	556.60	2.72			
	90.00	100.24	5.53	0.00	12.70	2.58	121.04	596.01	580.00	12.49			
	120.00	111.87	1.94	0.00	4.47	7.20	125.48	601.39	583.77	14.08			
	150.00	93.52	0.14	0.00	0.32	12.09	106.07	576.65	566.89	7.00			
	180.00	50.12	0.00	0.00	0.00	13.96	64.08	508.39	526.45	-9.60			
	210.00	0.00	0.14	0.00	0.32	12.09	12.55	338.19	466.82	-33.01			
	240.00	0.00	1.94	0.00	4.47	7.20	13.61	345.14	468.20	-32.49			
	270.00	0.00	5.53	0.00	12.70	2.58	20.81	383.76	477.31	-28.99			
	300.00	0.00	9.95	0.00	22.87	0.22	33.05	430.82	492.15	-23.23			
	330.00	0.00	14.01	0.00	32.20	0.00	46.21	468.48	507.22	-17.29			
	ENC	0.00	5.53	0.00	12.70	2.58	20.81	383.76	478.78	-29.61			
	ENC	86.81	5.53	0.00	12.70	2.58	107.62	578.74	568.01	7.76	504.50	526.16	-233.9
160.00													
	0.00	0.00	10.96	0.00	36.81	0.00	47.77	472.38	508.95	-16.61			
	30.00	20.43	9.58	0.00	32.20	0.00	62.21	504.64	524.51	-10.38			
	60.00	69.67	6.81	0.00	22.87	0.22	99.56	567.59	561.00	4.54			
	90.00	100.24	3.78	0.00	12.70	2.51	119.23	593.76	578.45	11.84			
	120.00	103.95	1.33	0.00	4.47	7.02	116.77	590.67	576.32	10.94			
	150.00	79.81	0.09	0.00	0.32	11.79	92.01	556.51	554.00	1.65			
	180.00	34.28	0.00	0.00	0.00	13.61	47.90	472.70	509.09	-16.55			
	210.00	0.00	0.09	0.00	0.32	11.79	12.20	335.83	466.37	-33.18			
	240.00	0.00	1.33	0.00	4.47	7.02	12.82	339.99	467.19	-32.87			
	270.00	0.00	3.78	0.00	12.70	2.51	18.99	375.12	475.06	-29.86			
	300.00	0.00	6.81	0.00	22.87	0.22	29.90	420.16	488.41	-24.69			
	330.00	0.00	9.58	0.00	32.20	0.00	41.78	456.83	502.25	-19.26			
	ENC	0.00	3.78	0.00	12.70	2.51	18.99	375.12	476.57	-30.50			
	ENC	94.19	3.78	0.00	12.70	2.51	113.19	586.09	572.87	9.88	498.13	522.91	-260.1
170.00													
	0.00	0.00	5.56	0.00	36.81	0.00	42.37	458.44	502.91	-19.00			
	30.00	35.05	4.87	0.00	32.20	0.00	72.11	523.61	534.65	-6.28			
	60.00	78.11	3.46	0.00	22.87	0.21	104.64	574.70	565.61	6.46			
	90.00	100.24	1.92	0.00	12.70	2.44	117.30	591.35	576.78	11.14			
	120.00	95.51	0.67	0.00	4.47	6.83	107.48	578.56	568.15	7.52			
	150.00	65.19	0.05	0.00	0.32	11.47	77.03	532.32	539.56	-4.28			
	180.00	17.41	0.00	0.00	0.00	13.24	30.65	422.77	489.30	-24.34			
	210.00	0.00	0.05	0.00	0.32	11.47	11.83	333.26	465.89	-33.37			
	240.00	0.00	0.67	0.00	4.47	6.83	11.97	334.23	466.09	-33.29			
	270.00	0.00	1.92	0.00	12.70	2.44	17.06	365.21	472.62	-30.79			
	300.00	0.00	3.46	0.00	22.87	0.21	26.54	407.83	484.36	-26.27			
	330.00	0.00	4.87	0.00	32.20	0.00	37.06	443.35	496.84	-21.39			
	ENC	0.00	1.92	0.00	12.70	2.44	17.06	365.21	474.22	-31.44			
	ENC	98.72	1.92	0.00	12.70	2.44	115.78	589.42	575.09	10.85	490.76	519.35	-290.6

HEAT TRANSFER COMPUTATION FOR MAN IN EARTH ORBIT (45) SEPT. 22, 1964 PAGE 6

γ (DEG)	ω (DEG)	ABSORBED HEAT FLUXES (BTU/HR-SQFT)-SPACE SUIT- DIRECT SOLAR	REFLECTED SOLAR PLANET	REFLECTED SOLAR VEHICLE	THERMAL EMISS. PLANET	THERMAL EMISS. VEHICLE	TOTAL	TS (R)	T(OUT) (R)	QRATE B/H-SF	AVERAGE VALUES TS (R)	AVERAGE VALUES T(OUT) (R)	AVERAGE VALUES Q(IN) BTU/HR
180.00													
	0.00	0.00	0.01	0.00	36.81	0.00	36.81	442.59	496.55	-21.50			
	30.00	50.12	0.01	0.00	32.20	0.00	82.32	541.24	544.75	-2.16			
	60.00	86.81	0.00	0.00	22.87	0.20	109.89	581.77	570.30	8.42			
	90.00	100.24	0.00	0.00	12.70	2.37	115.31	588.82	575.06	10.41			
	120.00	86.81	0.01	0.00	4.47	6.63	97.91	565.22	559.48	3.92			
	150.00	50.12	0.01	0.00	0.32	11.13	61.57	503.34	523.83	-10.65			
	180.00	0.01	0.00	0.00	0.00	12.86	12.86	340.24	467.22	-32.86			
	210.00	0.00	0.01	0.00	0.32	11.13	11.45	330.55	465.39	-33.56			
	240.00	0.00	0.01	0.00	4.47	6.63	11.10	327.97	464.93	-33.73			
	270.00	0.00	0.00	0.00	12.70	2.37	15.07	354.06	470.09	-31.76			
	300.00	0.00	0.00	0.00	22.87	0.20	23.08	393.82	480.13	-27.91			
	330.00	0.00	0.01	0.00	32.20	0.00	32.20	428.02	491.14	-23.63			
	END	0.00	0.00	0.00	12.70	2.37	15.07	354.06	471.75	-32.43			
	END	100.24	0.00	0.00	12.70	2.37	115.31	588.82	574.70	10.67	482.50	515.60	-324.8
190.00													
	0.00	17.41	0.00	0.00	36.81	0.00	54.22	487.58	516.02	-13.79			
	30.00	65.19	0.00	0.00	32.20	0.00	97.39	564.47	559.02	3.72			
	60.00	95.51	0.00	0.11	22.87	0.20	118.70	593.10	577.98	11.64			
	90.00	100.24	0.00	1.31	12.70	2.37	116.62	590.49	576.19	10.89			
	120.00	78.11	0.00	3.67	4.47	6.63	92.87	557.81	554.80	1.98			
	150.00	35.05	0.00	6.15	0.32	11.13	52.65	484.02	514.32	-14.47			
	180.00	0.00	0.00	7.10	0.00	12.86	19.96	379.80	476.25	-29.40			
	210.00	0.00	0.00	6.15	0.32	11.13	17.61	368.06	473.29	-30.54			
	240.00	0.00	0.00	3.67	4.47	6.63	14.76	352.22	469.69	-31.92			
	270.00	0.00	0.00	1.31	12.70	2.37	16.38	361.51	471.75	-31.13			
	300.00	0.00	0.00	0.11	22.87	0.20	23.19	394.31	480.26	-27.85			
	330.00	0.00	0.00	0.00	32.20	0.00	32.20	428.02	491.14	-23.63			
	END	0.00	0.00	1.31	12.70	2.37	16.38	361.51	473.36	-31.78			
	END	98.72	0.00	1.31	12.70	2.37	115.10	588.55	574.51	10.59	490.72	519.45	-292.1
200.00													
	0.00	34.28	0.00	0.00	36.81	0.00	71.09	521.76	533.62	-6.69			
	30.00	79.81	0.00	0.00	32.20	0.00	112.01	584.56	572.16	9.20			
	60.00	103.95	0.00	0.22	22.87	0.20	127.25	603.50	585.26	14.71			
	90.00	100.24	0.00	2.58	12.70	2.37	117.90	592.09	577.29	11.35			
	120.00	69.67	0.00	7.22	4.47	6.63	87.99	550.32	550.20	0.08			
	150.00	20.43	0.00	12.12	0.32	11.13	44.00	462.78	504.76	-18.27			
	180.00	0.00	0.00	13.99	0.00	12.86	26.85	409.02	484.74	-26.12			
	210.00	0.00	0.00	12.12	0.32	11.13	23.57	395.92	480.75	-27.66			
	240.00	0.00	0.00	7.22	4.47	6.63	18.32	371.74	474.19	-30.19			
	270.00	0.00	0.00	2.58	12.70	2.37	17.66	368.33	473.37	-30.51			
	300.00	0.00	0.00	0.22	22.87	0.20	23.30	394.77	480.42	-27.79			
	330.00	0.00	0.00	0.00	32.20	0.00	32.20	428.02	491.14	-23.63			
	END	0.00	0.00	2.58	12.70	2.37	17.66	368.33	474.93	-31.15			
	END	94.19	0.00	2.58	12.70	2.37	111.85	584.35	571.71	9.37	498.06	523.08	-262.8

γ (DEG)	ω (DEG)	ABSORBED HEAT FLUXES (BTU/HR-SQFT)-SPACE SUIT- DIRECT SOLAR	REFLECTED SOLAR PLANET	VEHICLE	THERMAL EMISS. PLANET	VEHICLE	TOTAL	TS (R)	T(OUT) (R)	QRATE B/H-SF	AVERAGE VALUES TS (R)	T(OUT) (R)	Q(IN) BTU/HR
210.00													
	0.00	0.00	0.00	0.00	36.81	0.00	36.81	442.59	496.55	-21.50			
	30.00	0.00	0.00	0.00	32.20	0.00	32.20	428.02	491.14	-23.63			
	60.00	0.00	0.00	0.33	22.87	0.10	23.30	394.78	480.42	-27.79			
	90.00	0.00	0.00	3.77	12.70	1.20	17.68	368.46	473.39	-30.50			
	120.00	0.00	0.00	10.55	4.47	3.37	18.39	372.09	474.29	-30.16			
	150.00	0.00	0.00	17.72	0.32	5.65	23.69	396.41	480.89	-27.61			
	180.00	0.00	0.00	20.46	0.00	6.53	26.98	409.54	484.91	-26.05			
	210.00	0.00	0.00	17.72	0.32	5.65	23.69	396.41	480.89	-27.61			
	240.00	0.00	0.00	10.55	4.47	3.37	18.39	372.09	474.29	-30.16			
	270.00	0.00	0.00	3.77	12.70	1.20	17.68	368.46	473.39	-30.50			
	300.00	0.00	0.00	0.33	22.87	0.10	23.30	394.78	480.42	-27.79			
	330.00	0.00	0.00	0.00	32.20	0.00	32.20	428.02	491.14	-23.63			
	END	0.00	0.00	3.77	12.70	1.20	17.68	368.46	474.97	-31.14			
	END	0.00	0.00	3.77	12.70	1.20	17.68	368.46	474.97	-31.14	397.53	481.41	-566.4
220.00													
	0.00	0.00	0.00	0.00	36.81	0.00	36.81	442.59	496.55	-21.50			
	30.00	0.00	0.00	0.00	32.20	0.00	32.20	428.02	491.14	-23.63			
	60.00	0.00	0.00	0.42	22.87	0.10	23.39	395.17	480.52	-27.75			
	90.00	0.00	0.00	4.85	12.70	1.20	18.76	373.95	474.76	-29.97			
	120.00	0.00	0.00	13.57	4.47	3.37	21.40	386.48	478.06	-28.70			
	150.00	0.00	0.00	22.78	0.32	5.65	28.75	416.07	487.02	-25.23			
	180.00	0.00	0.00	26.30	0.00	6.53	32.83	430.10	491.89	-23.33			
	210.00	0.00	0.00	22.78	0.32	5.65	28.75	416.07	487.02	-25.23			
	240.00	0.00	0.00	13.57	4.47	3.37	21.40	386.48	478.06	-28.70			
	270.00	0.00	0.00	4.85	12.70	1.20	18.76	373.95	474.76	-29.97			
	300.00	0.00	0.00	0.42	22.87	0.10	23.39	395.17	480.52	-27.75			
	330.00	0.00	0.00	0.00	32.20	0.00	32.20	428.02	491.14	-23.63			
	END	0.00	0.00	4.85	12.70	1.20	18.76	373.95	476.28	-30.61			
	END	0.00	0.00	4.85	12.70	1.20	18.76	373.95	476.28	-30.61	405.38	483.79	-547.5
230.00													
	0.00	0.00	0.00	0.00	36.81	0.00	36.81	442.59	496.55	-21.50			
	30.00	0.00	0.00	0.00	32.20	0.00	32.20	428.02	491.14	-23.63			
	60.00	0.00	0.00	0.50	22.87	0.10	23.47	395.51	480.62	-27.71			
	90.00	0.00	0.00	5.78	12.70	1.20	19.69	378.50	475.92	-29.53			
	120.00	0.00	0.00	16.17	4.47	3.37	24.00	397.72	481.28	-27.46			
	150.00	0.00	0.00	27.14	0.32	5.65	33.11	431.04	492.22	-23.20			
	180.00	0.00	0.00	31.34	0.00	6.53	37.87	445.74	497.77	-21.03			
	210.00	0.00	0.00	27.14	0.32	5.65	33.11	431.04	492.22	-23.20			
	240.00	0.00	0.00	16.17	4.47	3.37	24.00	397.72	481.28	-27.46			
	270.00	0.00	0.00	5.78	12.70	1.20	19.69	378.50	475.92	-29.53			
	300.00	0.00	0.00	0.50	22.87	0.10	23.47	395.51	480.62	-27.71			
	330.00	0.00	0.00	0.00	32.20	0.00	32.20	428.02	491.14	-23.63			
	END	0.00	0.00	5.78	12.70	1.20	19.69	378.50	477.42	-30.16			
	END	0.00	0.00	5.78	12.70	1.20	19.69	378.50	477.42	-30.16	411.31	485.83	-531.3

HEAT TRANSFER COMPUTATION FOR MAN IN EARTH ORBIT (45) SEPT. 22, 1964 PAGE 8

ϕ (DEG)	ω (DEG)	ABSORBED HEAT FLUXES (BTU/HR-SQFT)-SPACE SUIT- DIRECT SOLAR	REFLECTED SOLAR PLANET	REFLECTED SOLAR VEHICLE	THERMAL EMISS. PLANET	THERMAL EMISS. VEHICLE	TOTAL	TS (R)	T(OUT) (R)	QRATE B/H-SF	AVERAGE VALUES TS (R)	AVERAGE VALUES T(OUT) (R)	AVERAGE VALUES Q(IN) BTU/HR
240.00													
	0.00	0.00	0.00	0.00	36.81	0.00	36.81	442.59	496.55	-21.50			
	30.00	0.00	0.00	0.00	32.20	0.00	32.20	428.02	491.14	-23.63			
	60.00	0.00	0.00	0.56	22.87	0.10	23.54	395.79	480.69	-27.69			
	90.00	0.00	0.00	6.54	12.70	1.20	20.44	382.08	476.88	-29.16			
	120.00	0.00	0.00	18.28	4.47	3.37	26.11	406.19	483.85	-26.46			
	150.00	0.00	0.00	30.69	0.32	5.65	36.66	442.13	496.36	-21.58			
	180.00	0.00	0.00	35.43	0.00	6.53	41.96	457.32	502.46	-19.18			
	210.00	0.00	0.00	30.69	0.32	5.65	36.66	442.13	496.36	-21.58			
	240.00	0.00	0.00	18.28	4.47	3.37	26.11	406.19	483.85	-26.46			
	270.00	0.00	0.00	6.54	12.70	1.20	20.44	382.08	476.88	-29.16			
	300.00	0.00	0.00	0.56	22.87	0.10	23.54	395.79	480.69	-27.69			
	330.00	0.00	0.00	0.00	32.20	0.00	32.20	428.02	491.14	-23.63			
	ENC	0.00	0.00	6.54	12.70	1.20	20.44	382.08	478.34	-29.78			
	ENC	0.00	0.00	6.54	12.70	1.20	20.44	382.08	478.34	-29.78	416.81	487.49	-518.3
250.00													
	0.00	0.00	0.00	0.00	36.81	0.00	36.81	442.59	496.55	-21.50			
	30.00	0.00	0.00	0.00	32.20	0.00	32.20	428.02	491.14	-23.63			
	60.00	0.00	0.00	0.61	22.87	0.10	23.59	395.99	480.76	-27.66			
	90.00	0.00	0.00	7.09	12.70	1.20	21.00	384.65	477.56	-28.90			
	120.00	0.00	0.00	19.84	4.47	3.37	27.67	412.11	485.73	-25.73			
	150.00	0.00	0.00	33.30	0.32	5.65	39.27	449.80	499.39	-20.39			
	180.00	0.00	0.00	38.45	0.00	6.53	44.97	465.32	505.85	-17.84			
	210.00	0.00	0.00	33.30	0.32	5.65	39.27	449.80	499.39	-20.39			
	240.00	0.00	0.00	19.84	4.47	3.37	27.67	412.11	485.73	-25.73			
	270.00	0.00	0.00	7.09	12.70	1.20	21.00	384.65	477.56	-28.90			
	300.00	0.00	0.00	0.61	22.87	0.10	23.59	395.99	480.76	-27.66			
	330.00	0.00	0.00	0.00	32.20	0.00	32.20	428.02	491.14	-23.63			
	ENC	0.00	0.00	7.09	12.70	1.20	21.00	384.65	479.02	-29.51			
	ENC	0.00	0.00	7.09	12.70	1.20	21.00	384.65	479.02	-29.51	420.38	488.70	-508.8
260.00													
	0.00	0.00	0.00	0.00	36.81	0.00	36.81	442.59	496.55	-21.50			
	30.00	0.00	0.00	0.00	32.20	0.00	32.20	428.02	491.14	-23.63			
	60.00	0.00	0.00	0.64	22.87	0.10	23.62	396.11	480.79	-27.65			
	90.00	0.00	0.00	7.43	12.70	1.20	21.34	386.20	477.99	-28.73			
	120.00	0.00	0.00	20.79	4.47	3.37	28.62	415.61	486.88	-25.29			
	150.00	0.00	0.00	34.89	0.32	5.65	40.87	454.31	501.21	-19.67			
	180.00	0.00	0.00	40.29	0.00	6.53	46.82	470.02	507.91	-17.02			
	210.00	0.00	0.00	34.89	0.32	5.65	40.87	454.31	501.21	-19.67			
	240.00	0.00	0.00	20.79	4.47	3.37	28.62	415.61	486.88	-25.29			
	270.00	0.00	0.00	7.43	12.70	1.20	21.34	386.20	477.99	-28.73			
	300.00	0.00	0.00	0.64	22.87	0.10	23.62	396.11	480.79	-27.65			
	330.00	0.00	0.00	0.00	32.20	0.00	32.20	428.02	491.14	-23.63			
	ENC	0.00	0.00	7.43	12.70	1.20	21.34	386.20	479.43	-29.34			
	ENC	0.00	0.00	7.43	12.70	1.20	21.34	386.20	479.43	-29.34	422.52	489.45	-503.0

γ (DEG)	ω (DEG)	ABSORBED HEAT FLUXES (BTU/HR-SQFT)-SPACE SUIT- DIRECT SOLAR	REFLECTED SOLAR PLANET	REFLECTED SOLAR VEHICLE	THERMAL EMISS. PLANET	THERMAL EMISS. VEHICLE	TOTAL	TS (R)	T(OUT) (R)	QRATE B/H-SF	AVERAGE VALUES TS (R)	AVERAGE VALUES T(OUT) (R)	AVERAGE VALUES Q(IN) BTU/HR
270.00													
	0.00	0.00	0.00	0.00	36.81	0.00	36.81	442.59	496.55	-21.50			
	30.00	0.00	0.00	0.00	32.20	0.00	32.20	428.02	491.14	-23.63			
	60.00	0.00	0.00	0.65	22.87	0.10	23.63	396.15	480.81	-27.64			
	90.00	0.00	0.00	7.55	12.70	1.20	21.45	386.72	478.12	-28.68			
	120.00	0.00	0.00	21.11	4.47	3.37	28.94	416.77	487.26	-25.14			
	150.00	0.00	0.00	35.43	0.32	5.65	41.40	455.30	501.82	-19.43			
	180.00	0.00	0.00	40.91	0.00	6.53	47.44	471.58	508.61	-16.74			
	210.00	0.00	0.00	35.43	0.32	5.65	41.40	455.80	501.82	-19.43			
	240.00	0.00	0.00	21.11	4.47	3.37	28.94	416.77	487.26	-25.14			
	270.00	0.00	0.00	7.55	12.70	1.20	21.45	386.72	478.12	-28.68			
	300.00	0.00	0.00	0.65	22.87	0.10	23.63	396.15	480.81	-27.64			
	330.00	0.00	0.00	0.00	32.20	0.00	32.20	428.02	491.14	-23.63			
	END	0.00	0.00	7.55	12.70	1.20	21.45	386.72	479.58	-29.29			
	END	0.00	0.00	7.55	12.70	1.20	21.45	386.72	479.58	-29.29	423.24	489.70	-501.0

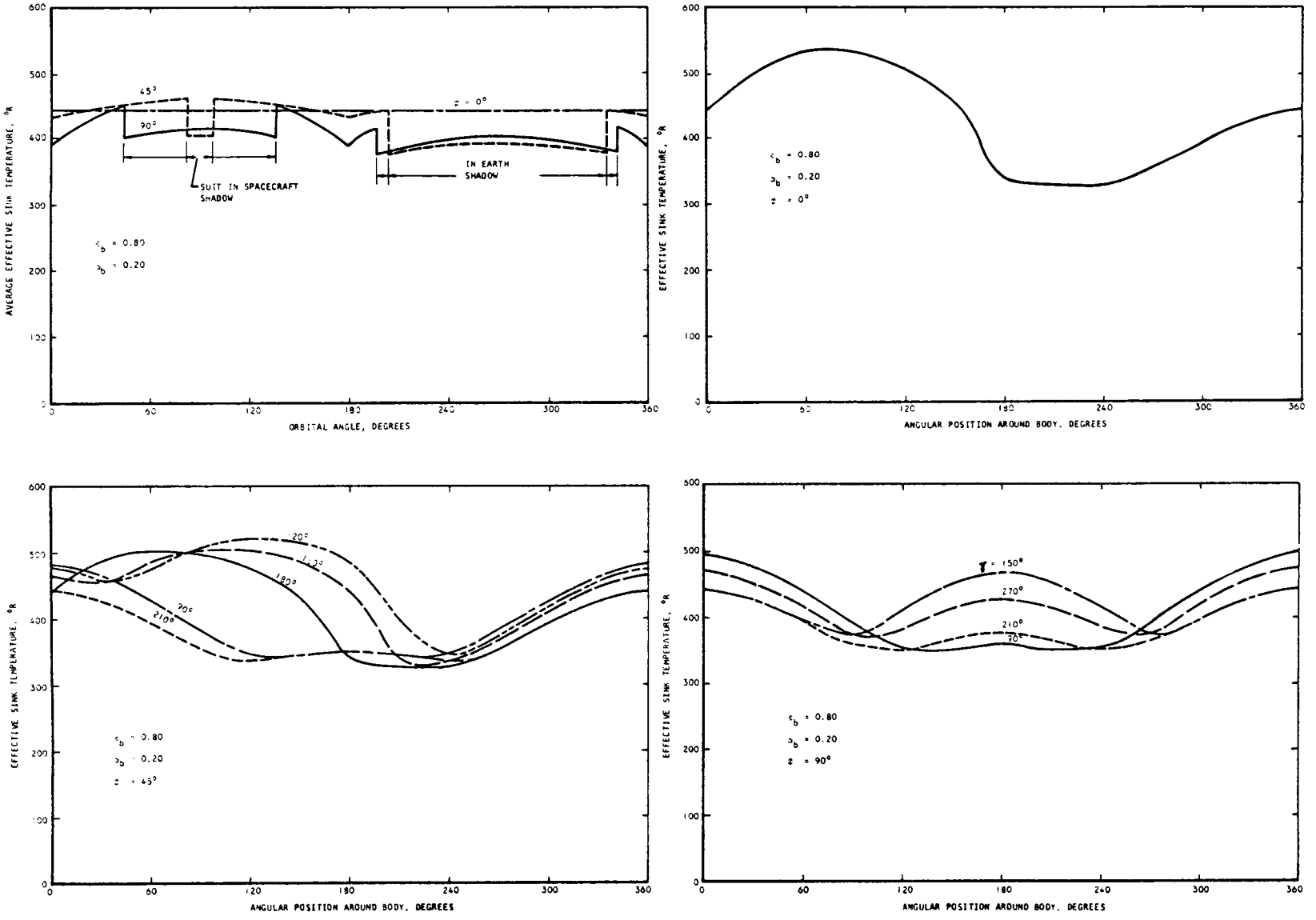

Figure 5-3. Effective Sink Temperature for Extravehicular Suit with Spectrally Selective Surface in a 160-nm Earth Orbit

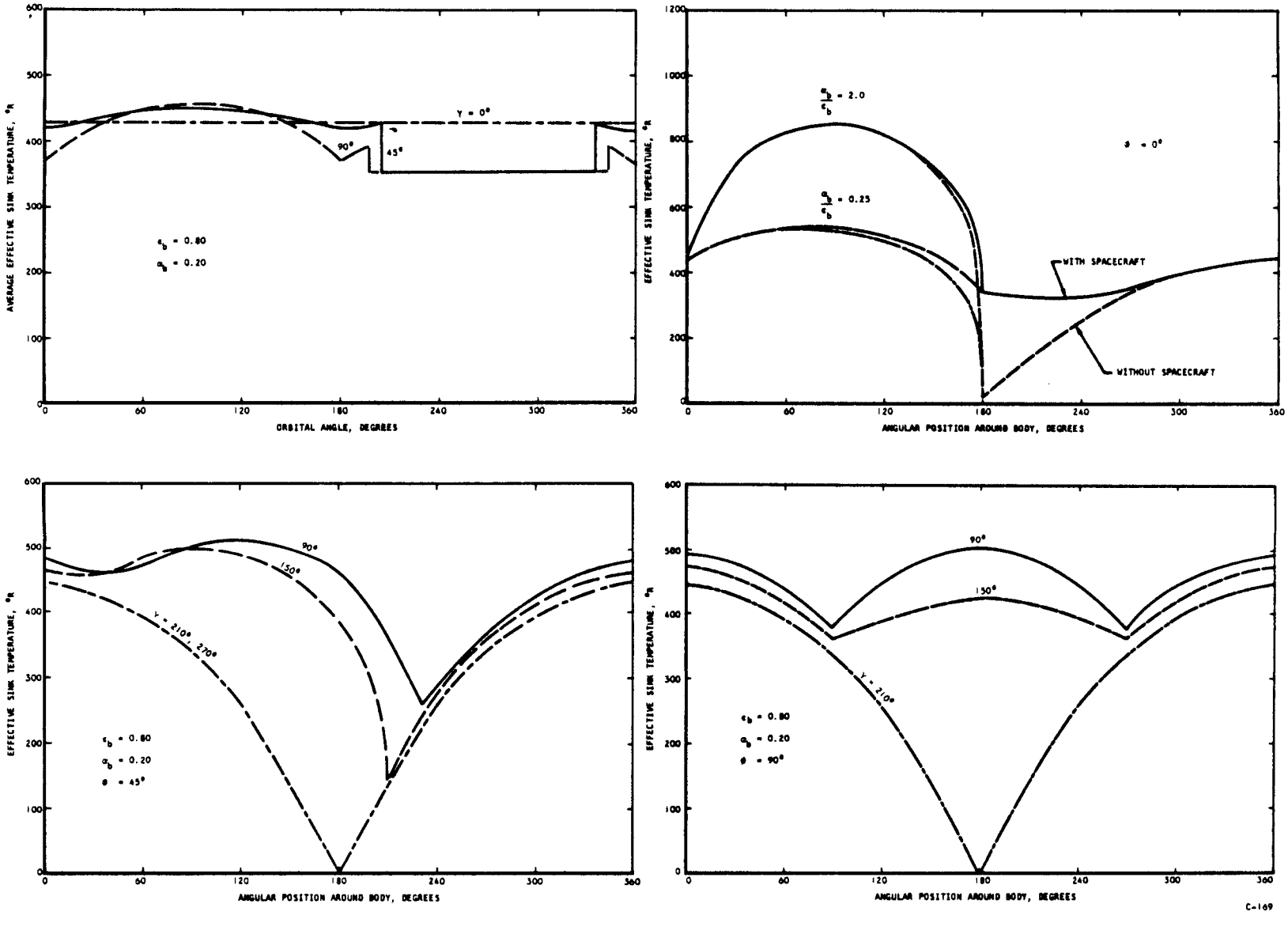

Figure 5-4. Effective Sink Temperature for Extravehicular Suit with Spectrally Selective Surface in a 160-nm Earth Orbit (Remote from Spacecraft)

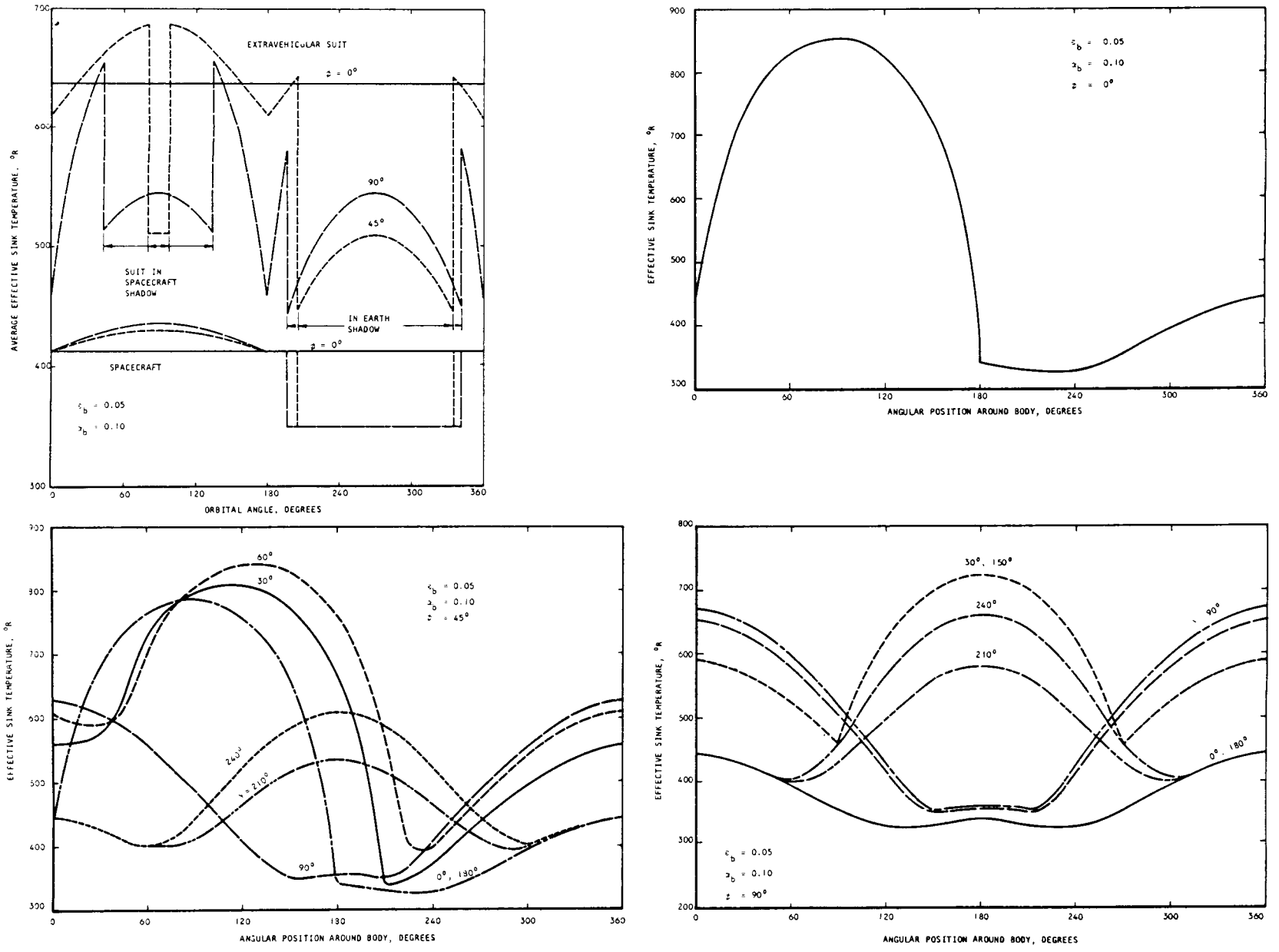

Figure 5-5. Effective Sink Temperature for Extravehicular Suit with Reflective Surface in a 160-nm Earth Orbit

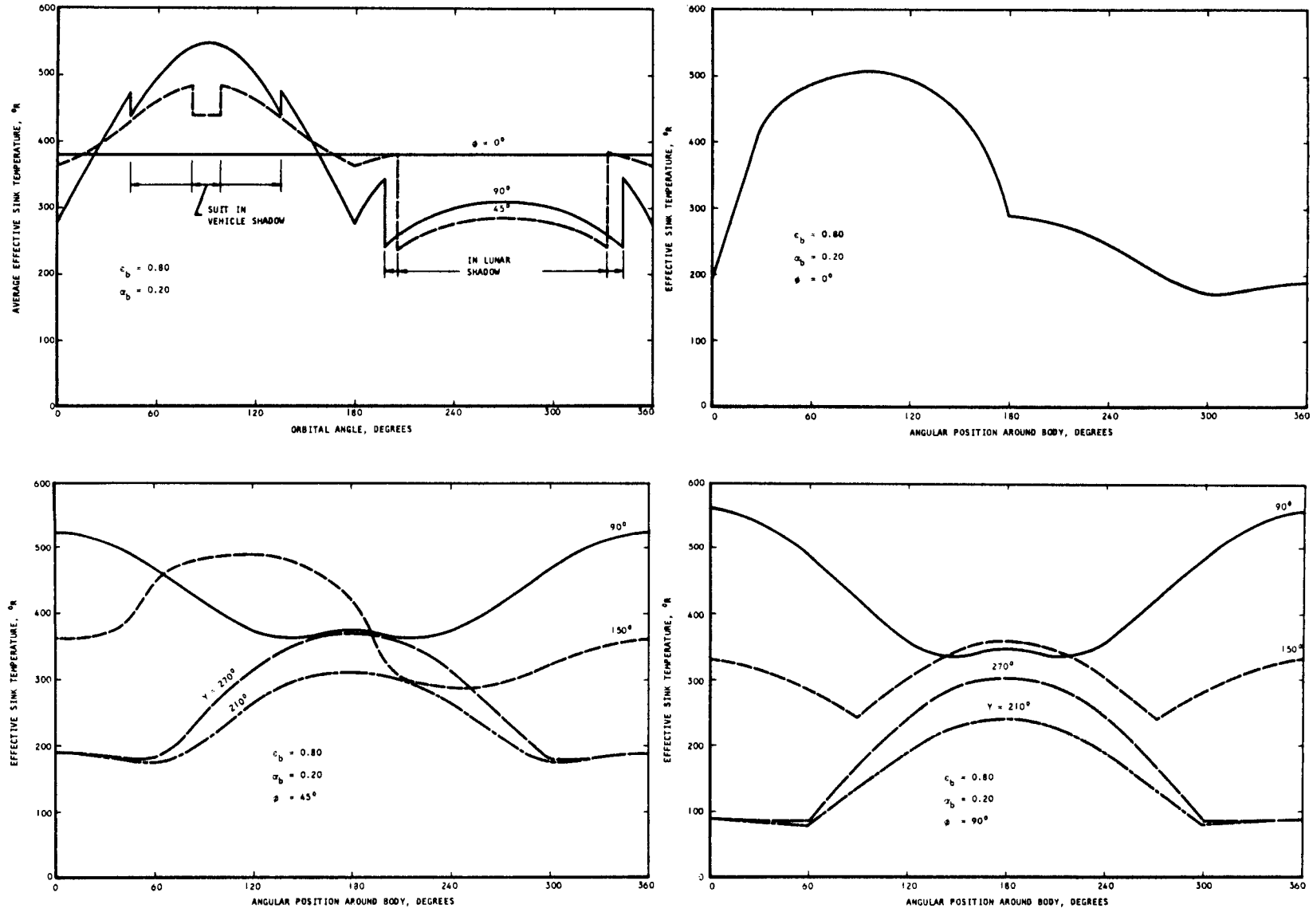

Figure 5-6. Effective Sink Temperature for Extravehicular Suit with Spectrally Selective Surface in a 50-nm Lunar Orbit

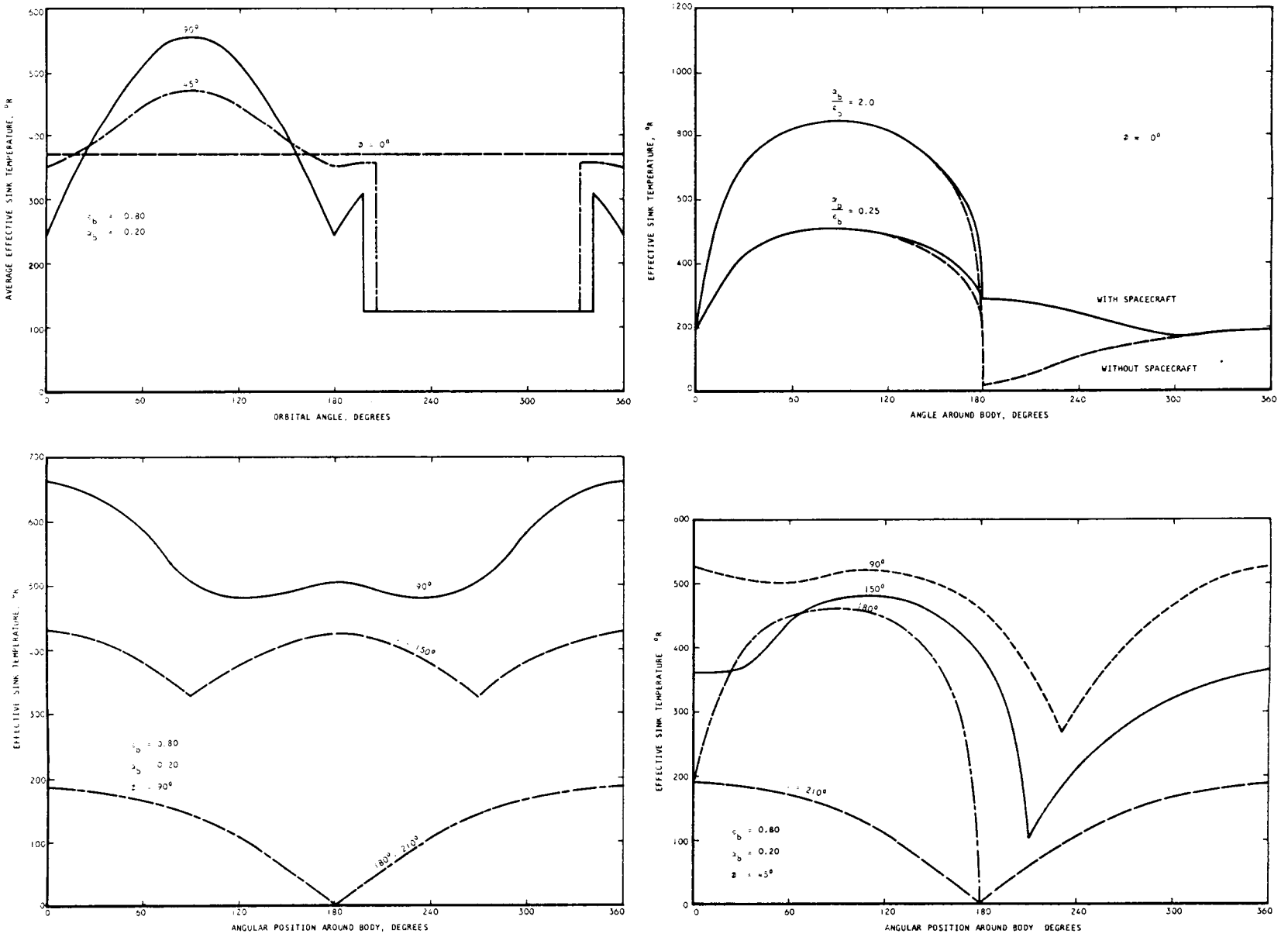

Figure 5-7. Effective Sink Temperature for Extravehicular Suit with Spectrally Selective Surface in 50-nm Lunar Orbit (Remote from Spacecraft)

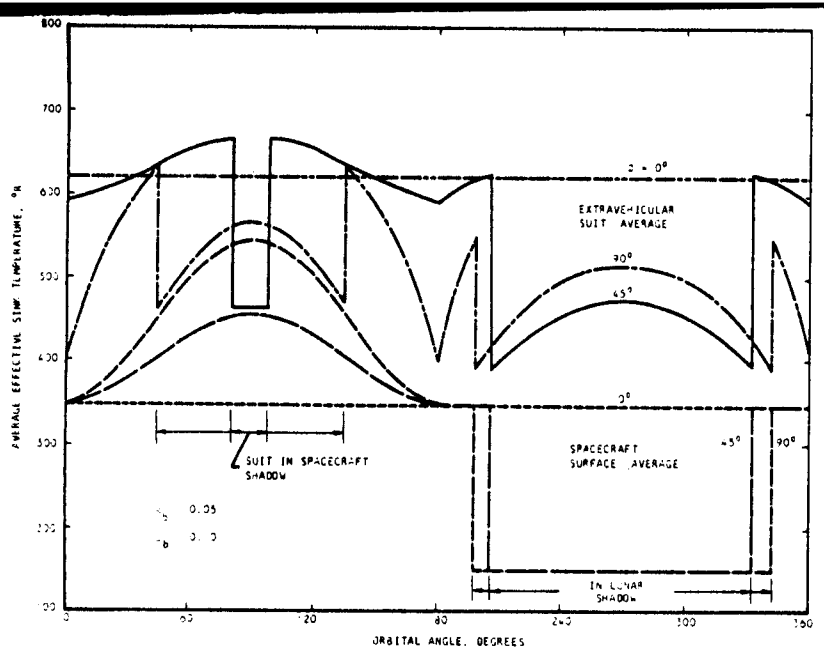

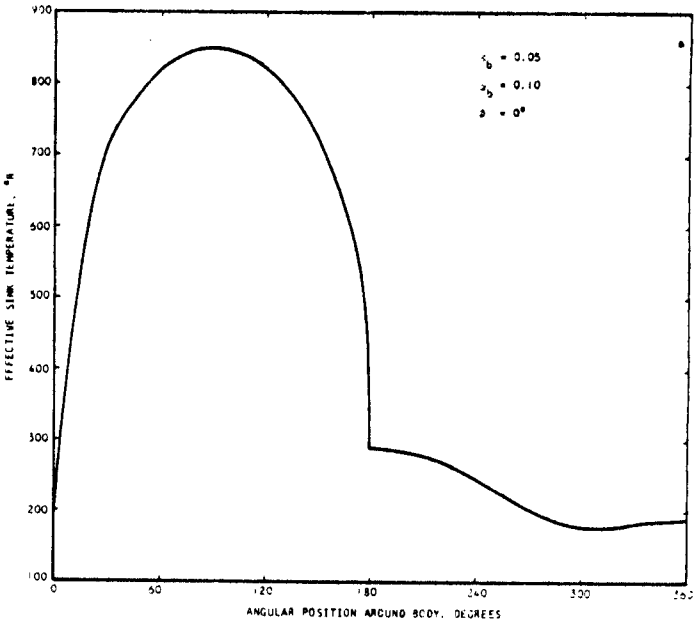

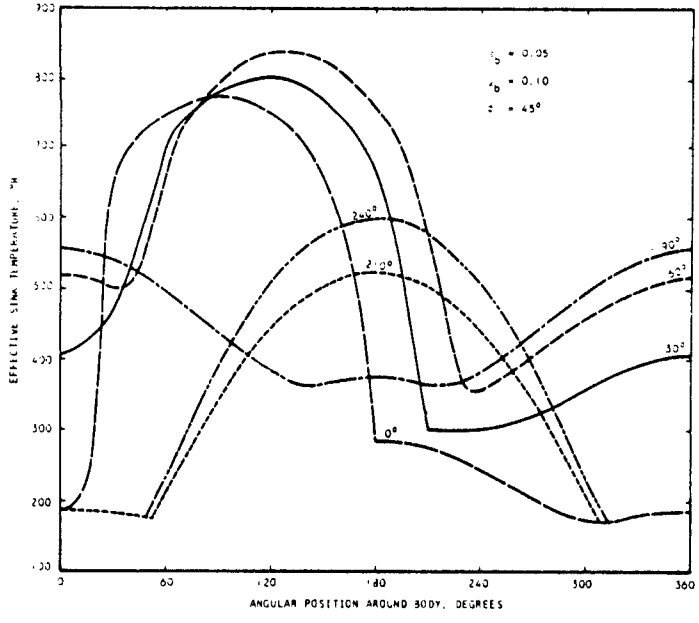

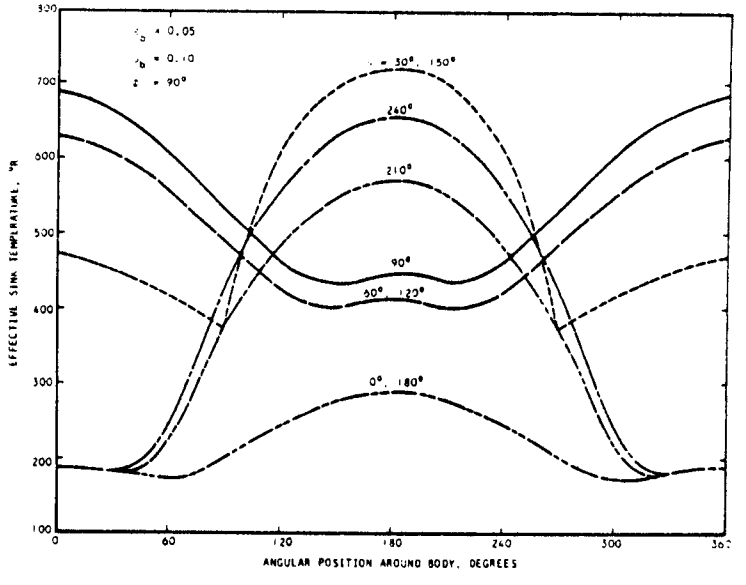

Figure 5-8. Effective Sink Temperature for Extravehicular Suit with Reflective Surface in a 50-nm Lunar Orbit

Table 5-4 shows typical heat balances for a 600-nm Mars orbit. Figure 5-9 shows the suit surface temperature distribution for no heat conduction through the suit wall (with and without the vehicle) and with heat leak through the suit wall. The temperature gradient is substantially eliminated for the rather high to l heat leak of -765 Btu/hr. As shown in Figure 5-10, the suit heat leak remains relatively high with variation in the orbital parameters. This is partly attributable to the assumed 600-nm Mars orbit, which is representative of present mission profiles for Mars missions.

LUNAR CRATERS

The computer program for the lunar crater environment (given in Appendix C), developed during this study for extravehicular suit thermal analysis, takes into account the temperature distribution obtained in the vicinity of a lunar crater wall. Figure 5-11 shows the geometry used in the heat balance analysis. The intensity of the thermal environment near lunar walls results from both an increase in the temperature of the base floor and the additional thermal radiation generated by the crater wall itself. Figure 5-12 shows the crater bottom temperature as a function of solar angle and distance from the wall.

Table 5-5 gives a typical heat balance computation for a solar angle of 40 degrees and a crater wall slope of 20 degrees (relative to the normal). A wall height of 14,000 ft and a slope of 20 degrees have been indicated by Correale and Guy (Ref. 33) as providing the most severe thermal lunar environment. The 40-degree solar angle has been found to provide the highest heat leak in the present studies. Table 5-5 gives the heat flux and temperature distributions as a function of thermal insulation thickness and distance from the crater wall.

Figure 5-13 shows the heat leak into the suit as a function of distance from the crater wall and solar angle for an insulating garment thickness of 0.1 in. It will be observed that the highest heat leak is obtained at a solar angle of 40 degrees for distances from the crater wall up to 4000 ft. This maximum heat leak at a 40-degree solar angle is also shown in Figure 5-14, which gives the heat leak into the suit as a function of the insulation thickness.

Figure 5-15 shows the effect of using a reflective outer surface on the extravehicular suit heat leak in the lunar crater thermal environment. Two results can be noted. One is the reduction in the peak heat leak with no thermal garment. The second is the displacement of the peak heat leak from a solar angle of 40 degrees with the previous surface characteristics to an angle of approximately 50 degrees. For the case of a 0.1-in.-thick thermal garment, however, the heat leak does not appear to be highly dependent upon the surface spectral characteristics. Figure 5-16 gives the heat leak as a function of thermal garment insulation thickness, illustrating the rapidly diminishing return with respect to performance improvement obtained after a heat leak into the suit of approximately 150 Btu/hr is reached.

TABLE 5-4

MARS ORBIT EXTRAVEHICULAR HEAT BALANCE

HEAT TRANSFER COMPUTATION FOR MAN IN MARS ORBIT (45) (10-2-64) PAGE 1

PLANET (SPHERICAL)
1799.000 = RADIUS (N.M.)
0.150 = ALBEDO
190.500 = SOLAR CONSTANT (BTU/HR-SQFT)

SPACECRAFT (SPHERICAL)
5.000 = RADIUS (FEET)
0.200 = SOLAR ABSORPTIVITY
0.900 = INFRARED ABSORPTIVITY
0.000 = INTERNAL HEAT LOAD (BTU/HR)

SUIT (CYLINDRICAL)
6.250 = RADIUS (INCHES)
69.100 = HEIGHT (INCHES)
0.350 = THICKNESS (INCHES)
600.000 = DISTANCE FROM PLANET SURFACE (N.M.)
2.000 = DISTANCE FROM VEHICLE SURFACE (FEET)

0.320 = SOLAR ABSORPTIBITY
0.560 = INFRARED ABSORPTIVITY
0.020 = THERMAL CONDUCTIVITY (BTU/HR-FT-R)
1.000 = INTERCHANGE FACTOR E(B-I)
550.000 = SKIN TEMPERATURE OF CREW (R)

ANGLES IN DEGREES
45.000 = ORBIT PLANE INCLINATION ANGLE
(W.R.T. PLANE PERPENDICULAR TO SUN DIRECTION)
90.000 = ANGLE BETWEEN BODY AXIS AND
BODY POSITION VECTOR

0.000 = ANGLE BETWEEN BODY-VEHICLE VECTOR AND
BODY POSITION VECTOR

SHADOW ANGLE INTERCEPTS	ENTER	EXIT
SUIT IN SHADOWS (PLANET)	249.322	290.678
(VEHICLE)	81.787	98.213
VEHICLE IN SHADOW (PLANET)	249.322	290.678

TABLE 5-4 (continued)

HEAT TRANSFER COMPUTATION FOR MAN IN MARS ORBIT (45) (10-2-64) PAGE 2

γ (DEG)	-ABSORBED HEAT FLUXES (BTU/HR-SQFT)-SPACECRAFT DIRECT SOLAR	REFTD. SOLAR	PLANET EMISSN	INSIDE HEAT	TOTAL	TS**4 (E-08)	TS (R)
90.00	9.53	0.68	6.17	0.00	16.37	106.21	321.03
100.00	9.53	0.67	6.17	0.00	16.36	106.14	320.97
110.00	9.53	0.64	6.17	0.00	16.33	105.94	320.82
120.00	9.53	0.59	6.17	0.00	16.28	105.61	320.58
130.00	9.53	0.52	6.17	0.00	16.21	105.17	320.24
140.00	9.53	0.44	6.17	0.00	16.13	104.62	319.82
150.00	9.53	0.34	6.17	0.00	16.03	103.99	319.34
160.00	9.53	0.23	6.17	0.00	15.92	103.29	318.80
170.00	9.53	0.12	6.17	0.00	15.81	102.54	318.22
180.00	9.53	0.00	6.17	0.00	15.69	101.77	317.62
190.00	9.53	0.00	6.17	0.00	15.69	101.77	317.62
200.00	9.53	0.00	6.17	0.00	15.69	101.77	317.62
210.00	9.53	0.00	6.17	0.00	15.69	101.77	317.62
220.00	9.53	0.00	6.17	0.00	15.69	101.77	317.62
230.00	9.53	0.00	6.17	0.00	15.69	101.77	317.62
240.00	9.53	0.00	6.17	0.00	15.69	101.77	317.62
250.00	0.00	0.00	6.17	0.00	6.17	39.99	251.47
260.00	0.00	0.00	6.17	0.00	6.17	39.99	251.47
270.00	0.00	0.00	6.17	0.00	6.17	39.99	251.47

τ	ω	ABSORBED HEAT FLUXES (BTU/HR-SQFT)-SPACE SUIT-									AVERAGE VALUES		
		DIRECT	REFLECTED SOLAR		THERMAL EMISS.			TS	T(OUT)	QRATE	TS	T(OUT)	Q(IN)
(DEG)	(DEG)	SOLAR	PLANET	VEHICLE	PLANET	VEHICLE	TOTAL	(R)	(R)	B/H-SF	(R)	(R)	BTU/HR
90.00													
	0.00	0.00	3.64	0.00	12.75	0.00	16.38	361.51	471.75	-31.13			
	30.00	0.00	3.15	0.00	11.04	0.00	14.19	348.74	468.96	-32.20			
	60.00	0.00	1.90	0.00	6.67	0.07	8.64	308.07	461.71	-34.95			
	90.00	0.00	0.72	0.00	2.54	0.86	4.13	256.09	455.68	-37.23			
	120.00	0.00	0.08	0.00	0.29	2.41	2.79	232.18	453.87	-37.91			
	150.00	0.00	0.00	0.00	0.00	4.05	4.05	254.93	455.58	-37.27			
	180.00	0.00	0.00	0.00	0.00	4.68	4.68	264.26	456.42	-36.96			
	210.00	0.00	0.00	0.00	0.00	4.05	4.05	254.93	455.58	-37.27			
	240.00	0.00	0.08	0.00	0.29	2.41	2.79	232.18	453.87	-37.91			
	270.00	0.00	0.72	0.00	2.54	0.86	4.13	256.09	455.68	-37.23			
	300.00	0.00	1.90	0.00	6.67	0.07	8.64	308.07	461.71	-34.95			
	330.00	0.00	3.15	0.00	11.04	0.00	14.19	348.74	468.96	-32.20			
	ENC	0.00	0.72	0.00	2.54	0.86	4.13	256.09	457.74	-37.99			
	ENC	0.00	0.72	0.00	2.54	0.86	4.13	256.09	457.74	-37.99	293.49	459.91	-735.6
100.00													
	0.00	0.00	3.58	0.00	12.75	0.00	16.33	361.20	471.69	-31.15			
	30.00	0.00	3.10	0.00	11.04	0.00	14.14	348.45	468.87	-32.23			
	60.00	16.11	1.87	0.00	6.67	0.07	24.72	400.65	482.15	-27.12			
	90.00	43.11	0.71	0.00	2.54	0.86	47.22	471.02	508.35	-16.85			
	120.00	58.56	0.08	0.00	0.29	2.41	61.34	502.86	523.59	-10.75			
	150.00	58.32	0.00	0.00	0.00	4.05	62.36	504.95	524.65	-10.32			
	180.00	42.45	0.00	0.00	0.00	4.68	47.13	470.79	508.25	-16.88			
	210.00	15.21	0.00	0.00	0.00	4.05	19.26	376.42	475.39	-29.73			
	240.00	0.00	0.08	0.00	0.29	2.41	2.78	232.12	453.85	-37.92			
	270.00	0.00	0.71	0.00	2.54	0.86	4.11	255.91	455.67	-37.24			
	300.00	0.00	1.87	0.00	6.67	0.07	8.61	307.81	461.68	-34.97			
	330.00	0.00	3.10	0.00	11.04	0.00	14.14	348.45	468.87	-32.23			
	ENC	0.00	0.71	0.00	2.54	0.86	4.11	255.91	457.73	-37.99			
	ENC	7.49	0.71	0.00	2.54	0.86	11.60	331.61	467.38	-34.17	402.87	483.72	-559.9
110.00													
	0.00	0.00	3.42	0.00	12.75	0.00	16.16	360.29	471.46	-31.24			
	30.00	0.00	2.96	0.00	11.04	0.00	14.00	347.57	468.71	-32.29			
	60.00	17.08	1.79	0.00	6.67	0.07	25.60	404.19	483.22	-26.71			
	90.00	43.11	0.68	0.00	2.54	0.86	47.19	470.94	508.31	-16.86			
	120.00	57.58	0.08	0.00	0.29	2.41	60.36	500.84	522.56	-11.16			
	150.00	56.63	0.00	0.00	0.00	4.04	60.67	501.49	522.89	-11.03			
	180.00	40.51	0.00	0.00	0.00	4.67	45.17	465.83	506.07	-17.75			
	210.00	13.53	0.00	0.00	0.00	4.04	17.57	367.87	473.26	-30.55			
	240.00	0.00	0.08	0.00	0.29	2.41	2.78	231.95	453.85	-37.92			
	270.00	0.00	0.68	0.00	2.54	0.86	4.08	255.37	455.61	-37.26			
	300.00	0.00	1.79	0.00	6.67	0.07	8.53	307.04	461.55	-35.01			
	330.00	0.00	2.96	0.00	11.04	0.00	14.00	347.57	468.71	-32.29			
	ENC	0.00	0.68	0.00	2.54	0.86	4.08	255.37	457.68	-38.01			
	ENC	14.74	0.68	0.00	2.54	0.86	18.82	374.27	476.36	-30.58	402.22	483.47	-561.1

HEAT TRANSFER COMPUTATION FOR MAN IN MARS ORBIT (45) (10-2-64) PAGE 4

γ (DEG)	ω (DEG)	ABSORBED HEAT FLUXES (BTU/HR-SQFT)-SPACE SUIT- DIRECT SOLAR	REFLECTED SOLAR PLANET	REFLECTED SOLAR VEHICLE	THERMAL EMISS. PLANET	THERMAL EMISS. VEHICLE	TOTAL	TS (R)	T(OUT) (R)	QRATE B/H-SF	AVERAGE VALUES TS (R)	AVERAGE VALUES T(OUT) (R)	AVERAGE VALUES Q(IN) BTU/HR
120.00													
	0.00	0.00	3.15	0.00	12.75	0.00	15.90	358.79	471.12	-31.37			
	30.00	0.00	2.73	0.00	11.04	0.00	13.77	346.12	468.39	-32.41			
	60.00	18.67	1.65	0.00	6.67	0.07	27.05	409.79	484.98	-26.03			
	90.00	43.11	0.63	0.00	2.54	0.86	47.13	470.80	508.26	-16.88			
	120.00	56.00	0.07	0.00	0.29	2.40	58.76	497.49	520.86	-11.85			
	150.00	53.88	0.00	0.00	0.00	4.03	57.91	495.68	519.97	-12.20			
	180.00	37.33	0.00	0.00	0.00	4.65	41.98	457.38	502.48	-19.17			
	210.00	10.78	0.00	0.00	0.00	4.03	14.81	352.47	469.73	-31.90			
	240.00	0.00	0.07	0.00	0.29	2.40	2.76	231.67	453.83	-37.93			
	270.00	0.00	0.63	0.00	2.54	0.86	4.02	254.49	455.53	-37.29			
	300.00	0.00	1.65	0.00	6.67	0.07	8.39	305.77	461.37	-35.08			
	330.00	0.00	2.73	0.00	11.04	0.00	13.77	346.12	468.39	-32.41			
	END	0.00	0.63	0.00	2.54	0.86	4.02	254.49	457.61	-38.04			
	END	21.55	0.63	0.00	2.54	0.86	25.58	404.09	484.51	-27.29	400.30	482.84	-565.3
130.00													
	0.00	0.00	2.79	0.00	12.75	0.00	15.53	356.72	470.67	-31.54			
	30.00	0.00	2.41	0.00	11.04	0.00	13.45	344.12	467.99	-32.56			
	60.00	20.82	1.46	0.00	6.67	0.07	29.02	417.03	487.36	-25.10			
	90.00	43.11	0.55	0.00	2.54	0.85	47.05	470.61	508.16	-16.92			
	120.00	53.84	0.06	0.00	0.29	2.39	56.59	492.82	518.55	-12.78			
	150.00	50.15	0.00	0.00	0.00	4.01	54.16	487.46	515.95	-13.82			
	180.00	33.02	0.00	0.00	0.00	4.63	37.65	445.11	497.53	-21.12			
	210.00	7.04	0.00	0.00	0.00	4.01	11.06	327.65	464.88	-33.75			
	240.00	0.00	0.06	0.00	0.29	2.39	2.74	231.28	453.81	-37.93			
	270.00	0.00	0.55	0.00	2.54	0.85	3.95	253.28	455.44	-37.32			
	300.00	0.00	1.46	0.00	6.67	0.07	8.20	304.02	461.12	-35.18			
	330.00	0.00	2.41	0.00	11.04	0.00	13.45	344.12	467.99	-32.56			
	END	0.00	0.55	0.00	2.54	0.85	3.95	253.28	457.51	-38.08			
	END	27.71	0.55	0.00	2.54	0.85	31.66	426.21	491.66	-24.39	397.11	481.85	-572.4
140.00													
	0.00	0.00	2.34	0.00	12.75	0.00	15.09	354.12	470.08	-31.77			
	30.00	0.00	2.02	0.00	11.04	0.00	13.06	341.61	467.49	-32.75			
	60.00	23.48	1.22	0.00	6.67	0.07	31.44	425.47	490.25	-23.97			
	90.00	43.11	0.47	0.00	2.54	0.85	46.96	470.37	508.06	-16.96			
	120.00	51.18	0.05	0.00	0.29	2.38	53.91	486.88	515.68	-13.92			
	150.00	45.55	0.00	0.00	0.00	3.99	49.54	476.71	510.91	-15.83			
	180.00	27.71	0.00	0.00	0.00	4.61	32.32	428.42	491.28	-23.57			
	210.00	2.44	0.00	0.00	0.00	3.99	6.43	286.18	458.78	-36.06			
	240.00	0.00	0.05	0.00	0.29	2.38	2.72	230.80	453.77	-37.95			
	270.00	0.00	0.47	0.00	2.54	0.85	3.85	251.77	455.30	-37.37			
	300.00	0.00	1.22	0.00	6.67	0.07	7.96	301.82	460.82	-35.29			
	330.00	0.00	2.02	0.00	11.04	0.00	13.06	341.61	467.49	-32.75			
	END	0.00	0.47	0.00	2.54	0.85	3.85	251.77	457.38	-38.13			
	END	33.02	0.47	0.00	2.54	0.85	36.87	442.79	497.63	-21.95	392.67	480.52	-582.3

γ	ω	ABSORBED HEAT FLUXES (BTU/HR-SQFT)-SPACE SUIT- DIRECT REFLECTED SOLAR THERMAL EMISS.						TS	T(OUT)	QRATE	AVERAGE VALUES TS	T(OUT)	Q(IN)
(DEG)	(DEG)	SOLAR	PLANET	VEHICLE	PLANET	VEHICLE	TOTAL	(R)	(R)	B/H-SF	(R)	(R)	BTU/HR
150.00													
	0.00	0.00	1.82	0.00	12.75	0.00	14.57	351.03	469.43	-32.01			
	30.00	2.89	1.57	0.00	11.04	0.00	15.50	356.54	470.63	-31.56			
	60.00	26.55	0.95	0.00	6.67	0.07	34.24	434.66	493.56	-22.68			
	90.00	43.11	0.36	0.00	2.54	0.85	46.85	470.10	507.95	-17.00			
	120.00	48.11	0.04	0.00	0.29	2.36	50.80	479.72	512.31	-15.27			
	150.00	40.22	0.00	0.00	0.00	3.97	44.18	463.27	504.95	-18.19			
	180.00	21.55	0.00	0.00	0.00	4.58	26.13	406.27	483.88	-26.45			
	210.00	0.00	0.00	0.00	0.00	3.97	3.97	253.59	455.47	-37.31			
	240.00	0.00	0.04	0.00	0.29	2.36	2.70	230.24	453.74	-37.96			
	270.00	0.00	0.36	0.00	2.54	0.85	3.75	249.98	455.17	-37.42			
	300.00	0.00	0.95	0.00	6.67	0.07	7.69	299.21	460.45	-35.43			
	330.00	0.00	1.57	0.00	11.04	0.00	12.61	338.63	466.92	-32.97			
	ENC	0.00	0.36	0.00	2.54	0.85	3.75	249.98	457.23	-38.19			
	ENC	37.33	0.36	0.00	2.54	0.85	41.08	454.89	502.35	-20.01	388.96	479.43	-590.2
160.00													
	0.00	0.00	1.24	0.00	12.75	0.00	13.99	347.52	468.69	-32.30			
	30.00	8.78	1.08	0.00	11.04	0.00	20.90	384.20	477.45	-28.94			
	60.00	29.96	0.65	0.00	6.67	0.07	37.35	444.20	497.17	-21.26			
	90.00	43.11	0.25	0.00	2.54	0.84	46.73	469.80	507.82	-17.06			
	120.00	44.70	0.03	0.00	0.29	2.35	47.37	471.40	508.52	-16.78			
	150.00	34.32	0.00	0.00	0.00	3.94	38.26	446.89	498.22	-20.85			
	180.00	14.74	0.00	0.00	0.00	4.55	19.29	376.58	475.43	-29.72			
	210.00	0.00	0.00	0.00	0.00	3.94	3.94	253.16	455.42	-37.33			
	240.00	0.00	0.03	0.00	0.29	2.35	2.67	229.62	453.70	-37.98			
	270.00	0.00	0.25	0.00	2.54	0.84	3.63	247.95	455.01	-37.48			
	300.00	0.00	0.65	0.00	6.67	0.07	7.39	296.24	460.04	-35.59			
	330.00	0.00	1.08	0.00	11.04	0.00	12.12	335.25	466.28	-33.22			
	ENC	0.00	0.25	0.00	2.54	0.84	3.63	247.95	457.07	-38.25			
	ENC	40.51	0.25	0.00	2.54	0.84	44.13	463.13	505.73	-18.62	386.31	478.65	-595.7
170.00													
	0.00	0.00	0.63	0.00	12.75	0.00	13.38	343.66	467.91	-32.60			
	30.00	15.07	0.55	0.00	11.04	0.00	26.66	408.29	484.52	-26.20			
	60.00	33.59	0.33	0.00	6.67	0.07	40.65	453.72	500.96	-19.77			
	90.00	43.11	0.13	0.00	2.54	0.83	46.60	469.48	507.68	-17.11			
	120.00	41.07	0.01	0.00	0.29	2.33	43.71	462.01	504.43	-18.40			
	150.00	28.03	0.00	0.00	0.00	3.91	31.95	427.19	490.86	-23.74			
	180.00	7.49	0.00	0.00	0.00	4.52	12.00	334.45	466.11	-33.28			
	210.00	0.00	0.00	0.00	0.00	3.91	3.91	252.70	455.39	-37.34			
	240.00	0.00	0.01	0.00	0.29	2.33	2.64	228.95	453.65	-38.00			
	270.00	0.00	0.13	0.00	2.54	0.83	3.50	245.73	454.83	-37.55			
	300.00	0.00	0.33	0.00	6.67	0.07	7.07	292.97	459.62	-35.74			
	330.00	0.00	0.55	0.00	11.04	0.00	11.59	331.52	465.59	-33.48			
	ENC	0.00	0.13	0.00	2.54	0.83	3.50	245.73	456.91	-38.31			
	ENC	42.45	0.13	0.00	2.54	0.83	45.95	467.82	507.73	-17.79	383.14	477.79	-602.5

HEAT TRANSFER COMPUTATION FOR MAN IN MARS ORBIT (45) (10-2-64) PAGE 6

γ (DEG)	ω (DEG)	ABSORBED HEAT FLUXES (BTU/HR-SQFT)-SPACE SUIT- DIRECT SOLAR	REFLECTED PLANET	REFLECTED VEHICLE	THERMAL EMISS. PLANET	THERMAL EMISS. VEHICLE	TOTAL	TS (R)	T(OUT) (R)	QRATE B/H-SF	AVERAGE VALUES TS (R)	AVERAGE VALUES T(OUT) (R)	AVERAGE VALUES Q(IN) BTU/HR
180.00													
	0.00	0.00	0.01	0.00	12.75	0.00	12.75	339.53	467.07	-32.92			
	30.00	21.55	0.01	0.00	11.04	0.00	32.59	429.33	491.62	-23.44			
	60.00	37.33	0.00	0.00	6.67	0.07	44.07	462.96	504.82	-18.24			
	90.00	43.11	0.00	0.00	2.54	0.83	46.47	469.15	507.52	-17.17			
	120.00	37.33	0.00	0.00	0.29	2.31	39.93	451.70	500.14	-20.09			
	150.00	21.55	0.00	0.00	0.00	3.88	25.43	403.53	483.02	-26.79			
	180.00	0.00	0.00	0.00	0.00	4.48	4.48	261.46	456.16	-37.05			
	210.00	0.00	0.00	0.00	0.00	3.88	3.88	252.22	455.35	-37.35			
	240.00	0.00	0.00	0.00	0.29	2.31	2.60	228.25	453.61	-38.01			
	270.00	0.00	0.00	0.00	2.54	0.83	3.37	243.38	454.66	-37.62			
	300.00	0.00	0.00	0.00	6.67	0.07	6.74	289.48	459.19	-35.91			
	330.00	0.00	0.01	0.00	11.04	0.00	11.04	327.53	464.87	-33.76			
	ENC	0.00	0.00	0.00	2.54	0.83	3.37	243.38	456.74	-38.38			
	ENC	43.11	0.00	0.00	2.54	0.83	46.47	469.15	508.29	-17.56	379.52	476.87	-610.4
190.00													
	0.00	7.49	0.00	0.00	12.75	0.00	20.23	381.09	476.61	-29.26			
	30.00	28.03	0.00	0.00	11.04	0.00	39.08	449.25	499.15	-20.48			
	60.00	41.07	0.00	0.05	6.67	0.07	47.86	472.61	509.07	-16.56			
	90.00	43.11	0.00	0.56	2.54	0.83	47.03	470.56	508.15	-16.93			
	120.00	33.59	0.00	1.58	0.29	2.31	37.77	445.44	497.66	-21.07			
	150.00	15.07	0.00	2.65	0.00	3.88	21.60	387.36	478.29	-28.61			
	180.00	0.00	0.00	3.06	0.00	4.48	7.54	297.73	460.26	-35.51			
	210.00	0.00	0.00	2.65	0.00	3.88	6.53	287.22	458.91	-36.01			
	240.00	0.00	0.00	1.58	0.29	2.31	4.18	256.93	455.75	-37.21			
	270.00	0.00	0.00	0.56	2.54	0.83	3.93	252.98	455.41	-37.33			
	300.00	0.00	0.00	0.05	6.67	0.07	6.79	290.00	459.25	-35.89			
	330.00	0.00	0.00	0.00	11.04	0.00	11.04	327.53	464.87	-33.76			
	ENC	0.00	0.00	0.56	2.54	0.83	3.93	252.98	457.48	-38.09			
	ENC	42.45	0.00	0.56	2.54	0.83	46.38	468.92	508.20	-17.60	366.76	478.80	-594.9
200.00													
	0.00	14.74	0.00	0.00	12.75	0.00	27.49	411.44	485.51	-25.82			
	30.00	34.32	0.00	0.00	11.04	0.00	45.36	466.32	506.29	-17.66			
	60.00	44.70	0.00	0.10	6.67	0.07	51.53	481.43	513.10	-14.95			
	90.00	43.11	0.00	1.11	2.54	0.83	47.58	471.92	508.76	-16.68			
	120.00	29.96	0.00	3.10	0.29	2.31	35.67	439.12	495.21	-22.03			
	150.00	8.78	0.00	5.21	0.00	3.88	17.88	369.48	473.65	-30.40			
	180.00	0.00	0.00	6.02	0.00	4.48	10.50	323.46	464.17	-34.02			
	210.00	0.00	0.00	5.21	0.00	3.88	9.09	312.03	462.32	-34.72			
	240.00	0.00	0.00	3.10	0.29	2.31	5.71	277.74	457.80	-36.43			
	270.00	0.00	0.00	1.11	2.54	0.83	4.48	261.36	456.15	-37.06			
	300.00	0.00	0.00	0.10	6.67	0.07	6.83	290.51	459.30	-35.87			
	330.00	0.00	0.00	0.00	11.04	0.00	11.04	327.53	464.87	-33.76			
	ENC	0.00	0.00	1.11	2.54	0.83	4.48	261.36	458.19	-37.81			
	ENC	40.51	0.00	1.11	2.54	0.83	44.98	465.34	506.67	-18.23	393.19	480.62	-580.7

γ	ω	ABSORBED HEAT FLUXES (BTU/HR-SQFT)-SPACE SUIT-									AVERAGE VALUES		
		DIRECT	REFLECTED SOLAR		THERMAL EMISS.			TS	T(OUT)	QRATE	TS	T(OUT)	Q(IN)
(DEG)	(DEG)	SOLAR	PLANET	VEHICLE	PLANET	VEHICLE	TOTAL	(R)	(R)	B/H-SF	(R)	(R)	BTU/HR
210.00													
	0.00	21.55	0.00	0.00	12.75	0.00	34.30	434.85	493.63	-22.65			
	30.00	40.22	0.00	0.00	11.04	0.00	51.26	480.79	512.81	-15.07			
	60.00	48.11	0.00	0.14	6.67	0.07	54.98	489.29	516.84	-13.46			
	90.00	43.11	0.00	1.62	2.54	0.83	48.09	473.19	509.32	-16.46			
	120.00	26.55	0.00	4.54	0.29	2.31	33.70	432.92	492.91	-22.93			
	150.00	2.89	0.00	7.62	0.00	3.88	14.39	349.96	469.19	-32.11			
	180.00	0.00	0.00	8.80	0.00	4.48	13.28	343.01	467.78	-32.64			
	210.00	0.00	0.00	7.62	0.00	3.88	11.50	330.90	465.46	-33.53			
	240.00	0.00	0.00	4.54	0.29	2.31	7.14	293.75	459.72	-35.71			
	270.00	0.00	0.00	1.62	2.54	0.83	4.99	268.54	456.84	-36.80			
	300.00	0.00	0.00	0.14	6.67	0.07	6.88	290.97	459.37	-35.84			
	330.00	0.00	0.00	0.00	11.04	0.00	11.04	327.53	464.87	-33.76			
	ENC	0.00	0.00	1.62	2.54	0.83	4.99	268.54	458.87	-37.54			
	ENC	37.33	0.00	1.62	2.54	0.83	42.32	458.30	503.74	-19.44	398.71	482.28	-568.3
220.00													
	0.00	27.71	0.00	0.00	12.75	0.00	40.46	453.17	500.75	-19.85			
	30.00	45.55	0.00	0.00	11.04	0.00	56.59	492.83	518.55	-12.78			
	60.00	51.18	0.00	0.18	6.67	0.07	58.10	496.09	520.16	-12.13			
	90.00	43.11	0.00	2.09	2.54	0.83	48.56	474.33	509.84	-16.25			
	120.00	23.48	0.00	5.83	0.29	2.31	31.91	427.08	490.81	-23.75			
	150.00	0.00	0.00	9.79	0.00	3.88	13.68	345.55	468.30	-32.45			
	180.00	0.00	0.00	11.31	0.00	4.48	15.79	358.20	471.00	-31.42			
	210.00	0.00	0.00	9.79	0.00	3.88	13.68	345.55	468.30	-32.45			
	240.00	0.00	0.00	5.83	0.29	2.31	8.44	306.25	461.45	-35.05			
	270.00	0.00	0.00	2.09	2.54	0.83	5.45	274.57	457.45	-36.56			
	300.00	0.00	0.00	0.18	6.67	0.07	6.92	291.40	459.41	-35.82			
	330.00	2.44	0.00	0.00	11.04	0.00	13.48	344.32	468.04	-32.55			
	ENC	0.00	0.00	2.09	2.54	0.83	5.45	274.57	459.48	-37.30			
	ENC	33.02	0.00	2.09	2.54	0.83	38.47	447.51	499.44	-21.21	404.75	484.15	-554.0
230.00													
	0.00	33.02	0.00	0.00	12.75	0.00	45.77	467.36	506.75	-17.48			
	30.00	50.15	0.00	0.00	11.04	0.00	61.19	502.55	523.43	-10.82			
	60.00	53.84	0.00	0.21	6.67	0.07	60.79	501.73	523.01	-10.99			
	90.00	43.11	0.00	2.49	2.54	0.83	48.96	475.30	510.27	-16.08			
	120.00	20.82	0.00	6.95	0.29	2.31	30.38	421.84	488.99	-24.46			
	150.00	0.00	0.00	11.67	0.00	3.88	15.55	356.84	470.69	-31.53			
	180.00	0.00	0.00	13.48	0.00	4.48	17.96	369.91	473.74	-30.36			
	210.00	0.00	0.00	11.67	0.00	3.88	15.55	356.84	470.69	-31.53			
	240.00	0.00	0.00	6.95	0.29	2.31	9.56	315.93	462.91	-34.50			
	270.00	0.00	0.00	2.49	2.54	0.83	5.85	279.47	458.01	-36.35			
	300.00	0.00	0.00	0.21	6.67	0.07	6.95	291.76	459.46	-35.81			
	330.00	7.04	0.00	0.00	11.04	0.00	18.08	370.54	473.89	-30.31			
	ENC	0.00	0.00	2.49	2.54	0.83	5.85	279.47	460.00	-37.09			
	ENC	27.71	0.00	2.49	2.54	0.83	33.56	432.48	493.85	-23.50	410.94	486.14	-538.8

HEAT TRANSFER COMPUTATION FOR MAN IN MARS ORBIT (45) (10-2-64) PAGE 8

γ	ω	ABSORBED HEAT FLUXES (BTU/HR-SQFT)-SPACE SUIT- DIRECT REFLECTED SOLAR THERMAL EMISS.						TS	T(OUT)	QRATE	AVERAGE VALUES TS	T(OUT)	Q(IN)
(DEG)	(DEG)	SOLAR	PLANET	VEHICLE	PLANET	VEHICLE	TOTAL	(R)	(R)	B/H-SF	(R)	(R)	BTU/HR
240.00													
	0.00	37.33	0.00	0.00	12.75	0.00	50.08	478.00	511.50	-15.59			
	30.00	53.88	0.00	0.00	11.04	0.00	64.92	510.05	527.32	-9.25			
	60.00	56.00	0.00	0.24	6.67	0.07	62.97	506.18	525.29	-10.07			
	90.00	43.11	0.00	2.81	2.54	0.83	49.28	476.09	510.64	-15.94			
	120.00	18.67	0.00	7.86	0.29	2.31	29.13	417.44	487.49	-25.05			
	150.00	0.00	0.00	13.20	0.00	3.88	17.08	365.28	472.63	-30.79			
	180.00	0.00	0.00	15.24	0.00	4.48	19.72	378.65	475.95	-29.51			
	210.00	0.00	0.00	13.20	0.00	3.88	17.08	365.28	472.63	-30.79			
	240.00	0.00	0.00	7.86	0.29	2.31	10.46	323.18	464.10	-34.05			
	270.00	0.00	0.00	2.81	2.54	0.83	6.18	283.27	458.43	-36.19			
	300.00	0.00	0.00	0.24	6.67	0.07	6.98	292.05	459.50	-35.79			
	330.00	10.78	0.00	0.00	11.04	0.00	21.82	388.34	478.58	-28.50			
	ENC	0.00	0.00	2.81	2.54	0.83	6.18	283.27	460.42	-36.93			
	ENC	21.55	0.00	2.81	2.54	0.83	27.73	412.33	487.08	-26.25	415.49	487.66	-527.3
250.00													
	0.00	0.00	0.00	0.00	12.75	0.00	12.75	339.53	467.07	-32.92			
	30.00	0.00	0.00	0.00	11.04	0.00	11.04	327.53	464.87	-33.76			
	60.00	0.00	0.00	0.26	6.67	0.03	6.96	291.81	459.48	-35.80			
	90.00	0.00	0.00	3.05	2.54	0.32	5.91	280.21	458.09	-36.32			
	120.00	0.00	0.00	8.53	0.29	0.91	9.73	317.35	463.14	-34.41			
	150.00	0.00	0.00	14.32	0.00	1.53	15.84	358.49	471.06	-31.39			
	180.00	0.00	0.00	16.53	0.00	1.76	18.29	371.61	474.17	-30.20			
	210.00	0.00	0.00	14.32	0.00	1.53	15.84	358.49	471.06	-31.39			
	240.00	0.00	0.00	8.53	0.29	0.91	9.73	317.35	463.14	-34.41			
	270.00	0.00	0.00	3.05	2.54	0.32	5.91	280.21	458.09	-36.32			
	300.00	0.00	0.00	0.26	6.67	0.03	6.96	291.81	459.48	-35.80			
	330.00	0.00	0.00	0.00	11.04	0.00	11.04	327.53	464.87	-33.76			
	ENC	0.00	0.00	3.05	2.54	0.32	5.91	280.21	460.07	-37.07			
	ENC	0.00	0.00	3.05	2.54	0.32	5.91	280.21	460.07	-37.07	322.88	464.26	-701.5
260.00													
	0.00	0.00	0.00	0.00	12.75	0.00	12.75	339.53	467.07	-32.92			
	30.00	0.00	0.00	0.00	11.04	0.00	11.04	327.53	464.87	-33.76			
	60.00	0.00	0.00	0.28	6.67	0.03	6.97	291.95	459.49	-35.80			
	90.00	0.00	0.00	3.20	2.54	0.32	6.06	281.93	458.28	-36.25			
	120.00	0.00	0.00	8.94	0.29	0.91	10.14	320.64	463.68	-34.21			
	150.00	0.00	0.00	15.01	0.00	1.53	16.53	362.32	471.93	-31.06			
	180.00	0.00	0.00	17.33	0.00	1.76	19.09	375.58	475.17	-29.82			
	210.00	0.00	0.00	15.01	0.00	1.53	16.53	362.32	471.93	-31.06			
	240.00	0.00	0.00	8.94	0.29	0.91	10.14	320.64	463.68	-34.21			
	270.00	0.00	0.00	3.20	2.54	0.32	6.06	281.93	458.28	-36.25			
	300.00	0.00	0.00	0.28	6.67	0.03	6.97	291.95	459.49	-35.80			
	330.00	0.00	0.00	0.00	11.04	0.00	11.04	327.53	464.87	-33.76			
	ENC	0.00	0.00	3.20	2.54	0.32	6.06	281.93	460.26	-36.99			
	ENC	0.00	0.00	3.20	2.54	0.32	6.06	281.93	460.26	-36.99	324.91	464.61	-698.8

HEAT TRANSFER COMPUTATION FOR MAN IN MARS ORBIT (45) (10-2-64) PAGE 9

γ	ω	ABSORBED HEAT FLUXES (BTU/HR-SQFT)-SPACE SUIT- DIRECT REFLECTED SOLAR THERMAL EMISS.						TS	T(OUT)	QRATE	AVERAGE VALUES TS	T(OUT)	Q(IN)
(DEG)	(DEG)	SOLAR	PLANET	VEHICLE	PLANET	VEHICLE	TOTAL	(R)	(R)	B/H-SF	(R)	(R)	BTU/HR
270.00													
	0.00	0.00	0.00	0.00	12.75	0.00	12.75	339.53	467.07	-32.92			
	30.00	0.00	0.00	0.00	11.04	0.00	11.04	327.53	464.87	-33.76			
	60.00	0.00	0.00	0.28	6.67	0.03	6.97	291.99	459.50	-35.79			
	90.00	0.00	0.00	3.25	2.54	0.32	6.11	282.50	458.34	-36.23			
	120.00	0.00	0.00	9.08	0.29	0.91	10.28	321.72	463.87	-34.13			
	150.00	0.00	0.00	15.24	0.00	1.53	16.76	363.58	472.23	-30.94			
	180.00	0.00	0.00	17.59	0.00	1.76	19.36	376.89	475.50	-29.69			
	210.00	0.00	0.00	15.24	0.00	1.53	16.76	363.58	472.23	-30.94			
	240.00	0.00	0.00	9.08	0.29	0.91	10.28	321.72	463.87	-34.13			
	270.00	0.00	0.00	3.25	2.54	0.32	6.11	282.50	458.34	-36.23			
	300.00	0.00	0.00	0.28	6.67	0.03	6.97	291.99	459.50	-35.79			
	330.00	0.00	0.00	0.00	11.04	0.00	11.04	327.53	464.87	-33.76			
	END	0.00	0.00	3.25	2.54	0.32	6.11	282.50	460.33	-36.96			
	END	0.00	0.00	3.25	2.54	0.32	6.11	282.50	460.33	-36.96	325.59	464.73	-697.9

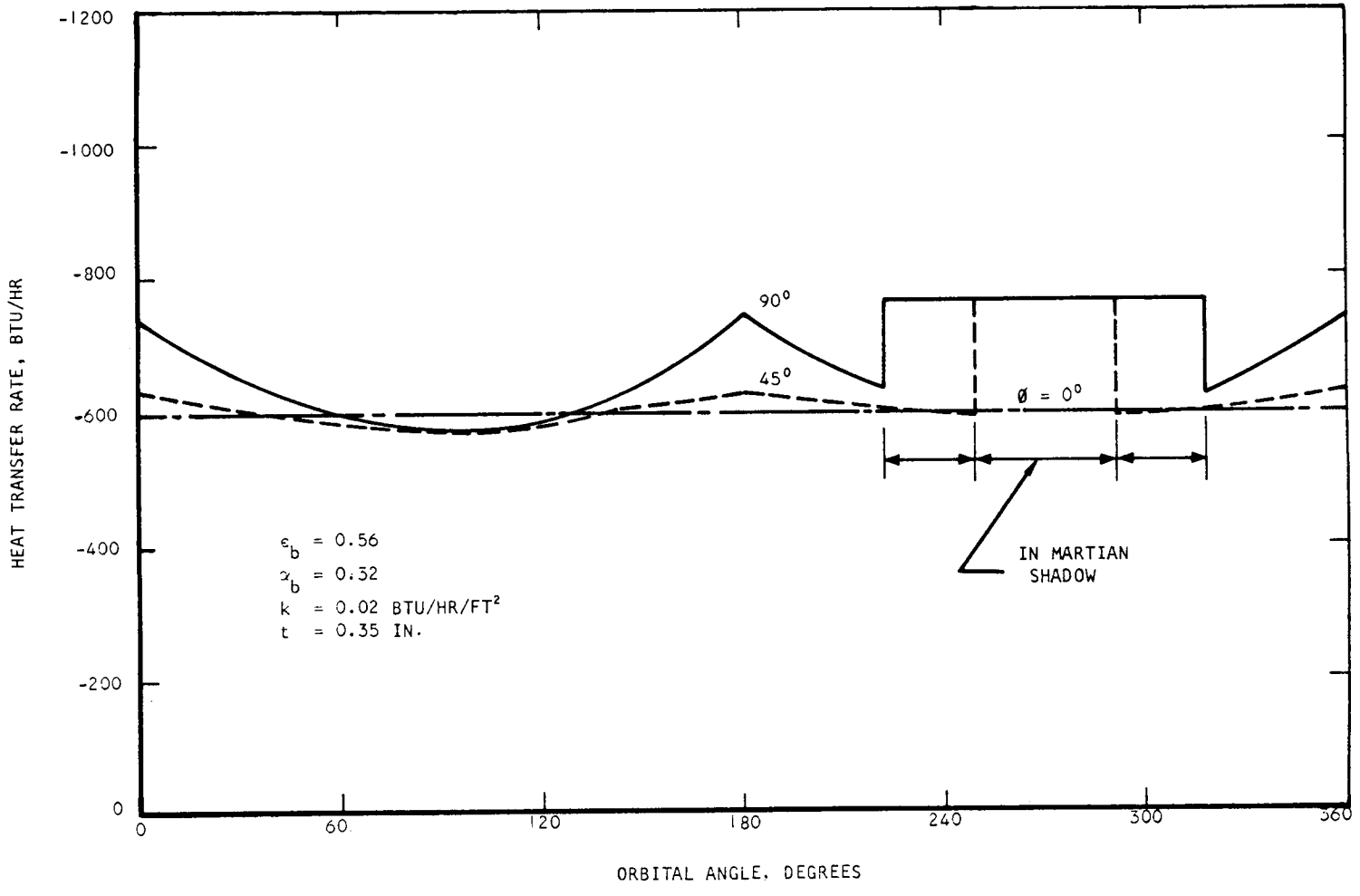

Figure 5-9. Extravehicular Suit Heat Balance in a 600-nm Mars Orbit

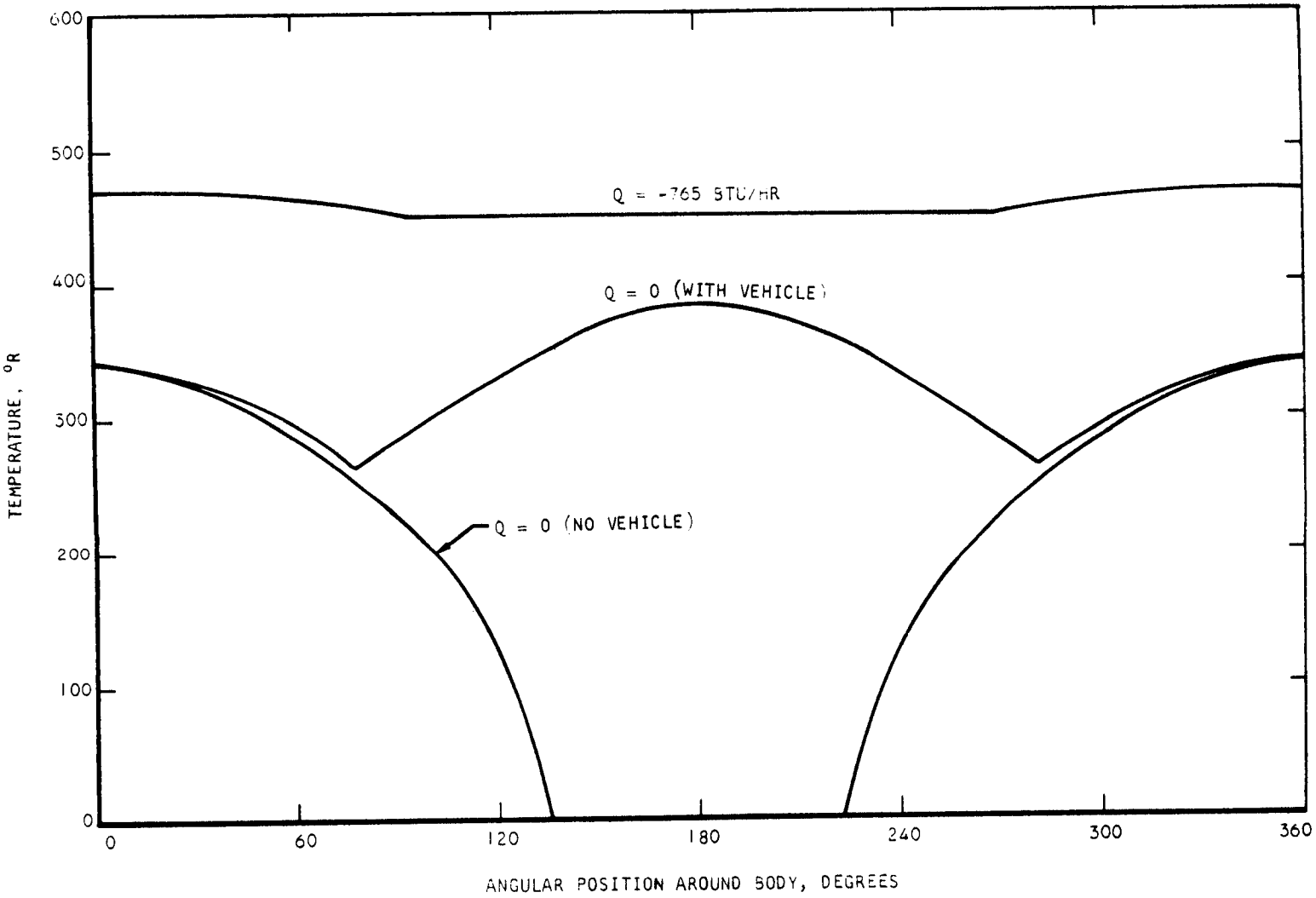

Figure 5-10. Extravehicular Suit Surface Temperature Distribution in a 600-nm Mars Orbit

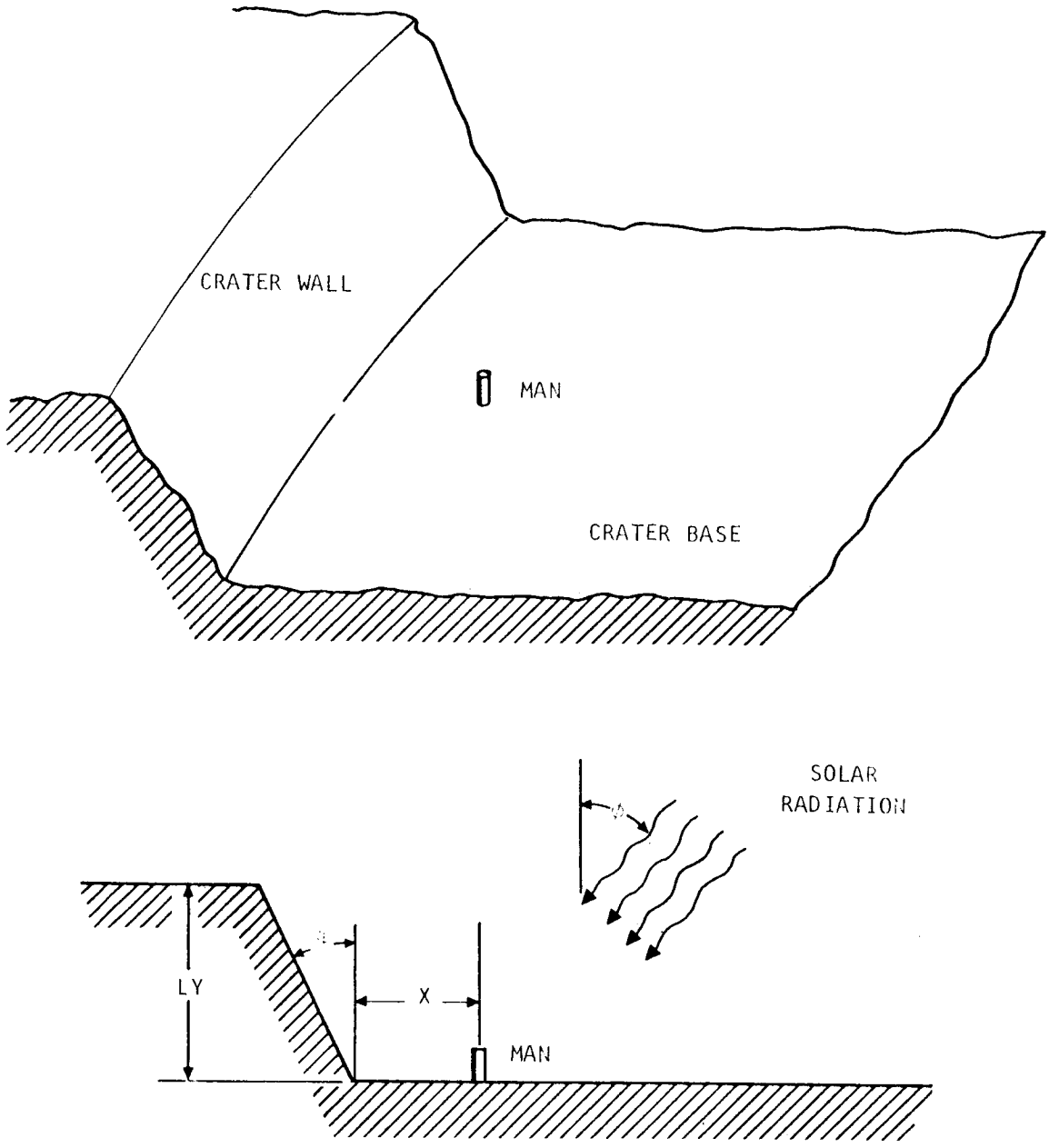

Figure 5-11. Geometry for Lunar Crater Extravehicular Suit Heat Balances

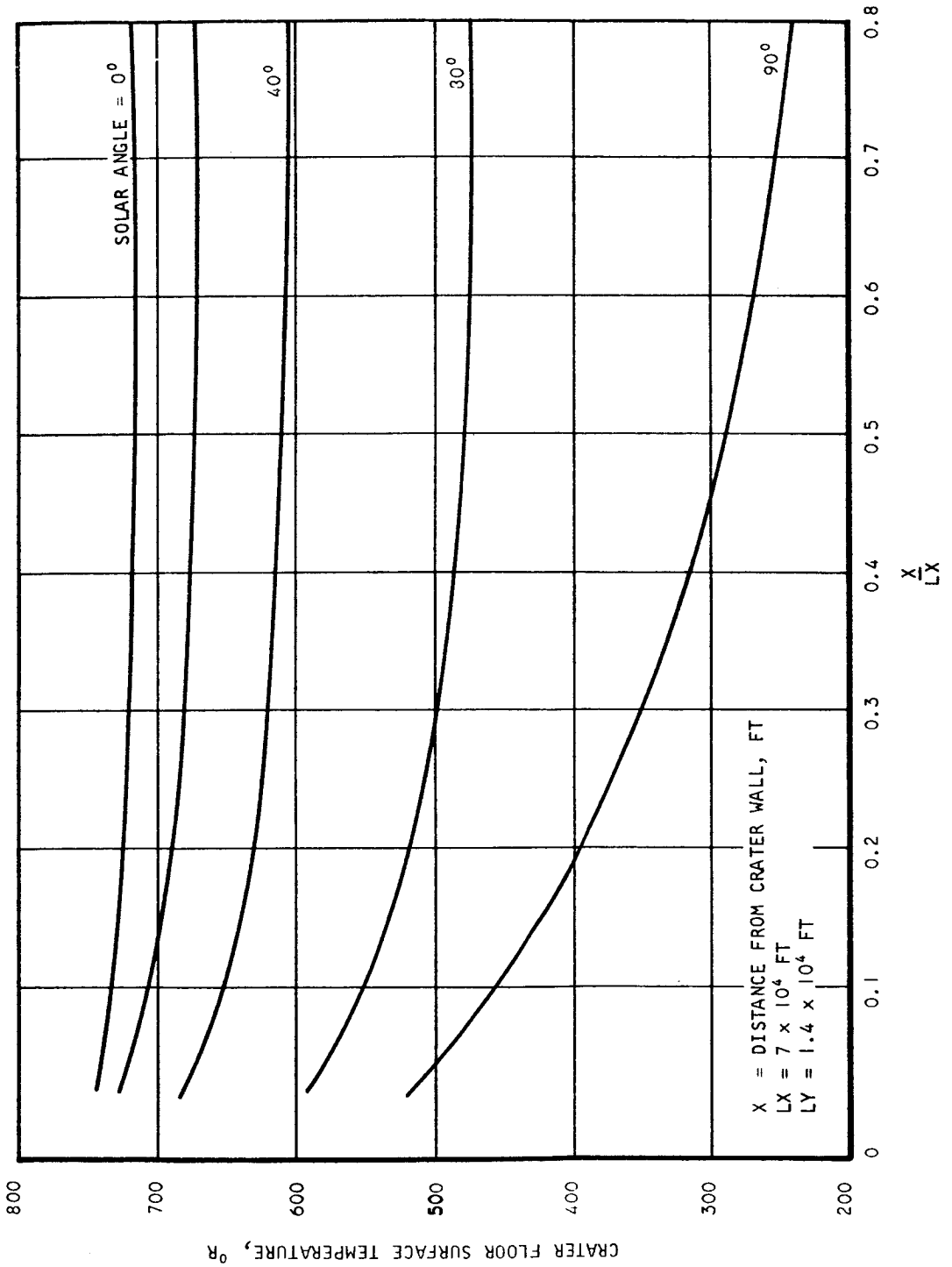

Figure 5-12. Crater Floor Surface Temperature Variation with Distance from Crater Wall

TABLE 5-5. LUNAR CRATER EXTRAVEHICULAR HEAT BALANCES

HEAT TRANSFER STUDY FOR MAN IN LUNAR CRATER (20/4C) (K1=0.0005) 10-21-64 PAGE 1

CRATER (V-GROOVE)

70000.000	= WIDTH OF BASE (FEET)
14000.000	= HEIGHT OF CLIFF (FEET)
443.000	= SOLAR CONSTANT (BTU/HR-SQFT)
20.000	= CLIFF-VERTICAL ANGLE (DEGREES)
40.000	= SUN RAYS-VERTICAL ANGLE (DEGREES)

SUIT (CYLINDRICAL)

6.250	= RADIUS (INCHES)
69.100	= HEIGHT (INCHES)
0.350	= SECOND LAYER THICKNESS (INCHES)
0.320	= SOLAR ABSORPTIVITY
0.560	= INFRARED ABSORPTIVITY
0.020	= 2-ND LAYER THERMAL CONDUCTIVITY (BTU/HR-FT-R)
1.000	= INTERCHANGE FACTOR E(S-I)
550.000	= SKIN TEMPERATURE OF CREW (R)

TABLE 5-5 (Continued)

HEAT TRANSFER STUDY FOR MAN IN LUNAR CRATER (20/40) (K1=0.0005) 10-21-64 PAGE 2

	FROM CORNER X/LX OR Y/LY	HEAT FLUX / SOLAR CONSTANT B(X)/S	B(Y)/S	TEMPERATURE (R) T(X)	T(Y)
1	0.0000	0.816	0.816	677.78	677.78
2	0.0250	1.085	1.018	727.75	716.23
3	0.0500	1.037	1.105	719.59	731.10
4	0.0750	0.996	1.148	712.32	736.14
5	0.1000	0.961	1.166	706.10	741.11
6	0.1250	0.933	1.173	700.84	742.09
7	0.1500	0.910	1.173	696.42	742.13
8	0.1750	0.890	1.171	692.69	741.75
9	0.2000	0.874	1.167	689.56	741.18
10	0.2250	0.861	1.163	686.92	740.54
11	0.2500	0.850	1.159	684.67	739.98
12	0.2750	0.840	1.155	682.76	739.22
13	0.3000	0.832	1.151	681.13	738.59
14	0.3250	0.825	1.147	679.72	737.98
15	0.3500	0.820	1.143	678.50	737.39
16	0.3750	0.814	1.140	677.45	736.82
17	0.4000	0.810	1.136	676.53	736.27
18	0.4250	0.806	1.133	675.72	735.74
19	0.4500	0.803	1.130	675.01	735.22
20	0.4750	0.800	1.127	674.38	734.73
21	0.5000	0.797	1.124	673.82	734.24
22	0.5250	0.795	1.121	673.32	733.78
23	0.5500	0.793	1.118	672.87	733.32
24	0.5750	0.791	1.116	672.47	732.88
25	0.6000	0.789	1.113	672.11	732.44
26	0.6250	0.788	1.110	671.79	732.02
27	0.6500	0.786	1.108	671.49	731.61
28	0.6750	0.785	1.105	671.22	731.20
29	0.7000	0.784	1.103	670.98	730.81
30	0.7250	0.783	1.101	670.75	730.42
31	0.7500	0.782	1.098	670.55	730.04
32	0.7750	0.781	1.096	670.36	729.66
33	0.8000	0.780	1.094	670.19	729.30
34	0.8250	0.779	1.092	670.03	728.94
35	0.8500	0.779	1.090	669.88	728.58
36	0.8750	0.778	1.088	669.74	728.23
37	0.9000	0.777	1.085	669.61	727.89
38	0.9250	0.777	1.083	669.50	727.55
39	0.9500	0.776	1.081	669.39	727.22
40	0.9750	0.776	1.080	669.28	726.89
41	1.0000	0.775	1.078	669.19	726.57

X = DISTANCE ON CRATER FLOOR

Y = HEIGHT ON CRATER WALL

LX = 7×10^4 FT

LY = 1.4×10^4 FT

T(X) = CRATER FLOOR TEMPERATURE, $^{\circ}R$

T(Y) = CRATER WALL TEMPERATURE, $^{\circ}R$

DISLM) = 1.800000E-06
ADIABATIC WALL CONDITION ASSUMED

HEAT TRANSFER STUDY FOR MAN IN LUNAR CRATER (20/40) (K1=0.0005) 10-21-64 PAGE 3

DISTANCE (FEET)	SPACE-SUIT 1-LAYER (IN.)	ELE-MENT	ABSORBED HEAT FLUXES (BTU/HR-SF) DIRECT SOLAR	CRATER BOTTOM	CRATER CLIFF	TOTAL	TS (R)	T(OUT) (R)	QRATE B/H-SF	AVERAGE VALUES TS (R)	T(OUT) (R)	T(INS) (R)	Q(I-J) BTU/HR
200.00	0.000												
		1	90.34	137.48	0.08	227.90	698.15	659.16	46.81				
		2	84.19	137.46	1.87	223.52	694.77	656.30	45.54				
		3	72.29	137.42	7.04	216.75	689.45	651.84	43.57				
		4	55.47	137.33	15.74	208.54	682.83	646.33	41.14				
		5	34.87	137.19	27.49	199.55	675.35	640.18	38.43				
		6	11.89	136.98	41.55	190.42	667.49	633.80	35.63				
		7	0.00	136.72	56.95	193.68	670.32	636.09	36.64				
		8	0.00	136.43	72.66	209.09	683.28	646.70	41.30				
		9	0.00	136.13	87.58	223.72	694.93	656.43	45.60				
		10	0.00	135.86	100.67	236.53	704.67	664.70	49.27				
		11	0.00	135.64	110.91	246.55	712.01	671.00	52.08				
		12	0.00	135.52	117.10	252.61	716.35	674.75	53.76				
		TOP	108.59	0.00	83.62	192.21	669.05	634.12	37.11	690.33	652.63	544.97	922.7
200.00	0.020												
		1	90.34	137.48	0.08	227.90	698.15	680.05	22.73				
		2	84.19	137.46	1.87	223.52	694.77	676.86	22.17				
		3	72.29	137.42	7.04	216.75	689.45	671.86	21.23				
		4	55.47	137.33	15.74	208.54	682.83	665.56	20.20				
		5	34.87	137.19	27.49	199.55	675.35	658.69	18.97				
		6	11.89	136.98	41.55	190.42	667.49	651.41	17.69				
		7	0.00	136.72	56.95	193.68	670.32	654.03	18.15				
		8	0.00	136.43	72.66	209.09	683.28	666.08	20.27				
		9	0.00	136.13	87.58	223.72	694.93	677.01	22.13				
		10	0.00	135.86	100.67	236.53	704.67	686.22	23.82				
		11	0.00	135.64	110.91	246.55	712.01	693.20	25.05				
		12	0.00	135.51	117.10	252.61	716.35	697.33	25.78				
		TOP	108.59	0.00	83.62	192.21	669.05	652.60	18.21	690.33	672.73	567.86	451.7
200.00	0.050												
		1	90.34	137.48	0.08	227.90	698.15	688.12	12.81				
		2	84.19	137.46	1.87	223.52	694.77	684.84	12.51				
		3	72.29	137.42	7.04	216.75	689.45	679.68	12.03				
		4	55.47	137.33	15.74	208.54	682.83	673.27	11.43				
		5	34.87	137.19	27.49	199.55	675.35	666.05	10.76				
		6	11.89	136.98	41.55	190.42	667.49	658.49	10.06				
		7	0.00	136.72	56.95	193.68	670.32	661.21	10.31				
		8	0.00	136.43	72.66	209.09	683.28	673.70	11.47				
		9	0.00	136.13	87.59	223.72	694.93	684.99	12.52				
		10	0.00	135.85	100.67	236.53	704.67	694.46	13.40				
		11	0.00	135.64	110.91	246.55	712.01	701.63	14.07				
		12	0.00	135.51	117.10	252.61	716.35	705.87	14.47				
		TOP	108.59	0.00	83.62	192.21	669.05	659.88	10.32	690.33	680.56	560.30	256.5

HEAT TRANSFER STUDY FOR MAN IN LUNAR CRATER (20/40) (K1=0.0005) 10-21-64 PAGE 4

SPACE-SUIT DISTANCE (FEET)	SPACE-SUIT 1-LAYER (IN.)	ELEMENT	ABSORBED HEAT FLUXES (BTU/HR-SF) DIRECT SOLAR	CRATER BOTTOM	CRATER CLIFF	TOTAL	TS (R)	T(OUT) (R)	CRATE B/H-SF	AVERAGE VALUES TS (R)	T(OUT) (R)	T(INS) (R)	Q(S) BTU/HR
200.00	0.100												
		1	90.34	137.48	0.08	227.90	698.15	692.41	7.40				
		2	84.19	137.46	1.87	223.52	694.77	689.08	7.23				
		3	72.29	137.42	7.04	216.75	689.45	683.85	6.96				
		4	55.47	137.33	15.74	208.54	682.83	677.34	6.62				
		5	34.87	137.19	27.49	199.55	675.35	670.01	6.24				
		6	11.89	136.98	41.55	190.42	667.49	662.31	5.84				
		7	0.00	136.72	56.95	193.68	670.32	665.08	5.98				
		8	0.00	136.43	72.66	209.09	683.28	677.79	6.64				
		9	0.00	136.13	87.59	223.72	694.93	689.24	7.24				
		10	0.00	135.85	100.68	236.53	704.67	698.33	7.74				
		11	0.00	135.63	110.91	246.55	712.01	706.03	8.11				
		12	0.00	135.51	117.10	252.61	716.35	710.37	8.34				
		TOP	108.59	0.00	83.62	192.21	669.05	663.77	5.99	690.32	684.72	556.02	143.7
200.00	0.200												
		1	90.34	137.48	0.08	227.90	698.15	695.07	3.99				
		2	84.19	137.46	1.87	223.52	694.77	691.72	3.90				
		3	72.29	137.42	7.04	216.75	689.45	686.45	3.76				
		4	55.47	137.33	15.74	208.54	682.83	679.88	3.58				
		5	34.87	137.19	27.49	199.55	675.35	672.48	3.37				
		6	11.89	136.98	41.55	190.42	667.49	664.70	3.16				
		7	0.00	136.72	56.96	193.68	670.32	667.50	3.23				
		8	0.00	136.43	72.66	209.09	683.29	680.33	3.59				
		9	0.00	136.12	87.59	223.72	694.92	691.87	3.91				
		10	0.00	135.85	100.68	236.53	704.67	701.54	4.17				
		11	0.00	135.63	110.92	246.55	712.01	708.83	4.37				
		12	0.00	135.50	117.11	252.61	716.35	713.14	4.49				
		TOP	108.59	0.00	83.62	192.21	669.05	666.70	3.26	690.31	687.30	553.29	42.5
200.00	0.500												
		1	90.34	137.47	0.08	227.90	698.15	696.38	1.65				
		2	84.19	137.46	1.87	223.52	694.77	693.01	1.61				
		3	72.29	137.42	7.04	216.75	689.45	688.21	1.55				
		4	55.47	137.33	15.74	208.54	682.83	681.61	1.48				
		5	34.87	137.18	27.50	199.55	675.35	674.16	1.39				
		6	11.89	136.97	41.55	190.42	667.49	666.34	1.31				
		7	0.00	136.71	56.96	193.67	670.32	669.16	1.34				
		8	0.00	136.42	72.67	209.09	683.28	682.06	1.48				
		9	0.00	136.11	87.60	223.71	694.92	693.67	1.61				
		10	0.00	135.83	100.69	236.53	704.67	703.38	1.72				
		11	0.00	135.61	110.93	246.54	712.01	710.70	1.81				
		12	0.00	135.49	117.12	252.61	716.35	715.03	1.85				
		TOP	108.59	0.00	83.62	192.21	669.05	667.85	1.38	690.27	688.04	551.35	36.7

HEAT TRANSFER STUDY FOR MAN IN LUNAR CRATER (20/40) (K1=0.0005) 10-21-64 PAGE 5

DISTANCE (FEET)	SPACE-SUIT I-LAYER (IN.)	ELE-MENT	ABSORBED HEAT FLUXES (BTU/HR-SF) DIRECT SOLAR	CRATER BOTTOM	CRATER CLIFF	TOTAL	TS (R)	T(OUT) (R)	CRATE B/H-SF	AVERAGE VALUES TS (R)	T(OUT) (R)	T(INS) (R)	Q(IN) BTU/HR
1000.00	0.000												
		1	90.34	137.46	0.07	227.88	698.13	659.14	46.80				
		2	84.19	137.46	1.76	223.41	694.68	656.23	45.51				
		3	72.29	137.46	6.83	216.58	689.31	651.72	43.52				
		4	55.47	137.44	15.57	208.49	682.78	646.30	41.12				
		5	34.87	137.42	27.57	199.86	675.61	640.40	38.53				
		6	11.89	137.39	42.06	191.34	668.29	634.44	35.92				
		7	0.00	137.34	58.05	195.39	671.80	637.29	37.16				
		8	0.00	137.28	74.46	211.75	685.44	648.49	42.09				
		9	0.00	137.23	90.16	227.39	697.76	658.42	46.66				
		10	0.00	137.17	104.03	241.21	708.13	667.66	50.59				
		11	0.00	137.13	114.96	252.09	715.98	674.43	53.62				
		12	0.00	137.11	121.55	258.66	720.60	678.45	55.42				
		TOP	108.59	0.00	83.72	192.32	669.14	634.19	37.14	691.92	653.98	585.38	934.7
1000.00	0.020												
		1	90.34	137.46	0.07	227.88	698.13	680.03	22.73				
		2	84.19	137.46	1.76	223.41	694.68	676.79	22.15				
		3	72.29	137.46	6.83	216.58	689.31	671.73	21.27				
		4	55.47	137.44	15.57	208.49	682.78	665.62	20.19				
		5	34.87	137.42	27.57	199.86	675.61	658.94	19.01				
		6	11.89	137.39	42.06	191.34	668.29	652.15	17.82				
		7	0.00	137.34	58.05	195.39	671.80	655.40	18.39				
		8	0.00	137.28	74.46	211.75	685.44	668.10	20.63				
		9	0.00	137.23	90.16	227.39	697.76	679.33	22.67				
		10	0.00	137.17	104.03	241.21	708.13	689.50	24.40				
		11	0.00	137.13	114.96	252.09	715.98	696.98	25.72				
		12	0.00	137.11	121.55	258.66	720.60	701.39	26.49				
		TOP	108.59	0.00	83.72	192.32	669.14	652.69	18.23	691.91	674.23	568.06	457.3
1000.00	0.050												
		1	90.34	137.46	0.07	227.88	698.13	688.11	12.91				
		2	84.19	137.46	1.76	223.41	694.68	684.76	12.50				
		3	72.29	137.46	6.83	216.58	689.31	679.54	12.02				
		4	55.47	137.44	15.57	208.49	682.78	673.23	11.43				
		5	34.87	137.42	27.57	199.86	675.61	666.31	10.79				
		6	11.89	137.39	42.06	191.34	668.29	659.26	10.13				
		7	0.00	137.34	58.05	195.39	671.80	662.63	10.44				
		8	0.00	137.28	74.46	211.75	685.44	675.79	11.67				
		9	0.00	137.23	90.16	227.39	697.76	687.74	12.78				
		10	0.00	137.17	104.03	241.21	708.13	697.84	13.72				
		11	0.00	137.13	114.96	252.09	715.98	705.51	14.43				
		12	0.00	137.11	121.55	258.66	720.60	710.03	14.85				
		TOP	108.59	0.00	83.72	192.32	669.14	659.97	10.33	691.91	682.10	560.41	253.4

SPACE-SUIT DISTANCE (FEET)	1-LAYER (IN.)	ELE-MENT	ABSORBED HEAT FLUXES (BTU/HR-SF) DIRECT SOLAR	CRATER BOTTOM	CRATER CLIFF	TOTAL	TS (R)	T(OUT) (R)	QRATE B/H-SF	AVERAGE VALUES TS (R)	T(OUT) (R)	T(INS) (R)	Q(IN) BTU/HR
1000.00	0.100												
		1	90.34	137.46	0.07	227.88	698.13	692.39	7.40				
		2	84.19	137.46	1.76	223.41	694.68	689.00	7.23				
		3	72.29	137.46	6.83	216.58	689.31	683.71	6.95				
		4	55.47	137.44	15.57	208.49	682.78	677.30	6.62				
		5	34.87	137.42	27.57	199.86	675.61	670.27	6.25				
		6	11.89	137.38	42.06	191.34	668.29	663.09	5.88				
		7	0.00	137.34	58.05	195.39	671.80	666.53	6.06				
		8	0.00	137.28	74.46	211.75	685.44	679.91	6.75				
		9	0.00	137.23	90.16	227.39	697.76	692.03	7.38				
		10	0.00	137.17	104.03	241.21	708.13	702.24	7.91				
		11	0.00	137.13	114.96	252.09	715.98	710.00	8.32				
		12	0.00	137.11	121.55	258.66	720.60	714.57	8.56				
		TCP	108.59	0.00	83.72	192.32	669.14	663.86	6.00	691.90	686.28	556.09	151.3
1000.00	0.200												
		1	90.34	137.46	0.07	227.38	698.13	695.05	3.99				
		2	84.13	137.46	1.76	223.41	694.68	691.63	3.90				
		3	72.29	137.46	6.83	216.58	689.31	686.31	3.75				
		4	55.47	137.44	15.57	208.49	682.78	679.84	3.57				
		5	34.87	137.42	27.57	199.86	675.61	672.74	3.38				
		6	11.89	137.38	42.06	191.34	668.29	665.49	3.18				
		7	0.00	137.34	58.05	195.39	671.80	668.96	3.24				
		8	0.00	137.28	74.46	211.75	685.44	682.47	3.65				
		9	0.00	137.23	90.16	227.39	697.76	694.68	3.98				
		10	0.00	137.17	104.03	241.21	708.13	704.97	4.27				
		11	0.00	137.13	114.96	252.09	715.98	712.78	4.48				
		12	0.00	137.11	121.55	258.66	720.60	717.37	4.61				
		TCP	108.59	0.00	83.72	192.32	669.14	666.24	3.26	691.33	686.97	553.31	83.2
1000.00	0.500												
		1	90.34	137.46	0.07	227.88	698.13	696.87	1.65				
		2	84.19	137.46	1.76	223.41	694.68	693.43	1.61				
		3	72.29	137.46	6.83	216.57	689.31	688.07	1.55				
		4	55.47	137.44	15.57	208.49	682.78	681.57	1.48				
		5	34.87	137.42	27.57	199.86	675.61	674.42	1.40				
		6	11.89	137.38	42.06	191.34	668.29	667.13	1.32				
		7	0.00	137.34	58.05	195.39	671.80	670.63	1.36				
		8	0.00	137.28	74.46	211.75	685.44	684.21	1.51				
		9	0.00	137.22	90.16	227.39	697.76	696.47	1.65				
		10	0.00	137.17	104.04	241.21	708.13	706.83	1.76				
		11	0.00	137.13	114.96	252.09	715.98	714.66	1.85				
		12	0.00	137.10	121.56	258.66	720.60	719.27	1.90				
		TCP	108.59	0.00	83.72	192.31	669.14	667.94	1.33	691.86	690.61	551.48	36.3

HEAT TRANSFER STUDY FOR MAN IN LUNAR CRATER (20/40) (K1=0.0005) 10-21-64 PAGE 7

SPACE-SUIT DISTANCE (FEET)	1-LAYER (IN.)	ELE-MENT	ABSORBED HEAT FLUXES (BTU/HR-SF) DIRECT SOLAR	CRATER BOTTOM	CRATER CLIFF	TOTAL	TS (R)	T(OUT) (R)	QRATE B/H-SF	AVERAGE VALUES TS (R)	T(OUT) (R)	T(INS) (R)	Q(IN) BTU/HR
5000.00	0.000												
		1	90.34	125.97	0.05	216.36	689.14	651.58	43.45				
		2	84.19	125.98	1.16	211.32	685.09	648.21	41.96				
		3	72.29	125.98	4.85	203.13	678.35	642.54	39.51				
		4	55.47	125.99	11.79	193.25	669.96	635.79	36.51				
		5	34.87	126.00	21.93	182.80	660.71	628.35	33.26				
		6	11.89	126.00	34.79	172.68	651.37	620.97	30.05				
		7	0.00	126.00	49.55	175.55	654.06	623.08	30.96				
		8	0.00	126.00	65.21	191.21	668.18	634.36	35.88				
		9	0.00	126.00	80.64	206.64	681.26	645.04	40.57				
		10	0.00	125.99	94.58	220.57	692.47	654.37	44.68				
		11	0.00	125.99	105.65	231.63	700.99	661.57	47.88				
		12	0.00	125.98	112.17	238.16	705.88	665.73	49.73				
		TCP	108.59	0.00	58.26	166.86	645.80	615.85	28.87	677.37	641.93	581.46	822.2
5000.00	0.020												
		1	90.34	125.97	0.05	216.36	689.14	671.57	21.24				
		2	84.19	125.98	1.16	211.32	685.09	667.78	20.57				
		3	72.29	125.98	4.85	203.13	678.35	661.49	19.46				
		4	55.47	125.99	11.79	193.25	669.96	653.69	18.09				
		5	34.87	126.00	21.93	182.80	660.71	645.17	16.60				
		6	11.89	126.00	34.79	172.68	651.37	636.63	15.10				
		7	0.00	126.00	49.55	175.55	654.06	639.08	15.53				
		8	0.00	126.00	65.21	191.21	668.18	652.05	17.81				
		9	0.00	126.00	80.64	206.64	681.26	664.20	19.94				
		10	0.00	125.99	94.58	220.57	692.47	674.70	21.79				
		11	0.00	125.99	105.65	231.63	700.99	682.74	23.20				
		12	0.00	125.98	112.17	238.16	705.88	687.36	24.02				
		TCP	108.59	0.00	58.26	166.86	645.80	631.37	14.43	677.36	660.54	566.13	405.1
5000.00	0.050												
		1	90.34	125.97	0.05	216.36	689.14	679.33	12.00				
		2	84.19	125.98	1.16	211.32	685.09	675.46	11.64				
		3	72.29	125.98	4.85	203.13	678.35	668.95	11.03				
		4	55.47	125.99	11.79	193.25	669.95	660.86	10.28				
		5	34.87	126.00	21.93	182.80	660.71	651.99	9.46				
		6	11.89	126.00	34.79	172.68	651.37	643.07	8.63				
		7	0.00	126.00	49.55	175.55	654.06	645.64	8.87				
		8	0.00	126.00	65.21	191.21	668.18	659.16	10.12				
		9	0.00	126.00	80.64	206.64	681.26	671.76	11.29				
		10	0.00	125.99	94.58	220.57	692.47	682.60	12.30				
		11	0.00	125.99	105.65	231.63	700.99	690.39	13.07				
		12	0.00	125.98	112.17	238.16	705.88	695.64	13.51				
		TCP	108.59	0.00	58.26	166.86	645.80	637.68	8.23	677.36	662.04	559.31	231.4

HEAT TRANSFER STUDY FOR MAN IN LUNAR CRATER (20/40) (K1=0.0005) 10-21-64 PAGE 3

DISTANCE (FEET)	SPACE-SUIT 1-LAYER (IN.)	ELEMENT	ABSORBED HEAT FLUXES (BTU/HR-SF) DIRECT SOLAR	CRATER BOTTOM	CRATER CLIFF	TOTAL	TS (R)	T(OUT) (R)	CRATE B/H-SF	AVERAGE VALUES TS (R)	T(OUT) (R)	T(INS) (R)	Q(I) BTU/HR
5000.00	0.100												
		1	90.34	125.97	0.05	216.36	689.14	683.55	6.94				
		2	84.19	125.98	1.16	211.32	685.09	679.57	6.74				
		3	72.29	125.98	4.85	203.13	678.35	672.95	6.39				
		4	55.47	125.99	11.79	193.25	669.95	664.73	5.96				
		5	34.87	126.00	21.93	182.80	660.71	655.63	5.49				
		6	11.89	126.00	34.79	172.68	651.37	646.58	5.02				
		7	0.00	126.00	49.55	175.55	654.06	649.20	5.16				
		8	0.00	126.00	65.21	191.21	668.18	662.99	5.87				
		9	0.00	126.00	80.64	206.64	681.26	675.81	6.54				
		10	0.00	125.99	94.58	220.57	692.47	686.92	7.11				
		11	0.00	125.99	105.65	231.63	700.99	695.21	7.55				
		12	0.00	125.98	112.17	238.16	705.88	700.03	7.80				
		TOP	108.59	0.00	58.26	166.86	645.80	641.11	4.80	677.35	672.00	555.45	135.3
5000.00	0.200												
		1	90.34	125.97	0.05	216.36	689.14	686.14	3.75				
		2	84.19	125.98	1.16	211.32	685.09	682.13	3.64				
		3	72.29	125.98	4.85	203.13	678.35	675.45	3.45				
		4	55.47	125.99	11.79	193.25	669.95	667.14	3.22				
		5	34.87	126.00	21.93	182.80	660.71	658.00	2.97				
		6	11.89	126.00	34.79	172.68	651.37	648.79	2.72				
		7	0.00	126.00	49.55	175.55	654.06	651.44	2.79				
		8	0.00	126.00	65.21	191.21	668.18	665.39	3.18				
		9	0.00	126.00	80.64	206.64	681.26	678.33	3.53				
		10	0.00	125.99	94.58	220.57	692.47	689.43	3.84				
		11	0.00	125.98	105.65	231.63	700.99	697.89	4.07				
		12	0.00	125.98	112.17	238.16	705.88	702.74	4.21				
		TOP	108.59	0.00	58.26	166.86	645.80	643.26	2.61	677.33	674.46	552.37	74.5
5000.00	0.500												
		1	90.34	125.97	0.05	216.36	689.14	687.90	1.55				
		2	84.19	125.98	1.16	211.32	685.09	683.87	1.50				
		3	72.29	125.98	4.85	203.13	678.35	677.16	1.43				
		4	55.47	125.99	11.79	193.25	669.95	668.79	1.33				
		5	34.87	126.00	21.93	182.80	660.71	659.59	1.23				
		6	11.89	126.00	34.79	172.68	651.37	650.30	1.13				
		7	0.00	126.00	49.55	175.55	654.05	652.97	1.16				
		8	0.00	126.00	65.21	191.21	668.18	667.03	1.31				
		9	0.00	126.00	80.64	206.64	681.26	680.05	1.46				
		10	0.00	125.99	94.58	220.57	692.47	691.22	1.59				
		11	0.00	125.98	105.65	231.63	700.99	699.71	1.68				
		12	0.00	125.98	112.17	238.16	705.88	704.59	1.74				
		TOP	108.59	0.00	58.26	166.96	645.80	644.72	1.11	677.29	676.10	551.23	32.5

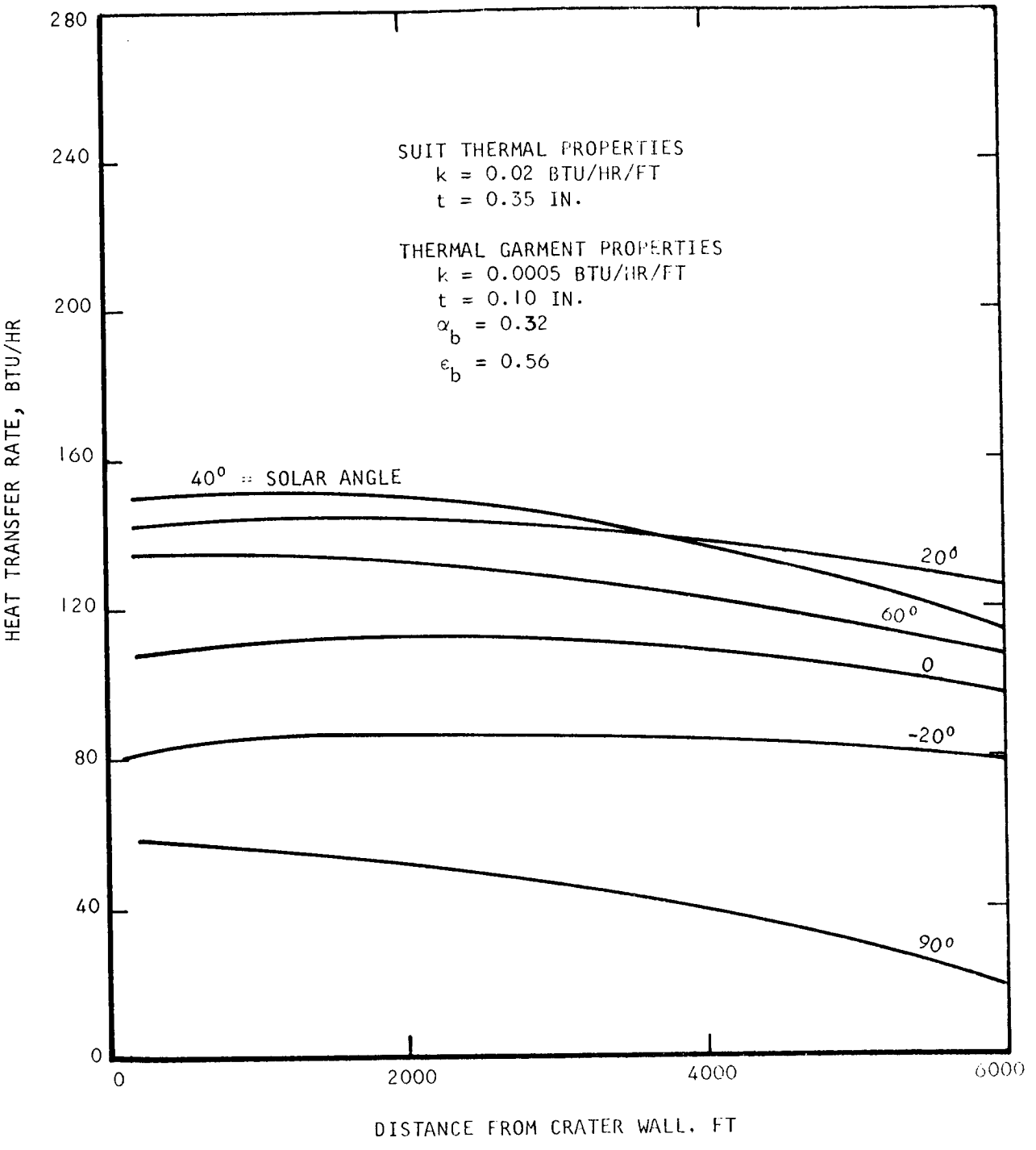

Figure 5-13. Extravehicular Suit Heat Leak Variation with Distance from Crater Wall

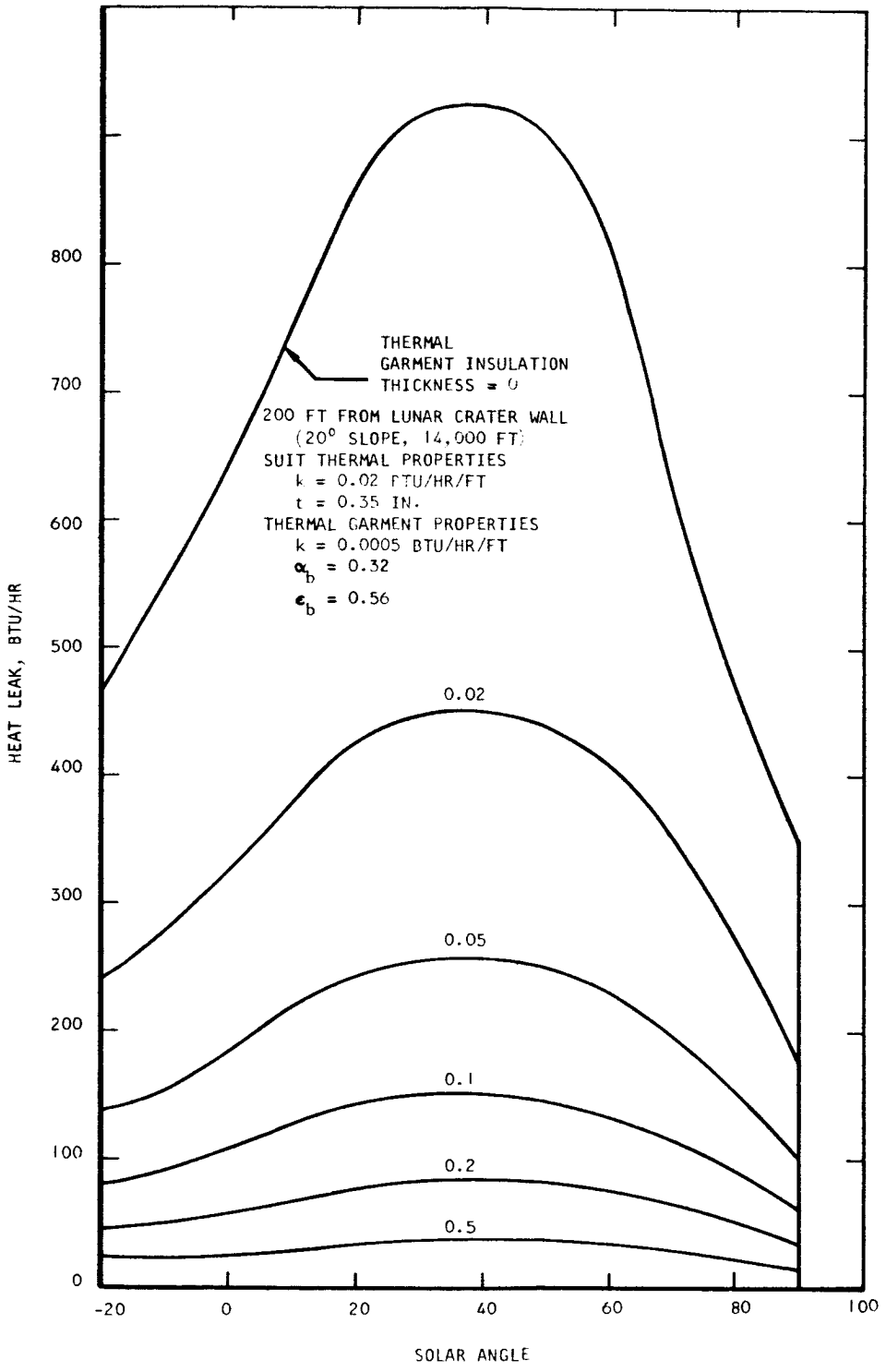

Figure 5-14. Extravehicular Suit Heat Leak Variation with Thermal Insulation for Lunar Crater Environment

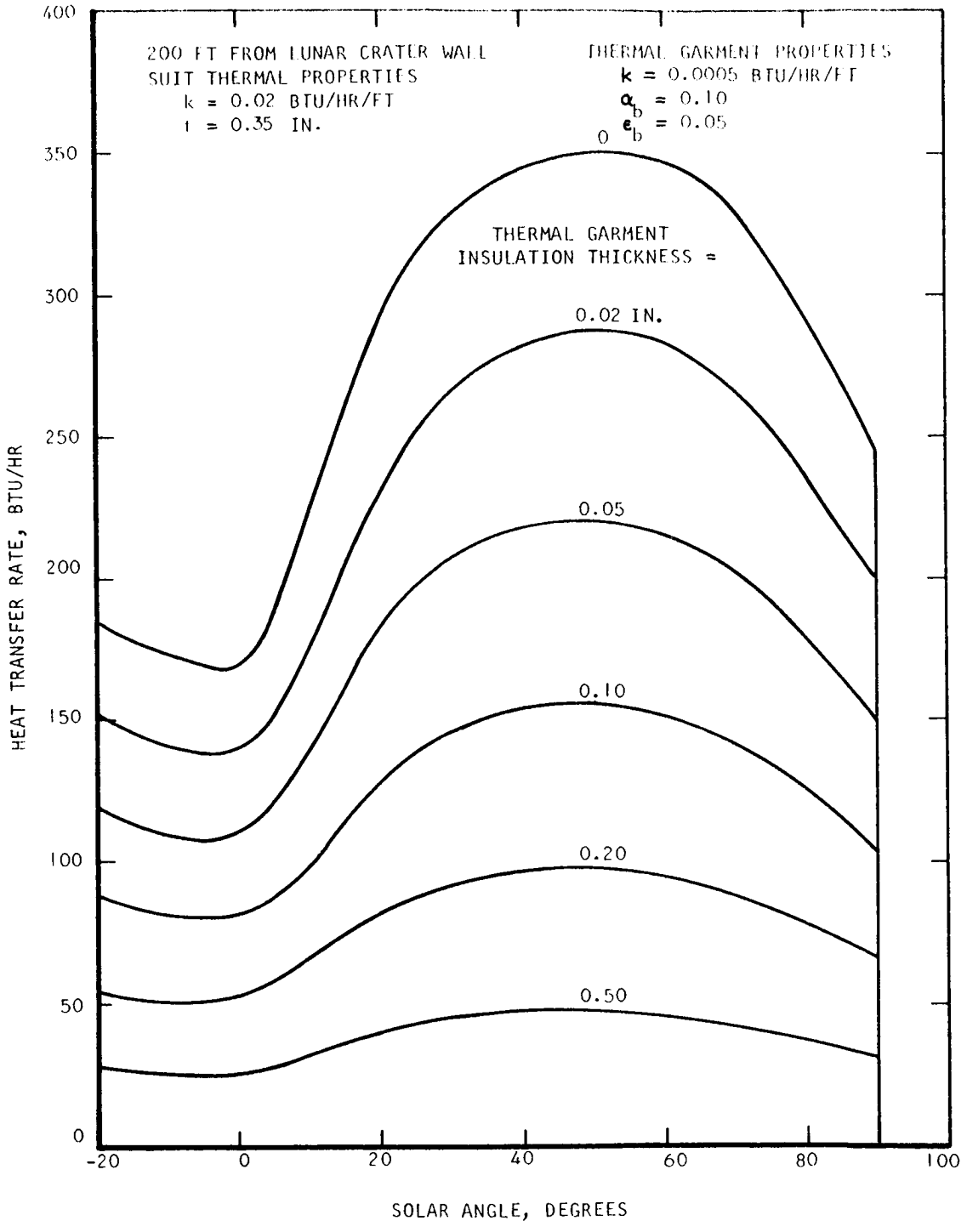

Figure 5-15. Heat Leak from an Extravehicular Suit with a Reflective Surface in a Lunar Crater

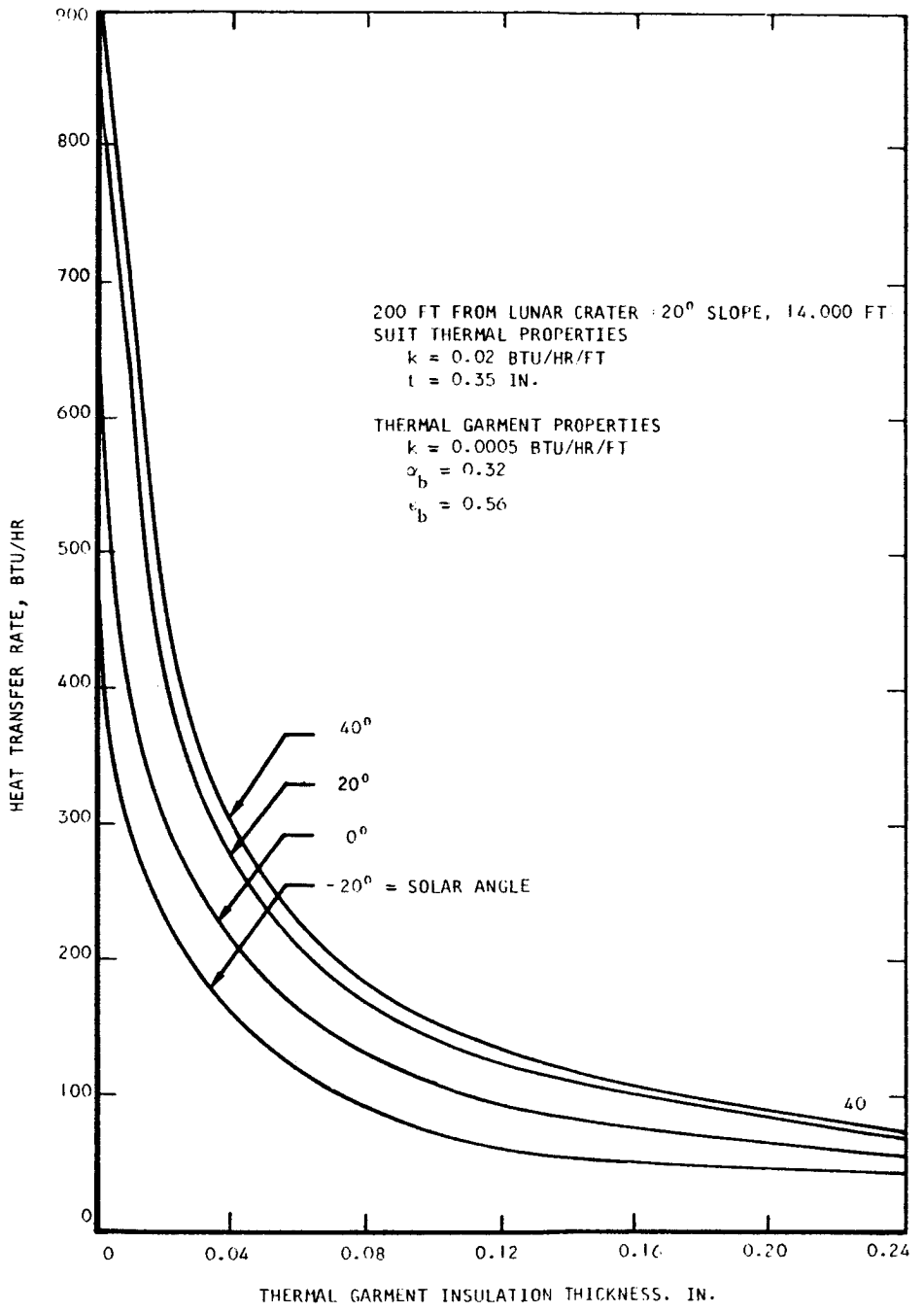

Figure 5-16. Heat Leak vs Insulation Thickness

LUNAR PLANES

Most of the lunar surface in the initial exploration areas will be represented by relatively flat planes. The computer program developed for the lunar plane surface environment is given in Appendix B. As indicated previously, these areas will be significantly less severe from the standpoint of the thermal environment. Figure 5-17 gives the lunar surface temperature for these areas as a function of solar angle. The surface temperature is shown as dropping to zero with sunset. Actually, the surface temperature starts at exponential decay from about 250°R at sunset to about 190°R at sunrise. The lunar surface temperature shown here is based upon heat balances for the lunar surface. Also shown in Figure 5-17 are the average effective sink temperatures for vertical cylindrical surfaces for the two surface characteristics.

Figure 5-18 shows the suit heat leak as a function of solar angle and insulation thickness. A maximum heat leak into the suit is obtained at a solar angle of approximately 20 degrees. At sunset, there will be a significant heat loss from the suit. Approximately 0.1-in. thickness for the insulating garment will keep the heat leak from the suit at or below 130 Btu/hr. In the previous analysis of the lunar crater thermal environment, it was determined that approximately the same amount of insulation would keep the heat leak into the suit from exceeding approximately 150 Btu/hr.

As shown in Figure 5-19, if the surface characteristics of the suit are changed to those obtained for reflective materials, a net heat leak into the suit is obtained for all solar angles during the lunar day. It will also be noted that for insulation thicknesses of more than about 0.02 in., a somewhat higher heat leak will be obtained with the reflective suit surface, although the difference will not be large.

MARS SURFACE

The Mars surface environment will be cold in comparison with that of the lunar surface. Figure 5-20 shows the extravehicular suit heat leak on the Mars surface. Under all conditions, a net heat loss from the suit is indicated. Other computations show that if the suit surface is changed to a reflective material ($\alpha_b = 0.10$ and $\epsilon_b = 0.05$), a negligible net thermal interchange is obtained during the Mars day. The analysis performed here used the lunar plane computer program (Appendix B) and neglects the effects due to forced or natural convection in the Mars atmosphere. There is reason for belief that high wind velocities are characteristic of the Mars surface (Ref. 38). Figure 5-21 gives the extravehicular suit heat loss rates for the Mars surface environments computed by Fejer and Seale (Ref. 38).

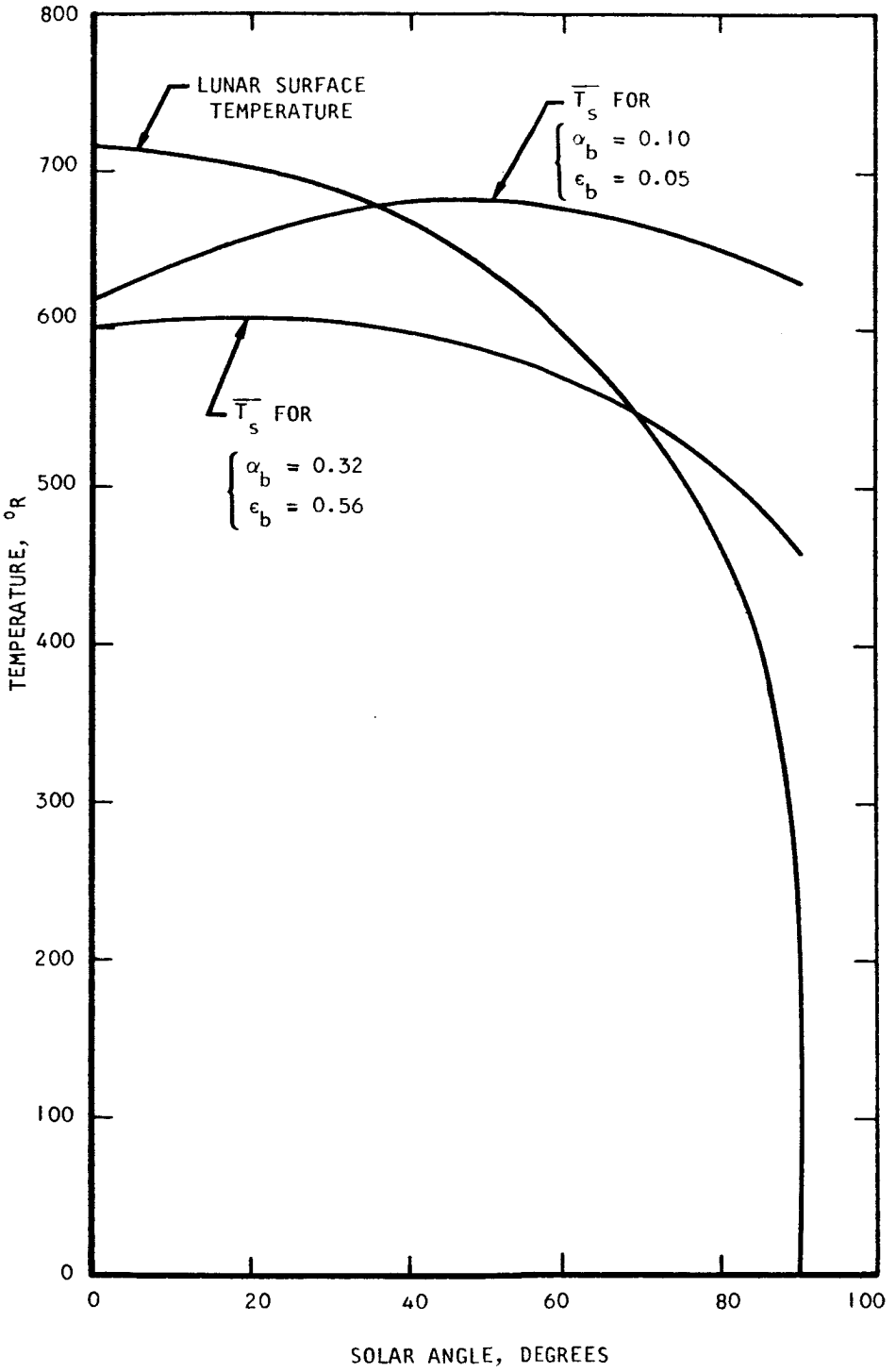

Figure 5-17. Lunar Planes Thermal Environment

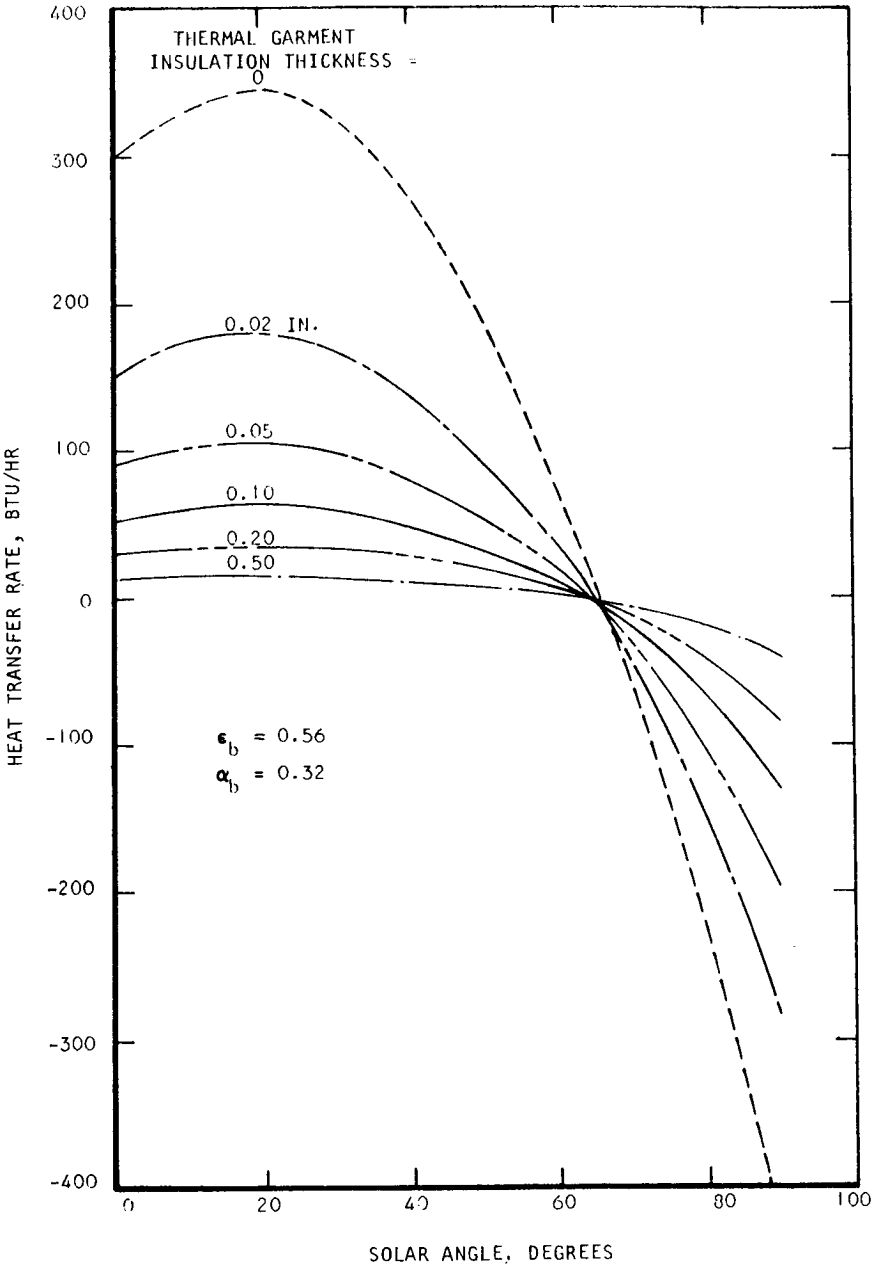

Figure 5-18. Heat Balance for an Extravehicular Suit on Lunar Planes

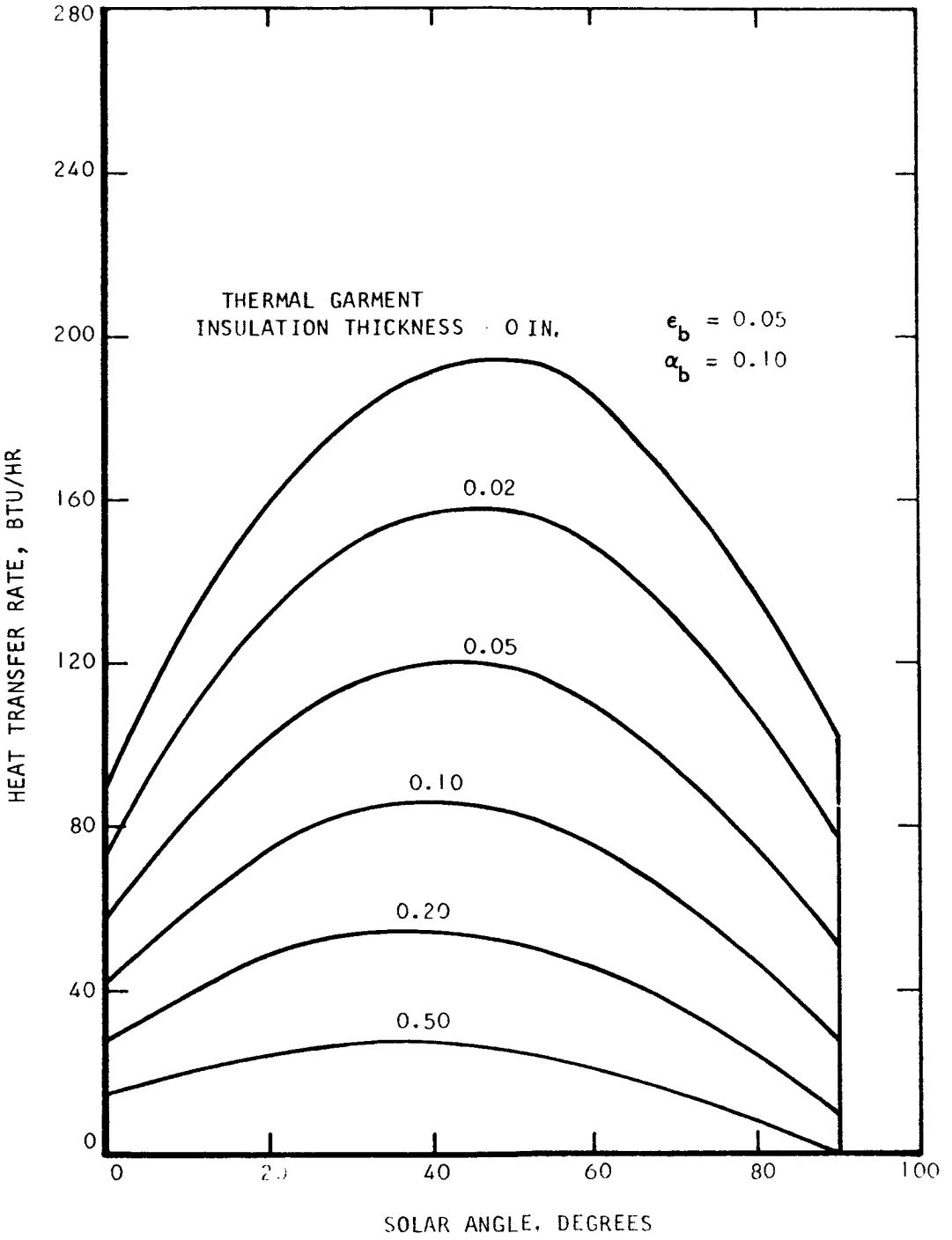

Figure 5-19 Heat Balance for an Extravehicular Suit with Reflective Surface on Lunar Planes

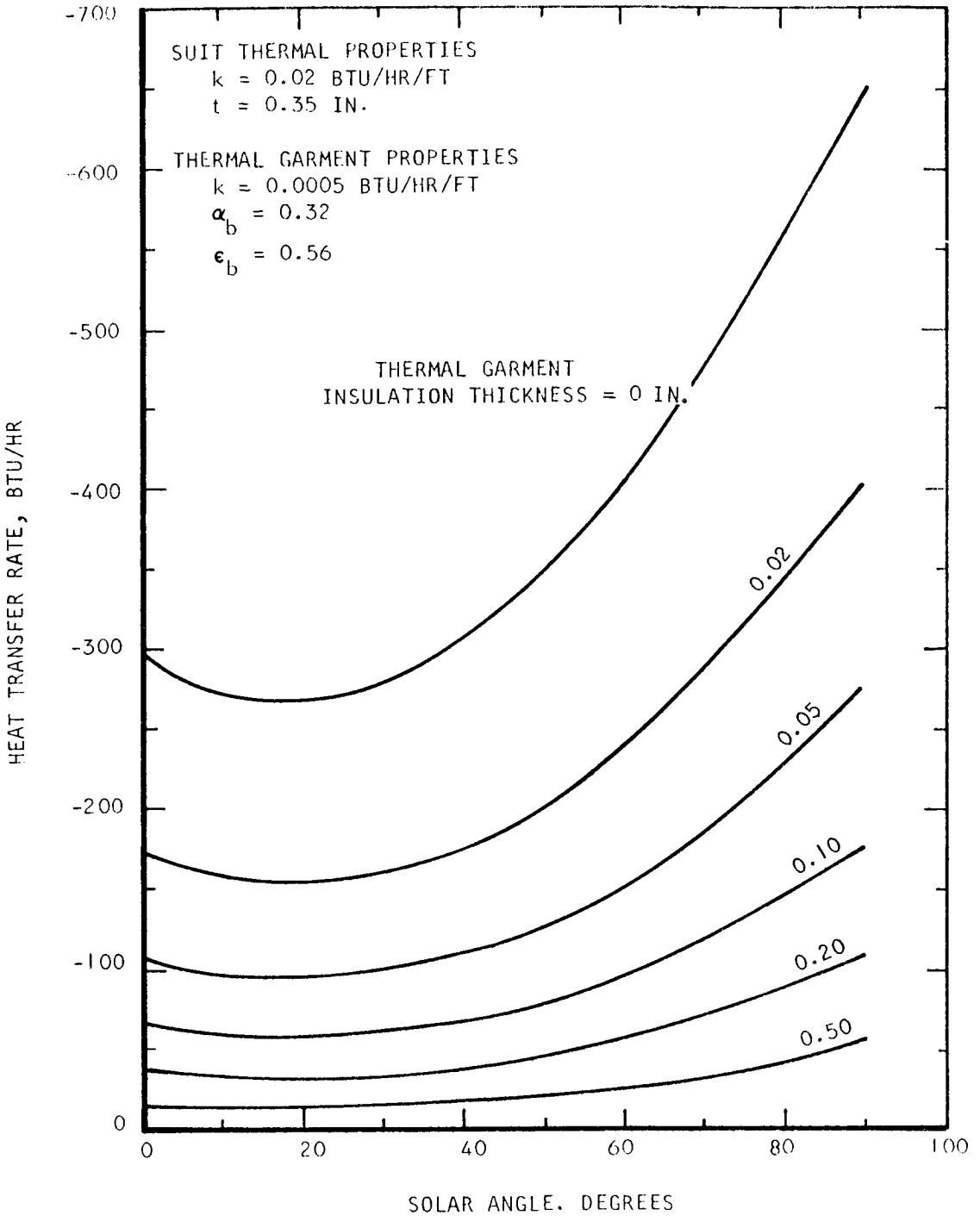

Figure 5-20. Heat Leak from Extravehicular Suit on Mars Surface

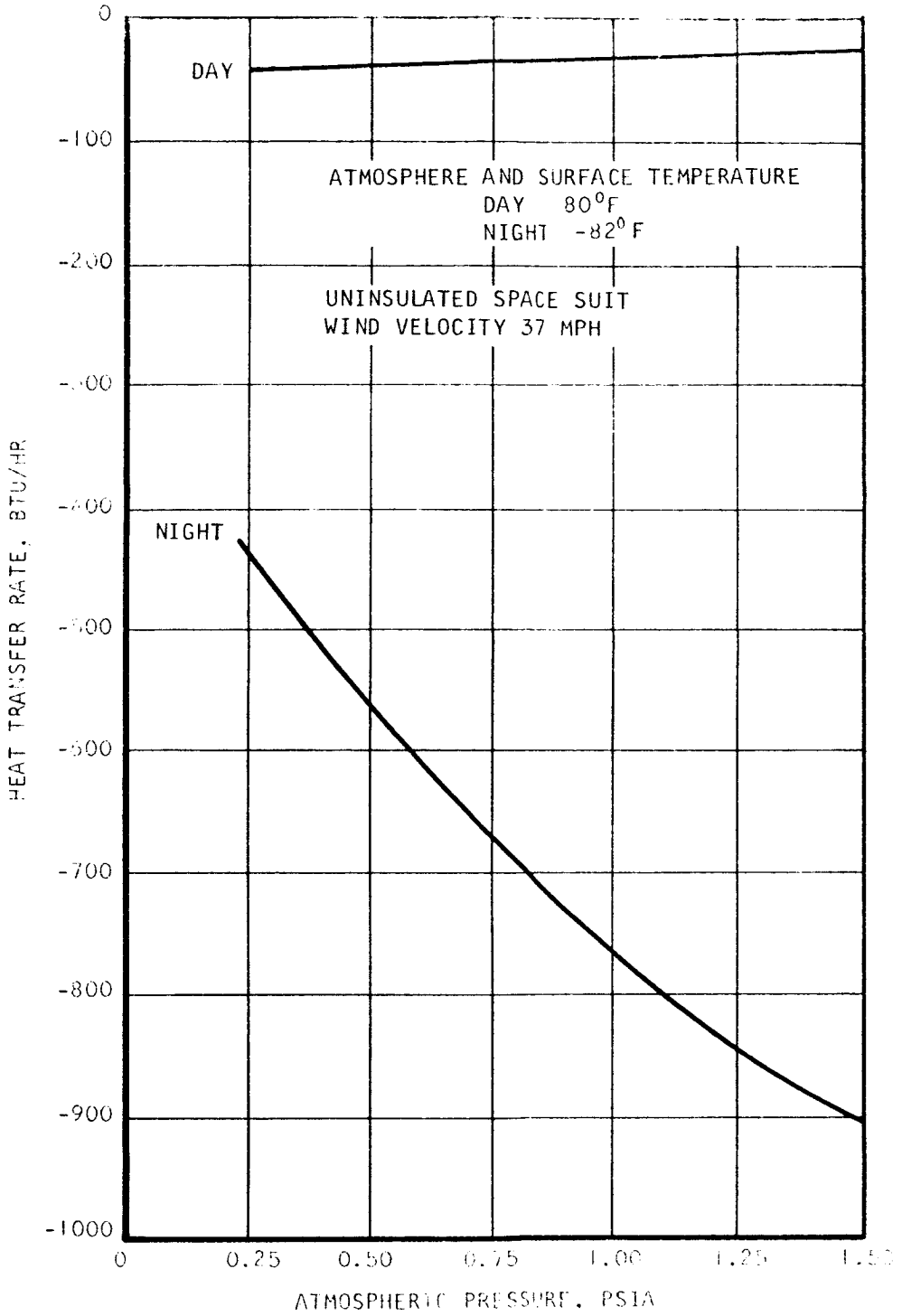

Figure 5-21 Extravehicular Suit Heat Balance for Mars Surface Considering Atmospheric Effects (Ref 38)

DISCUSSION AND CONCLUSIONS

In planetary orbital environments there is a tendency toward heat loss from extravehicular suits. It has been found that the situations in which there will be a net heat input into the suit from the external environment will be relatively few, although there may be a significant heat flux gradient between the hot and cold parts of the suit. This conclusion has been verified by the experimental work cited by Freedman (Ref. 40) for the Gemini suit in a space simulator. The magnitude of the heat loss from extravehicular suits in planetary orbits can be controlled by thermal insulation or by selection of materials with suitable surface spectral properties. It can be concluded that the radiative suit cooling schemes considered in Section 3 could be applied to orbital environments about earth, the moon, and Mars.

The thermal environments obtained on the lunar surface will tend to provide a net heat input into an extravehicular suit during the day. Use of a 0.1-in. layer of superinsulation should maintain the heat leak into the suit below 150 Btu/hr (in a lunar crater) or below 100 Btu/hr (on the lunar planes). It appears that the extravehicular suit spectral characteristics will be less important for the lunar environment than for the planetary orbital environments because of the insulation requirement resulting from the high thermal radiation flux (from the hot lunar surface), which reaches a peak intensity on the order of 435 Btu/hr-ft^2. Under the most severe thermal conditions, the view factor of the extravehicular suit to solar radiation will be relatively low. Therefore, the solar absorptivity will have relatively little effect upon the heat balance. For the case of thermal emissivity, there will be two counterbalancing effects, one associated with surface temperature (and the consequent heat conduction through the suit), and a second involving heat flux. For example, although high equilibrium surface temperatures are obtained with low-emissivity surfaces, because of the reduced heat flux, there will tend to be less heat conduction into the suit. Therefore, low-emissivity materials will tend to be favored for lunar extravehicular suits, although the overall differences will not be great.

The analysis of the Mars surface environment uses a computer program developed for lunar extravehicular heat balances and neglects atmospheric effects. Since the Martian atmosphere will undoubtedly affect the surface temperature and atmospheric convection will probably be an important factor in the extravehicular suit heat balance, the results given by these computations for the Mars surface environment are at best approximate.

SECTION 6

CONCLUSIONS

SHIRTSLEEVE ENVIRONMENT

Comfort Criteria

Design criteria applicable to the problem of providing comfort conditions in spacecraft cabins have been developed and correlated with established comfort criteria for normal terrestial environments. This comfort correlation is based upon maintenance of skin temperatures and latent cooling rates within specified limits, and considers the effects due to atmospheric pressure, gravity, ventilating gas flow, atmospheric temperature, water vapor partial pressure, atmospheric composition, and mean radiant (wall) temperature.

Reduced Gravity

In a zero-gravity space cabin, it will be necessary to provide a minimum ventilating gas velocity of approximately 20 ft/min to replace natural convection. In the lunar shelter environment, natural convection will provide adequate cooling of the body without ventilating other than that required for thermal and atmospheric control. The comfort zone for a sedentary subject in light clothing (1/2 CLO) in a normal terrestial environment is between environmental temperatures of 72 and 82°F, with the optimum near 77°F. The comparable comfort zone for a 6.0 psia lunar cabin will fall between 69 and 84°F, with the optimum near 74°F.

Atmospheric Pressure

The effect of decreasing the design atmospheric pressure is to reduce the sensible heat transfer and increase the latent cooling capacity (because of the increase in mass transfer coefficient resulting from the increased diffusivity of water vapor in air with decrease in pressure). Where minimum sweat rates are required, the effect of reduced pressure is to reduce the design environmental temperature by approximately 3°F. If increased sweat rates (well within the comfort and physiological limits) can be permitted, the effect is to allow an increase of approximately 2°F in comfort zone.

Humidity

The heat transfer studies conducted under this program have shown, in agreement with the latest ASHRAE findings, that the comfort zone is relatively independent of humidity over a relatively wide range of conditions.

EXTRAVEHICULAR SUITS

Metabolic Rates

It will be necessary to design for metabolic rates on the order of 2000 Btu/hr for walking on the lunar surface in a pressurized suit at relatively

low speeds (under 1.2 mph). For free-space extravehicular excursions, the design average level for metabolic output may be substantially lower because of the less sustained and less strenuous nature of the tasks to be performed, although it will probably be essential to have a high peak capability comparable to the lunar surface systems. The effect of reduced gravity on metabolic rate for performance of various tasks (including walking on the lunar surface) is somewhat speculative at the present time, since contradictory data have been obtained by different investigators. There is perhaps slightly more evidence to indicate a moderate increase (up to 30 percent) in metabolic rate in reduced gravity environments.

A portion of the high metabolic rates obtained in pressurized suit tests is a result of the q_{10} effect (the spontaneous increase in metabolism due to increased internal temperature) produced by inadequate cooling. Therefore, it appears that with adequate cooling, provided by conduction cooling of the body, for example, the metabolic rates required for working in pressurized suits may be 20 to 30 percent lower than those obtained in ventilated suit tests.

Ventilation Cooling

Ventilation cooling will provide a maximum heat removal rate on the order of 1300 Btu/hr. Most of this cooling capacity will be obtained by evaporation of sweat. The resulting high sweat rates and body temperatures represent an undesirable physiological stress. However, ventilation cooling offers an advantage over other methods in utilizing the thermoregulatory mechanism of the body to provide thermal control.

Liquid-Loop Cooling

The superiority of liquid-loop cooling over ventilation cooling of extravehicular suits for high metabolic rates has been well established. Heat removal rates in excess of 2500 Btu/hr appear to be feasible and practical where the body is cooled by conduction to the coolant tubes. Cooling of the body by radiation from the skin to the coolant tubes does not appear to be competitive with conduction cooling of the body from the heat transfer efficiency standpoint. However, since conduction cooling essentially bypasses the body's thermoregulatory controls and tends to provide constant heat removal rates (with constant coolant flow and temperature), it will be necessary to provide thermal controls that match system cooling capacity with the metabolic output. Development of suitable control methods can be considered to be a key problem area.

Conduction Cooling Comfort Criteria

Design methods for human comfort have been established for conduction cooling of the body. This comfort zone is based upon maintaining skin temperature between an upper limit for active sweating and a lower limit for the onset of shivering. The dependence of this zone on metabolic rate has been determined.

Radiative Cooling

By proper selection of surface spectral characteristics and suit wall thermal conductivity, in free-space environments it is possible to dissipate much of the metabolic waste heat by radiation from the suit outer surface, without excessively wide excursions in heat rejection rate with different external environmental conditions. It appears possible to hold the difference between maximum and minimum heat rejection to within ±50 Btu/hr, or a total spread of 100 Btu/hr, for radiative heat rejection rates up to 750 Btu/hr.

It is concluded that, because of the complexity of man's environmental requirements and the anticipated range of variation in metabolic output and external thermal environment, use of passive radiative thermal control methods to extravehicular suits is unlikely. However, there are significant incentives for employing radiation cooling to provide part of the required heat rejection (in conjunction with a conventional ventilating gas or liquid cooling system), as a means of reducing the size and weight of portable environmental control systems.

Planetary Orbital Environments

In earth, lunar, and Mars orbits, the extravehicular suit heat balances tend to result in net heat losses. The spectral characteristics of the outer surface of the suit will be important in determining the magnitude and excursions of the extravehicular suit heat balance. Where it is desired to use radiation from the suit to aid thermal control, an outer surface coating that provides high thermal emissivity ($\cong 0.9$) and a low solar absorptivity (< 0.10) is desired. Where minimum heat leak by radiation from the suit is desired, both thermal emissivity and solar absorptivity should be low.

Lunar Surface Environments

The day-time lunar surface thermal environments tend to provide heat input into an extravehicular suit. By use of a thermal insulating coverall with 0.1-in. layer of multiple-layer insulation, the maximum heat leak into the suit can be reduced to under 100 Btu/hr for lunar planes and to under 150 Btu/hr for lunar craters. The spectral characteristics of the outer suit surface were found to be less important for the lunar surface environments than free-space environments because of the predominant effect of thermal radiation from the lunar surfaces during the day.

SECTION 7

RECOMMENDATIONS FOR FUTURE WORK

SHIRTSLEEVES ENVIRONMENT COMFORT CRITERIA

Inadequate attention has been given the problem of providing man with a thermally adequate and subjectively comfortable environment in space cabins. Because of the different relationships that will be obtained for the various heat transfer processes in space cabin environments, conventional comfort criteria used for the design of terrestial air conditioning systems may not be applicable. In the present study, comfort criteria were developed which were based upon maintenance of skin temperatures and latent cooling rates at levels compatible with human comfort for varying atmospheric pressure, gravity, ventilating gas flow, atmospheric gas temperature, mean radiant temperature, and atmospheric composition. A good correlation was obtained between the ASHRAE comfort zone for a normal terrestial environment and the general comfort criteria established by the study. However, this represents a single point and additional verification by comfort tests at varying pressure, composition, and ventilating rate are highly desirable. The test conditions should simulate those to be encountered in space cabins as closely as possible with respect to subject selection, clothing, ventilating flow arrangements, and crew duty stations. By firmly establishing the thermal design criteria for space cabins, it will be possible to provide an acceptable environment consistent with the objectives of minimum equipment weight and power consumption.

HUMAN THERMAL ANALOG

Development of a general human thermal analog would permit the designer of space environmental control systems to predict the response of the human body in alien environments. A number of specialized thermal analogs have been created for special cases, such as those obtained in exposure to cold environments (see, for example, Ref. 46, 47, 49). However, a more general treatment is required that permits consideration of high metabolic rates, both hot and cold environments, and varying pathways for heat dissipation. Development of this analog will involve consideration of both the physiological and the heat transfer processes associated with body thermal control.

CONDUCTION COOLING OF THE HUMAN BODY

The advantages of conduction cooling of the human body have been established by the study. Improvements in conduction cooling methods appear to be possible and should be studied. One possibility involves a partial coverage cooling garment design (shown schematically in Figure 7-1). A cooling garment of this type would appear to be suited for extravehicular missions characterized by moderate metabolic rates or with extravehicular thermal systems using a combination of liquid-loop and radiative cooling. Another possible improvement in thermal garment design, shown in Figure 7-2, involves tubing design for improved mobility and heat transfer contact area characteristics.

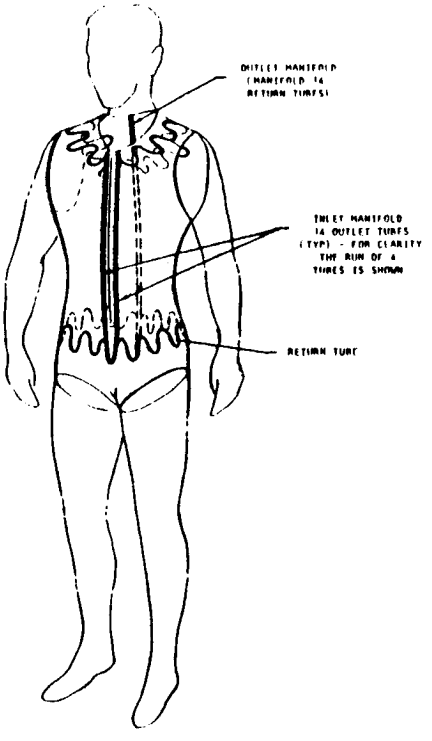

Figure 7-1. Partial Coverage Design

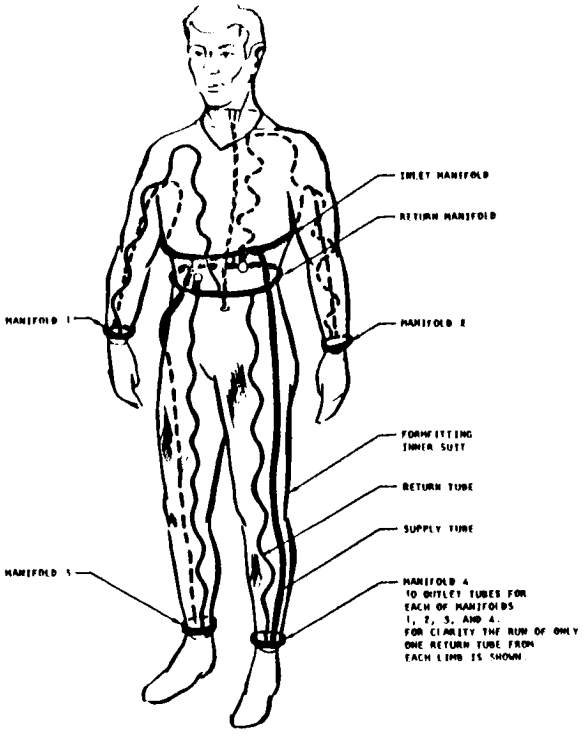

Figure 7-2. Improved Mobility Design

LOCAL BODY COOLING

Tests conducted by Wortz, et al. (Ref. 36, 37) indicate that subjective comfort may be obtained with limited area coverage of the body. The possibility of providing all of the required heat dissipation by cooling a limited area of the body should be investigated experimentally. From the conduction cooling data obtained and analyzed during the present study program, it appears that only a small skin area is actually in contact with the coolant tubes. The skin functioned to some extent as an extended surface or fin to the prime surface presented by the coolant tubes. The improvement in heat removal rate to be gained by increased prime surface area should be determined to provide data for optimizing the conduction cooling method.

SECTION 8

BIBLIOGRAPHIES

PHYSIOLOGICAL FACTORS

1. Benzinger, T. H., "The Diminution of Thermoregulatory Sweating During Cold-Reception at the Skin," Proc. Nat. Acad. Sci., 47, No. 10, pp. 1683-1688, October 1961.

2. Benzinger, T. H., A. W. Pratt, and C. Kitzinger, "The Thermostatic Control of Human Metabolic Heat Production," Proc. Nat. Acad. Sci., 47, No. 5, pp. 730-739, May 1961.

3. Benzinger, T. H., "Peripheral Cold- and Central Warm-Reception, Main Origins of Human Thermal Discomfort," Proc. Nat. Acad. Sci., 49, No. 6, pp. 832-839, June 1963.

4. Clifford, J., D. Kerslake, and J. L. Waddell, "The Effect of Wind Speed on Maximum Evaporative Capacity in Man," J. Physiol, 147, pp. 253-259, 1959.

5. Fahnestock, M. K., F. E. Boys, F. Sargent, W. E. Springer, and L. D. Siler, "Comfort and Physiological Responses to Work in an Environment of 75°F and 45 Percent Relative Humidity," American Society of Heating, Refrigerating, and Air-Conditioning Engineers, New York, January 1963.

6. Hazard, A., Personal Communication, Space-General Corporation, Monrovia, California, 1964.

7. Kerslake, D. McK., "Factors Concerned in the Regulation of Sweat Production in Man," J. Physiol., 127, pp. 280-296, 1955.

8. Kerslake, D., "The Physiological Requirements for Environment Comfort in Terms of the Microclimate," presented at the Full Pressure Suit Symposium, 1962, data given in Ref. 33.

9. Kuno, Y., Human Perspiration, C. C. Thomas, Springfield, Illinois, 1956.

10. Lomonaco, T., A. Scano, and G. Meineri., "Physiological Remarks on Man's Mobility upon Partial or Total Relief of Body Weight. I: Mechanics of Deambulation and Energy Expenditure," Riv. Med. Aero., 25, pp. 623-635

11. Margaria, R., and G. V. Cavagna, "Human Locomotion in Subgravity," Aerospace Medicine, 35, No. 12, pp. 1140-1146, December, 1964.

12. Nelson, N., L. W. Eichna, S. M. Harvath, W. B. Shelley and T. F. Hatch, "Thermal Exchanges of Man at High Temperature," Am. J. Physiol., 151, p. 626, 1947.

13. Robinson, S., "Circulatory Adjustments of Men in Hot Environments, "Temperature, Its Measurement and Control in Science and Industry," Vol. 3, Part 3, pp. 287-297, Reinhold, New York, 1963.

14. Streimer, I., D. P. W. Turner, C. A. Tardiff, and T. L. Stephens, "An Investigation of the Effects of Pressure Suit Wearing on Work Output Characteristics," Aerospace Medicince, 35, No. 8, pp. 747-751, August 1964.

15. Webb, P., ed., Biastronautic Data Book, Report No. NASA SP-3006, Office of Scientific and Technical Information, National Aeronautics and Space Administration, Washington, D. C., 1964.

16. Welch, B. E., et al., "Bioengineering Experiments in the SAM Space Cabin Simulator," ARS Paper, 1962.

17. Welsh, B. E., T. E. Morgan, Jr., and F. Ulvedal, "Observations in the SAM Two-Man Space Cabin Simulator," Aerospace Medicine, 32, pp. 583-590, 1961.

18. Wortz, E. C., et al., "Reduced Barometric Pressure and Respiratory Water Loss," Report No. LS-136, AiResearch Manufacturing Company, October 31, 1964.

HUMAN COMFORT CRITERIA

19. ASHRAE Handbook, American Society of Heating, Refrigerating, and Air-Conditioning Engineers, New York, 1963.

20. Gagge, A. P., G. M. Rapp, and J. M. Handy, "Mean Radiant and Operative Temperature for High Temperature Sources of Radiant Heat," ASHRAE J. pp. 67-71, October 1964.

21. Green, F. H., "Environmental Design Charts," AiResearch Manufacturing Company, Los Angeles, California, 1962.

22. Jannsen, J. E., "Thermal Comfort in Space Vehicles," ASME Paper 59-A-207, American Society of Mechanical Engineers, New York, November 1959.

23. Krantz, P., "Calculating Human Comfort," ASHRAE J., pp. 68-77, September 1964.

24. Waggoner, J. N. and W. L. Burriss, "Environmental Control of Manned Spacecraft for Durations up to Two Weeks," ARS Journal, 32, No. 7, pp. 1019-1028, 1962.

PRESSURE SUIT VENTILATION COOLING

25. Winslow, C. E. A.; L. P. Herrington and A. P. Gagge, "Relations Between Atmospheric Conditions, Physiological Reactions and Sensations of Pleasantness," Am. J. Hyg. 26, p. 103, 1937.

26. Albright, G., et al., "Ventilation Effectiveness of the Apollo Prototype Space Suit," Aerospace Medical Association, Washington, D. C., May 1964.

27. Nelson, W. G., L. Brown, and L. R. Krumland, "Preliminary Results of the Gemini Extravehicular Suit Pressurization-Ventilation Test Series," Report No. SS-3135, AiResearch Manufacturing Company, May 1964.

28. Nelson, W. G., "Final Report, Pressure Suit Test Program Project Apollo," Report No. SS-1018, AiResearch Manufacturing Company, September 26, 1962.

29. Wortz, E. C., T. J. Harrington, D. K. Edwards, and R. Diaz, "Heat Balance Study," NASA Contract 6-16139, Report No. SS-952, AiResearch Manufacturing Company, June 26, 1963.

30. Wortz, E. C., et al., "Full Pressure Suit Heat Balance Studies," Report No. LS-140, AiResearch Manufacturing Company, January 1965.

PRESSURE SUIT LIQUID-LOOP COOLING

31. Bowen, J. D., and R. F. Witte, "Thermal Transport for a Space Worker's Garment," AMRL Memo M-49, August 1963 (Classified).

32. Burriss, W. L., "Extravehicular Suit Thermal and Atmospheric Control," Report SS-3056, AiResearch Manufacturing Company, February 4, 1964.

33. Burton, D. R., and L. Collier, "The Development of Water Conditioned Suits," Tech. Note No. Mech Eng 400, Royal Aircraft Establishment, April 1964.

34. Crocker, J. J., P. Webb, and D. C. Jennings, "Metabolic Heat Balances in Working Men Wearing Liquid-Cooled Sealed Clothing," Proceedings of Third Manned Spaceflight Meeting, American Institute of Aeronautics and Astronautics, New York, 1964, pp. 111-131.

35. Felder, J. W. and A. P. Sholsinger, "Research on Methods for Thermal Transport in a Space Worker's Garment," Report No. AMRL-TDR-63-90, Aerospace Medical Research Laboratories, Wright-Patterson AFB, Ohio, November 1963.

36. Wortz, E. C., et al., "Technical Proposal, Internal Environment Management Program," Report No. SS-847, AiResearch Manufacturing Company, December 6, 1962.

37. Wortz, E. C., et al., "Progress Report, Internal Environment Management Program," Report No. LS-108, AiResearch Manufacturing Company, September 1963.

EXTRAVEHICULAR SUIT SYSTEMS

38. "A Study of Manned Locomotion and Protection Systems for Moon, Mars, and Venus," Contract No. NASW-613, Report No. D7183-920001, Bell Aerosystems, Buffalo, New York, October 1963.

39. Correale, J. V., and W. W. Guy, "Space Suits," NASA Manned Spacecraft Center, Houston, Texas, February 1963.

40. Freedman, G. F., "Control of Man's Thermal Environment During an Extravehicular Mission," pp. 126-131. Proceedings of the Third Manned Spaceflight Meeting, 1964, pp. 126-131.

41. Irvine, T. F., and K. R. Cramer, "Thermal Analysis of Space Suits in Orbit," WADD Tech. Note 60-145, Wright-Patterson AFB, Ohio, May 1960.

42. Kincaide, W. C., "Development of the Apollo Portable Life Support System," Lectures in Aerospace Medicine, USAF School of Aerospace Medicine, Brooks AFB, Texas, February 1964.

43. National Aeronautics and Space Administration, Mercury Suit Specifications, NASA-LS-62-2478.

44. Roth, E. M., "Bioenergetic Considerations in the Design of Space Suits for Lunar Exploration," Report II, Lovelace Foundation, July 12, 1963.

45. Woolsey, J., Personal Communication, Manned Spacecraft Center, National Aeronautics and Space Administration, Houston, Texas, September 1964.

HEAT TRANSFER

46. Brown, A. D., "Analog Computer Simulation of Temperature Regulation in Man," Report No. AMRL-TDR-63-116, Aerospace Medical Research Laboratories, Wright-Patterson AFB, Ohio, December 1963.

47. Crosbie, R. J., J. D. Hardy, and E. Fessenden, "Electrical Analog Simulation of Temperature Regulation in Man," Temperature Its Measurement and Control in Science and Industry, Vol. 3, Part 3, pp. 627-635, Reinhold, New York, 1963.

48. Eckert, E. R. G. and R. M. Drake, Jr., Heat and Mass Transfer, McGraw-Hill Book Co., Inc., New York, 1959.

49. "Heat and Mass Transfer through Composite Clothing Systems," U. S. Army Quartermaster Contract No. DA-19-129-AMC-183-N, Litton Systems, St. Paul, Minnesota.

50. Herrington, L. P., "The Biotechnical Problem of the Human Body as a Heat Exchanger," Trans. ASME, pp. 343-346, February 1957.

51. Jacob, M., Heat Transfer, John Wiley and Sons, Inc., New York, 1955.

52. McAdams, W. H., Heat Transmission, McGraw-Hill Book Co., Inc., New York, 1954.

53. Powell, R. W. "Note on the Distribution of Temperature and Vapor Pressure Around a Horizontal Wet Cylinder," Phil. Mag. (7), 29, pp. 274-284, 1940.

54. Woodcock, A. H., J. R. Breckenridge, R. L. Pratt, and J. J. Powers, Jr., "Analysis of Energy Exchange Between Man and His Environment," ASME Paper No. 57-SA-64, New York, 1957.

MISCELLANEOUS

55. Cannon, P., and W. R. Keatinge, "The Metabolic Rate and Heat Loss of Fat and Thin Men in Heat Balance in Cold and Warm Water," J. Physiol, 154, pp.329-344, 1960.

56. Nielsen, M., Skandinav. Arch. F. Physiol., 9, 5-6, 1938, data given in Ref. 34.

57. Iberall, A. S. "The Use of Ling of Nonextension to Improve Mobility in Full-Pressure Suits," Report No. AMRL-TR-64-118, Aeromedical Research Laboratory, Wright-Patterson AFB, Ohio, November 1964.

Appendix A

Computer Program for Extravehicular Heat Balance for Planetary Orbital Environments

```
*     JOB      H1440      S.H. LIN (MAN IN ORBIT)  (3501-110617-01-0100)
C     ORBITAL RADIANT HEAT FLUX AND SINK TEMPERATURE PROGRAM FOR MAN IN
C     SPACE.
      DIMENSION COS(26),SIN(26),CEN(26),CVN(26)
      DIMENSION XWD(200),XW(200),EMITV(200),HEADNG(16)
      DIMENSION PHID(26),FEB(26),FVB(26),CPSI(26),SPCI(26),AFEB(26),AFVB
     1(26)
      COMMON XID,BB,BBV,BBX,WW,SNI,XW3,XW4,YW3,YW4,ZW3,ZW4,XD
      COMMON S,ALBEDO,NCASE,XWD,XW,NW,EMITV,TMIN,DTEMP,EM,NPAGE,HEADNG
      COMMON HCD,HSD,FEV,CV1,CV2,CV3,DQV,AEV
      COMMON AFB,XDEL,NS,NS1,NS2,PHID,CPSI,SPCI,FEB,FVB,AFEB,AFVB,CB1,CB
     13,CB2,AREA,ASIDE,AEND,     TBI,SIDEK,SIDETK,ENDK,ENDTK,ES
      READ INPUT TAPE 41,4115,KMAX
      DO 99 K=1,KMAX
C     READ PROBLEM HEADING (ONE DATA CARD).
      READ INPUT TAPE 41,4105,HEADNG
 4105 FORMAT(16A5)
C     ORBIT PLANE INCLINATION,DEGREES,(XID).
C     ANGLE BETWEEN BODY AXIS AND BODY POSITION VECTOR,DEGREES,(XDELD).
C     ANGLE BETWEEN BODY-CRAFT VECOTR AND BODY POSITION VECTOR,DEGREES,(
C     XDD).
C     RV=RADIUS OF SPHERICAL SPACECRAFT (FEET).
C     HV=DISTANCE FROM BODY TO SPACECRAFT SURFACE (FEET).
C     QV=INTERNAL HEAT LOAD (BTU/HR) INSIDE SPACECRAFT.
C     READ THE ANGLES (DEG.) AND INFORMATION PERTAINING TO VEHICLE.
      READ INPUT TAPE 41,4110,XID,XDELD,     XDD,RV,HV,QV
C     IF NO RADIATION FROM THE VEHICLE IS TO BE CONSIDERED,(SET RV=0.0)
 4110 FORMAT(8F10.0)
C     RB=RADIUS OF CYLINDRICAL SUIT (INCHES).
C     HB=HEIGHT OF CYLINDRICAL SUIT (INCHES).
C     R=RADIUS OF PLANET (NAUTICAL MILES).
C     H=HEIGHT ABOVE SURFACE OF PLANET (NAUTICAL MILES).
C     TMAX=MAXIMUM PLANETARY SURFACE TEMPERATURE (DEG. RANKINE)
C     TMIN=MINIMUM PLANETARY SURFACE TEMPERATURE (DEG. RANKINE)
C     READ SUIT AND PLANETARY DATA.
      READ INPUT TAPE 41,4110,RB,HB,       R,H,TMAX,TMIN
C     WSTART=INITIAL ARGUMENT OF OMEGA,DEGREES
C     WEND=FINAL ARGUMENT OF OMEGA,DEGREES
C     NW=NUMBER OF INTERVALS INTO WHICH THE OMEGA RANGE IS DIVIDED
C     NS=NUMBER OF SUIT SURFACE ELEMENTS
C     LUNAR ORBIT (NCASE=1),EARTH ORBIT (NCASE=2)
C     READ ORBITAL ELEMENT RANGE (OMEGA,DEGREES)
      READ INPUT TAPE 41,4110,WSTART,WEND
C     READ ORBIT INTERVALS,SURFACE ELEMENTS AND PLANET IDENTIFICATION
      READ INPUT TAPE 41,4115,NW,NS,NCASE
 4115 FORMAT(8I10)
C     S=SOLAR CONSTANT,BTU/HR-FT**2
C     ALBEDO=PLANETARY ALBEDO(0.07 FOR MOON,0.35 FOR EARTH)
C     ASB=SOLAR(DIRECT AND REFLECTED) ABSORPTIVITY OF SUIT=ARB
C     AEB=INFRARED ABSORPTIVITY AND EMISSIVITY OF SUIT=AVB=EB
C     ASV=SOLAR (DIRECT AND REFLECTED) ABSORPTIVITY OF SPACECRAFT=ARV
C     AEV=INFRARED ABSORPTIVITY AND EMISSIVITY OF SPACECRAFT=EV
C     READ SURFACE RADIATION PROPERTIES AND PLANETARY ALBEDO
      READ INPUT TAPE 41,4110,S,ALBEDO,ASB,AEB,ASV,AEV
C     THICK=THICKNESS OF THE SPACE SUIT (INCHES)
C     BK=THERMAL CONDUCTIVITY OF SPACE SUIT MATERIAL (BTU/HR-FT-R)
C     TBI=INSIDE SURFACE TEMP. = BODY SKIN TEMP. (R)
C     EIB=EXCHANGE FACTOR FOR INSIDE SURFACE E(I-B)
      READ INPUT TAPE 41,4110,THICK,BK,TBI,EIB
C     PRELIMINARY CALCULATION OF ANGLE-DEPENDENT QUANTITIES. (SUIT)
```

```
      XI=XID*0.01745329252
      XDEL=XDELD*0.01745329252
      SNI=SINF(XI)
      CSI=COSF(XI)
      SNDEL=SINF(XDEL)
      CSDEL=COSF(XDEL)
C     COMPUTES COMMON TERMS FOR SUBSEQUENT SUBROUTINES.
      RR=R*R
      RH=R+H
      A=R/RH
      AA=A*A
      BB=SQRTF(1.0-AA)
      TH2=ATANF(A/BB)
      XWD(1)=WSTART
      XW(1)=WSTART*0.01745329252
      IF(XID)5,4,5
    4 NW=1
      GO TO 15
    5 FNW=NW
      DWD=(WEND-WSTART)/FNW
      DW=DWD*0.01745329252
      DO 10 I=2,NW
      XWD(I)=XWD(I-1)+DWD
   10 XW(I)=XW(I-1)+DW
   15 NS1=NS+1
      NS2=NS+2
      FNS=NS
      DPHID=360.0/FNS
      DPHI=6.2831853/FNS
      PHID(1)=0.0
      PHI=0.0
      COS(1)=1.0
      CPSI(1)=SNI
      SIN(1)=0.0
      SPCI(I)=0.0
      CEN(1)=SNDEL
      CEN(NS1)=-CSDEL
      CEN(NS2)= CSDEL
      DO 20 J=2,NS
      PHID(J)=PHID(J-1)+DPHID
      PHI=PHI+DPHI
      COS(J)=COSF(PHI)
      CPSI(J)=COS(J)*SNI
      SIN(J)=SINF(PHI)
      SPCI(J)=SIN(J)*CSI
   20 CEN(J)=SNDEL*COS(J)
      CB1=ASB*S
      CB3=CB1*ALBEDO
      AREA=3.1415927*RB
      AEND=AREA*RB/144.0
      AREA=2.0*AREA*HB/144.0
      ASIDE=AREA/FNS
      AREA=AREA+2.0*AEND
      SK=BK*12.0
      RATIO=RB/(RB-THICK)
      SIDEK=SK/(RB*LOGF(RATIO))
      ENDK=SK/THICK
      ENDTK=EIB*0.1713E-8
      SIDETK=ENDTK/RATIO
      ES=AEB*0.1713E-8
```

```
      DO 30 J=1,NS2
      FEB(J)=FEBFVB(J,CEN,A,AA,BB,TH2)
   30 AFEB(J)=AEB*FEB(J)
      GO TO (41,42),NCASE
   41 DTEMP=TMAX-TMIN
      EM=(1.0-ALBEDO)*S/((0.2*DTEMP**4+DTEMP**3*TMIN+2.0*DTEMP*DTEMP*TMI
     1N*TMIN+2.0*DTEMP*TMIN**3+2.0*TMIN**4)*4.0*0.1713E-08)
C     PRINT OUT INPUT VARIABLES OR PARAMETERS.
   42 NPAGE=1
      WRITE OUTPUT TAPE 42,4200,HEADNG,NPAGE
 4200 FORMAT(1H1,9X,16A5,4X,4HPAGE,I4)
      NPAGE=NPAGE+1
      WRITE OUTPUT TAPE 42,4201,R,ALBEDO,S
 4201 FORMAT(///,20X,18HPLANET (SPHERICAL),/,F33.3,16H = RADIUS (N.M.),/
     1,F33.3,9H = ALBEDO,/,F33.3,31H = SOLAR CONSTANT (BTU/HR-SQFT) )
      GO TO (43,44),NCASE
   43 WRITE OUTPUT TAPE 42,4202,EM,TMAX,TMIN
 4202 FORMAT(/,F33.3,22H = INFRARED EMISSIVITY,/,F33.3,33H = SURFACE TEM
     1PERATURE (R) (MAX.),/,F33.3,33H = SURFACE TEMPERATURE (R) (MIN.) )
   44 TESTRV=RV-0.005
      IF(TESTRV) 445,445,444
  444 WRITE OUTPUT TAPE 42,4203,RV,ASV,AEV,QV
 4203 FORMAT(///,20X,22HSPACECRAFT (SPHERICAL),/,F33.3,16H = RADIUS (FEE
     1T),/,F33.3,21H = SOLAR ABSORPTIVITY,/,F33.3,24H = INFRARED ABSORPT
     2IVITY,/,F33.3,30H = INTERNAL HEAT LOAD (BTU/HR) )
  445 WRITE OUTPUT TAPE 42,4204,RB,HB, THICK,H
 4204 FORMAT(///,20X,18HSUIT (CYLINDRICAL),/,F33.3,18H = RADIUS (INCHES)
     1,/,F33.3,18H = HEIGHT (INCHES),/,F33.3,21H = THICKNESS (INCHES),
     2/,F33.3,38H = DISTANCE FROM PLANET SURFACE (N.M.) )
      IF(TESTRV) 447,447,446
  446 WRITE OUTPUT TAPE 42,4246,HV
 4246 FORMAT(       /,F33.3,39H = DISTANCE FROM VEHICLE SURFACE (FEET) )
  447 WRITE OUTPUT TAPE 42,4247,ASB,AEB,BK,EIB,TBI
 4247 FORMAT(/,F33.3,21H = SOLAR ABSORPTIBITY,/,F33.3,24H = INFRARED ABS
     1ORPTIVITY,/,F33.3,37H = THERMAL CONDUCTIVITY (BTU/HR-FT-R),/,F33.3
     2,28H = INTERCHANGE FACTOR E(B-I),/,F33.3,
     331H = SKIN TEMPERATURE OF CREW (R) )
      WRITE OUTPUT TAPE 42,4205,XID,XDELD
 4205 FORMAT(///,20X,17HANGLES IN DEGREES,/,F33.3,32H = ORBIT PLANE INCL
     1INATION ANGLE, /,36X,45H(W.R.T. PLANE PERPENDICULAR TO SUN DIRECTI
     2ON)/,F33.3,30H = ANGLE BETWEEN BODY AXIS AND,/,36X,20HBODY POSITIO
     3N VECTOR )
      IF(TESTRV) 449,449,448
  448 WRITE OUTPUT TAPE 42,4248,XDD
 4248 FORMAT(  /,F33.3,40H = ANGLE BETWEEN BODY-VEHICLE VECTOR AND,/,36X
     1,20HBODY POSITION VECTOR)
C     PRELIMINARY CALCULATION FOR SPACECRAFT.
  500 MSHADE=2
      XD=XDD*0.01745329252
      SND=SINF(XD)
      CSD=COSF(XD)
      XX=XDEL-XD
      SNDD=SINF(XX)
      CSDD=COSF(XX)
      RHV=RV+HV
      AV=RV/RHV
      AAV=AV*AV
      BBV=SQRTF(1.0-AAV)
      THV2=ATANF(AV/BBV)
      RHV=RHV*0.000164579171
```

```
      HCD=RHV*CSD
      HSD=RHV*SND
      DOWN=RH*(RH+2.0*HCD)+RHV*RHV
      BBX=SQRTF(1.0-RR/DOWN)
      FEV=0.5*(1.0-BBX)
      DOWN=SQRTF(DOWN)
      UP=SNI/DOWN
      XX=HSD/DOWN
      DD=ATANF(ABSF(XX)/SQRTF(1.0-XX*XX))
      IF(XX)2,3,3
    2 DD=-DD
    3 WW=4.7123890-DD
      HCD=(RH+HCD)*UP
      HSD=HSD*UP
      CVN(1)=-SNDD
      CVN(NS1)=CSDD
      CVN(NS2)=-CSDD
      DO 520 J=2,NS
  520 CVN(J)=-SNDD*COS(
      CB5=CB1*(1.0-ASV)
      CV1=ASV*S
      CV2=AEV*FEV
      CV3=CV1*ALBEDO
      DQV=QV/(4.0*3.1415927*RV*RV)
      DO 530 J=1,NS2
      FVB(J)=FEBFVB(J,CVN,AV,AAV,BBV,THV2)
  530 AFVB(J)=AEB*FVB(J)
      CALL SHADOX(MSHADE,NSHADE)
      CALL TCRAFT(MSHADE)
      GO TO 99
  449 MSHADE=3
      CB5=0.0
      DO 533 J=1,NS2
  533 AFVB(J)=0.0
      CALL SHADOX(MSHADE,NSHADE)
   99 CALL TSUIT(NSHADE)
      CALL EXIT
      END
```

```
      FUNCTION FEBFVB(J,CSN,A1,A2,B2,AN2)
C     COMPUTES FORM FACTORS FOR PLANETARY OR VEHICULAR THERMAL RADIATION
      DIMENSION CSN(26)
      C=CSN(J)
      CC=C*C
      IF(C)     103,101,102
C     TH1=90.0 DEGREES OR 1.5707963 RADIANS
  101 FEBFVB=(AN2-A1*B2)                /3.1415927
      RETURN
  102 AN1=ATANF(SQRTF(1.0-CC)/C)
      GO TO 104
  103 AN1=3.1415927-ATANF(-SQRTF(1.0-CC)/C)
  104 ADD12=AN1+AN2
      SUB12=AN1-AN2
      IF(ADD12-1.5707963)110,110,105
  105 IF(SUB12-1.5707963)130,140,140
C     (TH1+TH2) SMALLER THAN 90.0 DEGREES (FULL VIEW),CASE 1
  110 FEBFVB=A2*C
      RETURN
C     (TH1+TH2) GREATER BUT (TH1-TH2) SMALLER THAN 90 DEGREES,CASES 2,3
  130 SINX=SINF(AN1)
      X=SQRTF(ABSF(A2-CC))/SINX
      Y=B2*CC/SINX
      ANG=2.0*ATANF(X/SQRTF(1.0-X*X))
      YB=ABSF(Y/(A1*C))
      ASIN=A2*ABSF(C      )*ATANF(YB/SQRTF(1.0-YB*YB))
      FEBFVB=0.5*A2*C      +(X*Y+ASIN+0.5*(ANG-SINF(ANG)))/3.1415927
      RETURN
C     (TH1-TH2) GREATER THAN 90 DEGREES (NO VIEW)
  140 FEBFVB=0.0
      RETURN
      END
```

```
      SUBROUTINE SHADOX(MSHADE,NSHADE)
C     COMPUTES THREE(3) SETS OF SHADOW ANGLE INTERCEPTS.
      COMMON XID,BB,BBV,BBX,WW,SNI,XW3,XW4,YW3,YW4,ZW3,ZW4,XD
      NSHADE=6
      IF(XID)220,250,220
  220 SS=ABSF(SNI)
      CSX=BB/SS
      IF(CSX-1.0)221,221,222
  221 ANG=ATANF(SQRTF(1.0-CSX*CSX)/CSX)
      XW3=4.7123890-ANG
      XW3D=XW3*57.29577951
      XW4=4.7123890+ANG
      XW4D=XW4*57.29577951
      NSHADE=NSHADE-3
  222 IF(MSHADE-3)223,250,223
  223 MSHADE=2
      CSX=BBV/SS
      IF(CSX-1.0)231,231,232
  231 ANG=ATANF(SQRTF(1.0-CSX*CSX)/CSX)
      YW3=1.5707963-ANG-XD
      YW4=YW3+2.0*ANG
      NSHADE=NSHADE-1
      IF(YW3)235,236,236
  235 YW3=6.2831854+YW3
  236 IF(YW4)237,238,238
  237 YW4=6.2831854+YW4
  238 IF(YW4-YW3)239,240,240
  239 NSHADE=NSHADE-1
  240 YW3D=YW3*57.29577951
      YW4D=YW4*57.29577951
  232 CSX=BBX/SS
      IF(CSX-1.0)241,241,250
  241 ANG=ATANF(SQRTF(1.0-CSX*CSX)/CSX)
      MSHADE=MSHADE-1
      ZW3=WW-ANG
      ZW3D=ZW3*57.29577951
      ZW4=WW+ANG
      ZW4D=ZW4*57.29577951
  250 WRITE OUTPUT TAPE 42,4210
 4210 FORMAT(///,20X,23HSHADOW ANGLE INTERCEPTS,11X,5HENTER,6X,4HEXIT)
      GO TO (251,251,253,254,254,256),NSHADE
  251 WRITE OUTPUT TAPE 42,4211,XW3D,XW4D,YW3D,YW4D
 4211 FORMAT(1H 25X,24HSUIT IN SHADOWS (PLANET),2X,2F10.3,/,41X,9H(VEHIC
     1LE),2X,2F10.3)
      GO TO 260
  253 WRITE OUTPUT TAPE 42,4212,XW3D,XW4D
 4212 FORMAT(1H 25X,24HSUIT IN SHADOWS (PLANET),2X,2F10.3,/,41X,9H(VEHIC
     1LE),5X,4HNONE,6X,4HNONE)
      GO TO 260
  254 WRITE OUTPUT TAPE 42,4213,YW3D,YW4D
 4213 FORMAT(1H 25X,24HSUIT IN SHADOWS (PLANET),5X,4HNONE,6X,4HNONE,/,41
     1X,9H(VEHICLE),2X,2F10.3)
      GO TO 260
  256 WRITE OUTPUT TAPE 42,4214
 4214 FORMAT(1H 25X,24HSUIT IN SHADOWS (PLANET),5X,4HNONE,6X,4HNONE,/,41
     1X,9H(VEHICLE),5X,4HNONE,6X,4HNONE)
  260 GO TO (261,262,270),MSHADE
  261 WRITE OUTPUT TAPE 42,4215,ZW3D,ZW4D
 4215 FORMAT(1H 25X,26HVEHICLE IN SHADOW (PLANET),2F10.3)
      GO TO 270
```

```
  262 WRITE OUTPUT TAPE 42,4216
 4216 FORMAT(1H 25X,26HVEHICLE IN SHADOW (PLANET),3X,4HNONE,6X,4HNONE)
  270 RETURN
      END
```

```
      SUBROUTINE TCRAFT(MSHADE)
C     COMPUTES SINK TEMPERATURES FOR A SPHERICAL SPACECRAFT.
      DIMENSION XWD(200),XW(200),EMITV(200),HEADNG(16)
      COMMON XID,BB,BBV,BBX,WW,SNI,XW3,XW4,YW3,YW4,ZW3,ZW4,XD
      COMMON S,ALBEDO,NCASE,XWD,XW,NW,EMITV,TMIN,DTEMP,EM,NPAGE,HEADNG
      COMMON HCD,HSD,FEV,CV1,CV2,CV3,DQV,AEV
      NLINE=51
      DO 350 I=1,NW
      IF(NLINE-50)302,302,301
  301 WRITE OUTPUT TAPE 42,4200,HEADNG,NPAGE
      WRITE OUTPUT TAPE 42,4201
      NPAGE=NPAGE+1
      NLINE=0
  302 W=XW(I)
      GO TO(300,315),MSHADE
  300 IF(W-ZW3)315,310,305
  305 IF(W-ZW4)310,310,315
  310 ONE=0.0
      GO TO 320
  315 ONE=0.25*CV1
  320 COSV=SINF(W)*HCD+COSF(W)*HSD
      IF(COSV)325,325,326
  325 THREE=0.0
      TE=TMIN
      GO TO 327
  326 THREE=FEV*COSV*CV3
      TE=DTEMP*COSV+TMIN
  327 GO TO(328,329),NCASE
  328 ET=0.1713E-08*EM*TE**4
      GO TO 330
  329 ET=0.25*(1.0-ALBEDO)*S
  330 TWO=CV2*ET
      EMITV(I)=ONE+TWO+THREE+DQV
      IF(AEV)350,350,349
  349 TV4=EMITV(I)/(AEV*0.1713)
      TV=TV4**0.25*100.0
      NLINE=NLINE+1
      WRITE OUTPUT TAPE 42,4251,XWD(I),ONE,THREE,TWO,DQV,EMITV(I),TV4,TV
 4251 FORMAT(1H F9.2,3X,5F8.2,7X,2F8.2)
  350 CONTINUE
 4200 FORMAT(1H1,9X,16A5,14X,4HPAGE,I4)
 4201 FORMAT(1H010X,46H-ABSORBED HEAT FLUXES (BTU/HR-SQFT)-SPACECRAFT,6X
     1,5HTS**4,5X,2HTS,/,5X,5HOMEGA,5X,6HDIRECT,2X,6HREFTD.,2X,6HPLANET,
     22X,6HINSIDE,/,5X,5H(DEG),6X,5HSOLAR,3X,5HSOLAR,2X,6HEMISSN,3X,4HHE
     3AT,4X,5HTOTAL,9X,6H(E-08),4X,3H(R),/)
      RETURN
      END
```

```
      SUBROUTINE TSUIT(NSHADE)
C     COMPUTES SINK TEMPERATURES FOR A CYLINDRICAL SUIT.
      DIMENSION XWD(200),XW(200),EMITV(200),HEADNG(16)
      DIMENSION PHID(26),FEB(26),FVB(26),CPSI(26),SPCI(26),AFEB(26),AFVB
     1(26)
      DIMENSION FSB(26),FREB(26),FRVB(26)
      COMMON XID,BB,BBV,BBX,WW,SNI,XW3,XW4,YW3,YW4,ZW3,ZW4,XD
      COMMON S,ALBEDO,NCASE,XWD,XW,NW,EMITV,TMIN,DTEMP,EM,NPAGE,HEADNG
      COMMON HCD,HSD,FEV,CV1,CV2,CV3,DQV,AEV
      COMMON AEB,XDEL,NS,NS1,NS2,PHID,CPSI,SPCI,FEB,FVB,AFEB,AFVB,CB1,CB
     13,CB5,AREA,ASIDE,AEND,     TBI,SIDEK,SIDETK,ENDK,ENDTK,ES
      NLINE=51
      DO 615 I=1,NW
      W=XW(I)
      IF(NLINE-47)205,205,200
  200 WRITE OUTPUT TAPE 42,4200,HEADNG,NPAGE
      WRITE OUTPUT TAPE 42,4201
      NPAGE=NPAGE+1
      NLINE=0
  205 WRITE OUTPUT TAPE 42,4205,XWD(I)
      NLINE=NLINE+1
 4205 FORMAT(1H F9.2)
      GO TO(310,310,310,330,320,340),NSHADE
  310 IF(W-XW3)315,335,311
  311 IF(W-XW4)335,335,315
  315 GO TO(330,320,340),NSHADE
  320 IF(W-YW3)340,335,321
  321 IF(W-YW4)335,335,340
  330 IF(W-YW3)331,335,335
  331 IF(W-YW4)335,335,340
  335 DO 337 J=1,NS2
  337 FSB(J)=0.0
      GO TO 360
  340 CDW=COSF(XDEL+W)
      FSB(NS1)=SINF(XDEL+W)*SNI
      FSB(NS2)=-FSB(NS1)
      DO 345 J=1,NS
  345 FSB(J)=CPSI(J)*CDW+SPCI(J)
      DO 350 J=1,NS2
      IF(FSB(J))347,350,350
  347 FSB(J)=0.0
  350 CONTINUE
  360 SEW=SINF(W)*SNI
      SVW=-SINF(W+XD)*SNI
      IF(SEW)410,410,405
  405 TE=DTEMP*SEW+TMIN
      DO 406 J=1,NS2
  406 FREB(J)=FEB(J)*SEW
      GO TO 415
  410 TE=TMIN
      DO 411 J=1,NS2
  411 FREB(J)=0.0
  415 IF(SVW)460,460,455
  455 DO 456 J=1,NS2
  456 FRVB(J)=FVB(J)*SVW
      GO TO 470
  460 DO 461 J=1,NS2
  461 FRVB(J)=0.0
  470 GO TO(471,472),NCASE
  471 ET=0.1713E-08*EM*TE**4
```

```
      GO TO 600
  472 ET=0.25*(1.0-ALBEDO)*S
  600 AVGT4=0.0
      QLOAD=0.0
      TK=SIDETK
      CK=SIDEK
      DO 610 J=1,NS2
      IF(NLINE-47)602,602,601
  601 WRITE OUTPUT TAPE 42,4200,HEADNG,NPAGE
      WRITE OUTPUT TAPE 42,4201
      NPAGE=NPAGE+1
      NLINE=0
  602 ONE=CB1*FSB(J)
      TWO=AFEB(J)*ET
      THREE=CB3*FREB(J)
      FOUR=AFVB(J)*EMITV(I)
      FIVE=CB5*FRVB(J)
      TOTAL=ONE+THREE+FIVE+TWO+FOUR
      TB4=TOTAL/ES
      TB=TB4**0.25
      IF(J-NS1)501,500,501
  500 TK=ENDTK
      CK=ENDK
  501 TERM=TK*TBI**4
      TMID=((CK*(TB-TBI)+TERM)/TK)**0.25
      DX=0.5*ABSF(TMID-TBI)
      X2=0.5*(TMID+TBI)
      XL=X2-DX
      XR=X2+DX
      KOUNT=0
  502 QRATE=TK*X2**4-TERM
      TOUT=X2+QRATE/CK
      YMID=ES*TOUT**4-TOTAL+QRATE
      IF(ABSF(YMID)-1.E-2) 510,510,503
  503 IF(YMID)504,510,505
  504 XL=X2
      GO TO 506
  505 XR=X2
  506 KOUNT=KOUNT+1
      X2=0.5*(XL+XR)
      IF(KOUNT-15)502,502,510
  510 X2=TOUT
      IF(NS-J)606,605,605
  605 AVGT4=AVGT4+TB4*ASIDE
      QLOAD=QLOAD+QRATE*ASIDE
      WRITE OUTPUT TAPE 42,4210,PHID(J),ONE,THREE,FIVE,TWO,FOUR,TOTAL,TB
     1,X2,QRATE
 4210 FORMAT(1H 9X,F9.2,3X,6F8.2,3X,3F8.2)
      GO TO 610
  606 AVGT4=AVGT4+TB4*AEND
      QLOAD=QLOAD+QRATE*AEND
      WRITE OUTPUT TAPE 42,4211,ONE,THREE,FIVE,TWO,FOUR,TOTAL,TB,
     1X2,QRATE
 4211 FORMAT(1H 14X,3HEND,4X,6F8.2,3X,3F8.2)
  610 NLINE=NLINE+1
      AVGT4=AVGT4/AREA
      AVGT=AVGT4**0.25
      TSKIN=(AVGT4-QLOAD/(AREA*ES))**0.25
      WRITE OUTPUT TAPE 42,4212,AVGT,TSKIN,QLOAD
 4212 FORMAT(1H+,96X,2F8.2,F7.1,/)
```

```
 615 NLINE=NLINE+1
4200 FORMAT(1H1,9X,16A5,14X,4HPAGE,I4)
4201 FORMAT(1H023X,46HABSORBED HEAT FLUXES (BTU/HR-SQFT)-SPACE SUIT-,
    129X,14HAVERAGE VALUES,/5X,5HOMEGA,5X,3HPHI,6X,22HDIRECT REFLECTED
    2SOLAR,2X,14HTHERMAL EMISS.,15X,2HTS,4X,6HT(OUT),3X,5HQRATE,4X,2HTS
    3,4X,6HT(OUT),2X,5HQ(IN),/,5X,5H(DEG),4X,5H(DEG),6X,5HSOLAR,2X,
    414HPLANET VEHICLE,2X,14HPLANET VEHICLE,3X,5HTOTAL,6X,3H(R),6X,3H(R
    5),3X,6HB/H-SF,3X,3H(R),5X,3H(R),3X,6HBTU/HR,/)
     RETURN
     END
```

Appendix B

Computer Program for Extravehicular Heat Balance for Lunar Surface Environments

```
*      JOB      H1494      S.H. LIN   (FOR ANY TS)  (10-22-1964)
C      SUIT HEAT TRANSFER STUDY FOR MAN ON LUNAR SURFACE.
       DIMENSION          TH(20),HEADNG(16),TCR(24),TCCR(24),TSSR(24),TSR(
      124),TCTR(24)
 4105 FORMAT(16A5)
C      READ SUIT DATA,SIZE,RADIANT AND THERMAL PROPERTIES.
       READ INPUT TAPE 41,4110,RI,HI,TB,EIB, CK2,TH2, CK1
 4110 FORMAT(8F10.0)
C      RI= INSIDE RADIUS OF SUIT(INCHES)
C      HI=LENGTH OF SUIT(INCHES)
C      TB=SKIN TEMPERATURE OF CREW(R).
C      EIB=EFFECTIVE INTERCHANGE FACTOR(INSIDE SURFACE-SKIN).
C      CK2=THERMAL CONDUCTIVITY OF SECOND LAYER(BTU/HR-FT-R).
C      TH2=THICKNESS OF SECOND LAYER(INCHES).
C      CK1=THERMAL CONDUCTIVITY OF FIRST  LAYER(BTU/HR-FT-R).
       READ INPUT TAPE 41,4115,NS,    KMAX
 4115 FORMAT(8I10)
C      NS=NUMBER OF ELEMENTS INTO WHICH (180 DEGREES) IS DIVIDED.
C      KMAX=NUMBER OF (CLIFF ANGLE AND SUN ANGLE COMBINATION) CASES.
C      PRELIMINARY COMPUTATION FOR SUBROUTINES.
       FNS=NS
       NMAX=NS+1
       DANG=3.1415927/FNS
       GAMMA=-0.5*DANG
       DO 20 N=1,NS
       GAMMA=GAMMA+DANG
       TCR(N)=COSF(GAMMA)
       TCCR(N)=TCR(N)*TCR(N)
       TSSR(N)=1.0-TCCR(N)
       TSR(N)=SQRTF(TSSR(N))
   20  TCTR(N)=TCR(N)/TSR(N)
       RM=RI+TH2
       THK=TH2/CK2
       TOPER=EIB*0.1713E-8
       TB4=TB**4
       TTERM=TCPER*TB4
       HM=HI+2.0*TH2
       DO 615 K=1,KMAX
       READ INPUT TAPE 41,4105,HEADNG
       READ INPUT TAPE 41,4110,SXDEG,BASE, S,ASB,AEB
       READ INPUT TAPE 41,4115,    NTH
       READ INPUT TAPE 41,4110,(TH(N),N=1,NTH)
C      TH(N)=FIRST LAYER THICKNESS(INCHES).
C      SXDEG=SUNRAY-VERTICAL PLANE ANGLE(DEGREES).
C      BASE=WIDTH OF CRATER BASE (FEET).
C      S=SOLAR CONSTANT(BTU/HR-SQFT)
C      ASB=SOLAR ABSORPTIVITY OF SUIT.
C      AEB=INFRARED ABSORPTIVITY AND EMISSIVITY OF SUIT.
       XMAX=BASE*12.0
       ES=AEB*0.1713E-8
       SA=S*ASB
       SE=S*AEB
       SS=S/0.1713E-8
       SN=SINF(0.01745329252*SXDEG)
       SX=SQRTF(1.0-SN*SN)
       SEX=0.159154941*SE*SX
       NPAGE=1
       WRITE OUTPUT TAPE 42,4200,HEADNG,NPAGE
```

```
      NPAGE=NPAGE+1
 4200 FORMAT(1H1,9X,16A5,4X,4HPAGE,I3)
      TX=(SX*SS)**0.25
      WRITE OUTPUT TAPE 42,4201,BASE,S,SXDEG,SX,TX
 4201 FORMAT(///,20X,17HFLAT SURFACE      ,/,F33.3,23H = WIDTH OF BASE (F
     1EET),/,F33.3,31H = SOLAR CONSTANT (BTU/HR-SQFT),/,
     2F33.3,36H = SUN RAYS-VERTICAL ANGLE (DEGREES),/,F33.3,29H = RADIOS
     3ITY / SOLAR CONSTANT,/,F33.3,20H = SURFACE TEMP. (R))
      WRITE OUTPUT TAPE 42,4202,RI,HI,    TH2,ASB,AEB,CK2,EIB,TB
 4202 FORMAT(///,20X,18HSUIT (CYLINDRICAL),/,F33.3,18H = RADIUS (INCHES)
     1,/,F33.3,18H = HEIGHT (INCHES),/,F33.3,34H = SECOND LAYER THICKNES
     2S (INCHES),//,F33.3,21H = SOLAR ABSORPTIVITY,/,F33.3,24H = INFRARE
     3D ABSORPTIVITY,/,F33.3,48H = 2-ND LAYER THERMAL CONDUCTIVITY (BTU/
     4HR-FT-R),/,F33.3,28H = INTERCHANGE FACTOR E(B-I),/,F33.3,31H = SKI
     5N TEMPERATURE OF CREW (R))
C     COMPUTES HEAT TRANSFER RATES OF SUIT.
      NLINE=51
      DB=0.5*BASE
      DX=0.5
      DO 615 M=1,NTH
      TH1=TH(M)
      RB=RM+TH1
      HB=HM+2.0*TH1
      ASIDE=2.0*RB*DANG*HB/144.0
      ATOP=3.1415927*RB*RB/144.0
      AREA=ASIDE*FNS+ATOP
      RLK=RB*LOGF(RM/RI)/CK2
      RL=RB*LOGF(RB/RM)
      CK=12.0/(RLK+RL/CK1)
      ER=TOPER*RI/RB
      TERM=ER*TB4
      RX=RB/XMAX
      HX=0.5*HB/XMAX
      XH=HX*HX
      QLOAD=0.0
      AVGT4=0.0
      IF(NLINE-44)105,105,100
  100 WRITE OUTPUT TAPE 42,4204,HEADNG,NPAGE
 4204 FORMAT(1H1,9X,16A5,4X,4HPAGE,I3,//,10X,10HSPACE-SUIT,8X,32HABSORBE
     1D HEAT FLUXES (BTU/HR-SF),34X,14HAVERAGE VALUES,/,3X,8HDISTANCE,2X
     2,7HI-LAYER,3X,4HELE-,2X,6HDIRECT,2X,6HCRATER,2X,6HCRATER,15X,2HTS,
     34X,6HT(OUT),3X,5HQRATE,4X,2HTS,4X,6HT(OLT),2X,6HT(INS),3X,5HQ(IN),
     4/,4X,6H(FEET),4X,5H(IN.),4X,4HMENT,3X,5HSOLAR,2X,6HBOTTOM,3X,5HCLI
     5FF,3X,5HTOTAL,6X,3H(R),6X,3H(R),3X,6HB/F-SF,3X,3H(R),5X,3H(R),5X,3
     6H(R),4X,6HBTU/HR,/)
      NPAGE=NPAGE+1
      NLINE=0
  105 WRITE OUTPUT TAPE 42,4205,DB,     TH1
 4205 FORMAT(1H F9.2,F9.3)
      NLINE=NLINE+1
      QWALL=0.0
      DO 610 N=1,NMAX
      IF(N-NMAX)114,111,111
  111 QSUN=SA*SX
      QFLAT=0.0
      CK=12.0/(THK+TH1/CK1)
      ER=TOPER
```

```
      TERM=TTERM
      GO TO 125
  114 CR=TCR(N)
      SC=SN*CR
      IF(SC)115,115,116
  115 QSUN=0.0
      GO TO 117
  116 QSUN=SA*SC
  117 CCR=TCCR(N)
      SSR=TSSR(N)
      SR=TSR(N)
      CTR=TCTR(N)
      B=-DX-RX*CR
      A=B/(HX*SR)
      ROOT=1.0/SQRTF(B*B+XH)
      ONE=ATANF(A)-HX*CR*ROOT*(1.57079635+ATANF(B*ROOT*CTR))
      B=-DX-RX*CR + 1.0
      A=B/(HX*SR)
      ROOT=1.0/SQRTF(B*B+XH)
      TWO=ATANF(A)-HX*CR*ROOT*(1.57079635+ATANF(B*ROOT*CTR))
      QFLAT=SEX*(TWO-ONE)
  125 TOTAL=QSUN+QFLAT
      TS4=TOTAL/ES
      TS=TS4**0.25
      TMID=CK*(TS-TB)+TERM
      IF(TMID) 126,126,127
  126 TMID=TS
      GO TO 128
  127 TMID=(TMID/ER)**0.25
  128 DX2=0.5*ABSF(TMID-TB)
      X2=0.5*(TMID+TB)
      XL=X2-DX2
      XR=X2+DX2
      KOUNT=0
  502 QRATE=ER*X2**4-TERM
      TOUT=X2+QRATE/CK
      YMID=ES*TOUT**4-TOTAL+QRATE
      IF(ABSF(YMID)-1.E-3)510,510,503
  503 IF(YMID)504,510,505
  504 XL=X2
      GO TO 506
  505 XR=X2
  506 KOUNT=KOUNT+1
      X2=0.5*(XL+XR)
      IF(KOUNT-20)502,502,510
  510 X2=TOUT
      IF(N-NMAX)606,605,605
  605 AVGT4=AVGT4+TS4*ATOP
      QLOAD=QLOAD+QRATE*ATOP
      WRITE OUTPUT TAPE 42,4210,QSUN,QFLAT,QWALL,TOTAL,TS,X2,QRATE
 4210 FORMAT(1H 23X,3HTOP,4F8.2,3X,3F8.2)
      GO TO 610
  606 AVGT4=AVGT4+TS4*ASIDE
      QLOAD=QLOAD+QRATE*ASIDE
      WRITE OUTPUT TAPE 42,4211,N,QSUN,QFLAT,QWALL,TOTAL,TS,X2,QRATE
 4211 FORMAT(1H I26,4F8.2,3X,3F8.2)
  610 NLINE=NLINE+1
```

```
      AVGT4=AVGT4/AREA
      AVGT=AVGT4**0.25
      TSKIN=(AVGT4-QLCAD/(AREA*ES))**0.25
      TDEEP=((TERM+QLCAD/AREA)/ER)**0.25
      WRITE OUTPUT TAPE 42,4212,AVGT,TSKIN,TDEEP,QLOAD
 4212 FORMAT(1H+,85X,3F8.2,F8.1)
  615 NLINE=NLINE+1
      CALL EXIT
      END
```

Appendix C

Computer Program for Man in Lunar Crater Environment

```
*       JOB       H1490      S.H. LIN (MAN IN CRATER) (3501-110617-01-0100)
C       SUIT HEAT TRANSFER STUDY FOR MAN IN CRATER.
        DIMENSION X(41),XS(41),BX(41),BY(41)
        DIMENSION DBC(20),TH(20),HEADNG(16),TCR(24),TCCR(24),TSSR(24),TSR(
       124),TCTR(24)
        COMMON RLK,RL,THK,TH1
        COMMON CR,CCR,SR,SSR,CTR,NH,NPT,STEP
      . COMMON XS,X,BX,BY,RR,RS,SY,SX,CY,CX,SS
        COMMON ND,NTH,DBC,TH,SIN,COS,RI,HM,RM,XMAX,YMAX,RYX,TB,TB4,SA,SE,S
       1N,ES,CK2,TOPER,TTERM,DANG,FNS,NMAX,NPAGE,HEADNG,TCR,TCCR,TSSR,TSR,
       2TCTR
 4105  FORMAT(16A5)
C       READ SUIT DATA,SIZE,RADIANT AND THERMAL PROPERTIES.
        READ INPUT TAPE 41,4110,RI,HI,TB,EIB, CK2,TH2
 4110  FORMAT(8F10.0)
C       RI= INSIDE RADIUS OF SUIT(INCHES)
C       HI=LENGTH OF SUIT(INCHES)
C       CK2=THERMAL CONDUCTIVITY OF SECOND LAYER(BTU/HR-FT-R).
C       TH2=THICKNESS OF SECOND LAYER(INCHES).
C       TB=SKIN TEMPERATURE OF CREW(R).
C       EIB=EFFECTIVE INTERCHANGE FACTOR(INSIDE SURFACE-SKIN).
        READ INPUT TAPE 41,4115,NS,NI,KMAX
 4115  FORMAT(8I10)
C       NS=NUMBER OF ELEMENTS INTO WHICH (180 DEGREES) IS DIVIDED.
C       NI=NUMBER OF INTERVALS INTO WHICH (XMAX OR YMAX) IS DIVIDED.
C       KMAX=NUMBER OF (CLIFF ANGLE AND SUN ANGLE COMBINATION) CASES.
C       PRELIMINARY COMPUTATION FOR SUBROUTINES.
        FNS=NS
        NMAX=NS+1
        DANG=3.14159277/FNS
        GAMMA=-0.5*DANG
        DO 20 N=1,NS
        GAMMA=GAMMA+DANG
        TCR(N)=COSF(GAMMA)
        TCCR(N)=TCR(N)*TCR(N)
        TSSR(N)=1.0-TCCR(N)
        TSR(N)=SQRTF(TSSR(N))
   20   TCTR(N)=TCR(N)/TSR(N)
        RM=RI+TH2
        THK=TH2/CK2
        TOPER=EIB*0.1713E-8
        TB4=TB**4
        TTERM=TOPER*TB4
        NH=NI/2
        NPT=NI+1
        FNI=NI
        DO 30 I=1,NPT
        AI=I-1
        X(I)=AI/FNI
   30   XS(I)=X(I)*X(I)
        STEP=X(2)/3.0
        HM=HI+2.0*TH2
        DO 99 K=1,KMAX
        READ INPUT TAPE 41,4105,HEADNG
        READ INPUT TAPE 41,4110,CSDEG,SXDEG,BASE,HIGH,S,ASR,AEB
        READ INPUT TAPE 41,4115,ND,NTH
        READ INPUT TAPE 41,4110,(DBC(N),N=1,ND)
        READ INPUT TAPE 41,4110,(TH(N),N=1,NTH)
C       TH(N)=FIRST LAYER THICKNESS(INCHES).
C       CSDEG=CRATER WALL-VERTICAL PLANE ANGLE(DEGREES).
```

```
C       SXDEG=SUNRAY-VERTICAL PLANE ANGLE(DEGREES).
C       BASE=WIDTH OF CRATER BASE (FEET).
C       HIGH=HEIGHT OF CRATER WALL (FEET).
C       S=SOLAR CONSTANT(BTU/HR-SQFT)
C       ASB=SOLAR ABSORPTIVITY OF SUIT.
C       AEB=INFRARED ABSORPTIVITY AND EMISSIVITY OF SUIT.
C       DBC(N)=DISTANCE FROM CORNER TO SUIT(FEET).
        XMAX=BASE*12.0
        SIN=SINF(0.01745329252*CSDEG)
        CC=1.0-SIN*SIN
        COS=SQRTF(CC)
        YMAX=HIGH/COS*12.0
        ES=AEB*0.1713E-8
        SA=S*ASB
        SE=S*AEB
        SS=S/0.1713E-8
        SN=SINF(0.01745329252*SXDEG)
        SX=SQRTF(1.0-SN*SN)
        SY=SN*COS+SX*SIN
        HSY=0.5*SY
        RYX=YMAX/XMAX
        CY=0.5*RYX*CC
        CX=CY*RYX
        RR=RYX*RYX
        HRS=RYX*SIN
        RS=2.0*HRS
        COMPUTES INITIAL BX(I) ALONG CRATER BASE.
        DO 40 I=2,NPT
   40   BX(I)=SX+HSY*(1.0-(HRS+X(I))/SQRTF(XS(I)+RR+RS*X(I)))
        NPAGE=1
        WRITE OUTPUT TAPE 42,4200,HEADNG,NPAGE
        NPAGE=NPAGE+1
 4200   FORMAT(1H1,9X,16A5,4X,4HPAGE,I3)
        WRITE OUTPUT TAPE 42,4201,BASE,HIGH,S,CSDEG,SXDEG
 4201   FORMAT(///,20X,17HCRATER (V-GROOVE),/,F33.3,23H = WIDTH OF BASE (F
       1EET),/,F33.3,25H = HEIGHT OF CLIFF (FEET),/,F33.3,31H = SOLAR CONS
       2TANT (BTU/HR-SQFT),/,F33.3,33H = CLIFF-VERTICAL ANGLE (DEGREES),/,
       3F33.3,36H = SUN RAYS-VERTICAL ANGLE (DEGREES))
        WRITE OUTPUT TAPE 42,4202,RI,HI,   TH2,ASB,AEB,CK2,EIB,TB
 4202   FORMAT(///,20X,18HSUIT (CYLINDRICAL),/,F33.3,18H = RADIUS (INCHES)
       1,/,F33.3,18H = HEIGHT (INCHES),/,F33.3,34H = SECOND LAYER THICKNES
       2S (INCHES),///,F33.3,21H = SOLAR ABSORPTIVITY,/,F33.3,24H = INFRARE
       3D ABSORPTIVITY,/,F33.3,48H = 2-ND LAYER THERMAL CONDUCTIVITY (BTU/
       4HR-FT-R),/,F33.3,28H = INTERCHANGE FACTOR E(B-I),/,F33.3,31H = SKI
       5N TEMPERATURE OF CREW (R))
        WRITE OUTPUT TAPE 42,4200,HEADNG,NPAGE
        NPAGE=NPAGE+1
        CALL GROOVE
   99   CALL SUIT
        CALL EXIT
        END
```

```
*       SUBROUTINE FOR H1490
        SUBROUTINE GROOVE
C       COMPUTES RADIOSITY DISTRIBUTIONS B(X) AND B(Y).
C       ADIABATIC WALL CONDITION REQUIRES B(I)=H(I). THAT IS
C       RADIOSITY OR EMITTED FLUX=INCIDENT FLUX.
        DIMENSION FK(41,41),GRAND(41)
        DIMENSION X(41),XS(41),BX(41),BY(41)
        COMMON RLK,RL,THK,TH1
        COMMON CR,CCR,SR,SSR,CTR,NH,NPT,STEP
        COMMON XS,X,BX,BY,RR,RS,SY,SX,CY,CX,SS
        GRAND(1)=0.0
C       COMPUTES K(X,Y) AND BY(J) ALONG CLIFF WALL.
        DO 30 J=2,NPT
        DO 25 I=2,NPT
        XY=X(I)*X(J)
        FK(I,J)=XY/(XS(I)+RR*XS(J)+RS*XY)**1.5
   25   GRAND(I)=BX(I)*FK(I,J)
   30   BY(J)=SY+CY*SUM(GRAND)
        TS2=SUM(BX)+SUM(BY)
        KOUNT=0
        WRITE OUTPUT TAPE 42,4204
 4204   FORMAT(///,7X,12HFROM  CORNER,4X,26HHEAT FLUX / SOLAR CONSTANT,5X,
       115HTEMPERATURE (R),/,7X,12HX/LX OR Y/LY,9X,6HB(X)/S,4X,6HB(Y)/S,11
       2X,4HT(X),6X,4HT(Y),/)
   100  TS1=TS2
        KOUNT=KOUNT+1
        DO 130 I=2,NPT
        DO 125 J=2,NPT
   125  GRAND(J)=BY(J)*FK(I,J)
   130  BX(I)=SX+CX*SUM(GRAND)
        DO 230 J=2,NPT
        DO 225 I=2,NPT
   225  GRAND(I)=BX(I)*FK(I,J)
   230  BY(J)=SY+CY*SUM(GRAND)
        TS2=SUM(BX)+SUM(BY)
        DTEST=ABSF(TS2-TS1)
C       TEST CONVERGENCE CRITERION SATISFIED OR NOT.
        IF(DTEST-1.E-5)250,250,245
   245  IF(KOUNT-30)100,100,250
   250  DO 300 I=2,NPT
        TX=(BX(I)*SS)**0.25
        TY=(BY(I)*SS)**0.25
   300  WRITE OUTPUT TAPE 42,4205,I,X(I),BX(I),BY(I),TX,TY
 4205   FORMAT(1H I5,F10.4,8X,2F10.3,5X,2F10.2)
        WRITE OUTPUT TAPE 42,4206,DTEST
 4206   FORMAT(////,10X,8HD(SUM) =,1P1E13.6,/,10X,32HADIABATIC WALL CONDIT
       1ION ASSUMED)
        RETURN
        END
```

```
*       SUBROUTINE FOR H1490
        SUBROUTINE SUIT
C       COMPUTES HEAT TRANSFER RATES OF SUIT.
        DIMENSION XD(41),YD(41),YH(41),XGRAND(41),YGRAND(41)
       1,BBX(41),BBY(41)
        DIMENSION X(41),XS(41),BX(41),BY(41)
        DIMENSION DBC(20),TH(20),HEADNG(16),TCR(24),TCCR(24),TSSR(24),TSR(
       124),TCTR(24)
        COMMON RLK,RL,TIP,TH1
        COMMON CR,CCR,SR,SSR,CTR,NH,NPT,STEP
        COMMON XS,X,BX,BY,RR,RS,SY,SX,CY,CX,SS
        COMMON ND,NTH,DBC,TH,SIN,COS,RI,HM,RM,XMAX,YMAX,RYX,TB,TB4,SA,SE,S
       1N,ES,CK2,TOPER,TTERM,DANG,FNS,NMAX,NPAGE,HEADNG,TCR,TCCR,TSSR,TSR,
       2TCTR
        RSH=0.5*RS
        BX(1)=2.0*BX(2)-BX(3)
        BY(1)=2.0*BY(2)-BY(3)
        DO 4 I=2,NPT
        BBX(I)=BX(I)+BX(I-1)
      4 BBY(I)=BY(I)+BY(I-1)
        SED=0.07957747705*SE
        SEQ=0.25*SE
        READ INPUT TAPE 41,4100,CK1
 4100 FORMAT(8F10.0)
        DO 615 K=1,ND
        NLINE=51
        DB=DBC(K)*12.0
        DX=DB/XMAX
        DY=DB/YMAX
        DXX=DX*DX
        RSX=RS*DX
        DO 5 I=2,NPT
        XD(I)=X(I)-DX
      5 YD(I)=-X(I)*SIN-DY
        DO 615 M=1,NTH
        TH1=TH(M)
        RB=RM+TH1
        HB=HM+2.0*TH1
        ASIDE=2.0*RB*DANG*HB/144.0
        ATOP=3.1415927*RB*RB/144.0
        AREA=ASIDE*FNS+ATOP
        RLK=RB*LOGF(RM/RI)/CK2
        RL=RB*LOGF(RB/RM)
        CK=12.0/(RLK+RL/CK1)
        CR=TOPER*RI/RB
        TERM=CR*TB4
        RY=RB/YMAX
        RX=RB/XMAX
        HY=0.5*HB/YMAX
        YMIN=2.0*HY
        HX=HY*RYX
        XH=HX*HX
        RH=RY*COS
        DO 10 I=2,NPT
     10 YH(I)= X(I)*COS-HY
        DH=DY*COS+HY*SIN
        QLOAD=0.0
        AVGT4=0.0
        IF(NLINE-44)105,101,100
    100 WRITE OUTPUT TAPE 42,4200,HEADNG,NPAGE
```

```
4200 FORMAT(1H1,9X,16A5,4X,4HPAGE,I3,//,10X,10HSPACE-SUIT,8X,32HABSORBE
     1D HEAT FLUXES (BTU/HR-SF),34X,14HAVERAGE VALUES,/,3X,8HDISTANCE,2X
     2,7H1-LAYER,3X,4HELE-,2X,6HDIRECT,2X,6HCRATER,2X,6HCRATER,15X,2HTS,
     34X,6HT(OUT),3X,5HQRATE,4X,2HTS,4X,6HT(OUT),2X,6HT(INS),3X,5HQ(IN),
     4/,4X,6H(FEET),4X,5H(IN.),4X,4HMENT,3X,5HSOLAR,2X,6HBOTTOM,3X,5HCLI
     5FF,3X,5HTOTAL,6X,3H(R),6X,3H(R),3X,6HB/H-SF,3X,3H(R),5X,3H(R),5X,3
     6H(R),4X,6HBTU/HR,/)
      NPAGE=NPAGE+1
      NLINE=0
  105 WRITE OUTPUT TAPE 42,4205,DBC(K),TH1
 4205 FORMAT(1H F9.2,F9.3)
      NLINE=NLINE+1
      DO 610 N=1,NMAX
      IF(N-NMAX)114,111,111
  111 QSUN=SA*SX
      YQ=0.
      YGRAND(1)=(DX+RSH*YMIN)/SQRTF(DXX+RR*YMIN*YMIN+RSX*YMIN)
      DO 112 I=2,NPT
      YGRAND(I)=(DX+RSH*X(I))/SQRTF(DXX+RR*XS(I)+RSX*X(I))
  112 YQ=YQ+BBY(I)*(YGRAND(I-1)-YGRAND(I))
      QWALL=SEQ*YQ
      QFLAT=0.0
      CK=12.0/(THK+TH1/CK1)
      ER=TOPER
      TERM=TTERM
      GO TO 125
  114 CR=TCR(N)
      SC=SN*CR
      IF(SC)115,115,116
  115 QSUN=0.0
      GO TO 117
  116 QSUN=SA*SC
  117 CCR=TCCR(N)
      SSR=TSSR(N)
      SR=TSR(N)
      CTR=TCTR(N)
      XQ=0.
      YQ=0.
      B=-DX-RX*CR
      A=B/(HX*SR)
      ROOT=1.0/SQRTF(B*B+XH)
      XGRAND(1)=ATANF(A)-HX*CR*ROOT*(1.57079635+ATANF(B*ROOT*CTR))
      B=DY+RY*CR
      UP=1./((DH+RH*CR)*SR)
      A=(B*SIN-HY*COS*SSR)*UP
      ROOT=1./SQRTF(B*B+HY*HY)
      YGRAND(1)=ATANF(A)+HY*CR*ROOT*(1.57079635-ATANF(B*ROOT*CTR))
      DO 120 I=2,NPT
      II=I-1
      B=XD(I)-RX*CR
      A=B/(HX*SR)
      ROOT=1.0/SQRTF(B*B+XH)
      XGRAND(I)=ATANF(A)-HX*CR*ROOT*(1.57079635+ATANF(B*ROOT*CTR))
      B=YD(I)-RY*CR
      C=YH(I)
      CC=C*C
      A=(C*COS*SSR-B*SIN)*UP
      ROOT=1./SQRTF(B*B+CC)
      YGRAND(I)=ATANF(A) -C*CR*ROOT*(1.57079635+ATANF(B*ROOT*CTR))
      XQ=DBX(I)*(XGRAND(I)-XGRAND(II))+XQ
```

```
120 YQ=BBY(I)*(YGRAND(I)-YGRAND(II))+YQ
    QFLAT=SEP*XQ
    QWALL=SEP*YQ
125 TOTAL=QSUN+QFLAT+QWALL
    TS4=TOTAL/ES
    TS=TS4**0.25
    TMID=((CK*(TS-TB)+TERM)/ER)**0.25
    DX2=0.5*ABSF(TMID-TB)
    X2=0.5*(TMID+TB)
    XL=X2-DX2
    XR=X2+DX2
    KOUNT=0
502 QRATE=ER*X2**4-TERM
    TOUT=X2+QRATE/CK
    YMID=ES*TOUT**4-TOTAL+QRATE
    IF(ABSF(YMID)-1.E-3)510,510,503
503 IF(YMID)504,510,505
504 XL=X2
    GO TO 506
505 XR=X2
506 KOUNT=KOUNT+1
    X2=0.5*(XL+XR)
    IF(KOUNT-20)502,502,510
510 X2=TOUT
    IF(N-NMAX)606,605,605
605 AVGT4=AVGT4+TS4*ATOP
    QLOAD=QLOAD+QRATE*ATOP
    WRITE OUTPUT TAPE 42,4210,QSUN,QFLAT,QWALL,TOTAL,TS,X2,QRATE
4210 FORMAT(1H 23X,3HTOP,4F8.2,3X,3F8.2)
    GO TO 610
606 AVGT4=AVGT4+TS4*ASIDE
    QLOAD=QLOAD+QRATE*ASIDE
    WRITE OUTPUT TAPE 42,4211,N,QSUN,QFLAT,QWALL,TOTAL,TS,X2,QRATE
4211 FORMAT(1H I26,4F8.2,3X,3F8.2)
610 NLINE=NLINE+1
    AVGT4=AVGT4/AREA
    AVGT=AVGT4**0.25
    TSKIN=(AVGT4-QLOAD/(AREA*ES))**0.25
    TDEEP=((TERM+QLOAD/AREA)/ER)**0.25
    WRITE OUTPUT TAPE 42,4212,AVGT,TSKIN,TDEEP,QLOAD
4212 FORMAT(1H+,85X,3F8.2,F8.1)
615 NLINE=NLINE+1
    RETURN
    END
```

```
*       FUNCTION FOR H1490
        FUNCTION SUM(GRAND)
        DIMENSION GRAND(41)
        COMMON RLK,RL,THK,TH1
        COMMON CR,CCR,SR,SSR,CTR,NH,NPT,STEP
C       PERFORMS INTEGRATION BY SIMPSONS RULE.
        SUM=GRAND(1)-GRAND(NPT)
        DO 51 K=1,NH
        K2=2*K
   51   SUM=SUM+4.0*GRAND(K2)+2.0*GRAND(K2+1)
        SUM=STEP*SUM
        RETURN
        END
```